SOLAR TERRESTRIAL EFFECTS

A STATUS REPORT 1994

Edited by

J.C. Bhattacharyya

DIAMOND JUBILEE PUBLICATION
1994

60
DIAMOND JUBILEE

INDIAN NATIONAL SCIENCE ACADEMY
Bahadur Shah Zafar Marg, New Delhi 110 002

SOLAR TERRESTRIAL EFFECTS

A STATUS REPORT ON SOLAR TERRESTRIAL PHYSICS RESEARCH

Edited by

J.C. Bhattacharyya

Diamond Jubilee Publication
1994

INDIAN NATIONAL SCIENCE ACADEMY
Bahadur Shah Zafar Marg,
New Delhi 110 002
INDIA

Issued in October 1994

Published by the Executive Secretary, Indian National Science Academy, New Delhi on behalf of the Academy and printed at Viba Enterprises, H-54-A, Kalkaji, New Delhi-110019, India Phone: 6428515, 6470666

PREFACE

The last time an attempt was made to review the status of Solar Terrestrial Physics (STP) studies in India was more than fifteen years ago when as a chapter of the report on Space Physics Efforts, a brief account of the subject was covered. Much progress has since been made in India and abroad, and this document is another attempt to review and record the progress. The document comprises a collection of review articles written by experts who have been engaged in researches in the respective areas of STP over this period. In the first three articles, reviews of some relevant aspects of Solar Physics have been made. The periodicity in solar activity has been known for over two centuries but the behaviour is still enigmatic. Prof. M.H. Gokhale has covered this aspect and described some of the recent attempts to understand the phenomenon.

Probing deeper into the subject, Prof. K.R. Sivaraman has discussed some new indications of short- and long-term variability of solar radiation. Astronomers have known for a long time that the Sun is a star, but efforts in searching for indications of similar effects in other stars are hampered due to enormous distances preventing detailed examination of the surface features. The new indications decipherable from radiations in wide bands of the electromagnetic spectrum not only find the solar-stellar connections, but also aim at understanding the underlying physical processes of generating these radiations.

The source of all particle streams affecting the terrestrial environment is the solar corona; the phenomenon of coronal activities has been covered by Dr. J. Singh in the third article. At one time, only a few brief seconds during the total solar eclipse supplied all our knowledge of the solar corona. The position has changed drastically. Space observations and the extended band of radiation from X-rays to the long radio waves are pouring out new information about this pearly white envelope of the Sun.

Linking the Sun and the Earth's environment is the interplanetary medium. At one time it was believed that this is an empty space; now we know better. Interplanetary probes have revealed the intricacies of this vast medium with its complex magnetic fields and plasma inhomogeneities. A brief review of this medium has been contributed by Prof. S.K. Alurkar.

The particle radiation emanating continuously from the Sun is the solar wind. It is this flow which reaches the Earth's environment and creates effects observable on the Earth. In a failrly extensive review, Prof. A.C. Das has covered the topic of how the plasma flow from the Sun interacts with the plasma environment in the Earth's magnetic field.

In the next article, Prof. J.H. Sastri discusses the different modes by which change in the magnetosphere affects the ionospheric medium much closer to the Earth's surface. This topic has been further discussed in another article by

Dr. A.P. Mitra, who has covered the modes of coupling between different layers in our upper atmosphere.

In the next two articles, two important aspects of the middle atmospheric phenomenon, chemistry and dynamics, have been discussed. The first is written by Prof. B.H. Subbaraya and the second by Dr. B.V. Krishna Murthy. In the final article the subject of atmospheres on the other planets in the solar system, and their reactions to the solar wind, have been discussed. This article has been contributed by Dr.K.K. Mahajan and his colleagues.

The topic which could not be covered is the lowest layer of our atmosphere, the troposhere, as this very important region is the subject of extensive investigations by other big groups in the country. I hope it will be discussed by atmospheric scientists of this country in a separate document, describing the complex phenomenon so vital to our existence.

I am most thankful to all the contributors who have made considerable efforts in spite of their busy schedule. Special thanks to my colleague Prof. J.H. Sastri who besides his contribution has lent valuable help in the compilation of this report.

J.C. Bhattacharyya
Indian Institute of Astrophysics
Bangalore 560 034

CONTENTS

PERIODICITIES IN SOLAR ACTIVITY

M.H. Gokhale*

WHAT IS SOLAR ACTIVITY ?

Conventionally, the term 'solar activity' has meant only the occurrence of sunspots and the associated phenomena like photospheric faculae, chromospheric emission plages, flares, active prominences, and the resulting planetary and interplanetary phenomena. Observations during recent decades have made it imperative to expand the meaning to include all the phenomena associated with concentrated magnetic fields that lead to excess heating, irrespective of where they occur and in what form they are observed.

Periodicities in Sunspot Activity

Most of the activity phenomena show the '11 year periodicity' which was first discovered in sunspot abundance by German amateur astronomer Heinrich Schwabe in 1843. Since then many observatories have kept day-to-day records of the numbers, locations and areas of sunspots in the form of white light photographs. Longest among and these are the records of Greenwich and Kodaikanal Observatories that date to 1874 and 1904 respectively. The number of sunspots on the Sun's disc occurring during a specified length of time, as counted according to a well-defined method to minimize observational uncertainties, is a commonly used index of the sunspot activity. The sum of the areas of sunspots corrected for projection effects is another such index. Waldmeier (1961) has published the monthly and the yearly sunspot numbers from 1610 to 1960. Indices of sunspot activity during earlier decades, centuries and millennia have been inferred, though with increasing uncertainties, from historical records of geophysical, biophysical and cosmic abundance parameters such as tree rings, isotope ratios in oceans and meteorites, and glacial flows, which have recently been identified as good measures of sunspot activity. Fourier spectra of the annual sunspot numbers by Cole (1973), Curie (1973) and Wolf (1976) show the presence of a large number of significant frequency bands at

* *Indian Institute of Astrophysics, Bangalore 560 034*

periodicities varying from 178 yr to a few months. All these periodicities are only approximate. Even the most prominent bands at 178 yr, 84 yr, 60 yr and 11 yr have relative frequency-widths ~ 10%.

The amplitude of the most prominent '11 yr' periodicity has substantial variations from cycle to cycle, leading to a modulation of ~ 100% over 3 or 4 cycles, (which in fact manifests as the '80 yr' periodicity). The historical and ancient parameters show that once in a few centuries the amplitude becomes so low, and remains so low for several decades, that sunspots rarely occur. One such period of near absence of sunspots started around 1640 (i.e. merely 30 years after the discovery of sunspots as solar phenomena) and lasted till 1715. Eddy (1975) has shown that at least three such 'long sunspot minima' must have occurred during the past one thousand years and probably the level of activity has a modulation on time scales exceeding several hundred years.

Sunspot Cycle as a Manifestation of the '22 yr' Magnetic Cycle

Most sunspots occur in groups, in majority of which the portions that are 'leading' and 'following' in the solar rotation are clearly separated, and have opposite magnetic polarities. The polarities of these so-called 'bipolar magnetic regions' are opposite in the northern and southern solar hemispheres. During each sunspot cycle the polarities of the bipolar regions in both the hemispheres are reverse of those during the previous cycle. Thus the magnetic fields associated with sunspots show a '22 yr' periodicity. In fact even the signs of the weak magnetic fields in the polar regions also reverse just after the sunspot maximum during each cycle. Thus the whole Sun shows a '22 yr' magnetic cycle. Since the darkness of sunspots is due to their strong magnetic fields, the '11 yr' sunspot cycle is in fact a manifestation of the Sun's '22 yr' magnetic cycle.

Distribution of Sunspot Activity on Solar Surface and in Time

Apart from the 'periodicities' mentioned so far in the distribution in time, the sunspot activity also shows some kind of periodicities in its distribution on the surface of the Sun.

For short durations of up to a year the activity seems to occur in a few 'preferred heliographic longitudes, giving an impression of a periodicity in distribution with respect to longitude. Longer periodicities with respect to longitude are difficult to detect (if existing owing to substantial variations in the Sun's rotation at any given latitude which has to be subtracted for uniquely determining the longitude of an event of activity).

At the starting 'minimum' of each '11 yr' sunspot cycle, sunspots occur at ~ 30° latitude in each solar hemisphere. During the increase of the sunspot numbers to maximum and its subsequent decrease to minimum the mean latitude of sunspot

occurrence in each hemisphere shifts systematically towards the solar equator, reaching ~ 5°. As a result, a two-dimensional display of the distribution of sunspot activity in latitude and time resembles a picture of a butterfly with its body along the time axis with tail towards increasing time and wings spread in the directions of the latitude axis.

A year or two before the end of any current sunspot cycle the small sunspots of the next cycle start appearing in latitudes ~ 30° in both hemispheres. Thus there are small overlaps between the successive sunspot cycles.

Periodicities in Other Activity Phenomena

Up to the middle of this century, faculae and eruptions of quiescent prominences were the only kinds of activity known to occur outside the sunspot latitudes.

The polar facular abundance varies with an '11 yr' periodicity, but in a phase opposite to that of the sunspot cycle.

The quiescent prominences,even before they erupt, are a kind of solar activity by virtue of their excess emission. Their index (sum of lengths) varies in a way similar to sunspot number, but with a small ($\sim \leq$ 1 yr) delay in phase. During each sunspot cycle a few latitude bands of their occurrence in each hemisphere migrate from ~ 35° to the respective poles.

With the advent of new observational techniques, small scale (e.g. $\leq 10^3$ km) solar activity has been detected to exist all over the Sun at all times. High resolution magnetograms show the presence of hundreds of tiny ($\sim 10^4$ km size) bipolar magnetic regions that last for a day or less (and hence called 'ephemeral active regions'), distributed all over the Sun's disc at any given time. Their abundance also shows '11 yr' periodicity approximately in phase with the sunspot numbers. X-ray images of the Sun show hundreds of similarly small bright points (XBP's) also distributed all over the Sun and also showing '11 yr periodicity' in their abundance. However, this abundance is *opposite* in phase with respect to the sunspot cycle.

One of the striking periodicities in solar activity, other than 11 yr is that of ~ '155 day' which is found in sunspot numbers, solar irradiance, 10.7 cm flux, plage index and in even in strong flares.

Periodicities in Solar Rotation

Solar and stellar activity is closely related to strengthening of the magnetic field by rotation. LaBonte and Howard (1982) detected '11 yr' periodicity in the variations of the coefficients *a*, *b* and *c* in the expression for Sun's photospheric rotation rate ω as a function of latitude λ in the form

$$\omega = a - b \sin^2\lambda + c \sin^4\lambda .$$

This corresponds to presence of two bands of latitudes in each hemisphere that rotate faster (or slower) than normal and seem to migrate from pole to equator in ~ 22 yr. The periodicity of rotation rate at each latitude however remains ~ 22 yr. They found that the latitude of sunspot activity remains coincident with that of the shear in the rotation. Javaraiah and Gokhale (1994) have found 44 yr, 22 yr and 7 yr periodicities in the temporal variation of the coefficient *b* in the rotation determined from sunspot data. The '7 yr' periodicity has been found earlier by Singh and Prabhu (1985) in the rotation rates of calcium emission plages. The '7 yr' periodicity is a third harmonic of the '22 yr' periodicity and may be responsible for the 'asymmetry' (viz the fast rise and the slow decline) in the '11 yr' sunspot cycle.

Theoretical Studies

A theoretical model of the solar activity cycle or solar magnetic cycle has to be based on magneto-hydrodynamical interaction of rotation and magnetic field. It must account for: (i) the '11' or '22' yr'period of the cycle, (ii) the latitude-time distribution ('butterfly' diagram), including the small overlaps, (iii) the 'shapes' of the sunspot cycles, (iv) modulation of the period and amplitude, including prolonged minima, (v) the long-term stability of the phase, (vi) the latitudinal distribution and relative phases of the non-sunspot activity, (vii) migration of weak magnetic fields and their neutral lines from middle latitudes to poles, and (viii) polar field reversals at appropriate epochs.

The first plausible theoretical reason for periodic nature of sunspot activity, based on MHD oscillations, was proposed by Alfvén (1943) and Walen (1949). A physical basis for this based on travel times of Alfvén waves was proposed by Alfvén. Pumpton and Ferraro (1955) showed the possibility that torsional oscillations of the Sun may have periods ~ decades However, these models depended on the presence of an internal magnetic field of primordial origin and on its strength. Babcock (1961) showed that the topology of the surface field is consistent with that expected from winding of poloidal field by differential rotation and diffusion due to the presence of convection. Parker (1955) pointed out the role of magnetic buoyancy in bringing out the strengthened toroidal fields. He also proposed the reversal of the toroidal field results from cyclonic turbulence of convection in the convection zone. The mean-field electrodynamics developed by Steenbeck and Krause (1969), Krause and Raddler (1971) provided mathematical basis for quantifying the statistical effects of cyclonic twisting and convective diffusion. However, the models of solar cycle based on this formulation, besides being merely kinematical and besides involving other limitations and conceptual difficulties, required contradiction with either the butterfly diagrams or the helio-seismologically determined radial gradient of Sun's internal rotation.

The Latest Developments

Legendre-Fourier analysis of the distribution of magnetic field as inferred from the sunspot data from 1874 to 1976 has shown that sunspot activity can be

considered as resulting from superposition of LF terms mainly of odd 'degrees' '$l = 1, 3, 5, \ldots, 13$', all with frequency $\nu_* = 1/21.4 \pm 1/103\ \text{yr}^{-1}$ (and a few odd harmonics of ν_*) with approximately constant relative amplitudes and phases (Gokhale *et al.*, 1992). These LF terms constitute four global MHD oscillations of the Sun. The superposition of the dominant terms reproduces not only the butterfly diagrams but also the distribution and migrations of solar magnetic fields in latitudes 35°-90°, though the analyzed data comes from latitudes < 35° (Gokhale and Javaraiah, 1992). A phenomenological model has been suggested for maintenance of the LF spectrum of torsional MHD waves by (i) cascade of energy supplied at $\nu = \nu_*$ and (ii) leakage of energy in the form of buoyant emergence of toroidal magnetic flux bundles wherever and whenever the critical buoyancy is reached by constructive interference of the waves (Gokhale and Javaraiah, 1994).

Summary

Solar activity constitutes a variety of phenomena which are manifestations of the heating of the Sun's atmosphere by dissipation of magnetic structures and MHD waves emerging from the solar interior The phenomena are distributed on Sun's surface and in time with a variety of periodicities, the prominent among which is the 11 yr periodicity in time The distribution on surface and in time is probably determined by the amplitude and phase spectra of the MHD waves, the prominent waves having period ~ 22 yr Among these the primarily excited modes and the mechanism of excitation have not yet been identified

REFERENCES

Alfvén, (1943), *Arkiv für Mathematik, Astronomi Och Fysik*, **29A**, No 12

Babcock, H.W. (1961), *Astrophy. J.*, **133**, 572.

Cole, T W. (1973), *Solar Phys*, **30**, 103.

Currie, R G. (1973), *Astrophys and Space Sci.*, **20**, 509.

Eddy, J.A. (1975), *Bull AAS*, **7**, 365

Gokhale, M H., Javaraiah, J ,Kutty, K.N. & Verghese, B A (1992), *Solar Phys.* **138**, 35.

Gokhale, M H. & Javaraiah, J. (1992), *Solar Phys.* **138**, 399

Gokhale, M.H & Javaraiah, J (1994), submitted to *Solar Phys*

Javaraiah, J. & Gokhale, M.H. (1994), in preparation.

Krause, F. & Raddler, K.H. (1971), in 'Solar Magnetic Fields', *IAU Symp.* **43**, 770.

LaBonte, B.J. & Howard, R . (1982) *Sol. Phys.* **75**, 161-178.

Parker, E N (1955), *Astrophys. J*, **122**, 293

Plumpton, C. & Ferraro, V.C.A. (1955), *Astrophys. J.* **121**, 168.

Schwabe, H. (1843), *Astr. Nach.*, **21**, 233

Singh, J & Prabhu, T P. (1985), *Solar Phys.*, **97**, 203.

Steenbeck, M. & Krause, F. (1969), *Astron. Nachr.* **291**, 49.

Walen, C. (1949), in *On the vibratory rotation of the Sun* (Hensik Lindstalls Bokhandel, Stockholm)

Waldmeier, M. (1961), *The Sunspot Activity in the Years 1610-1960* (Schultness, Zurich)

Wolf, C L. (1976), *Astrophys J* **205**, 612-621

RADIATION OUTPUT AND SPECTRUM VARIABILITY OF THE SUN AS A STAR

K.R. Sivaraman*

INTRODUCTION

For more than a decade, solar irradiance (both bolometric and at different wave lengths) has been monitored from space by different satellites as well as from ground-based telescopes The visible region pertains to the photosphere, the extreme ultraviolet, the far infrared regions as well as the centre of strong lines like Ca II H and K and H-alpha pertain to the chromosphere, whereas X-rays and long radio waves originate in the corona. In the solar interior, variations of convective efficiency resulting from magnetic field variations may cause luminosity and diameter changes. Magnetic fields associated with solar activity have a pronounced effect on the outer layers and the changes in the magnetic fields modulate the solar output correspondingly.

Magnetic fields organise in different ways to produce sunspots, faculae and coronal structures. The Sun's 27-day rotation causes these phenomena to transit on the solar disc and this gives rise to the rotational modulation of the magnetic related phenomena whereas the solar cycle causes the 11-year modulation on top of the rotational modulation. Thus the solar output variability is interpreted in terms of solar magnetic fields, the rotational modulation of these fields and the solar cycle.

VARIATIONS IN THE PHOTOSPHERE

Total irradiance variability

The basic parameter that characterises the output of the Sun is its luminosity. Sustained efforts to detect variability in the total solar irradiance (or the solar constant) began in the late 19th century. Experiments during the first three quarters

* *Indian Institute of Astrophysics, Bangalore 560 034*

of the present century from ground-based observatories, balloons and aircrafts could not detect any variation intrinsic to solar irradiance. The main problems were the corrections to instrumental performance and to Earth's atmospheric effects which were much larger than the precision sought for measuring the irradiance variation. The Earth Radiation Budget (ERB) experiment on board the Nimbus 7 spacecraft launched in late 1978 and continuing to the present day provides the longest database on the solar irradiance measurements[1]. The ERB can measure the solar insolation with an accuracy of 0 5%. The Active Cavity Radio Irradiance Monitor (ACRIM1) on board the Solar Maximum Mission (SMM) launched in February 1980 brought out a clear evidence of solar variability[2]. Observations from both the instruments show a systematic long-term decrease in total irradiance between 1980 and mid-1985. The decrease in total irradiance over this period is just below 0.1% or 0.02% per year[2]. Subsequent results from ACRIM1 show that the irradiance remained nearly constant from mid-1985 to early 1987 corresponding to the magnetic solar minimum years and then started rising steadily The increase in irradiance through mid-1989 is about 0.06% since early 1987[3,4] and if this upward trend continues into the activity maximum of solar cycle 22, then this would establish a direct relationship between the luminosity and the solar activity cycle.

Variability on time scales of days

The SMM measurements have for the first time shown evidences for the reduction in irradiance of as much as 0 25% when large sunspots cross the visible hemisphere of the Sun[5]. Also peaks in irradiance have been observed coinciding with the transit of active regions containing large facular areas. There have been occasions when the facular area has decreased the net deficit produced by the dark sunspots. Investigations on the nature of energy flow and balance in active regions seem to indicate that the irradiance deficits caused by sunspots are compensated for by excess persistent facular emission in the same active region on short time scales.

Photospheric absorption lines

If the solar luminosity shows changes independent of the variations in sunspots or faculae as is suggested by the downward trend in the SMM data, this should be reflected in the photospheric temperature. A search for this using lines formed in the upper photosphere as well as in the deeper layers is in progress at the Mc Math telescope on Kitt Peak since 1975. Low excitation lines such as Mn I 5394 Å and Fe I 5250 Å show both short- and long-term variability correlating with the variations seen in the H and K lines[6] and the CN band (3883 Å). These lines as well as the CN band are weakened by the same mechanism that weakens the H and K lines in active regions, namely the magnetic heating, whereas both the oxygen triplet (OI 7772 Å ,7774 Å, 7775 Å) and He I 10830 Å strengthen with solar activity or, in other words, their equivalent widths increase with solar activity. In contrast to these, the high excitation line CI 5380 does not show any modulation by the 11-year solar cycle. Other examples of lines invariant with the solar cycle are the weak line Fe I.5379Å

and the moderately strong line Fe I 5393 Å and the Si I 10827 Å[7].

Solar diameter

A few years ago claims of very large rates of diameter change were made[8]. Measurement of solar diameter at the High Altitude Observatory with precision of ~ 0.4 arc sec since 1981 has ruled out the claims that the Sun has been shrinking at the rate of 2 arc sec per century at the 1.8 σ level and also the suspected variation of 0.1 arc sec amplitude in phase with the solar cycle at the 2.8 σ level[9]. Analysis of white light images of 8 cycles in progress at Kodaikanal may be helpful in detecting any possible variations. However, very high precision measurements from spacecraft over a sufficiently long time may be required to establish any possible diameter variations.

Global convective efficiency

Several studies have investigated[10,11] the response of the solar radius and luminosity to postulated changes of efficiency of convection. Changes in the convective efficiency incorporating changes in magnetic field have been modelled by varying the mixing length parameter[12]. These models easily reproduce changes in luminosity at the 0.1% level but fail to reproduce diameter changes large enough to be observed with present-day techniques.

VARIATIONS IN THE CHROMOSPHERE

Ca II H and K lines

These lines have long been recognised as reliable diagnostic indicators of chromospheric activity on the Sun. Their sensitivity to activity and accessibility from ground-based facilities have made them the most often used lines for the study of the chromosphere. Temporal variations in the emission reversal in the two lines are caused by the evolution of structures associated with magnetic fields like plages, bright network, bright points, ephemeral active regions that represent the visible manifestations of the solar cycle. In addition to the solar cycle related changes the flux in these lines also exhibits the 27-day rotational modulation as these structures are brought into view and taken out of view by solar rotation.

Because of the success in detecting solar cycle changes and the rotational modulation on the Sun these have been the primary means of studying the stellar analogues of solar cycles and also the rotational modulation of slow rotating stars.

The monitoring of the irradiance variation in the K line has been in progress since 1960[13,14] at Kodaikanal using the tower telescope and high resolution spectrograph. These data provide irradiance variation over two solar cycles. Since 1977, similar measurements at the Mc Math telescope at the Kitt Peak have been in progress[15]

The parameter that is customarily used to characterise the K line emission is the 1Å Ca II K index (which is the integral of flux of the emission reversal over a 1Å band centred on the core normalised to the intensity of the nearby continuum) for both the integrated disc and for magnetically quiet region near the disc centre The latter gives the background variations of the quiet Sun. The full disc index shows an increase of about 28% in the mean from solar minimum to maximum for solar cycle 21 and an increase of about 34% for cycle 22[14]. The centre of the disc signal from a quiet region was shown to be invariant[15] but subsequent study using extensive material has brought out the variation in the contribution from the network boundaries over a solar cycle and this is quite significant[16].

UV and EUV lines

The measurements from the spacecrafts form the sources of data in these wave length regions Continuous observations in the EUV (10-1200Å) are available from July 1977 until December 1980 from the spacecraft Atmospheric Explorer-E (AE-E)[17] and in the range 1200-4000Å from Nimbus-7 since 1978. The Solar Mesosphere Explorer (SME) monitored the UV irradiance from 1150 to 3050Å with 7.5Å resolution since 1981[18]. The descending phase of solar cycle 21 (1982-86) and the ascending phase of cycle 22 (1986-1988) are covered well by continuous measurements from SME, NOAA-9 and NOAA-11 satellites[7].

From rocket and balloon measurements through 1975 a decrease of flux by a factor 2.5 at 1750Å and about 18% at 3000Å from the solar maximum to minimum were claimed[19]. But measurements from 1981 to 1985 show much smaller variations. The variation from the maximum to minimum over a solar cycle (with the solar rotation variation filtered out) in the Lyman α is only about 75%, in the range 1300-1600Å it is less than 20%, and in the range 1600 = 2000Å it is nearly 5% (ref. 20). The variation in the Lyman α and Mg II H and K lines follow closely that seen in Ca II H and K lines.[21]

The 27-day rotational modulation in the irradiance data can be clearly seen in the lines originating in the chromosphere and in the corona like Ca II K index, Lyman α, Lyman β, He II 304 Å, and Fe XV 284 Å[22]. The strength of the modulation varies with the ionic species and wavelength. Thus, for the flux at 2000 Å it is about 1.06, for He II 304Å it is about 1.6; for the coronal line Fe XV it is about 2.8 and for the X-ray flux 1-8 Å it is about 2 5[22].

VARIATIONS IN THE CORONA

Electron scattering corona

The long-term variations of the electron corona monitored by the K-coronameter reveal that over the solar cycle the mean polarization brightness (measured in units of 10^{-8} polarization percentage times solar disc brightness) varies from about 2.5 at

solar minimum to 5 at solar maximum. By inference the mass of the corona also must exhibit a variation by a similar factor over the solar cycle. The area of coronal holes is known to be anticorrelated with the solar cycle.

EUV radiation, 10.7 cm flux and X-rays

Among the EUV emission lines originating in the chromosphere-corona transition region and in the corona studied using the AE-E data during the ascending phase of cycle 21 (1977-1980) are Fe XVI (335 Å), Fe XIII (200-204 Å) and the Fe IX line (169-173 Å)[17]. These lines also show variations similar to Lyman β (1026 Å). The Fe XVI line originates in low density plasma at a temperature of 3×10^6 K while Lyman β originates from high density regions with temperatures in the range 20,000 = 50,000 K. The variation in the coronal line (Fe XVI 335 Å) is 2 to 100 times between solar minimum and maximum while the lower ionization lines vary by a factor of 2 or thereabouts[17]. This illustrates the high sensitivity of coronal emissions to the increased temperatures and densities due to solar activity.

The hot gas of the corona is the source of soft X-rays (free-free thermal emission) and has been monitored by the GOES series spacecraft. The 1-8 Å X-rays flux arises primarily from regions of the corona with temperatures higher than 2×10^6 QK while the 10.7 cm radio flux arises from the cooler regions and the transition region. The 1-8 Å X-ray flux shows a full range of two orders of magnitudes with very little quiet Sun component while the 10.7 cm radio flux has a substantial nonvarying component and shows a variation by a factor 4 between solar maximum and minimum.

A detailed comparison of the temperatral variations of the solar EUV, UV and 10830 Å radiations shows that the solar cycle variations are a factor of 2 larger than the short time scale variations (due to rotation modulation of evolving active regions) for the chromospheric UV, EUV and He I 10830 Å lines[22].

CONCLUSIONS

The Sun, although a run of the mill star, is still a variable star at levels both of astrophysical and geophysical interest. Quantitative estimates of the magnetically induced variations in the luminosity output in various bands particularly over time scale of a solar cycle are fairly well known today. These are both from ground-based facilities and from several spacecrafts. Definitely several fundamental questions and problems of interpretation remain to be answered. What is the nature and origin of the long-term drift of bolometric irradiance seen by SMM? What are the precise contributions from the sunspots and the faculae in this variation of irradiance? How does the slowly varying component of the Ca II K 1 Å index originate?

Answers to these questions are vital to understand the origin of these variations and to be able to interpret them in terms of solar models, both interior and atmospheres. Furthermore, efforts to look for variability in sunlike stars using the

Sun as a rosetta stone have resulted in such encouraging results that there is enough motivation for the stellar astronomers in this fertile field of investigation. The coming decades should see continued progress in this field with the data flowing from the spacecrafts which continue to be operational.

REFERENCES

Hickey, J.R., Alton, B.M., Lee Kyle, H. & Hoyt, D., *Space Sci. Rev.*, **48** (1988), 321-342.

Willson,. R.C., Hudson, H.S., Frohlich, C. & Brusa, R.W. *Science*, **234** (1986) 1114-1117.

Willson, R.C. & Hudson, H.S., *Nature*, **351** (1991), 42-44.

Hoyt, D.V., Kyle, H.L., Hickey, J.R. & Maschoff, R.H., *J. Geophys. Res.*, **97** (1992), 51-63.

Willson, R.C., Gulkis, S., Janssen, M., Hudson, H.S. & Champan, G.A., *Science*, **211** (1981), 700-702.

White, O.R., Livingston, W.C. & Wallace, L., *J. Geophys. Res.*, **92** (1987), 823-827.

Livingston, W.C., Donnelly, R.F., Grigoryev, V., Demidov, M.L., Lean, J; Steffen, M; White, O.R. & Willson, R.C., in *Solar Interior and Atmosphere*, edited by Cox, A N., Livingston, W C and Matthews, M.S. (University of Arizona Press, Tucson) (1991) 1109-1160

Eddy, J A & Booinazian, A A , *Bull Am Astron Soc.*, **11** (1979), 437

Brown, T M , Elmore, D.F., Lacey, L , & Hull, H , *Appl Optics*, **21** (1982), 3588-3596.

Dearborn, D S & Paud Newman, M J , *Science*, **201** (1978), 150-151

Gilliland, R.L., *Astrophys. J* , **253** (1982), 399-405.

Tayler, R.J., *Mon Not Roy Astron Soc* , **220** (1986), 793-797.

Sivaraman, K R , Jagdev Singh, Bagare, S P & Gupta, S.S., *Astrophys J* , **313** (1978), 456-462.

Sivaraman, K.R., Gupta, S S, Kariyappa, R., Aleem, P.S.M & Sunderaraman, K (1993), Presented at the IAU Col. 143; `The Sun as a variable star' held in 20-25 June, 1993, Boulder, Coloarado.

White, O.R & Livingston, W.C., *Astrophys. J* , **249** (1981), 798-816

Kariyappa, R. & Sivaraman, K.R , presented at IAU Coll. No. 143, `The Sun as a variable star', held in 20-25 June, 1993, Boulder, Colorado

Hinteregger, H E , Fukui, K & Gilson, B.R , *Geophys. Res. Lett.*, **8** (1981), 1147-1150.

Rottman, G J , in *Atmospheric Ozone* edited by C.S. Zerofos and A Ghazi. (D Reidel Publishing Co, Dordrecht) (1985), p.656.

Heath, D.F. & Thekakara, in *The solar output and its variation*, edited by O.R. White (Colorado Assoc Univ. Press.) 1977, 193.

Rottman, G.J., in *Solar Radiative Output Variations*, edited by P.V. Foukal, 1988, 71-86.

Lean, J.L. & Skumanich, A., *J. Geophys. Res.*, **88** (1983). 5751-5759.

Donnelly, R.F., Hinteregger, H.E. & Health, D.F , *J. Geophys. Res.*, **91** (1986), 5567-5578.

SOLAR CORONA

Jagdev Singh*

HISTORICAL BACKGROUND

The Sun is the only star close enough to provide detailed information about stellar atmospheres, and only during a total solar eclipse its prominences, chromosphere and corona can be directly viewed with naked eye and analysed in detail using telescopes During the total solar eclipse, the lunar shadow on the Earth darkens the sky to such an extent that the corona appears as a large brilliant halo surrounding the eclipsed Sun. We know that the corona consists of hot tenuous gases extending to large distances from the surface of the Sun; the sights of corona during total eclipses have always created great excitement and awe among the people all over the world since time immemorial. According to a Babylonian account, probably of the eclipse of 31 July 1063 BC "... the day was turned into night and there was fire in the midst of heaven ..." Plutarch wrote about the eclipse of 27 December, 83 AD: "There always appears around the circumference of the moon some light that does not permit total darkness." Kepler in 1608, Cassini in 1706 and Halley in 1715 commented on the existence of the corona, but Halley could not decide whether it was connected to the Sun or the Moon (Mitchell 1935).

At the eclipse of 18 July 1860, the chromosphere, the corona and the prominences were successfully photographed for the first time. Things changed with the advent of spectroscopic techniques which were employed by the British and French teams together with the Madras Observatory team at the eclipse of 18 August 1868 in India and they established the gaseous nature of prominences as inferred from emission lines of hydrogen. The hydrogen emission lines seen in prominences were so strong that the French astronomer Janssen, who was stationed at Guntoor, reasoned that they could be seen without an eclipse. The next day at the eclipse site the speculation was proved to be correct. The prominence spectrum also displayed a bright yellow line more refrangible than the well-known D-lines of sodium, later attributed to helium element. After Pierre Janssen and J. Norman Lockyer discovered

Indian Institute of Astrophysics, Bangalore 560 034.

a means of observing the prominences outside an eclipse in 1868, astronomers shifted their attention to the corona. The green coronal line at 5303 Å was discovered by Charles A. Young during the eclipse of 7 August 1869. It was attributed to a new unknown element 'coronium' since this line could not be identified with any of the known lines of different elements at that time. The eclipse of 12 December 1871 had a path of totality passing over Ootacamund and Pudukottai near the southern tip of India. This eclipse is memorable for the French astrophysicist Janseen's discovery of the Fraunhofer corona by the observations of weak dark absorption lines, especially those of sodium The next important eclipse in the Indian region, on 22 January 1898, was well observed. Naegamvala stationed at Jeur obtained very good high resolution photographs of solar corona, and chromospheric and coronal spectra. Evershed obtained ultraviolet spectra of the chromosphere and prominences and found continuous emission shortward of the Balmer limit, a feature which is most usefully exploited in the present-day studies for the determination of electron temperature and density. By this time corona was no longer merely the spectacular crown of the Sun, it was a giant cosmic laboratory worthy of detailed and repeated inspection.

Structure of solar corona

Now, we know that the corona, the silvery white halo seen around the Sun during the total solar eclipses, consists of very hot ionized gas containing mostly free electrons. The shape of the corona changes with the solar activity cycle of 11 years. It is highly symmetric at the maximum phase of the solar cycle as seen from the broad band (Fig. 1) photograph taken at Jawalgera, India, during the total solar eclipse of 16 February 1980. The corona becomes asymmetric, elongated over the equator of the Sun near the minimum phase of the solar cycle as indicated by the photograph (Fig. 2) obtained at Tanjung Kodok, Java, Indonesia, on 11 June 1983. At the sunspot minimum beautiful regular polar plumes are evident, suggestive of the magnetic alignments of a simple bar magnet. The photograph of the solar corona obtained at the 1980 eclipse has been processed further by Scaria (1983) using unsharp masking technique developed by Malin (1977). The processed photograph in Fig. 3 shows that there are large numbers of structures in the corona. Comparison of the structures in the corona with the potential field distribution, obtained by using the photospheric magnetic fields by Newkirk and Altschuler (1970), confirmed the role of magnetic fields in shaping the coronal structures. Features in the corona produced as ionized gas above the corona are gathered by the magnetic field, which appear bright because energy flowing along the magnetic field lines heats the gas (Bruning, 1992). Coronal loops formed right above an active region connect regions of opposite magnetic polarity. Coronal arches are much larger loop-like features that extend between two active regions. Prominences seen just above the solar limb are made up of relatively cold gases embedded in the hot ambient coronal gas. They are most probably supported by the magnetic fields against the gravity. Helmet streamers form over the neutral lines in large active regions with a long-lived prominence commonly embedded in the base of the streamer. The footpoints of the streamer are in the

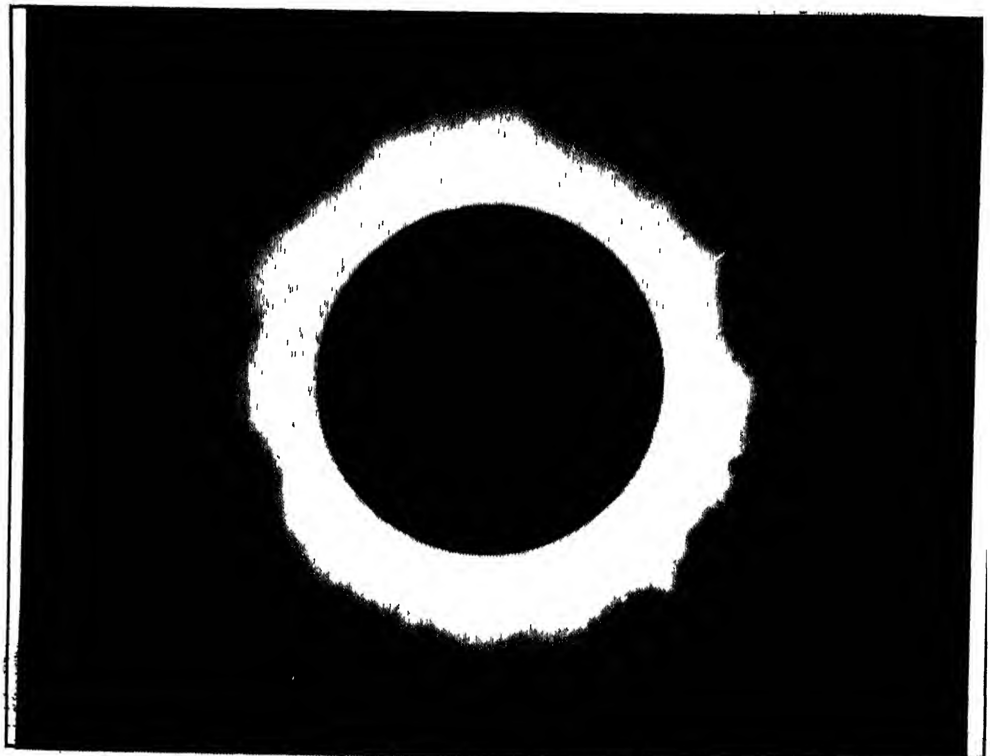

Fig. 1 The broad band picture of the solar corona near the maximum phase of the solar cycle obtained during the total eclipse of 16 February 1980 from Hosur, India (Courtesy, Indian Institute of Astrophysics, Bangalore)

Fig 2 The white light picture of the solar corona near the minimum phase of the solar cycle obtained during the eclipse of 11 June 1983 from Tanjung Kodok, Indonesia. (Courtesy: Charles Mahaffey, National Solar Observatory, Tucson)

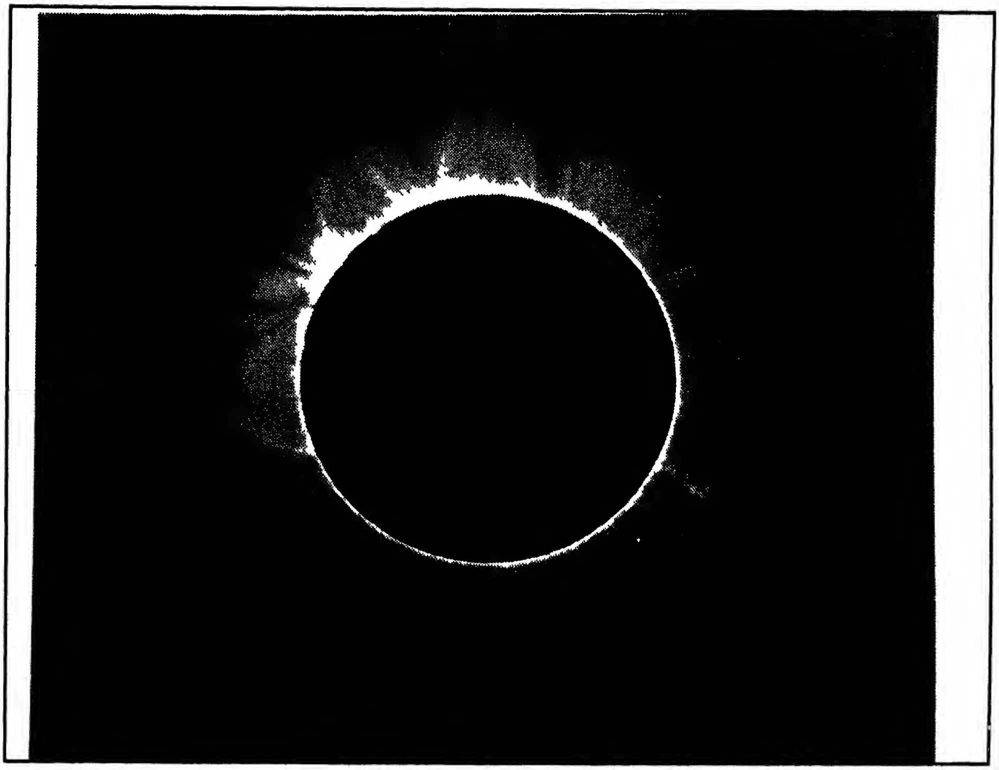

Fig 3 Processed image of the solar corona shown in Fig. 1 Unsharp masking technique was used to bring out the detailed structure in the corona. (Courtesy. Indian Institute of Astrophysics, Bangalore)

regions of opposite magnetic polarity. During an eclipse, the visible portion of a streamer extends to several times the Sun's radius outwards from the photosphere. Recent measurements suggest the streamers may reach at least half way to Earth. We shall discuss the role of streamers and magnetic field in the formation of coronal holes and solar wind in a separate section.

Brightness of solar corona

The solar corona is about a million times fainter than the intensity of the Sun at its centre. The relative brightness of the solar disc, solar corona and the sky brightness can be seen in Fig.4, which shows that under the best possible conditions at high altitudes the sky brightness is about 10^{-6} of the value of brightness on the centre of solar disc and coronal intensity close to the limb is marginally higher than that of sky. But, when the Moon blocks out the photospheric light, the sky brightness near the limb at mid-totality falls to such low levels that corona can be photographed out to almost four solar radii. It is also seen that coronal intensity drops exponentially with solar radii and corona close to the Sun has about the same intensity as that of the full Moon. Contribution to coronal light comes from three kinds of particles in the corona. Accordingly three components have been classified as K, E and F-corona. Fig.4 also shows a plot of the relative intensities' contribution of these three components as a function of solar radii due to Van de Hulst (1953). Most of the

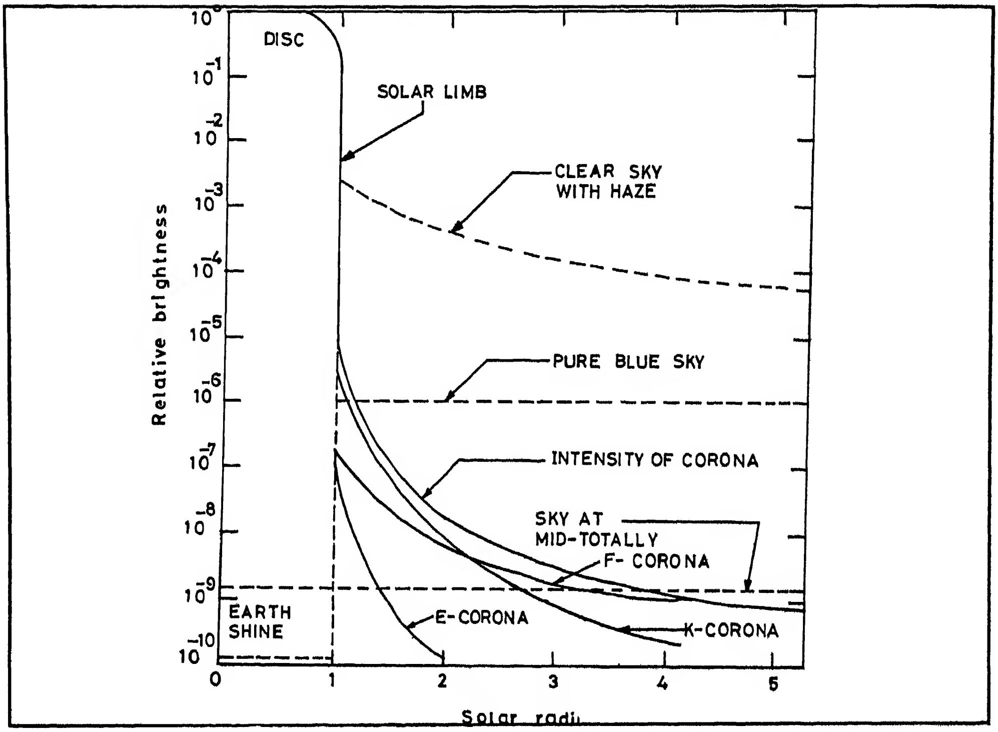

Fig 4 The relative intensities of the solar corona and sky brightness as a function of distance from the centre of the Sun are shown The relative intensities due to K,E and F-corona have also been plotted.

coronal light near the solar limb, viz. about 98 per cent, we see is simply sunlight from the photosphere which has been scattered off by the electrons in the corona towards our line-of-sight This component is known as K-corona. Since the density of the corona is extremely small, almost all of the sunlight escapes without being scattered. However, about one out of every million photons leaving the Sun does strike an electron in the corona and is scattered; some of these reach us and can be detected during a total eclipse or by coronagraphs or space telescopes. The brightness measurements yield a value of about 10^8 per cc for the electron density in the low corona. The rate at which the electron density drops off can be used to estimate the average temperature of solar corona. The computed value of density drop-off shows that the coronal temperature must be over 1,000,000 K (Van de Hulst, 1953). The results obtained by Sivaraman *et al.* (1985) from the data obtained at the 1980 and 1983 eclipses agree with those of Van de Hulst. About one per cent of the coronal intensity near the solar limb is due to the forbidden transitions in the highly ionized atoms in the corona. This component is called as E-corona. The rate of fall in the intensity with solar radii due to E-corona is similar to that in the K-corona. The contribution due to E-corona becomes negligible at 2 solar radii. The remaining part of coronal intensity near the limb, about 1 per cent, comes from the scattering of photospheric light by heavier particles. The rate of drop in intensity due to F-corona is not as rapid as that due to E and K-corona. Newkirk (1961) developed a detailed model for the electron density with solar radii for Quiet, Polar and Active regions in the solar corona.

Spectroscopy of solar corona

The bright crescent of the chromosphere, just before the totality, produces an emission line spectrum called 'flash' spectrum. Strongest among these is H_α, the red emission line that gives the chromosphere its characteristic colour and its name The crescent images of the chromosphere may last for several tens of seconds, as the Moon's limb gradually covers up the 10000 km thickness of the chromosphere However, there are a few other emission lines which do not vanish but remain visible even long after the Moon has completely blotted out the chromospheric emission. These are different spectral lines not seen in the chromospheric spectrum at all and at the time of their discovery in eclipse spectra, they had not been seen anywhere else. Brightest of these lines are a green line at 5303 Å, a red line at 6374 Å, and occasionally a yellow line at 5694 Å. The Swedish physicist Edlen (1942) showed that thirteen-times ionized iron atom would emit radiation at 5303 Å wavelength of the green line and coronal red line at 6374 Å could be produced by Fe X ion. A detailed list of observed coronal lines and their identification in the visible wavelength region was compiled by Jefferies *et al.* (1971). The flight of a rocket spectrograph into the eclipse path in 7 March 1970 (Speer *et al.*, 1970) permitted the recording of 28 coronal lines between 977 Å and 2200 Å. Jordan (1971) identified 20 of these lines with forbidden transitions between common coronal ions. A weak continuum has also been detected along with these emission lines. Because of its million-degree temperature, corona is a plasma of electrons, protons and some heavier ions. The continuous emission at the low coronal densities is negligible as compared to the photosphere except for the radio region. Therefore, the continuous spectrum is dominated by Thomson scattering of the bright photospheric emission by free electrons. The continuum observed consists of two components : the K-corona, which is polarised and free of absorption lines due to high thermal random velocity of free electrons, and the F-corona, which is unpolarized and shows all the Fraunhofer absorption lines of the photospheric spectrum. The F-corona component has nothing to do with the solar atmospheres as it is simply the sunlight diffracted by solid particles between the Sun and Earth in the plane of ecliptic. The absorption lines remain visible in the diffracted spectrum because the particles are heavy and slow moving.

Bappu *et al.* (1972) obtained a low dispersion spectrum of the solar corona during the eclipse of 7 March 1970 at Mexico, covering spectral range of 3400 - 7600 Å. Their analysis of the intensities of the emission lines of the Balmer series, D_3 and calcium H and K lines indicated that there exist cool columns of gases embedded in the hot corona. High resolution multislit-spectra were obtained by Livingston and Harvey (1982) at four eclipses between 1970 and 1983 to study the flow of gases in the polar region of the solar corona. Singh *et al.* (1982) have used the multislit technique to record coronal spectra (Fig.5) and studied the temperature and velocity structure of the solar corona. Singh *et al.* (1982) conclude that corona does not show any localized differential mass motions and that it co-rotates with the photospheric layers deeper down. On the other hand, Raju *et al.* (1993) interpret their 1980 eclipse

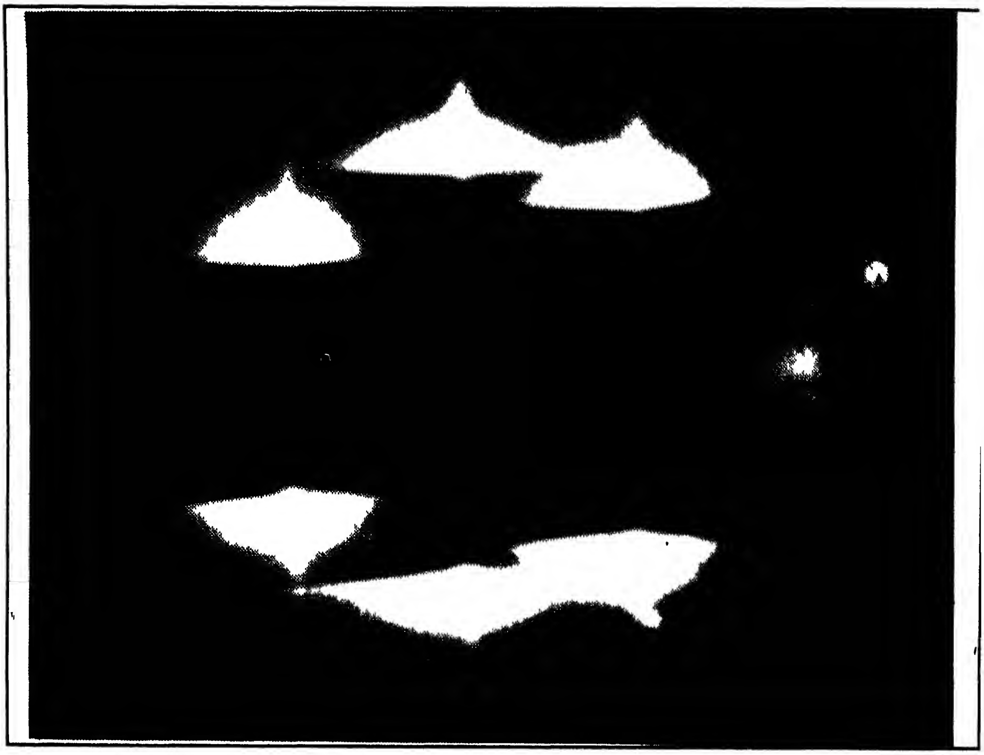

Fig 5 High-resolution spectra of 6374A (Fe X) coronal emission line obtained at the total solar eclipse of 16 February 1980 from Jawalgera, India, with the multislit spectrograph. (Courtesy: Indian Institute of Astrophysics, Bangalore)

data in terms of large scale systematic mass motions in the corona. Further, Singh (1985) shows that for R/R⊙ < 1.2, collisional excitation is the predominant mode. Collisional as well as radiative excitation is equally important for 1.2 <R/R < 1.4, whereas beyond 1.4 R ⊙ radiative excitation becomes dominant.

Temperature and heating of solar corona

It took a long time of 70 years to identify the green coronal line after its initial discovery by C A. Young in 1869. Following Germany's Walter Grotraian's suggestion, Swedish astronomer Bengt Edlen (1942) showed that ordinary elements such as iron, calcium and nickel emitted coronal lines but under conditions never before witnessed in any object. The radiations in these lines came from atoms that had a large number of electrons stripped away. In the case of the green coronal line, 13 out of 26 electrons of an iron atom have been removed. Edlen realized that the highly ionized state of atoms can only occur if the coronal gas is extremely hot, a million degrees or more. With Edlen's discovery, it became clear that all of the unusual characteristics of the corona and its spectrum were caused by its high temperature. Raju and Singh (1987) have computed ratios of the line flux to the square of continuum flux for green and red lines at different coronal temperatures. The comparison of computed values with those observed for Fe X (6374 Å) line in the 1980 eclipse indicated the temperature of corona to be 1.6×10^6 K. The

temperature profile of outer layers of the solar atmosphere can be seen in Fig.6 with the transition to coronal temperatures confined to a few hundred kilometres. What could cause the temperature of the Sun, after decreasing smoothly from the core to the surface, to reverse its decline above the surface and rise once again above the million-degree mark? In other words, what heats the corona?

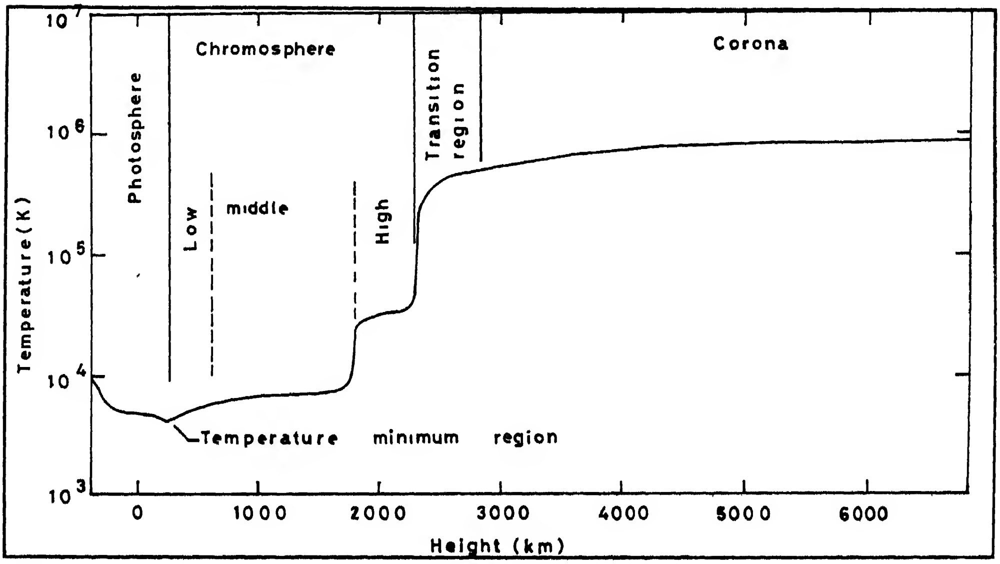

Fig 6 Variation of average temperature with height in the solar chromosphere, transition region and corona.

The photosphere has a temperature of roughly 6000 K, which is nowhere near the million degree of the corona. Thus, the Sun cannot simply transfer heat from the cooler photosphere to the hotter corona. The Sun needs some additional mechanism to concentrate the heat that escapes into the corona and to boost the temperature of the corona to a million degrees. Many theories have been proposed to explain this rise in temperature. Schwarzchild (1948) and Biermann (1948) pointed out that the turbulent kinetic motions of the granulation must generate violent shock waves in the solar atmosphere but the observations obtained from the space ruled out the existence of shock waves in the corona. Gokhale (1975) suggested that release of energy through X-ray bright points can play an important role in heating the solar corona. Generation of MHD waves by thermal overstability of surface MHD waves was considered as a possible source of waves to heat the corona by Joarder *et al.* (1987). Ruling out all the other possibilities, theorists and observers together have established that Sun's magnetic field plays a crucial role in the formation and heating of the corona. The active corona contains mostly loop-shaped features that form above active region in the photosphere and arch along the magnetic fields as they rise above the active region. Coronal loops appear hot and bright and emit strongly in X-ray (Golub, 1993). Observations show that active corona and strong magnetic fields are related, but the slow-changing magnetic field cannot explain the observed rapid variation of X-ray emission in coronal loops. High resolution X-ray and magnetic observations suggest that both magnetic and turbulent processes structure and heat the corona (Golub, 1993).

Coronal holes and solar wind

The first suggestion of significance of coronal holes came from studies in geomagnetism. Chapman and Bartels (1940) postulated the existence of 'M-region' on the Sun as source of geomagnetic disturbances with a marked 27-day recurrence. The first indication that regions of low coronal density might affect the Earth was the discovery by Bell and Glaser (1954) that peaks of geomagnetic activity were preceded a few days earlier by the central meridian passage of a minimum in green line emission observed at the east limb with coronagraphs. The existence of coronal holes was confirmed from the soft X-ray images obtained by skylab mission. In one of such pictures (Fig.7) obtained from a rocket-borne telescope, one can see an enormous dark region, covering more than half of the Sun. The low density of the gas makes this part of the corona appear dark as if there were a hole in the corona. The hole is created by a large region of weak magnetic field of single polarity that opens into the corona and extends out in space Particles from the Sun stream along the open magnetic field to form the high-speed part of the solar wind. Coronal holes form

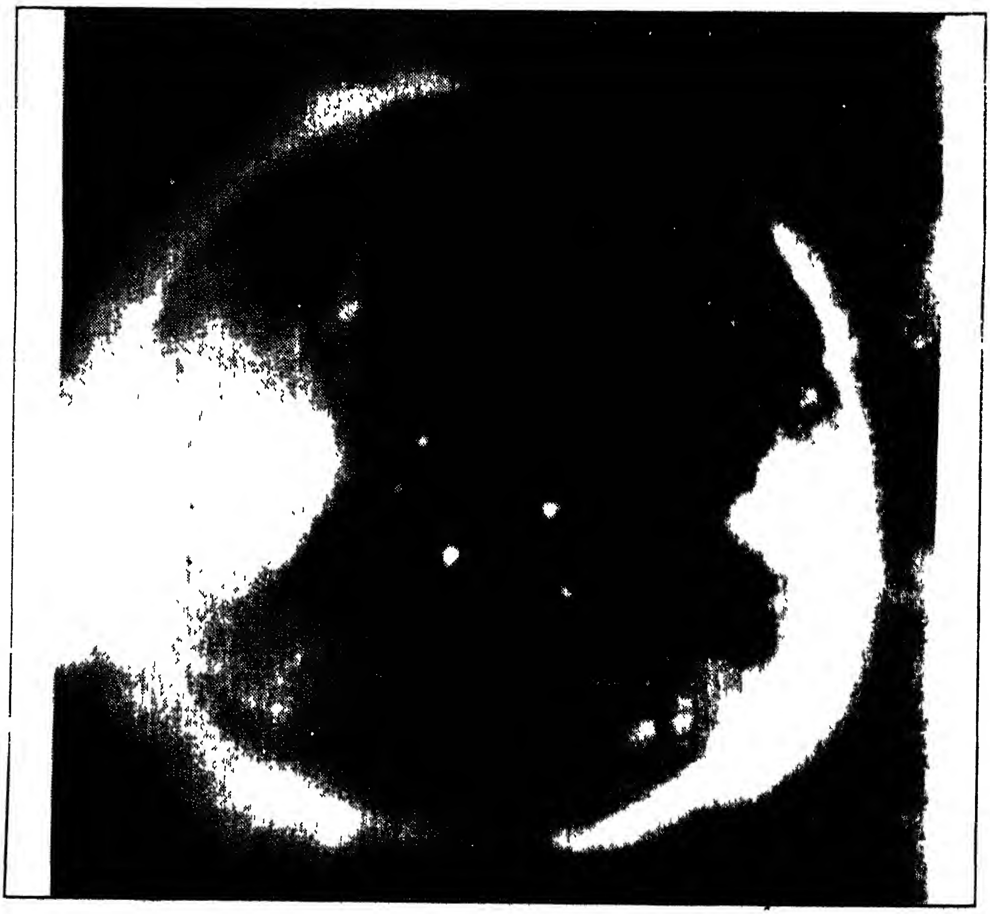

Fig 7 X-ray image of the Sun, obtained from a rocket – borne X-ray telescope on 27 June 1974 by John Davis, American Science and Engineering Co , shows a large size coronal hole, a dark region of very low coronal emission The bright points are tiny dipoles, spotless active regions called X-ray bright points.

during the evolution of active regions. Two magnetic polarities move apart as the active region evolves. One polarity moves towards the equator where it disappears. The other slowly migrates towards the nearest pole of the Sun and before it reaches the pole, the magnetic field from this large single polarity opens into space, forming a coronal hole.

Observation of comets showed sudden changes and gap in their tails. Biermann (1951) proposed the existence of a particle outflow from the Sun to explain the excess ionization and abrupt changes in the outflow of material in the comet tail. Parker (1958) showed that in the case of 'solar wind' particle outflow velocity is very small near the Sun and difficult to detect. The velocity increases with increasing distance from the Sun and becomes supersonic at a 'critical point' located at a distance of about 5 solar radii above the surface of the Sun. The computations indicated that the speed of solar wind would be several hundred kilometres per second at the distance of the Earth's orbit. This was confirmed when coronal outflow was detected by satellites and recorded particle outflow velocities of about 300 km per second in the interplanetary space near the Earth.

Nolte *et al.* (1976) showed that coronal holes coincide with the high velocity streams in the solar wind and they produce recurring geomagnetic disturbances known as M-regions. The direct connection of field lines to the solar wind permits these high speeds. Sheeley and Harvey (1980) showed the relation between the position of coronal holes, the interplanetary field direction, the solar wind speed and the magnitude of disturbances in the Earth's field. From the analysis of interplanetary plasma database compiled from near-Earth spacecraft measurements, Sastri (1987) showed the relevance of subsonic coronal processes to the low speed solar wind at 1 AU.

Coronal mass ejections

Coronal mass ejections (CME) were discovered from the photographs of the outer corona obtained by externally occulted coronagraph developed by High Altitude Observatory (HAO) and put into space on skylab and Solar Maximum Mission (SMM). Similar observations were also obtained using Solwind coronagraph of Naval Research Laboratory on the P78-1 spacecraft. The CME is seen in Fig. 8, as a great eruptive loop far above the surface of the Sun, moving outward with a great speed of 400-700 km/s. From these observations, Wagner (1984) and Howard *et al.* (1982) concluded that CME must be three-dimensional bubbles projected against the sky, and the material, directed at the Earth, appears as a bright halo around the Sun. Howard *et al.* concluded that the eruption is constrained near its base, expanding outward near the top as a cone. Wagner finds that CME occur at the average of 0.74 per day near the minimum and at 0.9 per day near the maximum phase of the solar cycle. These numbers should be doubled to take into account the events happening behind the solar disc. Sheeley *et al.* (1982) found the rate of CME to be about 2 per day with the Solwind data. About half the CME are related to flares and

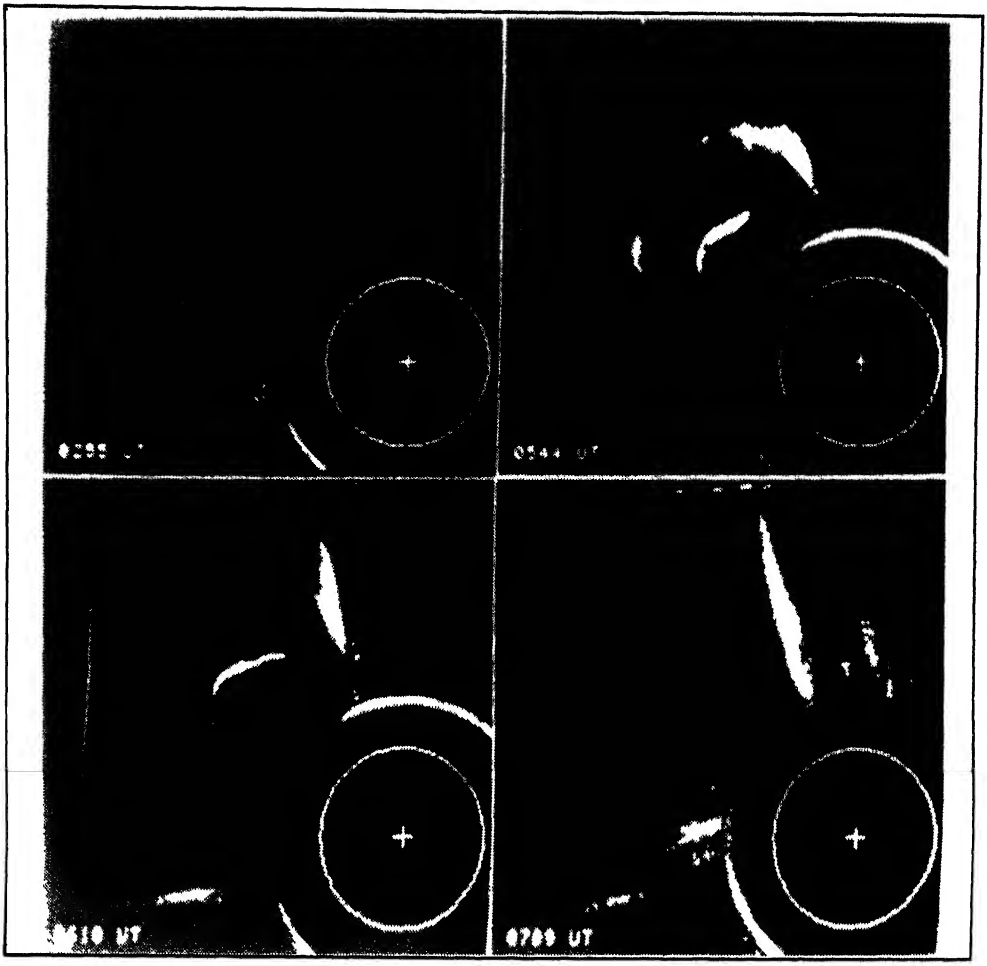

Fig.8 A coronal mass ejection (CME) or coronal transient observed by the Solar Maximum Mission coronagraph of High Altitude Observatory.

the rest to erupting prominences. In both cases, the phenomenon is associated with instabilities in the magnetic field structure. The CME accelerate as they move outward. A number of examples of MHD phenomena running ahead of the CME, including enhanced mass forerunners, pressure waves and rarefactions have been observed. Jackson (1981) reported increase in brightness in the K-corona a few hours before the CME. These data suggest that the eruption is not an explosion but a transformation of the entire magnetic structure.

Radio emission from solar corona

The corona is the main source of solar radio emission at $\lambda > 10$ cm and can be observed directly at these long wavelengths. Variation in brightness with frequency may be interpreted as variation of temperature with height. Systematic and extensive studies since 1946 have shown that radio emission from the Sun has three components, originating from the quiet Sun, from bright regions and from

transient disturbances such as flares. The radiations from quiet regions are due to thermal emission from the overlying layers of the solar corona and this component remains at a constant level for months together. The observations of the quiet Sun component have confirmed the high kinetic temperature of the corona, the rapid transition between the chromosphere and the corona, and the variation of coronal electron density with the solar activity cycle. The radiations from bright regions, slowly varying component, originate from the corona overlying the active regions on the Sun called 'condensations' and vary with a period of 27 days, rotation period of the Sun. High resolution observations made simultaneously over a wide range of wavelengths have indicated high density and brightness temperature of about 2×10^6 K in these regions of the corona. The strong magnetic field at the photospheric level plays an important role in the generation of intense radiations from these regions at short centimetre wavelengths. The third component, radio burst, generally associated with solar activity, originates from all levels of the solar atmosphere. Radiations associated with activity in millimetre and centimetre wavelength range are emitted from lower chromosphere, and metre and decametre waves from the outer corona up to several solar radii. It has also been seen that chromospheric structures influence the millimetre and centimetre radiations emitted from the overlying solar atmosphere, while the emission at metre wavelength is affected by the coronal streamers and coronal holes (cf Furšt, 1980). Monitoring of radio emission of the Sun was started in India in 1952 at Kodaikanal Observatory with a radio telescope operating at 100 MHz. From the measured values of slowly varying component of solar radio emission at decametre wavelengths during quiet phase of the Sun, Sastry *et al.* (1981) show that brightness temperatures vary within the limits of 0.3×10^6 to 1.5×10^6 K, and the average half power width of brightness temperature distribution on the Sun is about 3 R. They also show that thermal emission from the dense coronal regions can account for the observed brightness temperatures and half power widths. The world's largest radio telescope, called 'Giant Metrewave Radio Telescope', comprising 30 parabolic dishes, each 45 m in diameter, being installed near Pune to investigate primarily the origin of the universe will also be used to obtain high resolution images of the Sun.

Coronal studies with coronagraphs and from space

With the invention of a coronagraph by Bernard Lyot in 1930, it became possible to study corona even without the occurrence of a total solar eclipse. One can determine only the gross structure of corona and of emission corona using narrow band filters centred on the coronal emission lines. It is difficult to obtain information about the finer details of the solar corona and especially of the middle and outer corona using coronagraph and the best possible location on the surface of the Earth. Daily observations of corona made with coronagraphs, e.g. at Pic-du-Midi, Sac Peak, High Altitude Observatory have helped in understanding the relationship in magnetic structures at the photosphere and streamers in the corona, and the dynamics of the solar corona.

The coronagraphs and total solar eclipses permit us to study the corona above the solar limb only. It is not possible to see the corona against disc in the visible wavelength region because background light from the Sun is much stronger than the coronal emission. We know that most of the emission from the hot corona is concentrated in the extreme ultraviolet (EUV) and X-rays wavelength region and the Sun is not a good emitter at these wavelengths. Therefore, by making observations in EUV and X-rays, one will be able to study the corona against the solar disc, but the atmosphere of the Earth does not permit these radiations to reach at the surface of the Earth. Hence, one needs to put up the telescope in space above the atmosphere of the Earth to observe in EUV and X-rays. The age of space astronomy began on 10 October 1946 when a captured World War II German V-2 rocket was launched by American scientists from New Mexico The far ultraviolet spectrum of the Sun was recorded for the first time. It is interesting to note that Saha in (1937a) pointed out the practical feasibility of having a Stratosphere Solar Observatory for obtaining knowledge of the solar spectrum at the ultraviolet wavelengths, in particular the Lyman-alpha (1216 Å) line of hydrogen. Saha (1937b) also pointed out that the solar UV emission could not be of photospheric origin. Lyman-alpha line of hydrogen could be photographed for the first time on 12 December 1952 and found to be in emission (Tousey, 1963). The use of rockets permitted observations only for short duration of a few minutes. With the development of space satellites, a series of Orbiting Solar Observatories (OSO) were launched in the early 1960s which carried out solar observations from space until 1979. A number of telescopes capable of taking photographs and spectra of the Sun in EUV and X-rays were put into space e.g. Skylab, SMM, YOHKOH and others. These observations have helped in discovering coronal holes and coronal mass ejections apart from providing a large amount of information about other coronal features. Scientists at Indian Institute of Astrophysics, Bangalore in collaboration with US and European scientists have built a telescope to study the Sun in EUV radiations (Timothy *et al.*, 1990). This is scheduled to be launched by the end of 1994 using the NASA rocket. The data obtained will help in understanding the physical characteristics and dynamics of coronal bright points.

Current status

The studies of solar corona have already helped in uncovering why some stars have corona and others do not. But in spite of the fact that a large body of data is available from a number of eclipses, coronagraphs and space telescopes, the physical and dynamical processes in the corona and heating of the solar corona are not fully understood yet. Still there are controversies about the temperature, structure, turbulence, large-scale systematic mass motions, location of temperature maximum and short period intensity oscillations in the solar corona. The definitive answer to the above-mentioned parameters will help in understanding the heating and realistic modelling of the corona and especially coronal structures and the factors that contribute to the solar wind-flow. To find answers to some of the above-mentioned problems, scientists at the Indian Institute of Astrophysics have already finalized

plans to conduct three experiments: (i) High resolution multislit spectroscopy of solar corona in two emission lines simultaneously, (ii) Narrow band photometry in 6 emission lines with low spatial resolution, and (iii) Narrow band photometry in 2 emission lines with high spatial resolution, during the coming total solar eclipses of 3 November 1994 and 24 October 1995 The ratios of line intensities give the temperature at a given location in the corona and the excess in observed line width over the thermal width gives the strength of turbulence at that location. Correlation of temperature and turbulence with position on the corona, and comparison of these quantities in 'open'and 'closed' coronal structures will tell us about the role of turbulence in the heating of these coronal structures.

REFERENCES

Bappu, M K V , Bhattacharyya, J C & Sivaraman, K R. (1972) *Solar Phys* **26**,366

Bell, B & Glaser, H (1954) *J Geophys. Res.* **59**, 551

Biermann, L. (1948) *Z Astrophys.* **2**, 161

Biermann, L (1951) *Z Astrophys* **29**, 274

Bruning, D., (1992) *Astronomy*, **20** (1), 48

Chapman, S & Bartels, J , (1940). *Geomagnetism*, (Oxford Univ Press, Oxford)

Edlen, B , (1942). *Z Astrophys* , **22**, 30

Furst, E (1980). (eds Kundu M R and Gergely, T E.) Radio Physics of the Sun, IAU Symposium **86, 5**

Gokhale, M H , (1975) *Solar Phys* , **41**, 381

Golub, L., (1993). *Astronomy*, **21** (5), 28.

Howard, R.A., Michels, D.J., Sheeley, Jr N.R. & Koomen, M.J., (1982). *Astrophys. J Lett.*, **263** L101.

Jackson, B.V., (1981). *Solar Phys.*, **73**, 133.

Jefferies, J.T , Orrall, F.Q. & Zirker, J.B , (1971) *Solar Phys.*, **16**, 103.

Joarder, P.S , Gokhale, M.H and Venkatakrishnan, P , (1987). *Solar Phys* , **110**, 255.

Jordan, C., (1971). *Solar Phys* , **21**, 381.

Livingston, W. & Harvey, J. (1982). *Proc Indian Natl. Sci. Acad.*, **48A**, Suppl No.3, p.18

Malin, D.F., (1977). *AAS Photo-Bull*, No.**16**, 10.

Mitchell, S.A. (1935) *Eclipses of the Sun* (Columbia Univ.Press).

Newkirk, G.A. (1961). *Astrophys J.* **133**, 983

Newkirk, G.A. & Altschuler, M , (1970) *Solar Phys* , **13**, 131

Nolte, J.T , Krieger, A S., Timothy, A F , Gold, R E., Roelof, E.C , Vaina, G., Lazarus, A.J., Sullivan, J.D. & McIntosh, P.S , (1976). *Solar Phys* , **46**, 303

Parker, E.N., (1958). *Astrophys. J.* **128**, 669.

Raju, K.P., Desai, J.N., Chandrasekhar, T & Ashok, N M., (1993). *Mon.Not. R Astron. Soc* , **263**,789

Raju, K.P & Singh, J , (1987) *Solar Phys* , **110**, 271.

Saha, M N., (1937). *Bull. Harvard Coll. Obs.*, **905**

Saha, M.N., (1937b). *Proc R Soc.*, **A 160**.55

Sastry, Ch.V., Dwarkanath, K S., Shevgaonkar, R.K. & Krishan, V , (1981) *Solar Phys.*, **73**, 363

Sastri. J.H., (1987). *Solar Phys.*, **111**, 429.

Scaria, K.K., (1983). *Solar Phys.*, **85**, 235.

Schwarzschild, M., (1948). *Astrophys. J.*, **107**, 1.

Sheeley, Jr.N.R. & Harvey, J.W., (1980). *Solar Phys.*, **70**, 237.

Sheeley, Jr. N.R., Howard, R.A., Koomen, M.J., Michels, D.J., Harveey, K.L. & Harvey, J.W., (1982). *Space. Sci. Rev.*, **33**, 219.

Singh, J., Bappu, M.K.V. & Saxena. A.K., (1982). *J.Astrophys. Astron.*, **3**, 249.

Singh, J., (1985), *Solar Phys.*, **95**, 253.

Sivaraman, K.R., Singh, J., Kapoor, R.C. & Kariyappa, R., (1985). *Kodaikanal Obs.Bull.*, **5**, 51.

Speer, R.J., Garton, W.R.S., Morgan, J.F., Nicholls, R.W., Goldberg, L., Parkinson, W.H., Reeves, E.M., Jones, T.J.L., Paxton, H.J.B., Shenton, D.B. & Wilson, R., (1970). *Nature*, **226**, 249.

Timothy, J.G., Berger, T.E., Morgan, J.S., Walker, Jr. A.B.C., Bhattacharyya, J.C., Jain, S.K., Saxena, A.K., Huber, M.C.E., Tondello, G. & Naletto, G. (1990). *SPIE*, **1343**, 350.

Tousey, R., (1963). *Space Sci. Rev.*, **2**, 3.

Van de Hulst, H.C. (1953). *The Sun*, Edited by Kuiper, G.P., Univ of Chicago, Chicago.

Wagner, W., (1984). *Ann. Rev.Astron. Astrophys.*, **22**, 267.

THE INTERPLANETARY MEDIUM

S.K Alurkar*

INTRODUCTION

Extensive research over the last four decades has immensely contributed to our understanding of the interplanetary medium (IPM). At the beginning of this time-span, the understanding was that the changes in the Sun's output of waves and particle radiations produced the Earth's ionosphere by photoionization and magnetic storms and aurorae by streams of charged particles. The solar magnetic field, on the one hand, was thought to confine the solar plasma to the photosphere. On the other hand, the geomagnetic field enclosed the Earth's ionosphere, leaving the intermediate space or the interplanetary space nearly a huge void.

This situation was substantially changed in the late 1950s with the development of the magnetohydrodynamic theory, according to which the solar wind emanates from the lower corona, accelerating up to about 20 solar radii, and then steadily increasing its expansion rate to a supersonic speed of typically 400 km/s. The solar wind speed remains supersonic throughout the IPM.

Although the solar wind carries away from the Sun a small fraction (about 10^{-9} or less) of its energy, the particle flux, during disturbed condition, produces major effects on the Earth's atmosphere. The hot tenuous coronal plasma has very high thermal and electrical conductivity, so that the solar magnetic field is frozen in the plasma and is therefore dragged into the interplanetary space. The solar wind ultimately slows down to subsonic speed far beyond the minor planets where it encounters a shockfront at the boundary with the interplanetary gas. Beyond this shockfront the subsonic wind and the gas reach another boundary (heliopause) with interstellar medium. This huge volume up to the heliopause is called "heliosphere".

The Interplanetary Medium

The Sun-Earth environment is but a small part of the heliosphere, which has been formed by the radially outflowing solar wind plasma and its interaction with the

* *Physical Research Laboratory, Ahmedabad 380 009*

interstellar medium. It flows past the solar system up to the distance where its radiation pressure is balanced by the pressure of the interstellar gas and magnetic field.

Most of the physical phenomena which occur in the heliosphere are strongly influenced by the solar wind The study of the physics of the three-dimensional heliosphere is basic to the understanding of the solar-terrestrial relationship. In space research the solar wind is a common factor for the study of solar, geophysical, astronomical and plasma processes.

The belief that the interplanetary space was a vacuum was proved wrong in the early 1950s when two observational evidences were obtained for the continuous presence of an interplanetary gas. Observations made on cometary ion-tails, oriented in the anti-solar direction, indicated unaccountably high acceleration of the molecules in the tails. According to Biermann (1951) this and the ionization of the molecules was a result of the interaction with interplanetary background of ions continuously and radially outflowing from the Sun. The ion flux density required was estimated to be about 10^{10} ions/cm^{2}sec, which is two orders of magnitude higher than that measured directly. Similarly, zodaical light intensity and polarization observations of Behr and Siedentopf (1953), which were attributed to the scattering by electrons with a density of about 10^3/cm^3, were later interpreted as due to scattering of sunlight by particulate matter. The *in situ* measurements yielded electron density lower by two orders of magnitude than that estimated on the basis of electron scattering.

A great success in this direction was achieved when Parker (1958, 1963) presented a new hydrodynamic theory for a fast, continuously expanding solar corona, instead of a static, conducting corona (Chapman, 1957). He worked out for equations of motion solutions relevant to a steady hydrodynamic expansion of the corona or what he called "Solar Wind".

The hot coronal plasma, with its very high thermal and electrical conductivity, carries "frozen-in" solar magnetic field lines into the interplanetary space. As a result of the solar rotation (period 27 days for an Earth-based observer), the field lines are drawn out, by the radially flowing solar plasma, in the form of Archimedian spirals with constant heliographic latitude (Fig. 1), making an angle of ~ 45° at the Earth.

This spiral structure of the interplanetary magnetic field (IMF) is maintained throughout a solar cycle, except with opposite polarities in the northern and southern hemispheres. The polarity of the fields changes during alternate solar cycle, thus resulting in a 22-year magnetic cycle. Passing through the opposite polarity fields is a thin current sheet situated nearly in the equatorial plane of the Sun. This neutral sheet has warps whose amplitude reaches 15-20° on either side of the equatorial plane (Fig. 2).

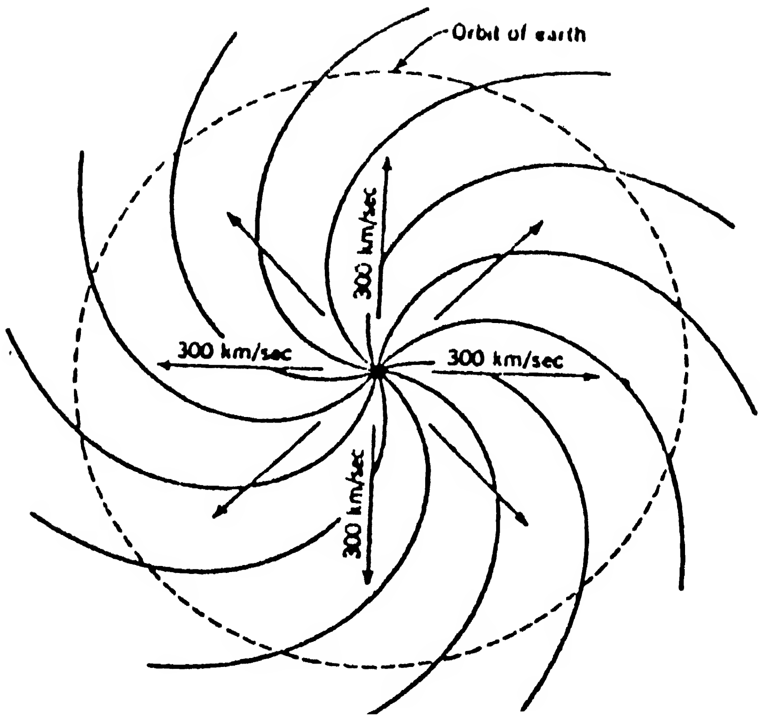

Fig. 1 Sketch of the Archimedian spiral of IMF resulting from solar rotation

The current sheet and the associated stream structures vary with helio-longitudes or in the east-west direction. Crossing the heliospheric current sheet (HCS) one comes across sector boundaries, which divide two high-speed regions with oppositely directed magnetic field lines (Wilcox & Ness, 1965). The rotating Sun is emitting high-speed streams, which are observed in the ecliptic plane and cause the structure in the IPM. Most of these streams originate from coronal regions which are cooler than the background and are characterized by unipolar, diverging magnetic lines of force (Nolte *et al.*, 1976). They are the well known "coronal holes".

Evidence has also been gathered which indicates that the average solar wind speed depends on the heliographic latitude of the region from which it flows out. Interplanetary scintillation (IPS) of radio galaxies has provided indirect evidence of higher speed solar wind emanating from high latitude coronal regions (Kojima & Kakinuma, 1987; Rickett & Coles, 1991; Alurkar *et al.*, 1993). Spacecraft coverage of $\pm 7^{\circ}.25$ of the heliolatitude about the solar equator has also indicated enhancement

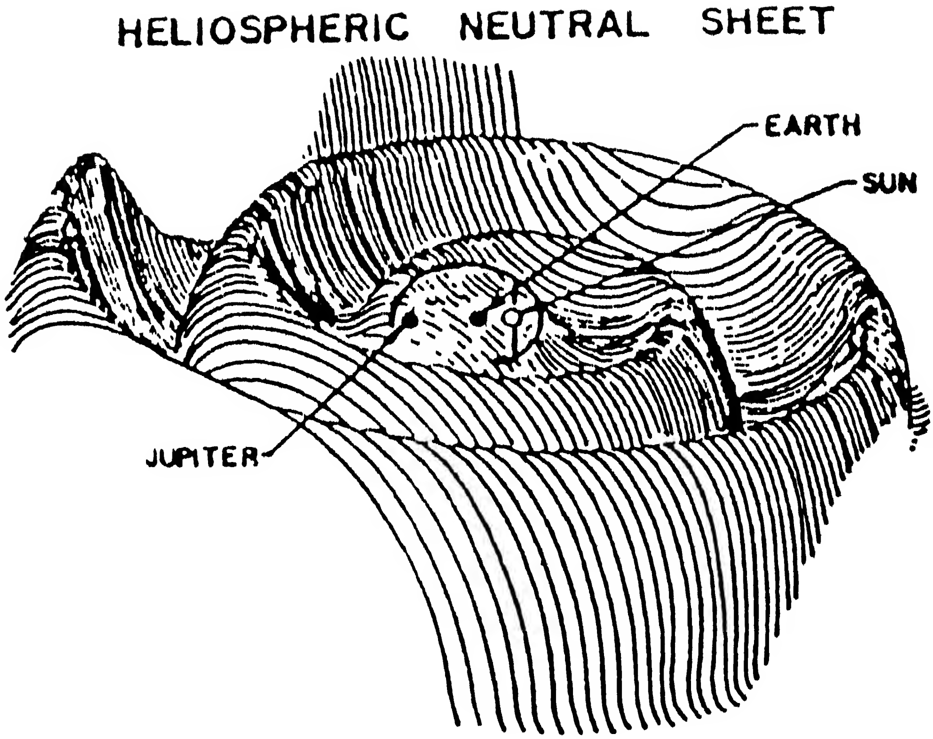

Fig. 2 Heliospheric current sheet (HCS) separates solar and IMF regions of opposite polarities.

in the solar wind speed. The "Ulyssis" mission, which will cover all the heliolatitudes from south to north poles during 1994-95, is expected to give direct evidence of the solar wind velocity gradient in latitude.

Three-dimensional view of solar corona, solar wind and solar magnetic field

Spacecraft observations in early 1960s revealed that the solar corona is highly structured with large density gradients. It is believed long that the solar magnetic field strongly controls the shape of the corona and determines the inner boundary conditions to facilitate the escape of the solar wind. The Skylab mission of the 70s convincingly showed that the solar corona and interplanetary magnetic field (IMF) exist in three dimensions (heliospheric view) and that they determine the global structure of the solar wind.

Solar corona

For a good understanding of the physical processes underlying the generation of the solar wind, a few models for the coronal magnetic field were developed. For example, Pneuman & Kopp (1971) and Endler (1971) numerically solved the MHD-equations for an isothermal coronal plasma embedded in a solar magnetic field with

the dipole field imposed on solar surface (Fig 3) The main features of these models are

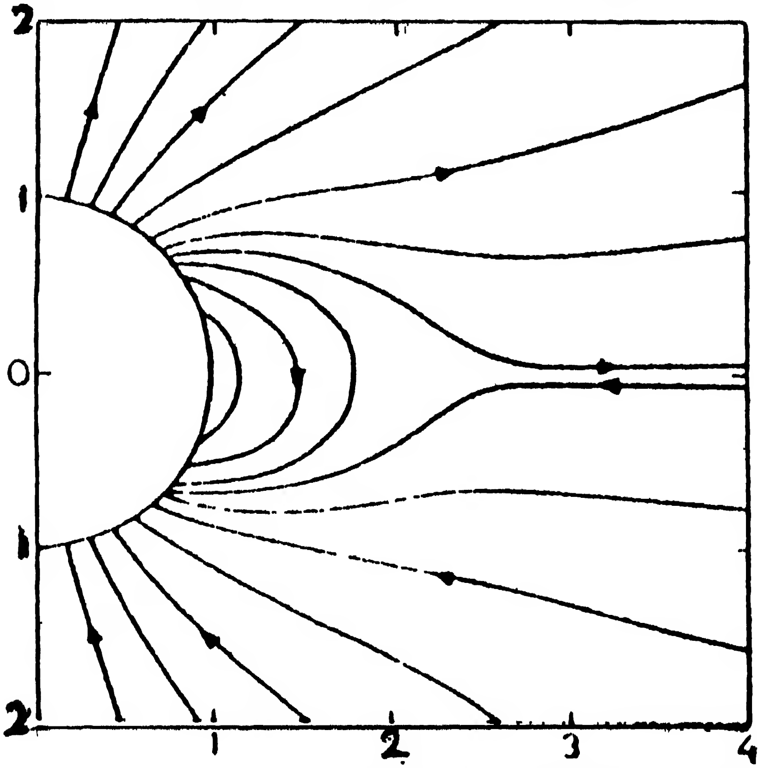

Fig 3 Model of magnetic field lines for equilibrium of an isothermal corona with a dipole magnetic field imposed at the source surface.

The streams of plasma flow coincide with the magnetic lines of force. The high pressure of the coronal plasma at high latitudes forces the field lines there to open out, whereby the plasma expands. A few closed lines appear near the equator, while a narrow belt around the equator encompasses closed field lines, hence no expansion of the plasma there. The field lines in the equatorial plane are separated by an equatorial current sheet encircling the Sun.

Another well-known model was suggested by Schatten *et al.* (1969), Altschuler & Newkirk (1969), Schatten (1976) Levine (1977) and Hoeksema (1984). Known as a "potential field model", it assumes that the expansion of the coronal plasma (solar wind) can occur by defining an outer equipotential spherical surface, called the "source surface", at which the field lines become radial. This surface is located at 2.5 radii from the Sun's centre. Large-scale magnetic structures dominate at great distances from the source surface in this model, which also enables calculation of the 3-dimensional polarity structure of the coronal magnetic field.

To identify the locations of the large-scale magnetic structures on the source surface, the IMF measured at the Earth is mapped back to the surface. This mapping-back technique was developed by Scherrer *et al.* (1977), Duvall (1977) and Hoeksema (1984). A synoptic contour map of the magnetic field at the photosphere is shown

in Fig. 4. The thick solid line (neutral line) divides the negative (dashed contours) and the positive (solid contours) polarity regions. Fig.5 shows a map of the computed radial component of solar magnetic field using photospheric field of Fig 4.

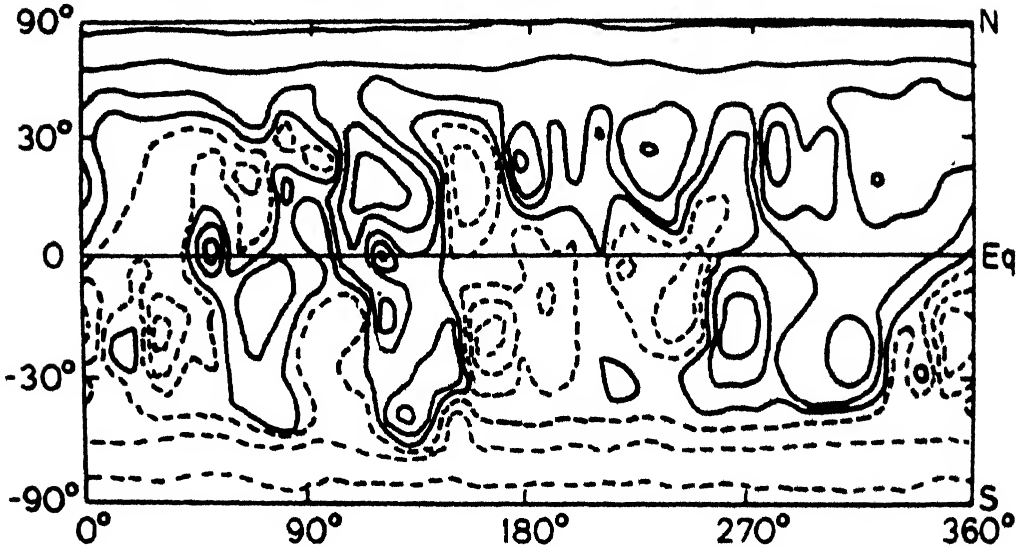

Fig. 4 Average synoptic map of line-of-sight phospheric magnetic field covering eighteen solar rotations during 5 May, 1976 to 7 August 1977. Solid lines show positive field direction away from the Sun, and dashed lines indicate negative field direction towards the Sun

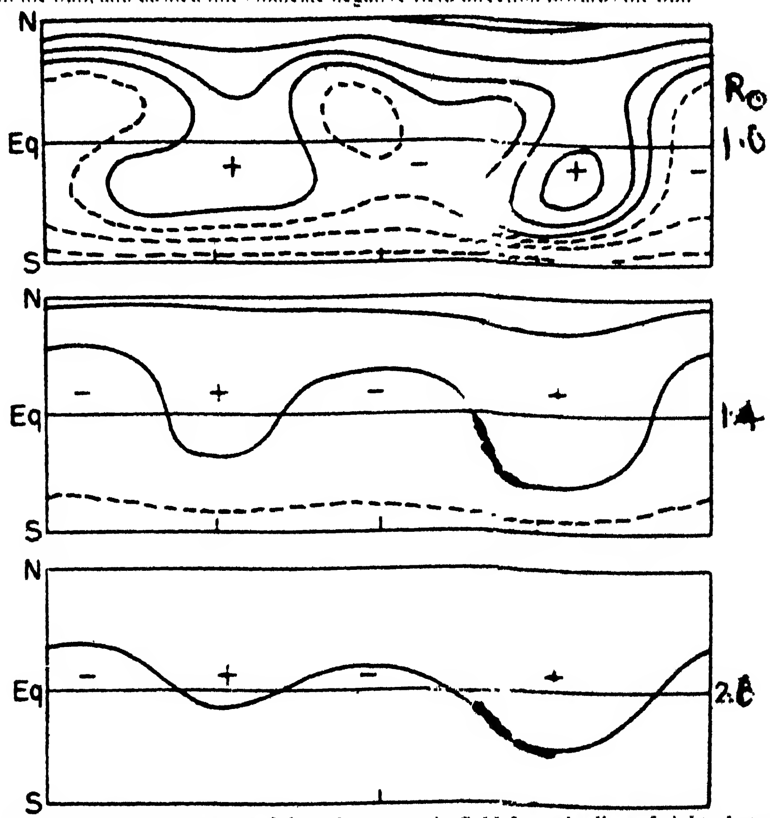

Fig 5 Computed radial component of the solar magnetic field from the line-of-sight photospheric magnetic field of Fig 4 The synoptic maps show the field on the surfaces at 1, 1.4 and 2.6 R⊙ from the Sun's centre

The IMF structure near the solar equatorial plane for a constant solar wind speed of 300 km/s is shown in Fig. 1.

The Structure of the IMF

Moving radially away from the neutral line on the source surface one encounters the warped current sheet which divides the oppositely polarized magnetic fields in the IPM. Now, the ecliptic is inclined at an angle of $\pm 7^{\circ}$ 25 with the Sun's equatorial plane; therefore, as the Sun rotates, the HCS crosses the Earth two, four or six times every solar rotation in 27 days, depending on the phase of the solar activity. Accordingly, the polarity of the IMF changes as many times, sweeping an equal number of sectors past the Earth every solar rotation (Wilcox & Ness, 1965). In the interplanetary space, however, only one sector boundary exists, and it is the heliospheric current sheet (HCS), which runs in between the opposite polarity fields (Schulz, 1973).

The sector-like structure of the photospheric magnetic field, with north-south boundaries between the polarities, causes the warps on the HCS. These warps sometimes reach 15 - 20° heliolatitudes.

Away from the Sun, these warps are depressed by the polar field to lower and lower latitudes. Fig.6 shows a sketch of a 4-sector situation of the warped HCS up to 6 AU. The solid lines show the region where the sheet bulges above the solar

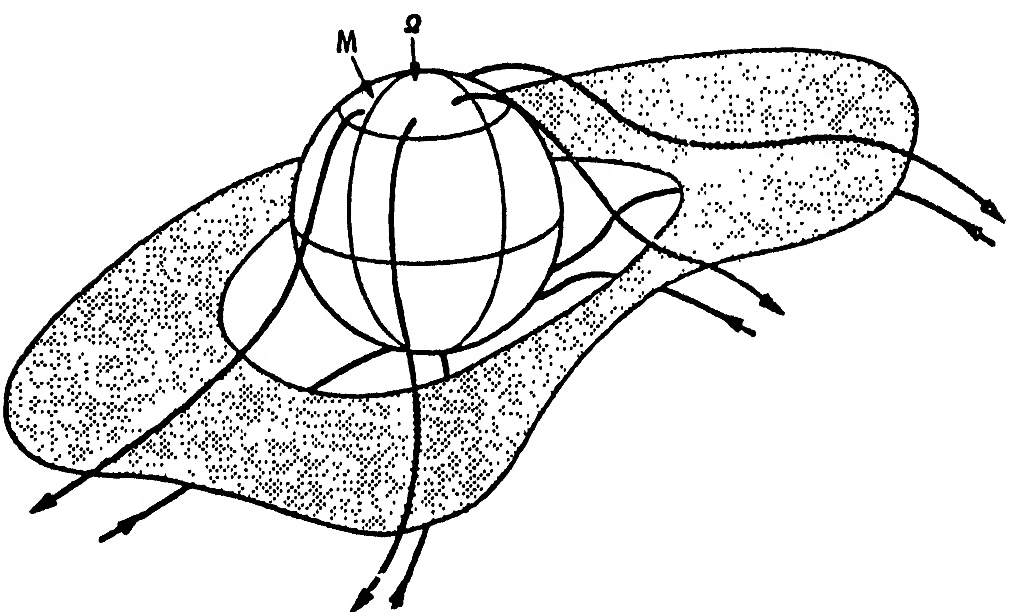

Fig. 6 HCS responsible for sector structure. The axix M of the HCS is tilted relative to the solar axis Ω

equatorial plane, while the dashed lines show where the HCS, flowing in the source surface, is depressed below the equatorial plane. This was confirmed when in February 1976 (solar minimum) pioneer 11 reached 16° north heliolatitude. For several months the magnetic field was found to be directed *away* from the Sun. (Fig.6).

It also observed a strong association between sector boundaries and large-scale coronal features, called "coronal streamers", which are visible in white light. This is observed around 1.5 radii above the solar limb using a coronagraph at 10830 Å wavelength Fe line from the K-corona (Hansen *et al.*, 1974; Howard & Koomen, 1974). The coronal streamers are believed to be emanating from the active regions with closed-loop systems. Furthermore, high-speed plasma streams were correlated with magnetic polarity of coronal holes, which were themselves associated with unipolar open-field regions (Fig. 7).

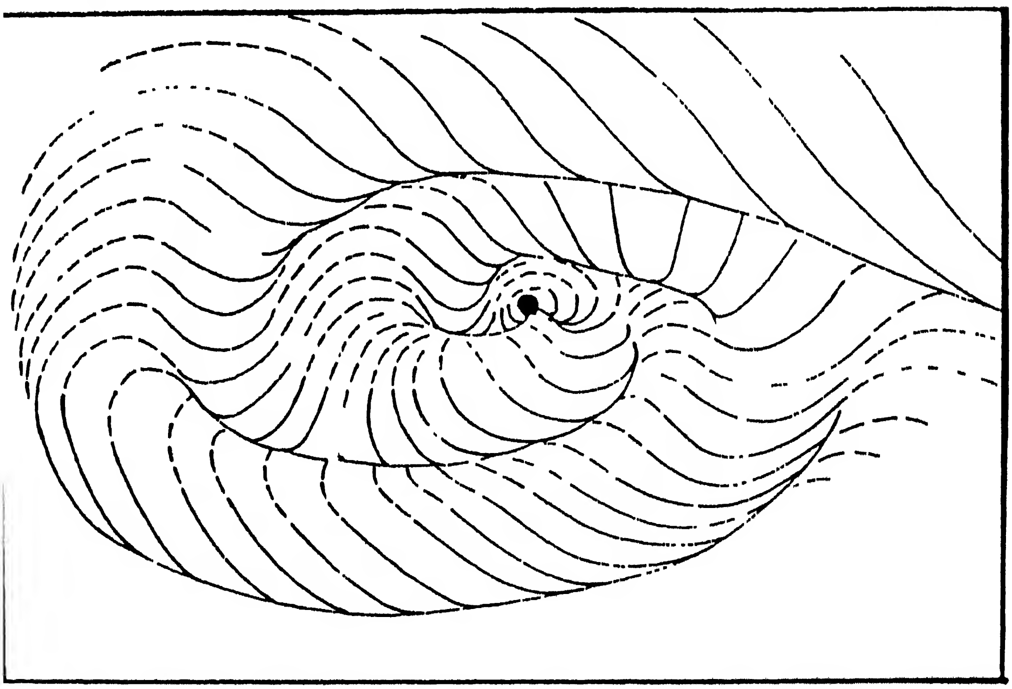

Fig. 7 Sketch of a warped HCS within 6 a u from the Sun This depicts a four-sector structure showing three-dimensional shape of a surface Solid lines show where the surface lies above the equatorial plane, while the dashed ones show where it lies below the plane. The Sun is at the centre.

These out-of-the ecliptic findings of Pioneer 11 were modelled, suggesting a heliospheric current sheet embedded in the narrow equatorial belt of coronal streamers around the Sun and inclined about 15° with the solar equatorial plane. Separating the oppositely polarised fields, the HCS perhaps extends throughout the heliosphere (Fig. 2).

Our knowledge about the interplanetary medium is greatly advanced owing to

the continuous observations at 1 AU by Mariner 2 in 1962 and by Skylab in 1973-74. The spatial and temporal variability of the solar wind confirmed the earlier view, based on eclipse observations that the corona was highly structured and underwent changes in shape over a sunspot cycle. Neugebauer & Snyder (1966) observed long-lived fast streams with a slow plasma flow in between them. Interestingly, the slow flow was considered a "quiet state" of the solar wind with its proton velocity of ~ 300 km/s, proton density of ~ 9 cm^{-3} and proton temperature of ~ 4 x 10^4K (Hundhausen, 1972). The fast flow was thought to be a "disturbed" condition of the quiet state, with values of the above quantities of 600 km/s, 3 cm^{-3} and 10^5 K (Feldman *et al.*, 1976).

This view of the solar wind was totally changed by the Skylab mission when it found that the coronal holes were located over the inactive polar cap regions of the Sun, where open field lines exist around solar minimum (Timothy *et al.*, 1975). The active regions, on the other hand, are associated with solar disturbances and bipolar magnetic loop structures. The fast wind represented the "quiet state" while the slow wind, which originated from the most active solar regions, was in fact the "disturbed state" of the solar wind (Feldman *et al.*, 1978).

These studies were made using data observed at 1 AU and beyond, leaving a wide gap of the inner heliosphere, which was bridged by the extensive observations made by the highly successful pair of spacecraft Helios 1 and 2. With the observations restricted to 1 AU and beyond, theoretical models of coronal expansion at 1 AU were produced at least for a slow solar wind (Hundhausen, 1972). But such attempts for a fast solar wind were unsuccessful (Schwenn, 1990). The Helios mission, with sophisticated plasma instruments on board, measured solar wind plasma parameters in the inner heliosphere as close to the Sun as 0.29 AU and considerably improved our understanding of several plasma processes in the heliosphere, as well as the large-scale structures of solar wind and their distribution throughout the heliosphere.

Helios 1 worked continuously from December 1974 through February 1986, while Helios 2 operated during the period 1976-80.

In an extensive review of the observational status of the large-scale structure of the IPM, based mainly on the findings of the Helios 1 and 2 missions, Schwenn (1990) draws, among others, the following conclusions:

* Approaching the solar minimum of cycle no. 20 in 1976, very large amplitude, several days wide, quasi-periodic fast streams resulting from two strong, co-rotating, high-speed streams emanating from the corona at constant heliolongitudes on opposite sides of the Sun, were observed.

* Ground-based techniques and optical observations made using Skylab instruments confirmed that coronal holes are sources of high-speed streams. This

association between coronal holes and high-speed streams was also observed when Helios 1 was at 0.3 AU from the Sun.

Latitudinal solar wind structure, which is normally impossible to derive, was studied using the Helios spacecraft. IPS observations had estimated an average latitudinal velocity gradient of about 2 km s^{-1} deg^{-1} (Coles & Rickett 1976).

Helios 1 observations with very high latitudinal and longitudinal resolutions showed that estimating long-term average gradients in a solar wind stream is meaningless. For Helios observations showed that the latitudinal boundaries, like the longitudinal ones, are narrower than 5°.

The 3-D structure of the solar wind in the heliosphere

The solar wind structure in the 3-D heliosphere must be considered in association with the magnetic field of the solar corona and IPM, since the magnetic field facilitates the coronal expansion and controls the properties of solar wind (Hundhausen, 1972).

Pioneer 11 reached 16° north heliolatitude during the solar minimum in 1976, when it observed mainly outward directed magnetic field (Smith *et al.*, 1978). A 3-D magnetic sector structure was therefore thought of by means of a "ballerina skirt" model for a heliospheric current sheet (HCS) (Alfven, 1977; Schulz, 1973; Saito, 1975). Consequently, some interesting studies were undertaken on the distribution of solar wind structure with heliomagnetic latitude.

Bruno *et al.* (1986) studied the dependence of solar wind speed structure in the IPM on the latitudinal separations from current sheet positions using the observations made by Helios 1 and 2 and IMP during 1976-77. The current sheet positions were estimated from synoptic white-light (K-coronal intensity) maps of the corona at a height of 1.75 solar radii from the limb. Fig. 8 shows that the slow wind was limited within ± 20° of the heliomagnetic latitude, and the fast wind appeared only beyond this limit during the solar minimum .

Another interesting finding relates to the narrow slow solar wind region lying between two fast-speed regions. Using superposed epoch analysis, 23 well-defined sector boundaries observed at 1 AU from IMP 6/7/8 spacecraft were studied (Gosling *et al.*, 1981) (Fig. 9). The quantities measured were proton velocity, temperature, helium abundance and density. Around the sector boundary crossing (marked 'O' on the X-axis) there is a sharp depletion in the helium abundance and an increase in the proton density. This narrow band of slow wind, high-density region of field reversals encompasses coronal streamers, which emanate from above photospheric active regions with bipolar closed-loop structures. Although correlated with one another, the mechanisms of generation of the slow flow in the sector boundaries, coronal streamers and HCS are poorly understood.

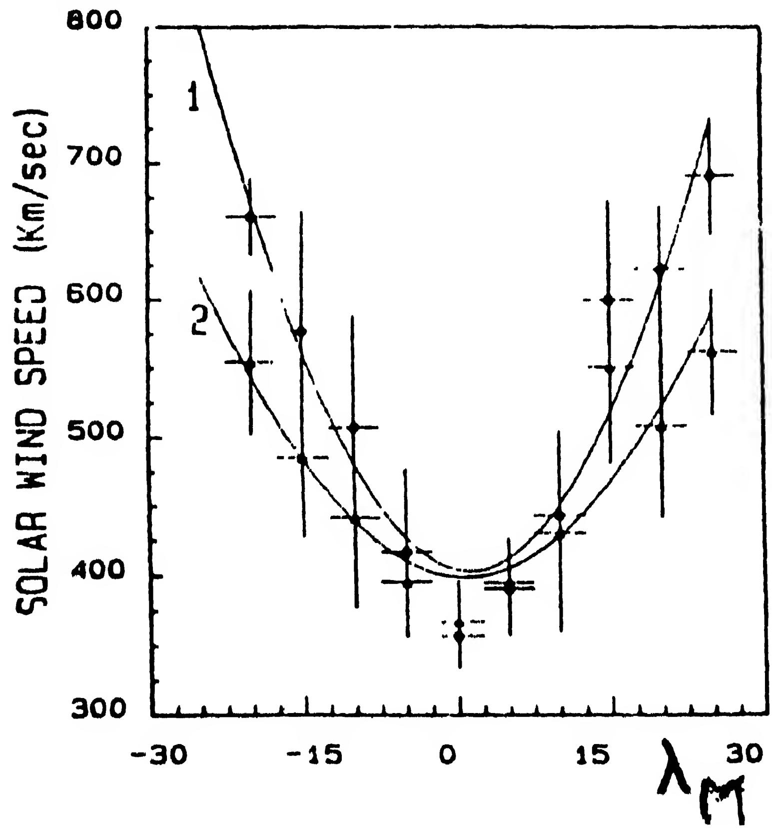

Fig. 8 Solar wind speed as a function of latitudinal separation λ M from the HCS Each data point is the average of speed values in 5° latitudinal interval Vertical bars show standard deviations in each interval. Horizontal bars are intervals of average Circles and triangles indicate data from 1976 and 1977. Solid curves 1 and 2 are best-fit lines for 1976 and 1977

It must be noted that this association between slow wind in the near-equatorial belt and low helium abundance cannot be generalised. For during solar maximum slow wind has been observed over a wide range of high heliolatitudes (Kojima & Kakinuma, 1987; Coles & Rickett, 1991; Alurkar *et al.*, 1993.) This solar wind might have been emitted from coronal regions far away from the streamers and HCS. Such a flow was found with high helium abundance (Schwenn, 1983).

There is thus a suggestion of a 3-component (fast streams, slow plasma flow near the solar equator at solar minimum and helium-rich slow wind at high latitudes at solar maximum) solar wind (Schwenn, 1990). Similarly a 3-component model for the solar magnetic field has been proposed by Axford (1977).

Associated with sector boundaries, coronal streamers and slow solar wind is another interesting phenomenon, which is transient in nature, and is known as coronal mass ejection (CME). These are a large class of events which are ejected at speeds between 100 and 400 km s^{-1} (Howard *et al.*, 1985). More work on this association would be rewarding.

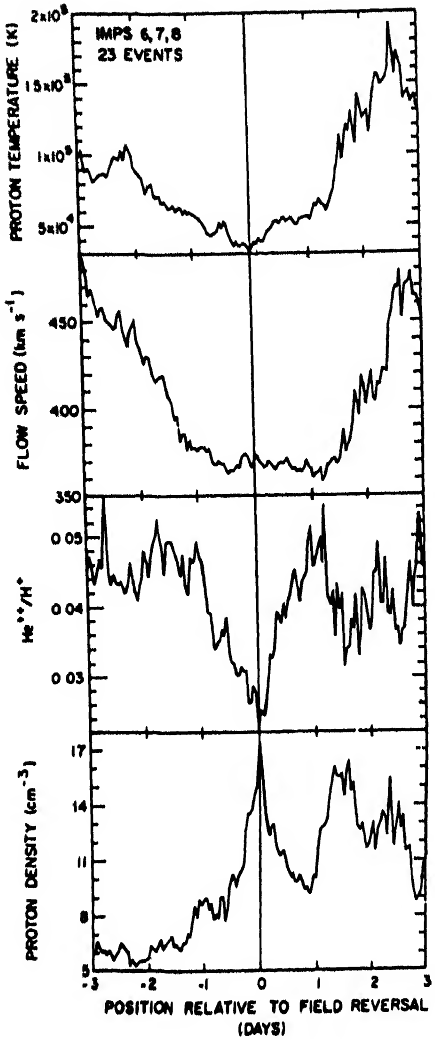

Fig. 9 Superposed epoch plots of solar wind proton temperature, speed, helium abundance and density for 23 sector boundaries one day away from speed enhancements due to high-speed streams. Pronounced minima in temperature, speed and helium abundance occurred near field reversals.

Structure of interplanetary medium through a solar cycle - Main features

In situ measurements of solar wind plasma parameters by spacecraft are so far restricted to the ecliptic, barring a few rare occasions mentioned earlier. Even then, several important results have been obtained. Slow solar wind is observed in the ecliptic plane during solar minima as well as maxima. Around maximum, helium-rich slow wind emanates from almost all heliolatitudes, whereas coronal holes with their high-speed streams disappear (Coles *et al.*, 1980; Kojima & Kakinuma, 1987; Alurkar *et al.*, 1993). At solar minimum, the heliomagnetic equator coincides with the ecliptic and the current sheet, with no warps, lies in a narrow belt of helium-poor slow wind (Nolte *et al.*, 1977). The fast wind at the same time emanates at latitudes beyond ± 20°. A few years before minimum, large coronal holes extend down to the equatorial regions and send out long-lived high-speed streams. Skylab observations a little before the solar minimum in 1976 showed that large fast streams persisted for nearly three years. A very relevant finding is the strong correlation between fast streams and recurrent geomagnetic storms (Sheeley *et al.*, 1976; Sheeley *et al.*, 1977; Sheeley & Harvey, 1981).

The character of the solar wind too changes over the poles during a solar cycle. The quiet, high-speed flow at solar minimum changes into a highly variable slow wind (Coles *et al.*, 1980; Kojima & Kakinuma, 1987). Helios found that the electron density in this flow within 0.4 AU of the Sun enhanced by a factor of two from minimum to maximum. It would be of interest to further study the plasma density and IPS velocity data together.

The issue of the effect of the solar cycle on the manifestations of the "active" corona is also being widely studied. Important among these are coronal transients and their effects on the IPM. Also, phenomena like occurrence of active centres and

emergence of new magnetic flux, prominences, CMEs, flares, radio bursts, particle acceleration, coronal and interplanetary shock waves, etc. are also very relevant for the study of solar-terrestrial relations.

CONCLUSIONS

Over the last three decades extensive observations of the interplanetary medium using both ground-based and satellite-borne techniques have enormously enriched our understanding of the inner (up to 1 AU from the Sun) heliosphere. A wealth of data on the solar wind plasma has been collected, the on-going analysis of which has already uncovered many hitherto unknown characteristics of the large-scale structures of the corona, solar magnetic field and the solar wind. Major results have come from the Helios 1 and 2 spacecraft, which could measure plasma parameters over the range from 0.29 (63 radii) to 1 AU, Also, UV and X-ray telescopes as well as sensitive coronagraphs have scanned the corona up to about 10 solar radii from the Sun. On the other hand, other deep space probes, such as the Pioneer, have reached beyond about 45 AU in the outer solar system.

The sophisticated plasma instruments on the twin Helios spacecraft and the powerful coronagraphs, UV and X-ray telescopes have helped establish strong associations among the solar wind, corona and solar magnetic field structures. This has been achieved using mapping-back on a source surface near the Sun, the measured solar wind velocity and IMF to identify their locations. Synoptic maps of the solar wind speed and magnetic field are then used for studying their behaviour through a solar cycle.

In spite of these important achievements, two most important questions about the solar wind have remained unanswered : the origin of the fast and slow solar wind, and mechanism of coronal heating.

The on-going ULYSSIS mission will be covering all the heliolatitudes between 1994 and 1995, a year near solar minimum. It might throw more light particularly on the distribution of the slow wind over the equator and fast wind over polar latitudes.

Suggestions for future work which may be done in India

Economically what is feasible for us in India is to undertake extensive observations of IPS of thousands of radio galaxies, so that a complete coverage of heliolatitudes and heliolongidutes is achieved. These observations should continue over a solar cycle High-density synoptic velocity maps will then identify on the source surface accurate, highly resolved regions of solar wind velocity structures. Lower resolution V-maps have already given encouraging results (Alurkar *et al.*, 1993). The much larger GMRT telescope, coming up near Pune, together with 103 MHz telescope at Thaltej, Ahmedabad (Alurkar *et al.*, 1989) are suitable for such

work, which has a great potential for studies on solar wind structure.

Using a grid of a couple of thousand scintillating radio galaxies around the Sun, day-to-day deviations of scintillation indices from their long-term mean have been used to define a scintillation enhancement factor, called "g" parameter. Daily g-values for all the sources are then plotted on a Sun-centred spherical coordinate system. These "g-maps" are then used to study solar disturbances travelling earthward through the IPM. This technique was pioneered at Cambridge, UK, by Hewish *et al.* (1985). Observing a large number of such events, Hewish *et al.* have concluded that these spherical shell shaped disturbances were emanated as eruptive plasma streams from mid-latitude, unstable coronal holes rather than from solar flares as is conventionally believed. Some of the major disturbances accompanied by proton showers have caused magnetic storms at the Earth. The g-maps have also been used to predict "interplanetary weather" about a day in advance of the geomagnetic disturbances (Hewish and Duffett-Smith, 1987).

The two large IPS telescopes in India should fully exploit the g-map technique.

REFERENCES

Alfven, H., (1977). *Rev. Geophys. Space Phys.*, **15**, 217.

Altschuler, M D. & Newkirk, G. (1969). *Solar Phys.*, **9**, 131.

Alurkar, S.K., Bobra, A.D , Nirman, N.S., Venat, P & Janardhan, P , (1989). *Indian J. Pure Appl. Phys.*, **27**, 322

Alurkar,S K , Janardhan, P & Vats, H O., (1993). *Solar Phys.*, **144**, 385.

Axford, W.I ,(1977) *Study of Travelling Interplanetary Phenomena*, edited by M.A. Shea, D.F. Smart, S.T. Wu, (Reidel Publishing Co , Holland) **145**

Behr, A & Siedentopf, H , (1951). *Z. Astrophys.*, **32**, 19.

Biermann, L., (1951). *Z Asrophys* , **29**., 274.

Bruno, R , Villane, U ,Bavassano, B., Schwenn, R & Mariani, F., (1986). *Solar Phys.*, **104**, 431.

Chapman, S. (1957) Smithsonian Contrib. *Astrophys* , **2**, 1

Coles, W A. & Rickett, B J.. (1976) *J. Geophys. Res* , **81**, 4797

Coles, W.A , Rickett, B.J., Ramsey, V.H., Kaufman, J.J. Turley, D.G., Ananthakrishanan, S , Armstrong, J.W., Harmons, J.K., Scot, L.S.L. & Sime, D G., (1980). *Nature*, **286**, 239.

Duvall,T K. Jr. (1977) Ph D Thesis, Stanford University.

Endler, F. (1971). Gottingen Univ , Math-Nat, Fak.

Feldman, W.C , Asbridge, J.R., Bame, S.J. & Glosling, J T., (1976). *J. Geophys. Res.*, **81**, 5054.

Feldman,W C ,Asbridge, J.R., Bame, S.J , Gosling, J.T. & Lemons, D.S., (1978). *J. Geophys. Res.*, **83**, 5285.

Gosling, J T , Borrni, G., Asbridge, J.R., Bame, S.J., Feldman, W.C. & Hansen, R.T., (1981). *J. Geophys. Res.*, **86**, 5438.

Hansen, S.F., Sawyer, C. & Hansen, R.T., (1974) *Geophys. Res. Lett.*, **1**, 13.

Hewish, A , Tappin, S.J. & Gapper, G.R , (1985) *Nature*, **314**, 137.

Hewish, A. & Duffett-Smith, P.J., (1987). *MNRS*, **229**, 485.

Hoeksema, J T. (1984) Ph.D. Thesis, Stanford University.

Howard, R A & Koomen, M.J., (1974). *Solar Phys.*, **37**, 469.

Howard, R A , Sheeley Jr , N R Koomen, M.J. & Michels, D J , (1985) *J. Geophys. Res.*, **90**, 8173.

Hundhausen, A J , (1972) *Coronal Expansion and Solar Wind*, (Springer, N Y)

Kojima, M & Kakinuma, T , (1987) *J Geophys Res* , **92**, 7269

Levine, R H., Alschule, M D & Harvey, J W , (1977) *J Geophys Res* , **82**, 1061

Neugebauer, M & Snyder, C W , (1966) *J Geophys Res* , **71**, 4469

Nolt J.T , Davis, J M , Gerassimenko, M , Lazarus, A J & Sullivan, J D , (1977) *Geophys Res Lett* , **4**, 291

Nolte, J T., Krieger, A.S., Timothy, A F., Gold, R E., Roelof, E C , Vaiana, G , Lazarus, A J , Sullivan, J D & McIntosh, P S , (1976). *Solar Phys* , **46**, 303

Parker, E N , (1958). *Astrophys. J* , **128**, 664.

Parker, E N , (1963) *Interplanetary Dynamical Processes* (Inter Science Pub)

Pneuman, G.W & Kopp, R.A , (1971) *Solar Phys.*, **18**, 258.

Ricket, B.J & Coles, W A , (1991) *J Geophys* , **96**, 1717

Saito, T , (1975). *Sci Rep.. Tohoku University, Ser.5, Geophys* , **23**, 37

Schatten, K H., (1976) *Nature*, **264**, 730

Scherrer, P H., Wilcox, J M., Svalgaard, L., Duvall, T.L Jr , Dittaur, P H & Gustafson, E K , (1977) *Solar Phys* , **54**, 353

Schulz, M , (1973) *Astrophys. Space Sci* , **24**, 371

Schwenn, R , (1983). *Solar Wind* 5, NASA Conf. Pub. **2280**, 489

Schwenn, R , (1990) *Phys. Inner Heliosphere* (Springer-Verlag), 99

Sheeley, N.R Jr . Harvey, J W & Feldman, W C , (1976) *Solar Phys.*, **49**, 271

Sheeley, N R Jr , Asbridge, J R , Bame, S.J & Harvey, J.W , (1977) *Solar Phys.*, **52**, 485

Sheeley, N.R. Jr & Harvey, J.W., (1981) *Solar Phys* , **70**, 237.

Smith, E J , Tsurutani, B.T. & Rosenberg, R.L , (1978) *J Geophys. Res* , **83**, 717

Svalgaard, L & Wilcox, J.M., (1978). *Ann. Rev A.A.*, **16**, 429.

Timothy, A.F., Krieger, A.S. & Vaiana, G.S., (1975). *Solar Phys.*, **42**, 135

Wilcox, J.M. & Ness, N.F., (1965) *J. Geophys. Res.*, **70**, 5793

SOLAR WIND - MAGNETOSPHERE INTERACTION

A.C. Das*

INTRODUCTION

The topic of solar wind-magnetosphere interaction is very wide and includes many physical processes and quantitative cause-effect relationships among different observed phenomena. Recent observations by ground-based instruments as well as by rocket and satellite probes have provided many important clues to understand the physical processes that are involved in solar wind-magnetosphere interactions. Reconnection of magnetic field lines is one of the most important processes that plays a very important role in shaping the magnetosphere of any planet and in producing many puzzling phenomena in the magnetosphere. A number of theoretical models of reconnection exist in MHD approximations (Dungey 1961; Parker 1963; Petscheck 1964) as well as in kinetic or microscopic description of plasma (Galeev and Zelenyi 1976; Schindler 1974) that can generate the steady state reconnection as well as spontaneous reconnection. The observations of flux-transfer events on the dayside magnetosphere and of plasmoids in the tail by satellite experiments are some of the important landmarks in the processes of solar wind interactions with the magnetosphere.

The prominent features of the frontside interaction of the solar wind with the Earth's magnetic field are: the bow shock, the flow diversion around the magnetosphere, the magnetopause, the polar cusp, boundary layer, field-aligned currents, convection and two loop currents in the polar ionosphere. A fairly good progress has been made in the theoretical understanding of these features.

It will not be possible in this review to include all the phenomena resulting from both the macroscopic and microscopic processes in the plasma environment in and around the magnetosphere. We will consider here some of the central issues of

* *Physical Research Laboratory, Ahmedabad 380 009.*

magnetospheric physics that include magnetic field reconnection, boundary layers, flux transfer events, and convection. An attempt has been made to bring out the state of art in the recent developments in the physics of solar wind-magnetosphere interaction and some important contributions made by the scientists working in the country.

MAGNETOPAUSE

A short historical account may be useful. Solar wind in the form of continuous emissions of plasma from the Sun was first postulated by Chapmann and Ferraro in 1931. The magnetic field of any planet prevents the direct entry of the solar wind plasma towards the planet and therefore a cavity is formed around any magnetized body that exists in the domain of streaming plasmas. In the models of interactions suggested earlier by Chapmann and Ferraro, and Dungey (1961), an electric current is produced at the boundary as it first encounters the magnetic field of the Earth and creates a well-defined sharp interface, the magnetopause, outside of which we find solar plasma and inside, the magnetic field which can be traced back to Earth. This becomes a problem of boundary layer between collisionless unmagnetized plasma and the vacuum magnetic field. The sheath can be described in the following manner (see Dungey 1958).

Suppose the particles, both electrons and ions, from the Sun move in x-direction and come back because of the magnetic field of the planet. This produces an electric field near the interface. Using a simple equation

$$m(\upsilon.\nabla)\mathbf{v} = q(\mathbf{E} + \mathrm{v} \wedge \mathbf{B})$$

in a simple model $B_x = B_y = 0$ and $\partial/\partial y = \partial/\partial z = 0$ and curl $\mathbf{E} = 0$, it can be seen that

$$u^2 + v^2 = U^2 + V^2 - \frac{2q}{m}\phi$$

and

$$v = V - \frac{q}{mc}A \qquad \text{... (1)}$$

where *U*, *V*, *W* are the velocities far away from the sheath. The current density is then given by $j_y = 2ne(\upsilon_p - \upsilon_c)$ and the magnetic potential *A* can be determined by solving $(curl\,\mathrm{B})_y = \frac{4\pi}{c} j_y$

$$i.e.\ \frac{d^2A}{dx^2} = \frac{8\pi ne^2}{c^2}\left(\frac{1}{m_p} + \frac{1}{m_e}\right)A. \qquad \text{... (2)}$$

It is obvious from Eq. (1) that there exists a current sheet along y-direction. The thickness of the sheet is determined by Eq. (2) and is given by c/ω_{pc} where $\omega_{pe} = 4\pi ne^2/m_c$.

The magnetopause as defined above is a free boundary created by the solar wind flow around the Earth's magnetic field. This is not a very simple boundary problem but it has been solved by considering a simple model that takes into account (i) simple pressure low outside, (ii) no plasma pressure inside, and (iii) zero magnetic field on the outside [e.g. Midgley and Davis 1963]. In equilibrium the pressure outside the boundary will therefore be balanced by the magnetic field pressure inside and the field sources are the Earth's dipole and the magnetopause current. The total magnetic field B at the magnetopause is then given by $B = B_d + B_{mc}$, where B_d is the dipole magnetic field and B_{mc} represents the magnetic field associated with the magneto-pause current. The condition of pressure balance is

$$\frac{B_m^2}{8\pi} = P_m \qquad \text{... (3)}$$

where B_m and P_m are the magnetic field and pressure on the respective sides of the magnetopause. The pressure can be described by

$$P = P_{st}\cos^2\psi$$

where P_{st} is the pressure at the stagnation point and is given by

$$P_{st} = K\rho_s \upsilon_s^2 \qquad \text{... (4)}$$

and ψ is the angle between the boundary normal $\hat{n}_m$ and the velocity vector at ∞. Numerical value of K has been estimated to be about 0.8 on the basis of gasdynamic modelling of the interaction of a supersonic stream with a blunt body.

The standoff distance of the stagnation point can be calculated easily from Equations (3) and (4). If one realizes that $B_m = 2B_d$ since the contribution of surface current must be approximately equal such that the unperturbed dipole field is cancelled outside the magnetopause. Since $B_d = \mu/r^3$, the standoff distance r_{st} is given by

$$r_{st} = \left(\frac{\mu^2}{K 2\pi \rho_s v_s^2}\right)^{1/6} \qquad \text{... (5)}$$

where μ is the Earth's dipole moment. This provides the magnetopause distance from the surface of the Earth as a function of P_s, v_s and K. One can thus obtain a very reasonable model for the shape of the magnetopause by this simple first order description (approach). Figure 1 shows the noon-midnight meridian cross-section of the magnetosphere. Apart from the magnetopause there are other important features like polar-cusp, entry layer, and plasma mantle. There exists one more discontinuity ahead of the magnetopause. Since the solar wind flows towards the planets with supersonic and super-Alfvenic speeds, a bow shock of nearly parabolic shape is formed which enables the flow to be deflected around the magnetopsheric obstacles. The general characteristics of the bow shock are reasonably well described in the gasdynamics analogy (Spreiter *et al.* 1966) although the gas in the solar wind is collisionless. Recently, a three-dimensional gasdynamic model for

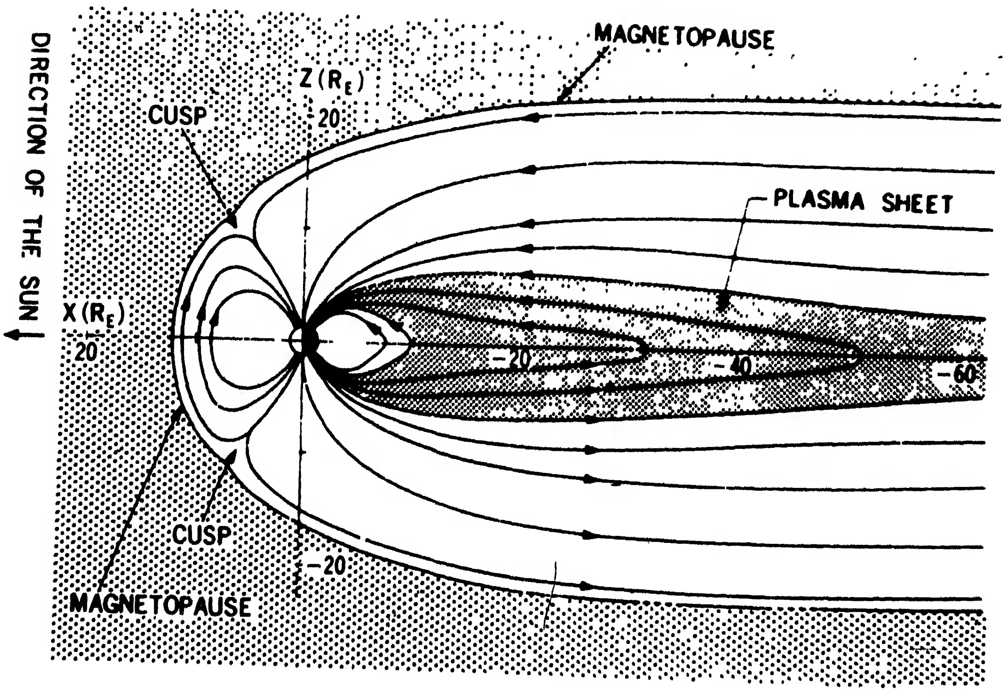

Fig.1 Noon-midnight meridian cross-section of the magnetosphere (after Nishida, A , 1982)

solar wind flow past nonaxisymmetric magnetospheres has been considered by Stahara *et al.*,(1989). Comparison of the model results with the observations of the location of bow shock and magnetopause shows a remarkable agreement.

It is obvious from Eq. (3) and from this above discussion that the solar wind pressure variation can make a substantial change in the location of magnetopause and other related phenomena. The pressure variations are common and have a large amplitude. Sibeck (1990) has shown that the variation can drive a large-amplitude (~ IR_E) magnetopause motion with velocities of ~ 60 km s^{-1} and the transient dayside ionospheric flow of 2 km s^{-1} which are organised into double convection vortices. Ground magnetometer also shows pronounced enhancements under the auroral ionosphere where they reach 60-300 nT. The effects on the equatorial region are also dominant. A correlation study made by Sibeck (1990) of transient ground magnetometer events at the south pole station and geosynchronous orbit indicates that almost all the strong ground events are associated with clear compressional signature at the dayside geosynchronous orbit.

On the nightside the shape of the magnetosphere is different. It has an extended tail called magnetospheric tail. In the case of Earth the tail extends to about 100 R_E, which is about 10 times the subsolar distance. Although the magnetic field lines in the tail originate from the planet, the structure of the magnetic field in tail no more resembles a dipole. It is modified by the electric current that flows across the tail. A schematic view of the magnetosphere with the tail associated with cross-field current is shown in Fig.2. We will however discuss the tail dynamics a little later.

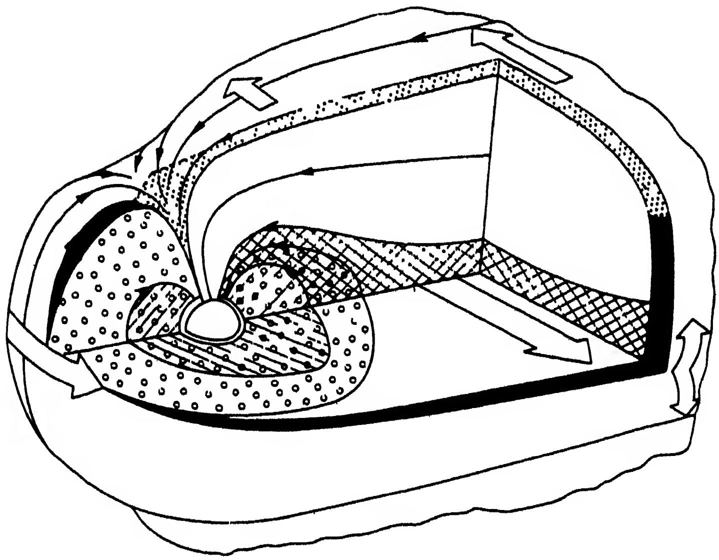

Fig 2 Schematic view of the internal structure of the magnetosphere with tail current.

MICROSTRUCTURE OF MAGNETOPAUSE

We have already discussed the magnetopause boundary based on the field-plasma interaction. A very simplified microstructure of the boundry is given by Willis (1975) and is reproduced in Fig.3. The two charged particle species, ions and electrons, are incident normally on a plane boundary layer. The solar wind is considered magnetic-field free. The ions tend to penetrate deeper than the electrons because of their heavier mass. This produced charge separation and generated an electric field pointing outward. Owing to this field the ions are returned before they are deflected by the magnetic field. The electrons however experience Lorentz force and get accelerated. The translation motion due to this electric field accounts for the currents in the boundary and is known as Chapmann-Ferraro current, which has already been discussed in plasma-field interaction at the boundary. If one uses $p = 2n\ (m_i + m_e)\ \upsilon^2_0$ in the pressure balance equation and replaces υ_0/B by the gyroradius, one finds the thickness of the order of plasma skin depth $d = 1/\sqrt{2}\ c/w_{pe}$, where w_{pe} is the plasma frequency. Hence the thickness of the magnetopause could be around 1 km.

The situation becomes different if the electric field is short-circuited by the current flowing along the magnetic field line and closing through the ionosphere. This becomes possible if there exists enough plasma inside the boundary. In such a case the ions can penetrate unimpededly and the thickness of the current layer would

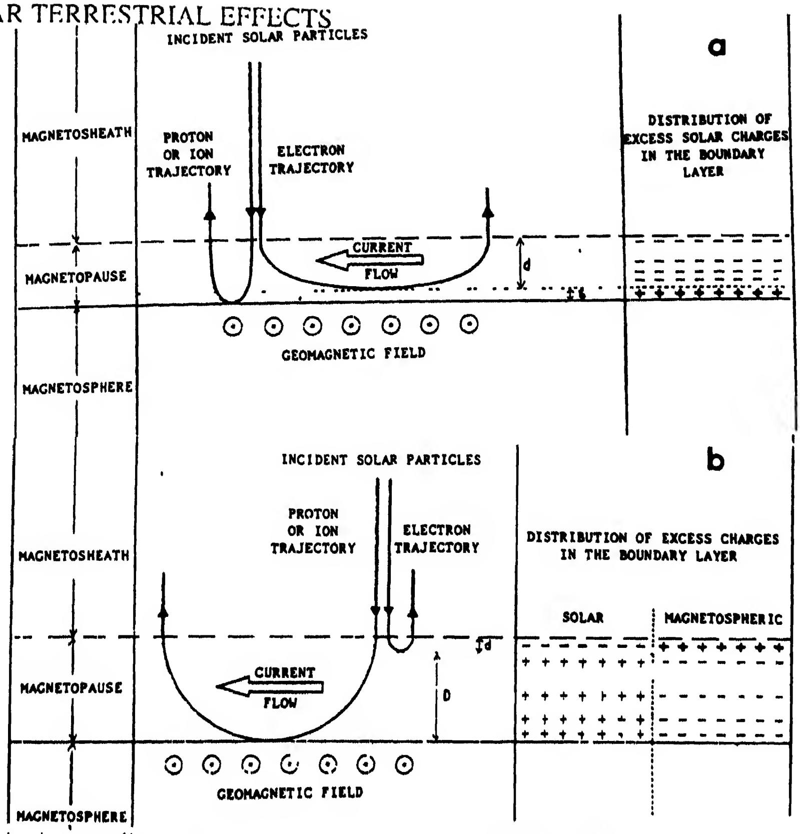

Fig 3 A schematic illustration of magnetopause boundary on the basis of the trajectories of electrons and ions (from Willis, 1975).

be of the order of ion-gyroradius which is about 100 km. The currents in the magnetopause may produce some instabilities and turbulence and the thickness may get enhanced because of scattering of particles in the trapped orbit.

Berchem and Okuda (1990) have developed a two-dimensional particle simulation to study the formation and stability of the magnetopause current layer. They have computed the trajectory of electrons and ions in their self-consistently generated electromagnetic field and an externally imposed two-dimensional vacuum dipolar magnetic field so that the results can be applied to the interaction of solar wind with magnetosphere. A self-consistent current layer due to both diamagnetic drift and $E_\wedge B$ drift has been found to have formed. It is shown that during the establishment of this current layer, thickness is of the order of the hybrid gyroradius ($\rho \simeq (\rho_c \rho_i)^{1/2}$, which is close to a value suggested by Rosenbluth (1963). However, there is enough indication that the current sheet is subjected to instabilities which broaden the width of the current layer. Perturbations with wavelength of the order of ion-gyroradius are seen at the surface between the fields and particles. These are observed both on electrostatic field and on the compressional magnetic field.

Surface waves are now shown to be important in the magnetopause boundary. Uberoi (1984) has shown that the criterion of the onset of Kelvin-Helmboltz (K-H) instability in the magnetopause may be obtained directly from the marginal instability condition for the pure Alfven surface waves propagating along the interface

between two incompressible media in the limit when the propagation direction is nearly perpendicular to the largest magnetic field.

Field-line resonance is one of the important mechanisms for the generation of micropulsations. It has been demonstrated successfully by Uberoi (1989) that the surface waves generaged at the magnetopause are capable of producing field-line resonance that in turn generates micropulsations. Resonant absorptions of Alfven compressional surface wave are also shown to be an important part of interaction for transfer of energy from solar wind plasma.

INTERPLANETARY MAGNETIC FIELD AND MAGNETOSPHERIC MODEL

The model suggested by Chapmann and Ferraro does not include the effect of the interplanetary magnetic field. The interplanetary magnetic fields are now measured rather accurately and they play a very important role in an interesting and important process of reconnection of magnetic field lines. The concept of magnetic field reconnection has provided an important clue for a unified theoretical framework for the generation of substorm and large-scale dynamics of the magnetosphere.

A radically different type of magnetopause structure has been introduced by Dungey (1961). He has first shaped the reconnection model for the Earth's magnetosphere and it is now certain that it has been able not only to explain many observations but also to generate extensive research work both in space and in laboratory plasma..

The basic process of reconnection depends on (i) the topology of magnetic field and (ii) the motion of plasma flow near the neutral point. A simple model of magnetic field line configurations in the Earth's magnetosphere has the topology shown in Fig.4. There are three classes of field lines:

(i) Closed field lines that connect to the Earth at both ends.

(ii) Open field lines that connect to the Earth at one end, the other end being indistinguishable from the interplanetary magnetic field.

(iii) Interplanetary magnetic field lines that do not connect to the Earth at all.

Each group is separated from the other by a line called separatrix. The separatrix intersects along x-lines which encircle the Earth. If now the magnetic flux in one regime is to be increased or diminished, it requires the motion of field lines across the separatrix. One visualizes how an individual field line is transported across the separatrix in the following way. A field line of class (iii) and one of class (i) must be simultaneously cut and reconnected to make two field lines of class (ii) if the open flux is increased, or reverse if the flux is diminished. If one considers the topology of the magnetic field alone, the transfer of these fluxes does not produce any remarkable effect. The importance of this process in space plasma arises from the

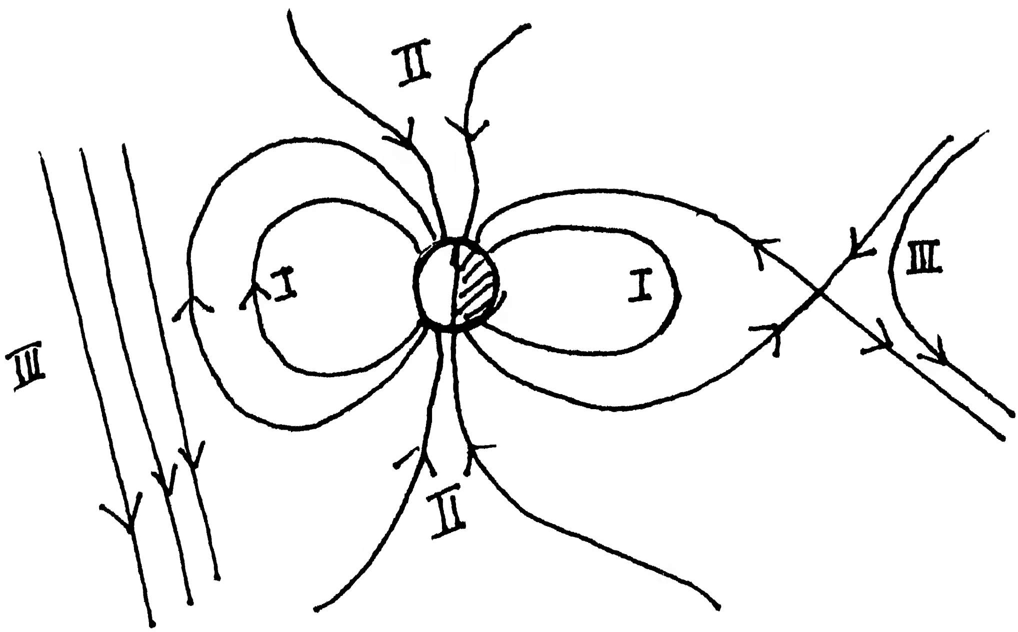

Fig.4 Topology of the magnetic field There are three classes of magnetic field lines, each class is separated from the other by a line called separatrix

fact that the magnetic field line is closely coupled to the plasma motion. (Dungey 1961; Petscheck 1964; Vasyliunus 1975).

The large-scale plasma motion in the magnetosphere has important effects in many magnetospheric phenomena. However, there are many difficulties to this motion. The collisions are rare and the flow is quite complicated. Boltzman equation is valid even for negligible collisions and by taking moments the usual equation of motion can be obtained except that the pressure takes the form of asymmetrical tensor. It is difficult to obtain the different components of the pressure tensor and the motion cannot be described in a simple manner. However, the pressure can be neglected in some regions and the Ohm's law for infinite conductivity is given by

$$\mathbf{E} + \frac{1}{c}\,\mathbf{v}\Lambda\mathbf{B} = 0 \qquad \text{... (6)}$$

where **E** and **B** are the electric and magnetic fields respectively, **v** is the bulk flow velocity of plasma and *c* is the velocity of light. Equation (6) is valid in many regions of cosmic plasma. The nature of plasma flow can virtually be obtained from Eq. (6)

and it implies that the magnetic flux through any element of plasma initially coincident with a magnetic flux tube continues to form a flux tube at all times. Hence a transport of magnetic flux near the separatrix is always associated with the plasma motion. However, finite conductivity becomes essential for such transport across the separatrix. This flow is for all practical purposes the essential element in the definition of reconnection concept. The magnitude of plasma flow is a measure of the reconnection rate.

Equation (6) is not valid near the neutral point and the flow has a special pattern around this point. Dungey (1958) pointed out that it was only in such a region that a large current could be produced in a plasma without being opposed by electromagnetic force $\mathbf{j} \wedge \mathbf{B}/c$. The equations governing the motion are Maxwell's equation, the continuity equation, the hydrodynamic equation of motion and the Ohm's law given by

$$E + \frac{1}{c}\,\mathbf{v} \Lambda \mathbf{B} = \eta j \qquad \text{... (7)}$$

where η is the electrical resistivity and j, the current density. The flow pattern and the magnetic field lines are shown in Fig. 5. The current direction is perpendicular to the plane of the paper. An oversimplified microscopic picture of this current has been presented by Cowley (1971).

The main point about the large current is the existence of finite resistivity in such a plasma. The resistivity has the classical value when it is entirely due to particle scattering by Coulomb collisions. However in a collisionless plasma, a higher

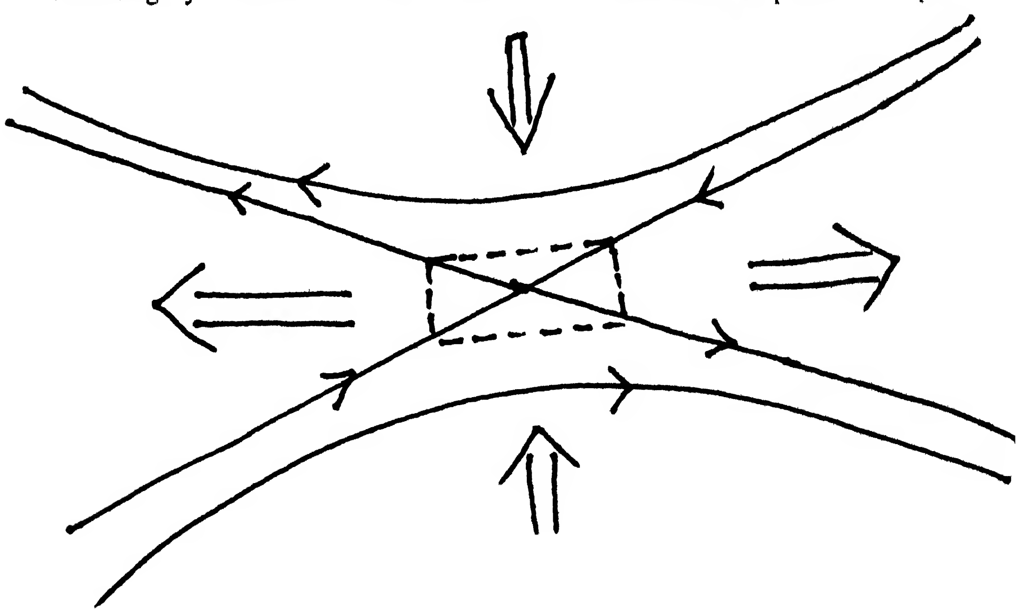

Fig.5 Flow pattern and magnetic field lines near the neutral point

anomalous resistivity can occur from the scattering by many microscopic processes which will be discused later. It may be useful to reproduce the scenario of electric field in the region discussed by Dungey (1958). Near the neutral point some electric field is necessary to drive the current which is given by $\mathbf{E} = \eta j$ where j is not very large. Far away from the neutral sheet or line Eq. (6) is valid and the fluid flows towards it with velocity v. The electric field determined by $\mathbf{v}\Lambda\mathbf{B}$ has the same sign as that of the electric field near the neutral point. Thus the occurrence of reconnection rate can be stated in two ways (Vasyliunus 1975) and there exists an electric field **E** parallel to neutral line with pointing vector $c\frac{\mathbf{E}\Lambda\mathbf{B}}{4\pi}$ directed so as to represent a flux of magnetic energy to the reversal region from both sides. In other words, plasma flow with bulk velocities $\pm\mathbf{v}$ from both sides transporting magnetic energy in the field reversal region. The magnitude **E** or **v** is then the measure of reconnection rate. However, the process of transport fails in the region where the magnetic field tends to zero and therefore the process of diffusion must take place to transport the energy to the neutral line.

We have discussed above a very simple picture of reconnection under the assumption that there exists a finite conductivity near the neutral line. Parker (1963) suggested a model with diffusion length l and width δ. Assuming that the plasma is convected to the region of neutral sheet with velocity u and leaves with velocity v, l and δ may be related. Steady state has been assumed by considering that there is a balance between magnetic field convection by inward moving fluid and magnetic diffusion due to finite resistivity. The annihilation occurs by Ohmic dissipation. However, the rate of annihilation in a thin sheet is found to be very low to account for observations. Petschek (1964) however overcome these difficulties by matching the diffusion region to a region of standing wave or slow shock by which the magnetic field energy may be converted into kinetic energy. In this case the merging rate is enhanced considerably. Yeh and Axford (1970) have also obtained a shock solution showing effective energy transfer in the system.

It is clear from Fig. 4 that the reconnection occurs both in the frontside and in the magnetotail. However, the dynamics of the tail reconnection depends on the dayside reconnection. We shall now consider these two cases separately. It is also seen that the reconnection is expected with a southward component of the interplanetary magnetic field and this will be considered primarily for the discussion of the indirect evidence for reconnection.

The Boundary Layer

A boundary layer consisting of plasma with the same temperature and other similar flow properties of the solar wind plasma is found to exist first adjacent to magnetopause. This layer of plasma is different from the magnetopause current layer or plasma sheet boundary layer in the tail lobe. This is an important signature of the interaction between solar wind and the magnetosphere and it shows that the

magnetopause is not impenetrable by the solar wind. Plasma instabilities and surface waves at the magnetopause (Uberoi 1984) play an important role.

The boundary layer in the noon-midnight meridian cross-section of the magnetosphere is shown in Fig.5. It is evident that the boundary extends over the entire region of magnetopause. However, there are different characteristics for different portions of the boundary layers. Three distinct regions have been observed: the low-latitude boundary layer (LLBL), the entry layer (EL) and plasma mantle (Paschmann *et al.*, 1976; Haerendel *et al.*, 1978; Eastman and Hones, 1979). Some of the characteristics are given below.

In the plasma mantle a gradual increase of plasma density by three order of magnitude over a distance of several Earth radii has been observed. The plasma velocity along the field line in this region can be as high as 100 km/s.

In the entry layer, the density at the inner edge is seen to be almost the same as at the magnetosheath region. The lack of density jump suggests the direct local entry of plasma from the solar wind plasma. The plasma β is also found to be larger than 1 throughout the entry layer in contrast to the plasma mantle where it is less than 1. The flow direction at the entry layer crossing is very striking as most of the time it shows the sunward flow. Different and irregular flows are observed at other times. At low latitudes a variety of plasma profiles is obtained. Sometimes it is seen to have sharp density changes at the magnetopause and at the inner edge of the layers (Paschmann, 1979).

These regions are characterized by different thicknesses. It is obvious from Fig.6 and the density profiles that the smallest thickness is seen at the subsolar point and then it slowly increases as one moves away from the subsolar point to plasma mantle, the maximum being at the mantle of around 10 R_E.

Strong and sometimes organized flow pattern also forms a part of distinct features of different regions. These are already mentioned above. Typical flows in the boundary layer observed by various satellites have been illustrated in Fig.7 [*see* Eastman, 1979]. Lee and Akasofu (1989) have recently obtained an analytic formula that relates the particle flux to the average plasma density and the total open flux at the magnetopause. The particle flux through the closed part of magnetopause is also estimated to understand the generation process of low-latitude boundary layer. It is also found that the flux of solar wind particles across the tail magnetopause is greater than through the dayside magnetopause. On the other hand, Bryant and Riggs (1989) have made a survey of the interaction between plasmas of solar and terrestrial origin at the outer edge of the Earth's magnetosphere by using measurements from AMPTE-UKS experiment. A statistical relation of the location of boundary with the solar wind dynamic pressure and its variation and the nature of boundary layer have been shown on the basis of a new analysis.

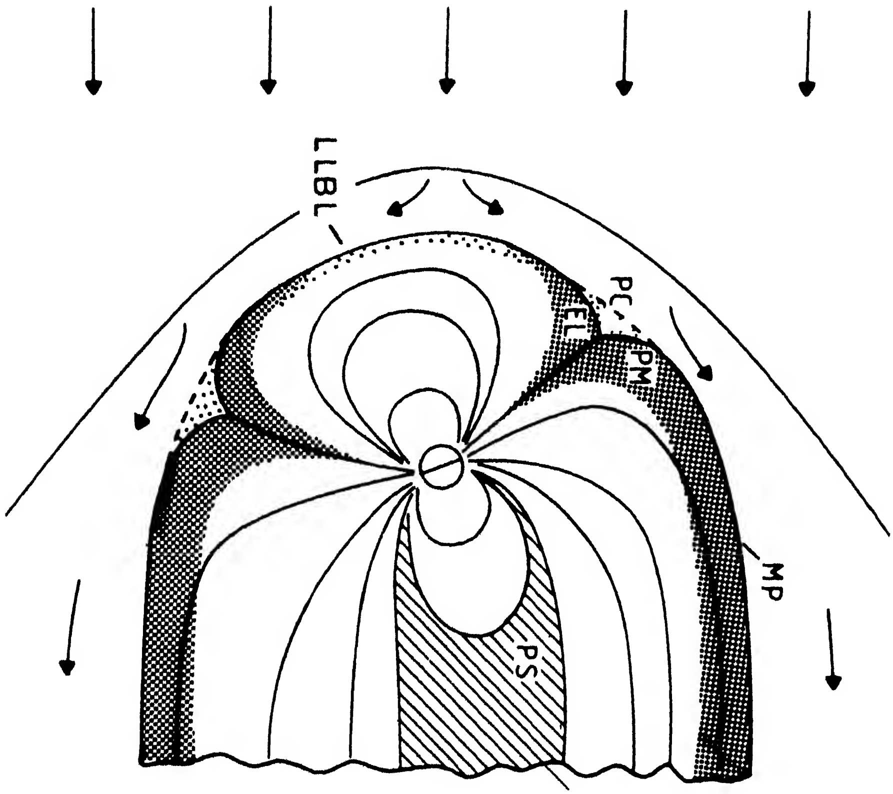

Fig.6 Illustration of the boundary layer in the noon-midnight meridian cross-section of the magnetosphere LLBL represents the low latitude boundary layer, EL the entry layer, MP the magnetopause, PC the polar cusp, etc. (from Haerendel *et al.*, 1976)

Flux Transfer Events and Dayside Reconnection

Twisted ropes of reconnected magnetosheath and magnetospheric field lines and the disturbances which they create in the surrounding media are known as flux transfer events. The first report of flux transfer events was given by Haerendel *et al.*(1978) and Russell and Elphic (1978). These ropes are interpreted by Russell and Elphic (1978) as the transient flux erosion of the magnetospheric magnetic field as a result of sporadic, non-stationary nature of reconnection in the dayside of the magnetosphere. Large spikes are seen in the magnetic data for an inbound crossing of the magnetopause by HEOS-2 and they are interpreted as the events of impulsive erosion of magnetic flux tube (Haerendel *et al.*, 1978). The solar wind can do work on the magnetic field at a location where an interplanetary magnetic field flux tube is connected with the terrestrial magnetic field and can erode magnetic flux that

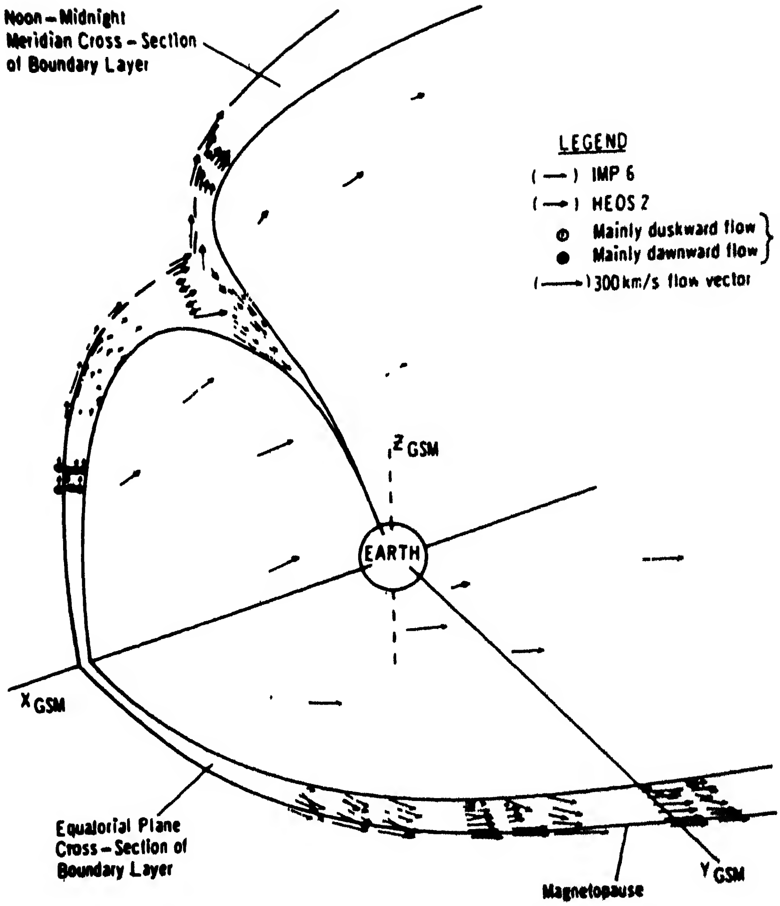

Fig.7 Plasma flows in the boundary layer observed by various satellites (Eastman and Hones, 1979).

formerly belonged to the magnetosphere. When mechanical work is done against magnetic tension, the result will be increased in the field strength. Consequently one sees enhancement of the magnetic field strength in the region.

The bipolar nature of the magnetic field along the local magnetopause normal, observed by satellites ISEE-1 and ISEE-2, is also the characteristic of flux transfer events. The qualitative picture of the flux transfer events is shown in Fig.8. Magnetosheath field lines denoted by slanted arrows are connected with the magnetospheric (closed) field lines represented by vertical lines. The connected flux tube is then carried away by the magnetosheath flow in the direction shown by the big arrow. The magnetosheath field lines which are not connected with the magnetospheric field lines are drapped around the connected flux and pass through the spacecraft and then show the bipolar characteristics in the magnetopause normal component of the magnetic field.

The reconnection process for these flux tubes in the polar cusp region is transient because the events last only for a short duration. There exist two classes of models

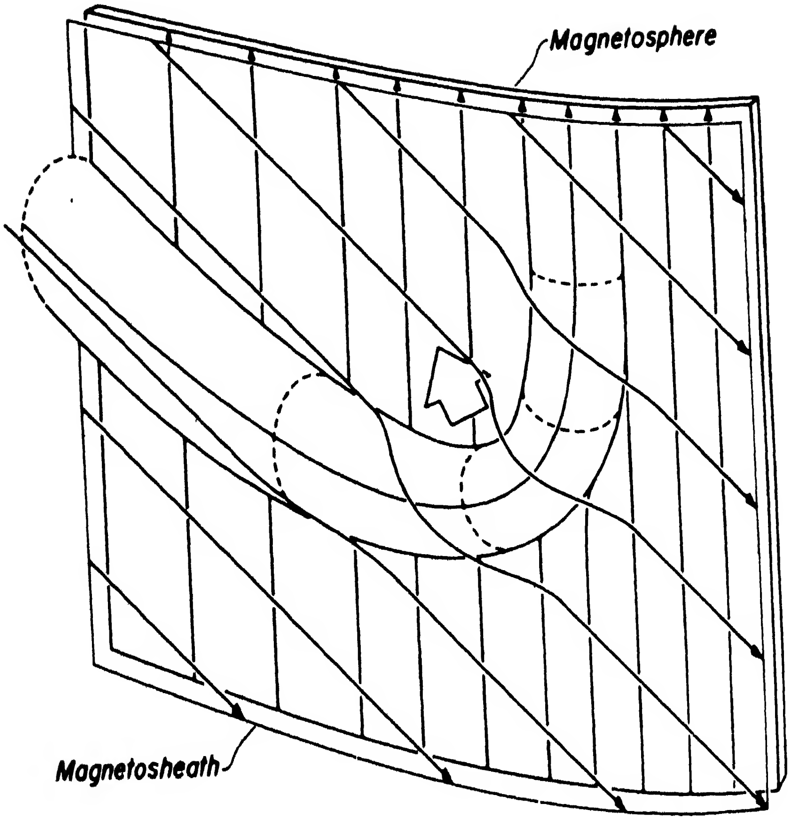

Fig.8 Qualitative picture of flux transfer events

for transient reconnection. Lee and Fu (1985) suggested a model of multiple X-line formation across the magnetopause to account for the twisting of the magnetic field in the central part of the FTEs. A number of 2-D (two-dimensional) computer simulations have been made to study the multiple X-line configuration (Fu and Lee, 1985; Shi *et al.*, 1988). In a 3-D model Ogino *et al.* (1986) have been able to show that the open field flux can indeed be twisted by the process of reconnection in the cusp region during the period of southward interplanetary magnetic field. In a recent paper, Ip and Jin (1992) have considered compressible plasma and have shown the time-dependent behaviour of driven reconnection process (*see* Fig.9). The results show recurrent formation of magnetic islands by bursty reconnection with multiple X-line configurations.

Southwood *et al.* (1988) and Scholer (1989) have suggested a different model in which it was shown that FTEs are 2-D magnetic structures generated by the bursty reconnection process with one single X-line. The transient ionospheric features stretched across a large longitudinal range in the dayside polar cusp boundary may be the result of the mapping of FTEs on the ground. In a 3-D resistive MHD computational model, Otto (1990) has concentrated on the local dynamics of the magnetopause with special emphasis on the formation of flux transfer event (FTE).

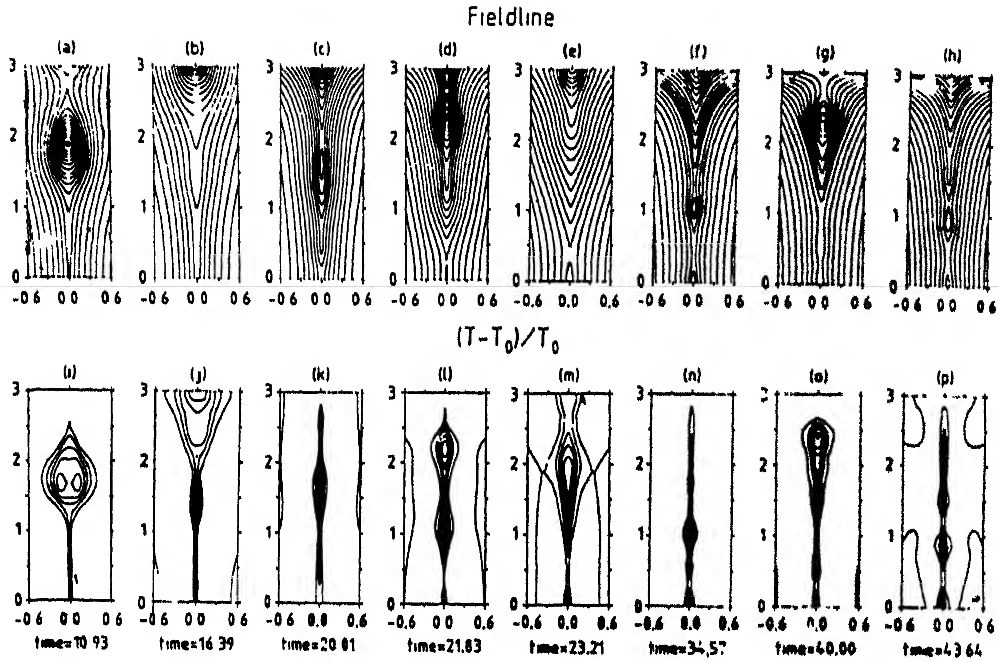

Fig.9 Recurrent formation of magnetic island with multiple x-line configuration (simulation results by Ip and Jin, 1992).

According to his computation, FTEs contribute a significant, if not a dominant, part of the plasma and energy transport from the solar wind into Earth's magnetosphere.

MAGNETOSPHERIC TAIL DYNAMICS AND SUBSTORM

Solar wind energy is primarily deposited to the nightside magnetosphere due to dayside reconnection and flux transfer events that result from the combination of high speed solar wind and strong southward interplanetary megnetic field. The tail current or equivalently the lobe magnetic flux is enhanced and the energy associated with this would eventually be converted into the other form through nightside reconnection. A part of this energy will be carried away by plasma jet down the tail and the rest would be ejected towards the Earth consistent with the basic features of plasma motion around the neutral point shown in Fig.5. The plasma flows towards the Earth and then produces convection and field-aligned potential that generate energetic electrons in the auroral region. If the reconnection at the nose of the magnetosphere occurs, there must also be reconnection in the tail to balance the rates of flux transport.

Following MHD model calculations described earlier, the magnetic islands can be generated in the tail near X-type neutral line. Dynamic reconnection in the magnetotail is also studied numerically by means of three-dimensional MHD code (Min, 1990). As a result of interaction between solar wind-magnetosphere the magnetic fields are stretched and the plasma sheet becomes thinner and thinner and

the magnetic reconnection is triggered by ohmic dissipation. The resulting plasma jetting is found to be supermagnetosonic. Although plasmoid formation and its tailward motion are not clear, the rarefaction of the plasma near the X-type neutral point is observed. Field-aligned currents are observed in the late expansion stage of magnetospheric substorm. It supports the earlier theoretical model that the field-aligned currents flow from the tail towards the ionosphere on the dawn side and from the ionosphere towards the tailside on the dusk side. The field-aligned currents and the cross tail currents are found to be strongly coupled. However, in all these models, resistivity near the neutral line is assumed, which is not very appropriate because of the long mean free path and it becomes useful to consider microscopic description.

The plasma and the magnetic field distribution within the magnetotail become unstable against excitation of a number of plasma collective modes. If the wavelength $\lambda << L$, where L is the characteristic length scale of plasma configuration, then one excites microinstabilities of different modes. Among many models based on microinstabilities that can be generated in the tail, the tearing mode instability (Schindler, 1974; Galeev and Zelenyi, 1976) is the most successful one to produce reconnection leading to substorm phenomenon, which is one of the most important phenomena in the magnetospheric physics. The concept of tail reconnection for substorm is supported by various evidences. The principal argument in its favour is the fact that the long magnetospheric tail, which has a diameter of the order of 30 Earth radii and extends by 50 R_E, provides a huge reservoir for substorm energy. The magnetic field inside the magnetotail shows an increase of its strength prior to substorm break-up. The diameter of the magnetotail also increases, suggesting that the magnetic flux is transferred from the dayside magnetopause into the tail.

The tearing mode instability may be understood qualitatively in the following manner. The simplest magnetic field model in the magnetotail is described in Fig.10. Such a configuration is supported by the plane current sheet which could be represented in the form of an elementary current filament uniformly distributed along the sheet. The attraction between a pair of filaments grows quickly as they draw together and the attraction of filaments from neighbouring pairs decreases as they move away. This redistribution of current changes the magnetic field topology. Part of the open field lines in the middle of the sheet current now reconnect and close around the pair of current filaments drawn together. It is seen that the development of tearing mode needs the dissipation process which could violate the frozen-in-field condition. In this mode, the electromagnetic wave is created by the periodic structure of current filaments in the narrow layer in the neutral sheet.

It is evident from the above description that in the tearing mode process, the current sheet spontaneously breaks up into a series of current filaments and the magnetic field associated with these forms a series of islands. A configuration consisting of a series of magnetic islands in equilibrium is subject to coalescence instability in which the islands move towards one another (Finn and Kaw, 1977; Pritchett and Wu, 1979). In the presence of resistivity this instability leads to a single

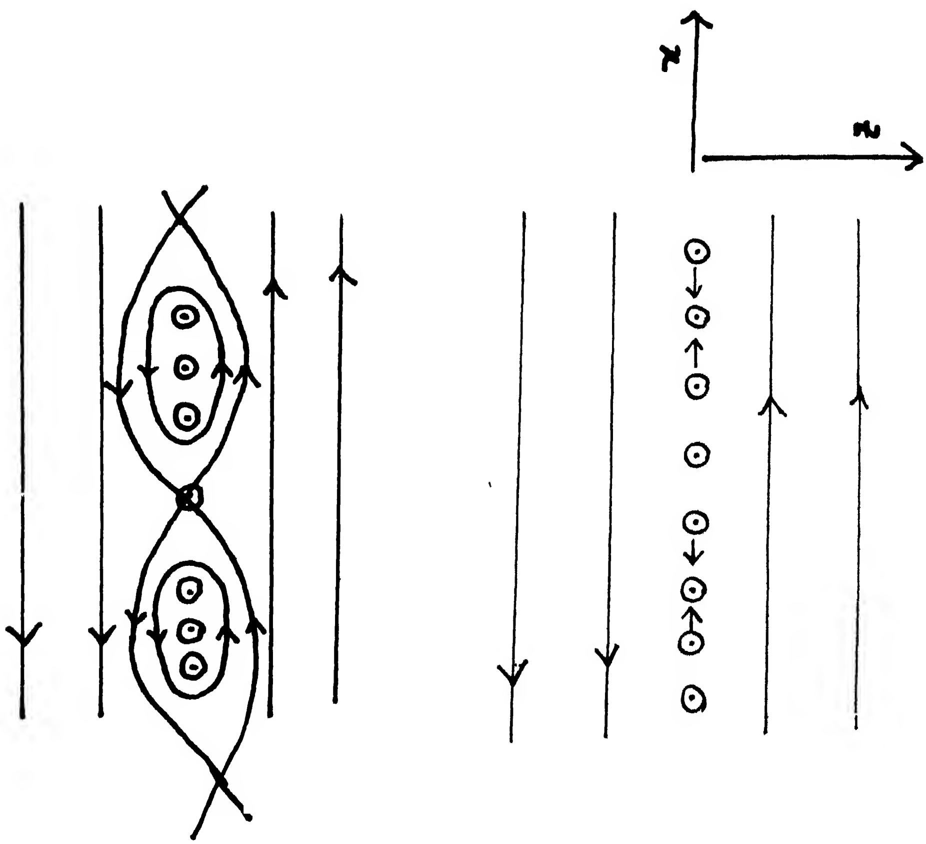

Fig 10 The simplest magnetic field model in the magnetotail Plane current is represented in the form of elementary current filaments uniformly distributed along the sheet. Physical process of tearing mode instability and the formation of island are shown.

island which is called plasmoid. Magnetic reconnection also occurs during this process of coalescence. There exists therefore a two step process : island formation followed by the rapid coalescence of small islands into larger ones.

The onset of a substorm takes place in a short time scale of the order of 5-10 min. If the tail reconnection caused by the tearing mode is responsible for this, then a much higher resistivity in the tail would be needed for this model to operate efficiently.

The presence of a small normal component of the magnetic field could lead to the suppression of electron tearing mode completely because of the fact that the electrons get magnetized and the flow is destroyed. Ion-tearing mode in two-dimensional configuration has been developed to overcome this difficulty, but the normal component is still seen to prevent the growth of ion-tearing mode if $B_{\perp}/B_0 \sim r_0/\Omega_0$ where r_0 represents the growth of one-dimensional tearing mode (Galeev and Zelenyi, 1976). One of the important contributions made by Lakhina and Schindler (1983, 1988) is the development of a model in which the plasma bulk flow in plasma

sheet boundary layer and in plasma mantle is considered. It is found to have an important destabilizing effect excitation of tearing mode in the Earth's plasma sheet region and thereby enhancing the growth rate and increasing the upper limit of B_z for ion-tearing mode. Recently Büchner and Zelenyi (1987) have suggested that the ion-tearing mode instability can be sustained when the electron orbits become chaotic (Chen and Palmadeso, 1986; Martin, 1986). However, the more recent simulation results by Pritchett *et al.* (1991) suggest that even for a thin sheet where the electron orbits become chaotic, the normal component field prevents the growth of ion-tearing mode. A possibility that still remains is of external influence and time-dependent effects which may help in driving the tearing mode leading to reconnection of field lines. This has been emphasized also by Pritchett *et al.* (1991).

The perturbation at the boundary in tail as a kind of external influence to drive the reconnection by tearing mode instability has been considered by Zelenyi and Kuznetsova (1984) and Horton and Tajima (1988) in one-dimensional model. A two-dimensional model of this driven reconnection theory in kinetic description of plasma has been developed by Lakhina (1992). It is found that the driven reconnection can occur in two steps, namely exponential and bursty type. These are new results and are very interesting. Some more work will probably be necessary to tackle the problem of equilibrium with high amplitude perturbation and to obtain suitable growths for substorm onset.

Sundaram *et al.* (1980) had taken a different view and studied the effect of background turbulence of lower hybrid and/or ion-cyclotron modes as a kind of external source to excite tearing mode. Such turbulence or fluctuations can exist in the vicinity of the neutral sheet as a result of microscopic instabilities driven by strong current layer or strong gradients in this region (Bowers, 1973 a, b; McBride *et al.* 1972) and it was possible to excite the electron tearing mode which otherwise would have been stabilized by the normal component of the magnetic field. However, the growth time was found to be rather large to account for the onset of substorm.

Recent satellite observations of plasma waves at the magnetopause (Labelle and Treumann, 1988) suggest that one of the most interesting instabilities which exists in the region of current sheet at the dayside magnetopause is the lower hybrid instability. The amplitude of these waves is reported to be as high as 3×10^{-2} V/m.

On the basis of these observations, Das (1992) has reinvestigated the earlier model of Sundaram *et al.* (1980) and with E ~ 10^{-2} V/m the growth time of tearing mode is found to be of the order of 60 s in the case of lower hybrid turbulence. Electrostatic ion-cyclotron mode waves can also be excited by the cross-field current at the magnetopause (Drummond and Rosenbluth, 1962; Porkalob, 1968 and many others) and if the effect of fluctuations in this mode is considered, then growth time can even be reduced to 12 s. These are very interesting numbers and can account for substorm onset. Physically these waves enhance the diffusion and not allow the

particles to get trapped completely, and consequently free streaming will not get lost. It makes the growth rate high and keeps B_i/B_0 at a level that is necessary to maintain the flow. Thus the lower hybrid turbulence makes the process very efficient and the instability will be able to produce rapid and variable reconnection rate to support explosive phenomena like solar flares and magnetic substorm

Recently many computer simulations have been done for the development of magnetic islands which are subjected to coalescence. In a model of magnetohydrodynamic and particle simulation, Wu *et al.* (1980) have demonstrated the formation of magnetic islands in a current sheet which subsequently coalesced. The coalescence growth rate is also reported to be ten times faster than the tearing mode growth. However, these two processes cannot take place simultaneously because the energy sources are different, e.g. islands have to be formed before coalescence takes place. Figure 11 shows the development of the coalescence process. The full island nearest

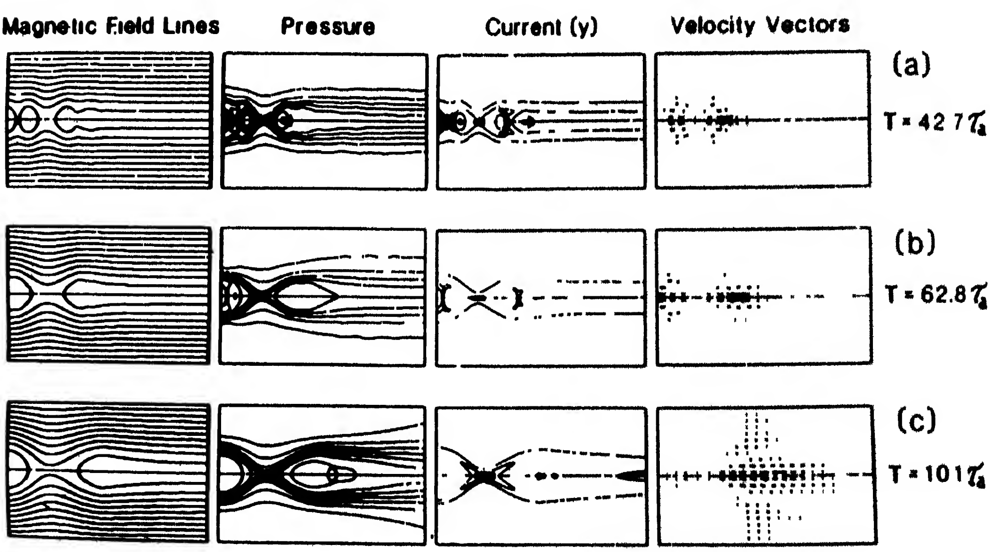

Fig 11 Development of the coalescence process of island formation (Wu *et al.*, 1980).

to the Earth merges with closed field lines while the three islands farther down the tail merge to form a large plasmoid-like island.

EVIDENCES OF RECONNECTION

Indirect Evidences

The observation of the association of southward component of interplanetary magnetic field with the magnetic field disturbance in the auroral region of Earth's ionosphere is an indirect evidence of the reconnection because it confirms the prediction of the model. Fairfield and Cahil (1966) from their analysis observe that when the interplanetary magnetic field is southward, there tends to be an associated magnetic disturbance on the ground. Arnoldy (1971) showed strong correlation of IMF north-south component with the auroral electrojet (AE) index, which is a measure of auroral electrojet current intensity based on magnetic records. Another important contribution is the prediction of magnetic activity index D_{st} on the basis of southward component of the magnetic field. D_{st} is the measure of ring current system inside the magnetosphere which is enhanced because of a large injection of particles from the tailside of the magnetosphere due to reconnection process. The observation of two-loop current system in the high latitude ionosphere also shows a close relationship with the southward component of the interplanetary magnetic field. The northward component which is associated with the quiet period has, however, shown sometimes complicated four-loop current system (Burke *et al.*, 1979) which can probably be explained by reconnection process associated with northward component of interplanetary magnetic field (Fig.13 in Das, 1990).

Direct Evidences

The most appropriate scenario for reconnection of magnetic fields at the subsolar magnetopause is seen in Fig.12 (Sonnerup *et al.*, 1981). Solid lines with arrows represent the magnetic field. The magnetopause (MP) is shown at the region of current layer and the boundary layer (BL) is just adjacent to it. The magnetosphere is on the right while the magnetosheath is on the left. The magnetosheath field and the magnetospheric field lines are connected at X-type neutral point seen as the intersection of two separatrixes S_1 and S_2. The plasma flow is shown by dotted double lines. The topology of the field lines is similar to Fig.4 and the flow pattern is similar to Fig.5 which are obtained on the basis of MHD model of reconnection.

This configuration may now be compared with the magnetic field and plasma data from ISEE-1 and ISEE-2 magnetosphere crossing of 6 September 1978 shown in Fig.13. The satellite moved from the outer magnetosphere into magnetosheath through the boundary layer (BL) and magnetopause (MP). The crossing of outer separatrix is denoted by S. The observations of plasma density, bulk velocity, north-south components of the magnetic field, the total magnetic field and pressure, etc. are shown from top to bottom of the figure. The transition of north-south component

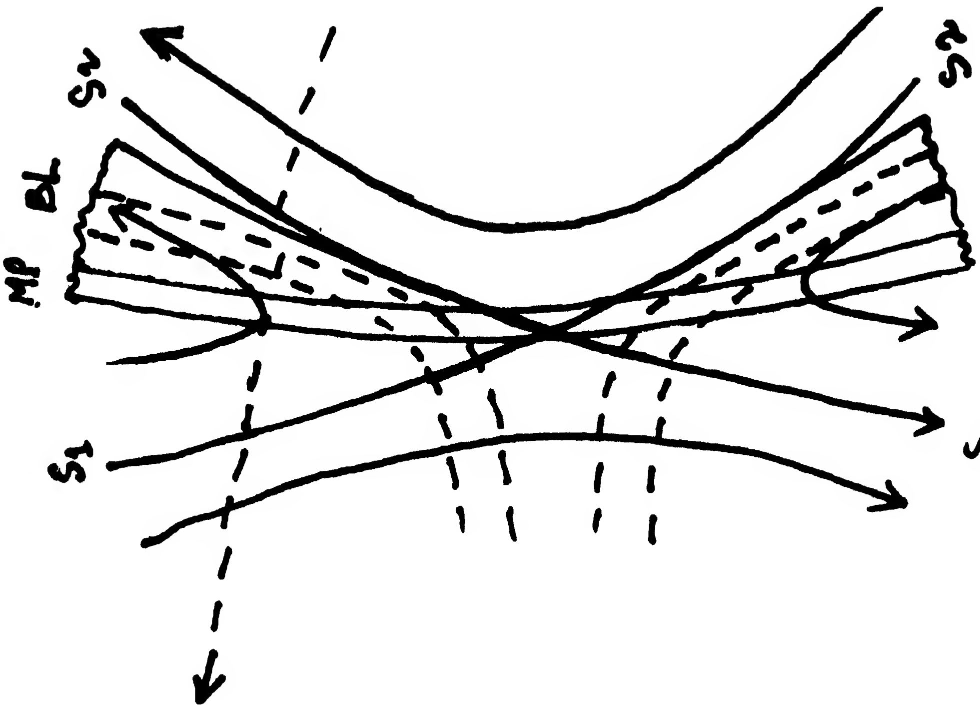

Fig 12 Appropriate scenario for reconnection of magnetic field at the subsolar magnetopause (Sonnerup *et al* 1981)

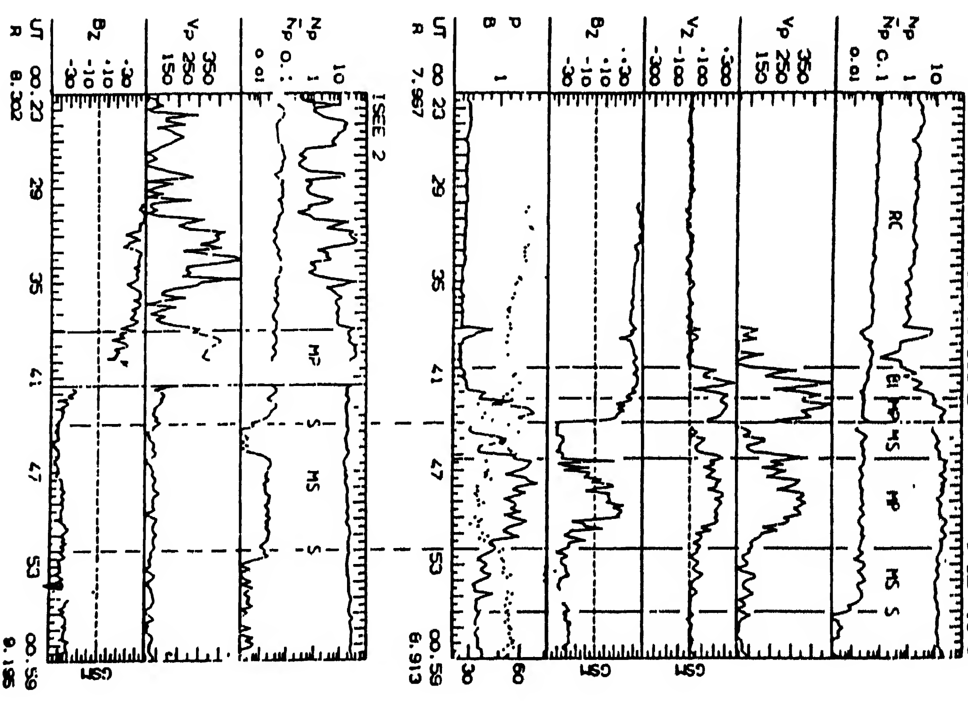

Fig 13 Magnetic field and plasma data from ISEE-1 and ISEE-2 magnetosphere crossing of 6 September 1978 (Sonnerup *et al*, 1981)

of the field also is confirmed by the multiple magnetopause crossing depicted in the figure. Comparison of these data with the configuration described in figure (earlier figure) supports the reconnection on the dayside magnetosphere.

Observation of Plasmoid

The discovery of plasmoid in the magnetospheric tail by ISEE-3 is an important step towards establishing the reconnection in the tail of the magnetosphere. Baker *et al.* (1984) have examined the plasma and field data in detail for a period during which ISEE-3 is in the tail region between 80 and 140 R_E. They have found several examples of strong southward magnetic field followed by a strong northward field when ISEE-3 in the plasma neutral sheet. Significant changes in plasma properties and magnetic field topology have been seen during the onset of substorm. These are shown schematically in a model in Fig.14. Before substorm, the neutral lines appear

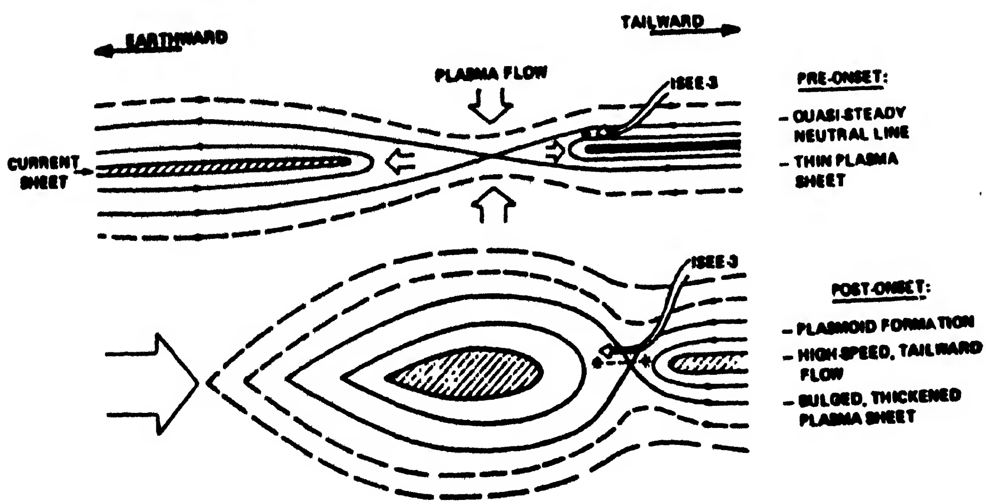

Fig.14 Magnetic field topology, plasmoid formation and plasma properties observed during the onset of substorm (Baker *et al.*, 1984).

to be located near $x \approx -100\ R_E$. The plasma sheet is thin and flattened during this phase. When the ISEE-3 was at 100-140 R_E, the plasma and the field data were consistent with an earthward neutral point (top panel). The significant changes in the configuration of tail around $x \approx -100\ R_E$ occur in a short time after the onset of expansion phase. Within a few minutes after the substorm, high-speed tailward plasma flows begin. The plasma sheet starts becoming thick and bulges just after the substorm onset. Plasmoid is formed and the release of plasmoid pushes the plasmasheet ahead of it and steepens the field line inclination throughout the region.

Another example of plasmoid travelling tailward through the distant plasmasheet consequent to the occurrence of substorm at Earth has been reported by Hones *et al.* (1984). The detailed characteristics of a plasmoid were obtained from the analysis of plasma and magnetic field observations by satellite ISEE-3 at a distance $\approx -220 R_E$ (*see* Fig. 15). The plasmoid was 75-150 R_E long and it was travelling tailwards at 500 ~ 1000 km/s. It was wrapped around by a separatrix layer within which energetic particle streamed freely toward the tail along the field line. In a recent work on plasmoid, Renuka *et al.* (1992) have shown that the energy content in the plasmoid is large for the larger extent of plasmoid. It is also found that the amplitude of oscillation, which is caused as a result of interaction between the plasma inside the island and the magnetic field outside, is relatively larger for larger islands.

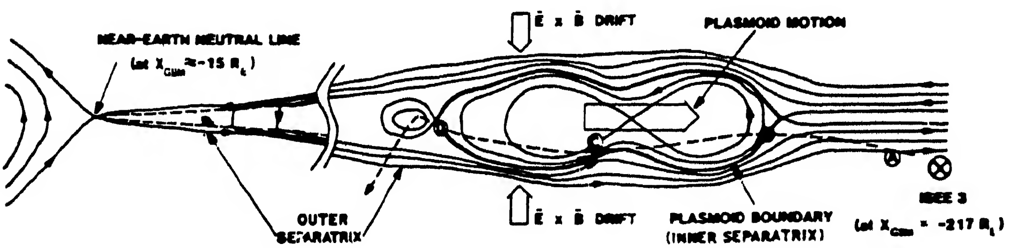

Fig 15 Schematic diagram of a plasmoid observed by ISEE-3 at distant tail (Hones Jr *et al*, 1984).

Summary

In this report a short historical account and a brief review of some recent works done in the field of solar wind-magnetosphere interactions have been presented to describe the present state of art in the field and to bring out the importance of the work done by the scientists in India in comparison with the work done elsewhere. Most of the work done in this field in India is on the theoretical models based on plasma processes including waves and instabilities in the current sheet formed both on the dayside and on the nightside of the magnetosphere owing to the solar wind interaction with magnetosphere.

It has been already been emphasized that the reconnection of the magnetic field plays a central role in the understanding of solar wind-magnetosphere interaction processes, particularly the onset and growth of substorm. Some discussions have

therefore been included on the evidences of reconnection although we do not have contributions in this aspect.

Scientists working in India have made significant contributions not in terms of volume of research papers but in terms of new ideas and models. In particular, the contribution to the theories of driven reconnection suggested by Sundaram *et al.* (1980), Lakhina (1992) and Das (1992) are remarkable. The necessity of an external source for triggering tearing mode leading to reconnection process in the magnetosphere has only recently been realized (Pritchett *et al.* 1991). We believe that the problem of onset of substorm can be understood by these models.

Field-line resonance is another important phenomenon that is related to magnetopause boundary. Many instabilities are possible at the magnetopause and K-H instabilities are considered to be important for the physics of field line resonance that leads to different types of micropulsations. The suggestion made by Uberoi (1989) that the surface waves generated at the magnetopause can successfully lead to field-line resonance has become very useful in understanding the process of micropulsations.

REFERENCES

Arnoldy, R L, (1971) *J. Geophys Res.*, **76**, 5189

Baker, D.N., Bame, S.J., Birn, J., Fieldman, N.C., Gosling, J.T, Hones, E W Jr., Zwicke, R.D, Slarin, J A, Smith, E J, Tsurutani, B T & Sibeck, D G. (1984), *J. Geophys Res, Lett* **11**, 1042

Beichem, J & Okuda, H., (1990) *J Geophys Res.*, **95**, 8133.

Bryant, D.A. & Rigg, S, (1989) Royal Soc. Discussion Meeting· The Magnetosphere, the High Latitude Ionosphere, and their Interactions, p.7-20

Burke, W J, Kelley, M.C., Sagalyn, R C, Smiddy, M. & Lai, S.T (1979) *J Geophys Res., Lett*, **6**, 21

Bowers, E C., (1973a) *Astrophys. Space Sci.* **21**, 339.

Bowers, E C, (1973b) *Astrophys & Space Sci.* **24**, 349.

Buchner & Zelenyi, (1987) *J Geophys. Res.*, **92**, 13456

Chen, J & Palmedesso, P.J, (1986). *J Geophys Res*, **91**, 1499

Cowley, S.W H. (1971). *Cosmic Electrodyn.* **2**, 90.

Das, A C (1990) *Indian J. Radio & Space Phys* **19**, 241

Das, A.C. (1992). *J. Geophys. Res*, **97**, 12275.

Drummond, W E & Rosenbluth, M.N (1962). *Phys. Fluids* **5**, 1507

Dungey, J W., (1958) *Cosmic Electrodynamics* (Cambridge University Press, London)

Dungey, J W., (1961). *Phys. Res. Lett* **6**, 47.

Eastman, T E & Hones E.W, (1979). *J. Geophys. Res*, **84**, 2019.

Fairfield, D H. & Cahil, L.J, (1966) *J. Geophys Res.*, **71**, 155.

Finn, J M & Kaw P K (1977). *Phys Fluids* **20**, 72.

Fu, Z F. & Lee L.C (1985) *Geophys Res., Lett* **12**, 291

Galeev, A A. & Zelenyi L M (1976). *Sov. Phys. J.E T.P* **43**, 1113

Galeev, A A, (1984) *Handbook of Plasma Physics*, Vol. 2, edited by M N. Rosenbluth and R Z Sagdeev, p 305

Haerendel, G, Paschmann, G, Sckopke, N, Rosenbuer H & Hedgecock P C., (1978). *J. Geophys Res.*, **83**, 3195.

Hones Jr, E.W, Birn J., Baker, D W, Baine, S.J., Feldman, W C, McComas D J & Zwicke R.D., (1984). *Geophys. Res. Lett* **11**, 1046

Horton, W & Tajima T, (1988). *J Geophys Res, Lett* **17**, 2741

Ip, W-H & Jin S P, (1992). *J Geophys Res*, (in press).

Lakhina, G S, (1992) *J. Geophys Res*, **97**, 2961

Lakhina, G.S & Schindler K, (1983) *Astrophys & Space Sci* **89**, 293

Lakhina, G S & Schindler K., (1988) *J. Geophys Res*, **93**, 8591

Lee, L C & Fu, Z F, (1985) *J Geophys Res, Lett.* **12**, 105

Lee, L C. & Akasofu S I, (1989) *J. Geophys Res*, **94**, 12020.

Labelle, J & Treumann, R A (1988). *Space Sci. Rev* **47**, 175.

Lambege, B & Pellat R (1982) *Phys Fluids* **25**, 1995

Martin, R F., (1986). *Geophys. J Res*, **91**, 11985

McBride, J.B, Ott, E, Boris, J P. & Orens, J H, (1972) *Phys Fluids*, **15**, 2367

Midgley, J E & Davies L, (1963) *J Geophys Res.*, **68**, 5111.

Min, K W., (1990) *Astrophys. Space Sci.*, **163**, 95.

Nishida, A, (1982) *Magnetospheric Plasma Physics*, edited by A. Nishida (Reidel D. Publishing Company).

Ogino, T, Walker, R T, Ashour-Abdalla M & Dawson J M, (1986) *J. Geophys. Res.*, **91**, 10029.

Otto, A, (1990) *Comput Phys. Commun* **59**, 185.

Parker, E.N, (1963) *Astrophys. J (Suppl Ser.)*, **77**, 177

Paschmann, G, Haerendel, G, Sckopke, N, Rosenbauer, H. & Hedgecock, P.C., (1976). *J. Geophys. Res.*, **81**, 2883

Pachmann,G., Sckopke, N., Baine, S.J, Asbridge, J R., Gosling, J.T., Russel, C.T. & Greenstadt, E.W., (1979). *Geophys Res Lett*, **6**, 209.

Petscheck, H.E (1964) *AAS-NASA Symposium on the Physics of the Solar Flare*, NASA, Special Publ. (ed. W.N. Hess) SP-50, 425

Porkalob, M, (1968) *Phys Fluids* **11**, 834.

Pritchett, P.L. & Wu, C C., (1979) *Phys. Fluids* **22**, 2140

Pritchett, P L, Coroniti, F V., Pellat R & Karimabadi H., (1991). *J. Geophys. Res.*, **96**, 11523.

Renuka, G, Sindhu, M S, & Venugopal, C (1992) *Indian J. Phys.* **66B**, 339.

Rosenbluth, M.N, (1963) *Plasma Physics and Thermonuclear Research*, Vol. 2, edited by M.L. Longmine, J.L. Tuck, & W B., Thompson, p 271.

Russell, C T. & Elphic, R C, (1978) *Space Sci. Rev.* **22**, 681.

Scindler, K, (1974) *J. Geophys Res.*, **79**, 2803.

Scholer, M, (1989) *J. Geophys. Res*, **94**, 8805

Shi, Y, Wu, C C & Lee L.C, (1988). *J. Geophys. Res., Lett.* **15**, 295.

Sibeck, D.G, (1990) *Joint Varenna-Abastumani ESA-Nagoya Potsdam Workshop on Plasma*, p. 63-68.

Sonnerup, B U O., Paschmann, G, Papamastorakis, I, Sckopke, N., Haerendel, G., Barne, S.J, Ashbridge, J.R., Gosling, J.T & Russel, C.T., (1981) *J Geophys Res.*, **86**, 10049.

Southwood, D.J Farrugia, C F & Saunders M A, (1988) *Planet Space Sci* **36**, 503

Spreiter, J R, Summers, A L s & Alksne, A K, (1966) *Planet Space Sci.* **14**, 223

Staharie, S S., Rachide, R R., Spreiter, J.R. & Slaun, J.A., (1989). *J. Geophys Res.*, **94**, 13353

Sundaram, A K, Das, A C. & Sen, A., (1980). *J. Geophys Res., Lett.* **7**, 921.

Uberoi, C., (1984). *J Geophys. Res.*, **89**, 5652

Uberoi, C., (1989) *J. Geophys. Res.*, **94**, 2745.

Vasyliunas, V.M., (1975) *Rev. Geophys. Space Phys.* **13**, 303.

Willis, D M., (1975). *Geophys J R Astron., Soc.* **41**, 355.

Wu, C C Leboent, J N, Tajima, T. & Dawson, J.M, (1980). UCLA. PPG-551 (Center for Plasma Physics and Fusion Engineering, University of California, Los Angeles, USA)

Yeh, T & Axford, W.I (1970). *J. Plasma. Phys*, **4**, 207.

Zelenyi, L M & Kuznetsova, M.M. (1984). *Sov. J. Plasma Phys*, **10**, 190.

MAGNETOSPHERE IONOSPHERE COUPLING

J.H. Sastri*

INTRODUCTION

Satellite exploration of the Earth's near-space environment since the dawn of the space era has greatly helped comprehend the configuration and large-scale characteristics of the magnetosphere. Our knowledge of the global behaviour of the magnetospheric domains and magnetospheric processes is however far from being comprehensive (*see* review of Williams, 1992). Magnetospheric physics thus continues to be an area of concerted research under the on-going Solar-Terrestrial Energy Programme (STEP) and allied ones. Studies especially over the past decade and half using a variety of instrumentation on ground and on orbital/sub-orbital platforms led to the realization that the magnetospheric processes have a profound effect on the other domains of the Earth's near-space environment. It is now established that the magnetosphere and the ionosphere-thermosphere system at high latitudes are strongly coupled and interdependent. The coupling prevails through electric fields, precipitating particles, field-aligned currents, heat flows and frictional interactions. Electrodynamical coupling is by far the most important process linking the magnetosphere with the high-latitude ionosphere-thermosphere system. Electric fields generated in the magnetosphere as a result of solar wind-magnetosphere interaction (magnetospheric dynamo) are mapped down the geomagnetic field lines onto the high-latitude ionosphere where they induce a large scale motion or convection of the ionospheric plasma. The plasma convection induced by magnetospheric electric field affects the characteristics of not only the ionosphere but also of the thermosphere. As the plasma convects through the neutral atmosphere (thermosphere) the ion temperature is elevated owing to ion-neutral frictional heating and this alters the topside plasma scale heights, chemical reaction rates and ion composition. Moreover, at F-region altitudes the neutral atmosphere tends to follow, but lags behind the convecting ionospheric plasma. The resulting ion-neutral frictional heating causes neutral vertical winds and O/N_2 composition changes.

**Indian Institute of Astrophysics, Bangalore 560 034*

These changes, in turn, affect the ionospheric density and temperature structure. Studies based on data from the Dynamics Explorer-2 (DE-2) satellite mission have been quite useful in elucidating the extent of the plasma-neutral coupling at high latitudes and its ramifications (*see* Schunk, 1988 and references therein).

Auroral electron precipitation is another important mode of coupling between the magnetosphere and the high latitude ionosphere-thermosphere This mechanism is responsible for not only the well-known auroral optical emissions (aurora) but is also a source of ion production (due to impact ionization of the neutral atmosphere) and bulk heating of both the ionosphere and neutral atmosphere, and a downward flow of heat from the lower magnetosphere into the ionosphere. The downward precipitating auroral electrons are responsible for an upward field-aligned (Birkeland) currents. The field-aligned currents are concentrated in two principal areas that encircle the geomagnetic pole. At any given local time, the poleward current regions (Region 1 current system) exhibit current flow into the ionosphere in the morning sector and away from the ionosphere in the evening sector, while the equatorward current regions (Region 2 current system) contain current flows in opposite directions. The Birkeland currents that flow into and out of the ionosphere are connected via horizontal currents that flow in the lower ionosphere. These large-scale currents, the auroral conductivity enhancements due to precipitation electrons and the convection electric fields are interdependent and are governed by Ohm's law and the current continuity equation. Models of the 'average' or 'statistical' patterns of high latitude convection, particle precipitation, Birkeland currents and their variations with magnetic activity and IMF B_y and B_z components are available. What is not yet known are the 'instantaneous' patterns of these parameters and their temporal variability on substorm and storm time scales. One of the major theoretical tasks now is to relate the behaviour of these parameters (in space and time) in a self-consistent and quantitative manner.

The high latitude upper atmosphere also exerts a significant influence on the magnetosphere Conductivity enhancements due to auroral particle precipitation can modify convection electric fields, large-scale current systems and the electrodynamics of the entire magnetosphere-ionosphere system. On polar cap and auroral field lines an additional feedback mechanism operates through a direct flow of plasma from the ionosphere to the magnetosphere. In the polar cap, continual outflow of thermal plasma from the ionosphere (polar wind) represents a significant source of mass, momentum and energy for the magnetosphere. On auroral field lines, hot ionospheric plasma is injected into the magnetosphere via ion beams, conics, rings and toroidal distributions all of which, along with the polar wind distributions, are non-Maxwellian and potentially unstable. The outflowing ionospheric plasma may thus be a source of turbulence for the magnetosphere. Though the ionospheric ions feed the magnetosphere at all latitudes, the fraction of magnetospheric plasma that has its origin in the ionosphere is yet to be established. The reason why energetic ion flows are more frequent at solar maximum than at minimum is not known. Much is yet to be learned about the auroral acceleration mechanisms and altitudes of

acceleration It is clear that although significant progress has been achieved in identifying the major routes of the two-way coupling between the magnetosphere and the high latitude ionosphere-thermosphere system, there are a large number of important physics issues to be resolved regarding the coupling processes. Further details of the scientific problems in this area of much current research can be found in the review by Schunk (1988)

The influence of magnetospheric processes, though dramatic at the high latitudes, is not restricted to that region but extends to lower latitudes as well because of electrodynamical coupling of the high latitude-low latitude ionospheres especially during disturbed geomagnetic conditions The well-known changes in the geomagnetic field at low latitudes during geomagnetic storms (which reflects in the equatorial D_{st} index) and the attendant ionospheric storms, which were the topics of much early research in Geomagnetism and Aeronomy both in India and elsewhere, are pointers to the coupling of the equatorial upper atmosphere to that at high latitudes and the magnetosphere. The perspective that the equatorial ionosphere is not really as isolated as is commonly believed but responds sensitively to high latitude and magnetospheric processes is, however, a fairly recent development. There is currently a great scientific interest in evaluating and understanding the response of the equatorial upper atmosphere to processes involved in the linked interactions of the solar wind with the magnetosphere, and of the magnetosphere with the high latitude ionosphere on various time scales from tens of seconds (micropulsations), to minutes (micropulsations, sudden commencements), to tens-and-hundreds of minutes (substorms) and finally to one-to-three days (geomagnetic storms). In the following I shall try to summarise the current status of our knowledge of the subject, the major unresolved scientific problems and the approaches to be followed to tackle them. Further details on some of the topics covered in this report can be found in the recent reviews by Reddy (1989), Sastri (1990), Abdu *et al.* (1991), Fejer (1991), Rostoker (1993) and Somayajulu and Cherian (1993).

Geomagnetic sudden commencements (sc's)

The geomagnetic sudden commencement (sc) is conventionally understood in terms of a compressional hydromagnetic (HM) wave set up by the impact of a shock in the solar wind with the magnetosphere. The impulsive increase in H-component of geomagnetic field at ground level that characterises the main impulse (mi) of the sc is generally attributed to the abrupt increase in magnetopause current due to shock-induced compression and accompanying dynamic processes in the magnetosphere. The complex latitudinal and local time dependence of the sc waveforms, nevertheless, indicated that the structure and amplitude of the sc is determined not only by magnetospheric current sources but also by those nearer to the Earth. Observations with magnetometers on ground and in space, VHF coherent backscatter and forward scatter radars and HF Doppler radars have, in fact, shown a definite contribution of ionospheric electric fields and currents to the sudden. commencement part of geomagnetic storms at high latitudes as well as dip equatorial latitudes. Indian

scientists have made noteworthy contributions to the realisation of the role of ionosphere in the manifestation of the sc (e.g. Rastogi, 1976; Reddy *et al.*, 1981).

According to the current understanding (Araki, 1977) the disturbance field of an sc, D(sc), is composed of three components as follows:

$$D(\mathrm{sc}) = DP(\mathrm{pi}) + DL\,(\mathrm{mi}) + DP(\mathrm{mi})$$

where DP(pi) and DP(mi) are electric fields of polar origin that manifest during the preliminary impulse (pi) and main impulse (mi) of the sc respectively, and DL(mi) is the field due to magnetospheric sources that predominates at low latitudes. The pi that precedes the mi of the sc manifests as a distinct negative impulse (duration about 1 min) in H-field simultaneously near the dip equator on the dayside and at high latitudes in the afternoon sector, and also as a positive impulse at high latitudes in the forenoon sector. It is therefore termed as the preliminary reverse impulse (pri) and the corresponding sc as sc^r. It is widely accepted now that the equatorial pri is due to the extension to the dayside equator of the DP2 type ionospheric current system driven by the dusk-to-dawn electric field transmitted to the polar ionosphere along the magnetic lines of force by anisotropic HM waves from the compressional wavefront propagating tailward in the dayside magnetosphere. Theoretical studies showed that the Earth-ionosphere waveguide facilitates instantaneous transmission of a suddenly imposed electric field on the polar ionosphere to the dip equator as a zeroth order transverse magnetic (TM) electromagnetic wave. Moreover, multidimensional numerical calculations of the global distribution of ionospheric currents caused by field-aligned current flows into and away from the ionosphere (source currents) predict that the intensity of the current reduces with decrease of latitude, but gets enhanced at the dayside equator in spite of the shielding effect of the enhanced Cowling conductivity. This prediction is in good agreement with the observed latitudinal variation of the pri amplitude.

The HF Doppler radar observations of the mid-eighties showed that the polar electric field responsible for the pri of sc* penetrates to lower latitudes not only on the dayside but also on the nightside. But detection of its extension to the nightside dip equator eluded researchers because it is rather difficult to detect the pri in ground level magnetic recordings in the nightside dip equatorial region due to the much reduced ionospheric conductivity at night (partly also due to the fact that the sense of the pri is the same as of mi). Careful analysis did, however, show that the pi current system extends to the nightside equator and produces a small but observable magnetic effect as a stepwise sc (or sc with double-step mi) simultaneous with the sc* on the dayside equator (Araki *et al.*, 1985). Independent verification of this identification particularly from F-region vertical plasma motions that are to be expected has not been made. The most recent HF Doppler radar observations in India (Sastri *et al*, 1993a) did provide the first and direct experimental evidence of F-region vertical plasma motions due to sc-associated electric fields in the night time dip equatorial ionosphere (Fig.1). They substantiate the view based on theory and

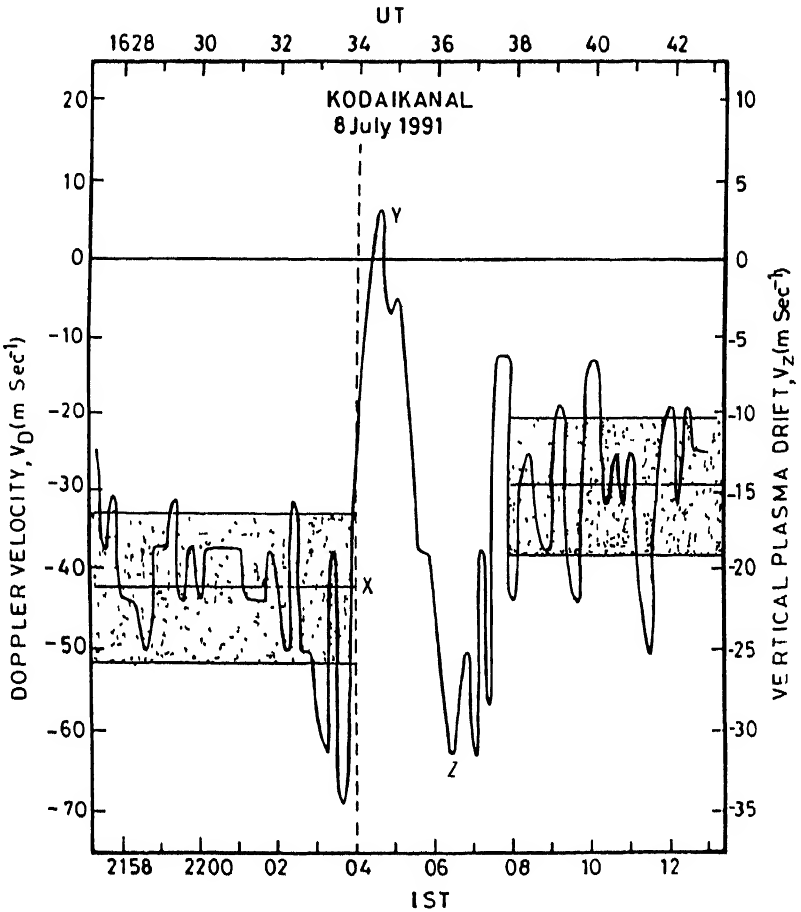

Fig.1 Time variation of F-region Doppler velocity, Vd (vertical plasma drift= Vd/2) over Kodaikanal around the time of the geomagnetic sudden commencement on 8 July 1991. Note the unambiguous cessation and small upward reversal of the ambient downward plasma drift at the time of the preliminary reverse impulse (pri) of the sc* (vertical dotted line) at high latitudes (after Sastri *et al*, 1993a)

ground level magnetic observations that the dusk-to-dawn electric field imposed on the polar ionosphere with the onset of pri of sc* is instantaneously transmitted to the dip equator on the nightside as on the dayside. Although progress has been achieved in understanding the complex electrodynamical coupling of the magnetosphere polar ionosphere-equatorial ionosphere domains at the time of sc's there is need for further theoretical and experimental work. For example, there are points of disagreement between observations and theoretical simulations particularly of the amplitude of pri at the nightside dip equator even from the sparse database available. Experimental characterization of the local time variation of the amplitude of the perturbation electric fields at dip equatorial latitudes associated with pri of sc* is essential for a rigorous assessment of the theoretical models (which are under continuous refinement), and to understand the physical factors that control the penetration of polar electric fields to lower latitudes. Measurements of equatorial electric fields along with rapid-run magnetograms are also needed for a large number of sc events occurring at different local times to ascertain the relative contributions of *DL*(mi) and

DP (mi) fields, both of which prevail during and after mi of the sc (the polarity of the electric field due to *DP*(mi) will be opposite between day and night while that due to *DL*(mi) will be independent of local time).

A fundamental issue that has received very little attention so far is the plausible response of the polar and equatorial ionosphere to sudden magnetospheric expansions, i.e. to negative sudden impulses, SI's (SC and SI are the same except that the latter are not followed by geomagnetic storms). The lone Japanese work of late-eighties based on magnetic observations on ground and by satellites showed that the SI waveform is quite complex and dependent on local time and latitude, and that magnetospheric electric fields transmitted via the polar ionosphere are involved (Araki and Nagano, 1988). The physical situation that is obtained during sudden magnetospheric expansions, therefore, merits to be explored with VHF backscatter radar, magnetometer and HF Doppler radar experiments available in the country complemented by theoretical work.

Geomagnetic micropulsations

Rapid variations in the Earth's magnetic field are called micropulsations which manifest as continuous (Pc) or irregular pulsations (Pi). Continuous pulsations (Pc) are classified into five groups, Pc 1 to Pc5, according to their periods. The period ranges in seconds of Pc 1 to Pc 5 are 0.2-5, 5-10, 10-45, 45-150 and 150-600 respectively. The corresponding frequency range is 1.6 mHz to 5 Hz which is the ultra low frequency (ULF) domain. Significant additions to our knowledge of geomagnetic micropulsations caused by ULF hydromagnetic (HM) waves have been made over the past decade both on the theoretical and experimental fronts. Noteworthy theoretical investigations are the modelling of the impulse excitation of compressional cavity mode oscillations and their coupling to toroidal mode field line resonance oscillations. On the experimental side, satellite data have been analysed to characterise the various modes of HM waves in the magnetosphere. Moreover, coherent and incoherent scatter radars have been employed to evaluate the latitudinal, longitudinal and altitude structures of the ionospheric electric fields associated with the ULF waves. Despite the progress achieved, our knowledge of ULF HM waves in the Earth's near-space environment is deficient with regard to their propagation in the ionosphere in general and to equatorial latitudes in particular. The observational knowledge of the ground-level geomagnetic micropulsations at equatorial latitudes remains very sparse and that of ionospheric pulsations associated with ULF waves practically nonexistent. Information on ionospheric electric fields associated, for example, with Pc5 pulsations is confined to only the high latitude zone It is pertinent to mention here that the nature and origin of ionospheric perturbations at equatorial latitudes associated with geomagnetic micropulsations is a subject of considerable interest and importance especially from the view point of magnetosphere-ionosphere coupling.

Noteworthy developments have taken place in India in the past two years

regarding studies of equatorial geomagnetic micropulsations and related ionospheric effects. One is the operation since 1991 of a 3-station network for recording of pulsations in the Pc3 - Pc4 range using induction sensors. The three stations which are carefully chosen are Tirunelveli (under the influence of equatorial electrojet), Sabhawala (close to the Sq focus) and Alibag (in between the two stations). The other is the realisation of HF Doppler radar stations at Waltair, Trivandrum, Nagpur and Delhi for studies of small-scale (in space and time) dynamics of F-region. Doppler radars are in operation at Kodaikanal and Trivandrum for a long time. Data from this network along with those from the magnetometer network in the country can be expected to yield new information on the characteristics of Pc 3 to Pc 5 pulsations which, together with theoretical work, will help in understanding the resonant regions and modes of propagation of HM waves in the equatorial ionosphere. It is to be highlighted here that the HF Doppler radar is the most sensitive tool available for studies of pulsation-related ionospheric variations. The potential of the Doppler radar was demonstrated by Indian scientists recently through a study of the ionospheric response to the Pc5 pulsation event on 24 March 1991 (Sastri *et al.*, 1993b). Measurements of Doppler velocity of F-region echoes over Kodaikanal near the dip equator on this day revealed quasi-periodic variations in the period band 6.4 to 10.7 min, concurrent with ground level pulsations in the Pc5 range (Fig.2). The characteristics of the F-region Doppler velocity oscillations strongly suggest that they are due to variations in the vertical plasma drift induced by time-varying electric fields associated with the ULF magnetic pulsation activity. Signatures of pulsation electric fields are also observed at E-region altitudes for this event with the VHF backscatter radar at Trivandrum. The source region and mode of propagation of the pulsation electric fields evidenced in this event are not clear at the moment. Further work on these lines is, therefore, necessary to comprehend the nature and origin of micropulsations and related ionospheric effects at equatorial latitudes.

Effects associated with geomagnetic activity

Geomagnetic activity (represented by indices like AE and D_{st} derived from ground-level geomagnetic recordings) is an insignia of changes in the magnetospheric and ionospheric current systems at times of southward IMF B_z and enhanced solar wind flow speed. Studies of the characteristics of the equatorial ionosphere (electric fields, neutral winds and composition, latitudinal structure of F-region plasma density, occurrence of irregularities, etc.) under disturbed geomagnetic conditions (storms and substorms) have a long history with the pioneering works devoted to the characterization of ionospheric storms as seen, for example, in the F-region plasma density. Equatorial recordings of electric and magnetic fields being cleaner than those at auroral latitudes (particularly from the viewpoint of spatial structuring) have the potential to contribute to the overall understanding of substorms/storms, which are telltale signatures of solar wind-magnetosphere-ionosphere coupling. Impressive studies made over the past three decades stand testimony to the merit of equatorial observations for the understanding of magnetosphere-ionosphere coupling.

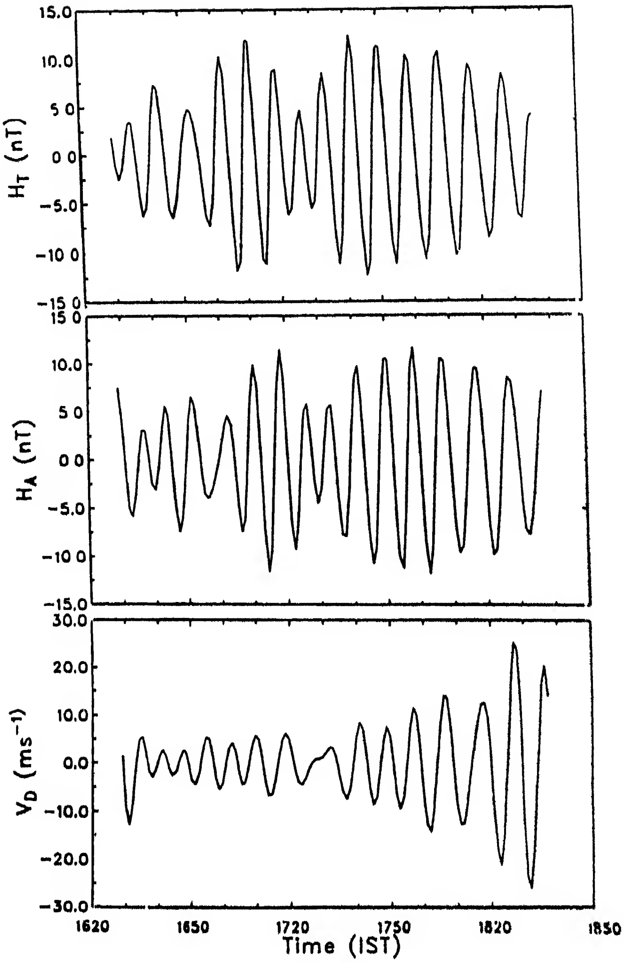

Fig.2. Variation of geomagnetic H-field at Trivandrum (Ht) and Alibag (Ha) and Doppler velocity (Vd) of F-region reflections over Kodaikanal on 24 March 1991. The time series shown are filtered (6.4 < T < 10 67 min) versions of the raw data. Note the concurrent oscillations in the Pc5 range in H-field at Trivandrum and Alibag and in ionospheric Doppler velocity at Kodaikanal (after Sastri *et al.*, 1993b).

As far as ionospheric electric fields are concerned, it is known from early sixties that the equatorial dynamo region currents in general and the equatorial electrojet in particular exhibit a close temporal relationship to high latitude geomagnetic disturbances. This relationship was later shown to extend to IMF B_y, which effectively controls the solar wind-magnetosphere-high latitude ionosphere interactions. The B_y modulation of the equatorial electric field or the F-region vertical drift associated with it is spectacularly seen on short time scales of 1-2h during DP2 events, and at times of sudden transitions in B_y orientation from south to north or vice versa. The current understanding is that two broad categories of electric field disturbances prevail at equatorial latitudes under magnetic storm/substorm conditions. The first category are the transient (1-2h duration) fields that manifest in association with sudden swings in the B_y and isolated substorm activity. The amplitude and frequency of occurrence of these perturbation fields depend on local time. Simultaneous measurements of electric fields at a latitudinal network of incoherent scatter radars showed that the transient disturbances in equatorial electric fields are closely

associated with rapid changes in magnetospheric convection which is controlled by B_z. They thus represent the signatures of prompt penetration of magnetospheric/high latitude electric fields into the equatorial ionosphere. Studies based on magnetometer and ionosonde recordings at equatorial stations distributed in longitude substantiate the understanding. Theoretical studies, in particular the global models of electric fields based on the convection approach, which treat the problem of electric field penetration in a comprehensive and realistic manner, have been quite successful in explaining the basic characteristics of the equatorial transient electric fields observed at times of sudden changes in B_z and substorm activity (i.e. with sudden changes in the polar cap potential drop). There is, however, a need for further theoretical studies as there are some points of major disagreement between theory and experiment and some ill-understood features of transient electric fields. The models are not able to explain, for example, the preferential response of equatorial electric field to northward turnings of B_z than to southward turnings and their persistence for about 2 h. It is also not clear why composite electric field disturbances (due to both increases and decreases in magnetospheric convection), evidence for which was recently unearthed by Sastri *et al.* (1992 a, b), are not commonly seen during substorms as expected from theory. The amplitude of the transient electric fields estimated from observations is also sometimes much larger than model predictions. Innovative theoretical studies and refinement of global convection models are necessary to comprehend the physical processes that control the penetration of high-frequency magnetospheric/high latitude electric fields into the dip equatorial region. This work is challenging as it involves handling of subtle points of magnetospheric physics and the complex magnetosphere-ionosphere-thermosphere interactions. On the experimental side, sizeable and reliable databases of equatorial electric fields need to be developed for the different longitude sectors (such a database is currently available only for the American sector) to help assess the theoretical predictions of substorm-related electric fields. The databases will also help develop eventually models of electric field patterns for different levels of geomagnetic activity, which serve as vital inputs for quantitative modelling of related phenomena like the equatorial ionization anomaly and equatorial spread-F.

The second category of electric field disturbances are the long-lasting (several hours, duration) and slowly-varying types which manifest long after the onset of magnetic storms and usually in their recovery phase. These persistent disturbances, whose polarity is opposite to the normal quiet day pattern at all local times, are widely considered to result from the ionospheric 'disturbance dynamo' mechanism. The current status of understanding of the physical processes that control the manifestation of these electric fields is not satisfactory. This is typified by several unsettled questions like why such fields are not always seen even when clearcut signatures of modifications in global thermospheric circulation (the important ingredient of 'disturbance dynamo' process) are evidenced at mid-latitudes. The origin of persistent electric field perturbations seen in some storms that do not seem to be of 'disturbance dynamo' type is also not known. Further in-depth theoretical and data-based studies are essential to advance our knowledge of the delayed and enduring

electric field disturbances in the dip equatorial region

It is known for a long time that the equatorial ionization anomaly (EIA), a characteristic daytime feature of the latitudinal distribution of F-region plasma density in the equatorial ionosphere, undergoes significant modifications during geomagnetic storms. This is not surprising because the essential element of the 'fountain' process responsible for the EIA is the vertical plasma drift associated with the zonal electric field. Since the electric field gets modified on different time scales during storm conditions as detailed before, so will the EIA. It is important to realise in this context, however, that besides electric fields, the properties of the equatorial thermosphere can also get modified during storms due to high-latitude heating effects, and must be given due attention (Burrage *et al.*, 1992; Burns and Killeen, 1992). Though versatile numerical models to simulate EIA are available, quantitative studies of EIA response to specific substorms/storms are not done on the scale required. This is primarily due to lack of simultaneous information on the forcing parameters (electric fields, neutral winds, neutral composition, etc.) and their temporal variations during the time period of interest. It is, therefore, important to pursue further studies focusing on the disturbance component of the forcing parameters, their relationship to the phase of the geomagnetic disturbance and their individual and combined effect on the specific observed features of EIA for individual substorm/storm events. Some progress has already been achieved through analysis and modelling of data obtained from the campaigns of international programmes like SUNDIAL, in which Indian scientists have actively participated (e.g. Abdu *et al.*, 1993). These efforts should be continued in the coming years under the Indian Solar-Terrestrial Energy Programme (I-STEP) to advance our understanding of the storm-time behaviour of EIA in quantitative terms.

There is compelling evidence for energetic particle precipitation from the magnetospheric ring current into the equatorial ionosphere, particularly in the South Atlantic magnetic anomaly region during magnetic storms. Particle precipitation is also known to occur even during geomagnetically quiet times although the precise diurnal pattern is unknown at the moment. Knowledge of the global characteristics of particle precipitation in the equatorial zone is necessary for different levels of geomagnetic activity to evaluate its role, for example, in the storm-time thermospheric heating and in causing 'negative' ionospheric storms. It is pertinent to add here that the origin of the 'negative' ionospheric storms which are sometimes seen at equatorial stations in association (*see* Sastri, 1990; Batista *et al.*, 1991 and references therein) is unclear at the moment. Though changes in the neutral composition are widely considered as responsible for the reductions in F-region peak plasma density that characterise the 'negative' storms, the physical mechanism(s) responsible for the composition changes is yet to be understood. The feasible way to advance our knowledge of the energetic particle precipitation and its effects is to attempt groundbased photometry of night airglow emissions (N2 1N 391.4 nm; OI 777.4 nm) that bear signatures of particle precipitation. This requirement is already projected in the I-STEP proposal.

Indian researchers have made significant contributions to the current knowledge of magnetosphere-high latitude ionosphere-low latitude ionosphere coupling. The key to further progress in this area of interdisciplinary research lies in vigorously pursuing the programme of systematic measurements of the key parameters of the equatorial ionosphere-thermosphere system using the multistation/multidiagnostic approach. These equatorial data sets are to be collated with those at other latitudes/ longitudes and satellite observations of solar wind plasma and magnetic field and indices (AE, AU, AL, AO, D_{st}) derived from groundbased magnetic observation, and interpreted through complementary modelling work. The ground situation of facilities in the country for experimental work of this nature is fairly comfortable, owing to funding infused in national programmes like AICPITS in recent times. The existing and upcoming facilities should be effectively used for addressing the unresolved problems in a concerted manner. The current scene of theoretical and modelling work in the country is rather unsatisfactory. Specific well-planned initiatives are to be made to develop theoretical expertise in the country that finds direct and immediate application in interpreting the observations The fusion of experiment and theory, if planned and organised well, will go a long way in unravelling the obviously complex physical processes underlying the magneto-sphere-ionosphere coupling.

REFERENCES

Araki, T , (1977). *Planet. Space Sci*, **25**, 373

Araki, T , Allen, J.H. & Araki, Y., (1985) *Planet. Space Sci*, **33**, 11.

Araki, T & Nagano, H (1988). *J. Geophys Res*, **93**, 3983.

Abdu, M.A., Walker, G.O., Reddy, B M., de Paula E.R., Sobral, J.H A , Fejer, B G & Szuszczewicz, E.P., (1993). *Ann. Geophysicae*, **11**, 585.

Abdu, M.A., Sobral, J.H.A., de Paula, E R., & Batista, I.S., (1991). *J. Atmos Terr. Phys*, **53**, 757.

Batista, I.S., de Paula, E.R., Abdu, M.A.,Trivedi, N.B & Greenspan, M.E. (1991). *J. Geophys Res*, **96**, 13943.

Burns, A.G., & Killeen, T.L., (1992) *Geophys. Res. Lett*, **19**, 977

Burrage, M.D., Abreu, V.J., Orsini, N , Fesen, C.G. & Roble, R.G. (1992). *J Geophys Res*, **97**, 4177.

Fejer, B.G., (1991). *J. Atmos. Terr. Phys*, **53**, 677.

Rastogi, R.G., (1976). *J. Geophys. Res.*, **81**, 687.

Reddy, C.A. Somayajulu, V.V. & Visvanathan, K.S , (1981). *J. Atoms. Terr. Phys*, **43**, 817.

Reddy, C A., (1989). *Pure Appl. Geophys*, **131**, 485

Rostoker, G , (1993). *J. Atmos. Terr. Phys*, **55**, 985.

Sastri, J.H , Ramesh, K.B. & Karunakaran, D., (1992a). *Planet Space Sci*, **40**, 95

Sastri, J.H., Ramesh, K.B. & Rao, H.N.R., (1992b). *Geophys. Res. Lett.* **19**, 1451.

Sastri, J.H., Rao, J.V.S V. & Ramesh, K.B., (1993a). *J. Geophys. Res*, **98**, 17517

Sastri, J.H., Ramesh, K.B., Rao,D.R K. & Rao, J.V.S.V. (1993b). *J. Atmos. Terr. Phys*, **55**, 1271.

Sastri, J.H., (1990). *Indian J.Radio Space. Phys*, **19**, 225.

Schunk, R.W., (1988). *Proc. XXVII Cospar Meeting*, pp 52-110

Somayajulu, V.V. & Cherian, L., (1993). *Curr. Sci*, **64**, 579.

Williams, D.J., (1992). *Rev. Geophys*, **30**,183.

THE MIDDLE ATMOSPHERE : COUPLING FROM ABOVE AND BELOW

A.P. Mitra*

In this article, an outline is given of recent activities in the middle atmosphere following the International Middle Atmosphere activities in the 80s with special reference to progress in India in terms of establishment of new facilities (such as the MST Radar) and new angles (such as global change-related changes in the middle and upper atmosphere and the ionosphere). In the international scene, three major programmes requiring quantitative identification of the role of the middle atmosphere are: The IGBP (International Geosphere-Biosphere Programme), the SPARC (the Stratospheric Processes And their Role in Climate) and the STEP (Solar Terrestrial Energy Programme). These are discussed in the context of the middle atmosphere, as also some of the new questions raised, in particular the question of global change and the Ionosphere.

1. IMAP AND FOLLOW-UP PROGRAMMES

The middle atmosphere, defined as the region between the tropopause and the mesopause (i.e. roughly between 10 and 85 km), was studied very intensively during the International Middle Atmosphere Programme in the 80s: the Indian programme spanned over a period of seven years from 1982 to 1989. The thrust was quantitative assessment of the dynamics, energetics and the composition of this region and the forcing functions from above and below. The Indian results relating to these programmes have been published extensively.[1] A major aim, from the Indian point of view, was to evolve a first order Reference Middle Atmosphere over India including at least the following elements:

(i) Concentrations of the main atmospheric constituents: N_2, O_2 and the neutral temperature,

(ii) Distribution of the interacting minor constituents: greenhouse molecules CO_2, CH_4, NO_x, CFCs, Ozone and Aerosols,

* *Bhatnagar Fellow (CSIR), National Physical Laboratory, New Delhi 110 012*

(iii) Electron and ion distributions; preferably also the nature of the ions, and
(iv) Profiles of wind motions of different types.

There were two special Ozone Intercomparison Campaigns: the Ozone Intercomparison (23-31 March 1993) and Diurnal Variation (3-8 Dec. 1987) carried out jointly with Soviet scientists with payloads from both India and the USSR using a total of 37 M-100 Rockets fired within two periods of roughly a week each. There were two Equatorial Wave Campaigns, first in June 1984 and later in January to February 1986 involving deployment of a total of 77 RH-200 Rockets from all the three ranges. Measurements of special interest in the context of global change activities were those of a number of halogenated hydrocarbons with balloon flights launched from Hyderabad on 27 March 1985 and 26 March 1987 by the Physical Research Laboratory, Ahmedabad, jointly with the Max Planck Institut für Aeronomy. Three comprehensive reports dealing with different IMAP Campaign-related experiments, the first for conductivity measurements[2], the second on estimates of aerosol features derived from UV-B and Multiwavelength Radiometers[3], and the third on D and E region electron and ion densities[4].

After the IMAP, the initial efforts were primarily focussed on an analysis of the large quantity of data collected during this period on dynamics, ionization, minor species and radiation. But soon the focus changed with the emergence of large-scale activities on global change-related problems and the introduction of SCOSTEP Programme STEP (Solar Terrestrial Energy Programme). Nevertheless, information generated during the MAP came to be of special value even for this activity. Of special importance were the balloon-borne measurements of ozone carried out intensively during this period, the profiles of CH_4, N_2O, H_2O and aerosol composition and information generated on turbulence and gravity waves. Since an inventory of greenhouse gases (particularly CO_2, CH_4, N_2O) is of special importance in global change activities, new measurement systems came up involving sensitive gaschromotography to estimate methane emission from paddy fields, from wetlands and ship-borne measurements of CO_2 flux in ocean areas. Although IGBP as such was limited to the tropospheric region and to the interaction of minor species of biogenic origin only, it soon became clear that a key role is played by stratosphere-troposphere interchange processes, and , in particular, the transport of ozone from the stratosphere to troposphere and water vapour from troposphere to stratosphere. SPARC is a result of this recognition. In this, a major contribution came from the availability of long-term measurements of the Lidars in France and monitoring of tropospheric "breaks" by ST/MST Radar systems. Since the changing composition of the middle atmosphere results in a changing scenario of radiative energy transfer, major efforts came up in modelling the nature of the changing stratosphere and the mesosphere. The USA introduced a new programme called "The Middle Atmosphere Research Initiative (MARI)". A programme of far-reaching consequence is the Central Equatorial Pacific Experiment (CEPEX) conducted over the Central Equatorial Pacific Ocean during March 1993 under the overall leadership of the Centre for Clouds, Chemistry and Climate at San Diego to test the "thermostat

hypothesis" that could contain a runaway warming. Another remarkable development was the discovery of the "ozone hole" in the Antarctic in 1985 and the series of follow-up campaigns relating to the mechanisms causing this depletion (formation of polar stratospheric clouds, low temperatures, composition of the cloud, changes in the concentrations of ClO, NO_x and H_2O, etc.). In this, Indian contributions are also fairly appreciable. India has been participating in the balloon-borne measurements over the Antarctic at its own station, Dakshin Gangotri, and later at Maitri from 1987 onwards.

The emergence of a network of MST Radars (including one at Gadanki in India–(Fig. 1), capable of sensing not only the troposphere and the stratosphere but also the mesosphere, and the various coupling processes between the regions have brought in a new dimension in the whole area. Of special interest are the conditions of "tropopause break", the discovery of a polar mesospheric structure (coupled with noctilucent clouds) and a new capability of looking at turbulence and gravity waves with very high resolution.

These various aspects are outlined in this article. Certain projections for future activities are also outlined.

Fig 1 Indian MST Radar Antenna Array System (Courtesy MST Radar Facility)

2. PRINCIPAL QUESTIONS

In the context of global change problems and existence of coupling between different levels in the Earth space system, the middle atmosphere questions have

taken a different shape from that originally envisaged at the beginning of the MAP Programme One significant difference is the addition of anthropogenic trace gases into the atmosphere causing changes in atmospheric composition and in the global climate.

The solar-terrestrial connection as visualized by the STEP Programme is shown in Fig. 2 and the specific elements of coupling between chemistry, radiation and dynamics in the middle atmosphere are given in Fig. 3. The biogenic connection of the trace gases of greenhouse interest are given in Fig. 4

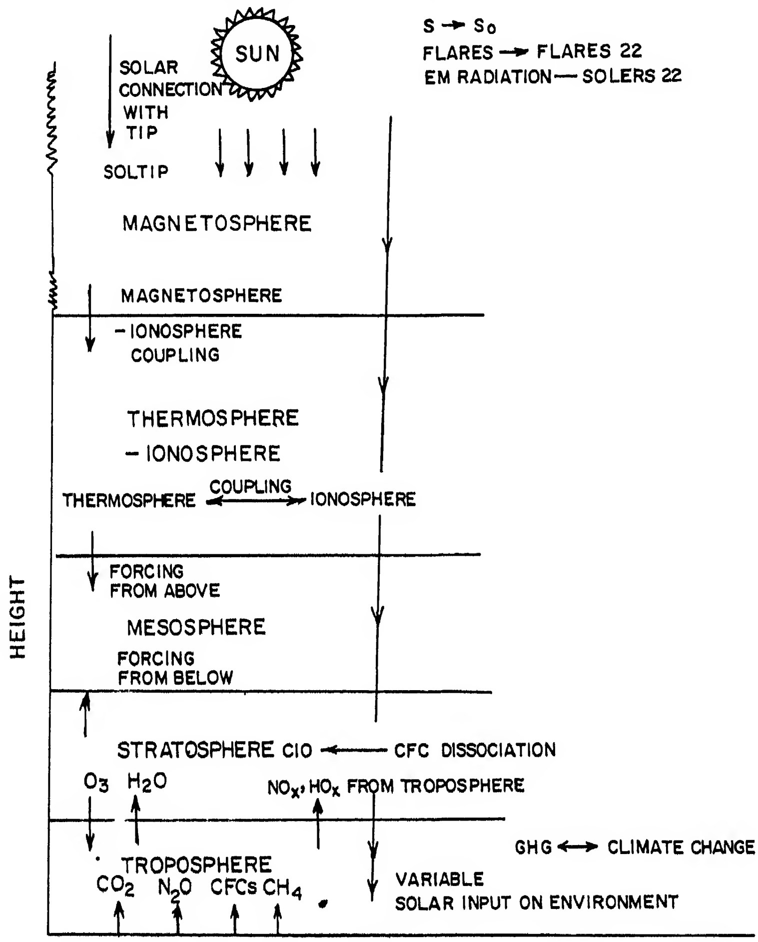

Fig.2 Solar-Terrestrial Environment Connections (Reference STEP Document)

It is clear that the connections (or coupling) are of different kinds. One kind is the transport of gases of biogenic origin into the atmosphere (and, for long-lived species, also into the stratosphere either in original form or in modified form). Fig. 5 shows the various transformations that occur as greenhouse gases rise through troposphere to stratosphere to mesosphere. This is a coupling from below. Another kind is the entry from above of chemically important trace gases, such as nitric oxide generated from impact of solar protons during flare events (penetrating during large

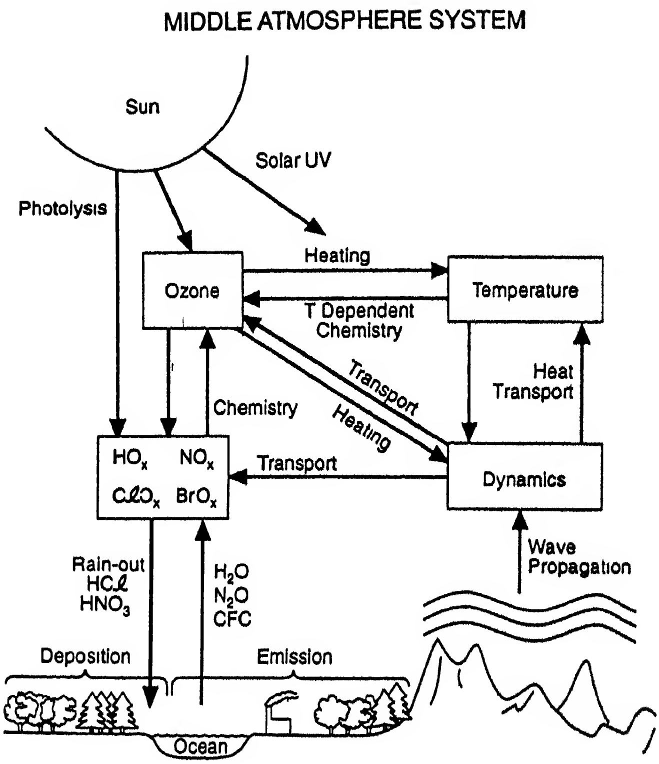

Schematic picture of the coupled physical/chemical processes in the middle atmosphere Arrows indicate major external inputs and internal links

Fig 3 Chemical-Radiative-Dynamic Connections in the Middle Atmosphere (from U.S. Middle Atmosphere Research Initiative Document)

events to levels as low as 50 km) and from the ionic reaction NO$^+$ + e. A third kind of connection is through the electric field and the process of global electrical circuit through the positive-negative ions that exist in equal numbers even in the so-called non-ionized region below 60 km.

The main questions arising now can be summarized as follows:

(i) *Radiative processes at all levels which determine the basic structure of temperature and hence those of winds and chemical constituents of the atmosphere:* In this connection one should know the nature of variation in solar absorption at each particular level: absorption at each level is linked to the Earth's surface, to all other levels and to space. One is concerned not only with the solar UV output but also with energetic particles from the Sun and aurora.

(ii) *The role of long-lived chemicals (both in radiative processes and in chemistry) emitted from the biosphere and from anthropogenic sources,*

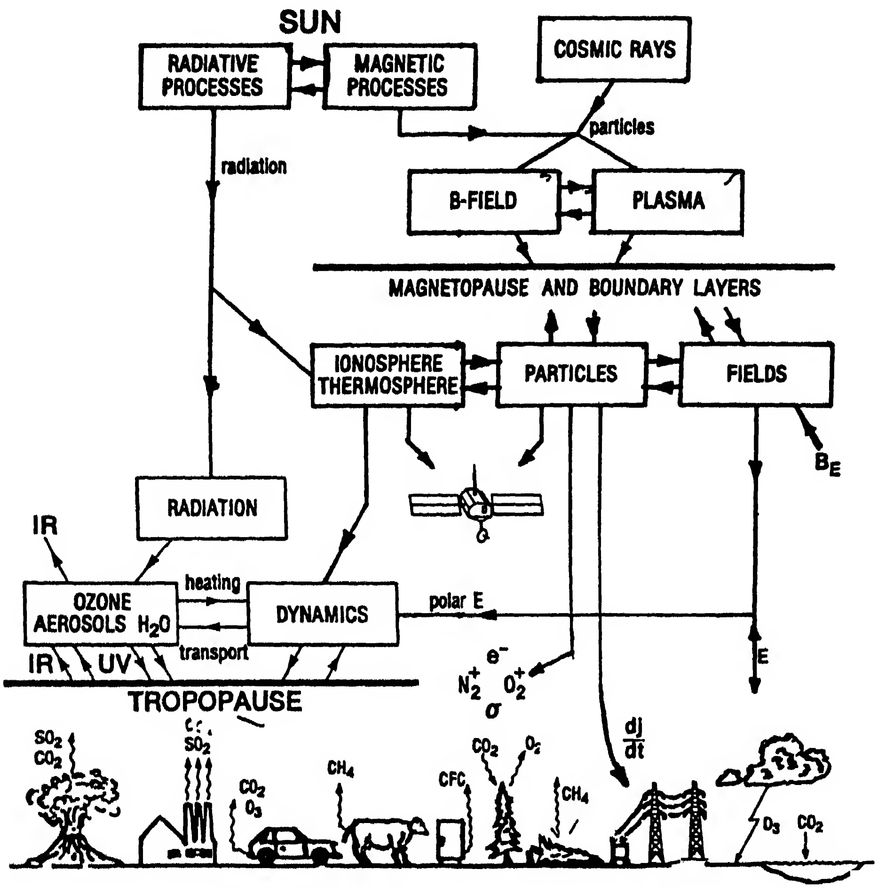

Fig.4 Interaction between principal domains of solar-terrestrial system (after STEP document)

such as CFCs, CO_2, CH_4, and N_2O: Each one of these constituents contributes to the radiative part directly and also exerts a control over the distributions of other constituents controlling the chemistry of the troposphere and the stratosphere, such as ozone and water vapour.

(iii) *The question of whether changes in the greenhouse gases affect the mesospheric region, and, if so, to what extent :* This has been receiving attention only very recently. There is an important question of relative contributions between natural and anthropogenic forcing functions which arise from: (a) solar radiation, (b)volcanic eruptions, (c) the increase in concentrations of greenhouse gases, and (d) aerosols.

(iv) *The generation, propagation, interaction and absorption of waves on all scales including gravity waves, Rossby waves and tides.*

(v) *The problem of ozone hole:* conditions of formation and differences between the arctic and the antarctic holes and the mechanisms for reduction at lower latitudes.

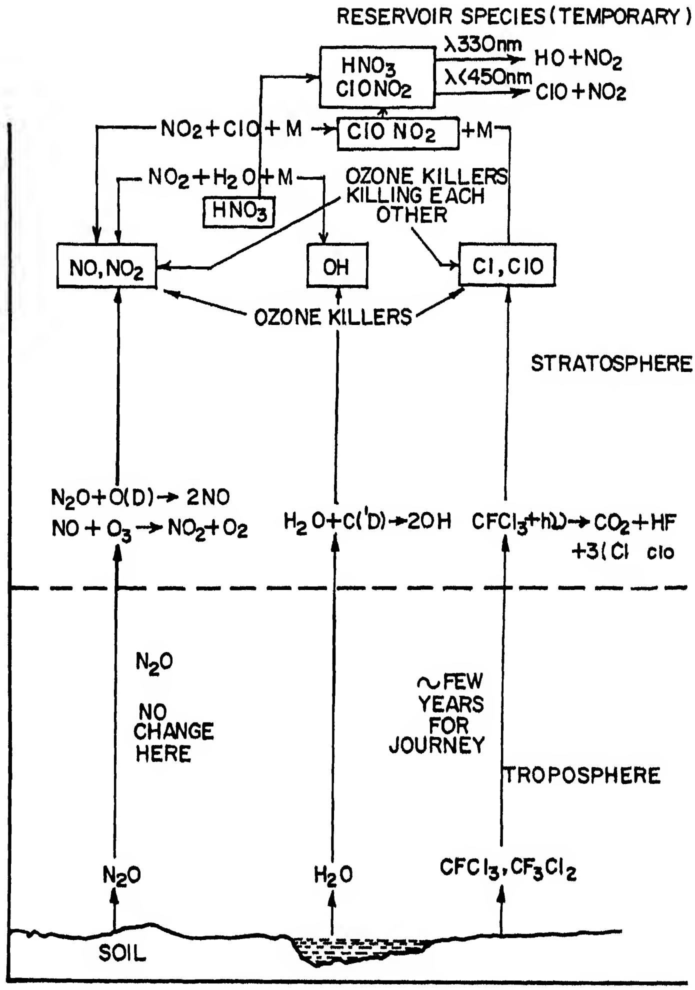

Fig.5 Transformation of important minor species as these travel upwards from the surface through troposphere to the middle atmosphere and the upper atmosphere

(vi) *The problem of ozone changes from specific events and antropogenic inputs:* natural events include volcanic eruptions like Mt Pinatubo; anthropogenic inputs such as NO_x emissions from biomass burning.

(vii) *How the middle atmospheric ionization changes when atmospheric composition changes under global change conditions.*

4. DISTRIBUTION OF MINOR SPECIES IN THE ATMOSPHERE : CURRENT SITUATION

One major objective of the Middle Atmosphere Programme was to generate reference profiles of minor constituents of the atmosphere for India on the basis of measurements of ozone, nitric oxide (in the mesosphere), water vapour, CH_4, ClO, etc. (with balloons). A set of reference profiles have been derived. This is given in Table 1 as well as in Fig.6. Theoretical profiles obtained with 2-d models by Beig

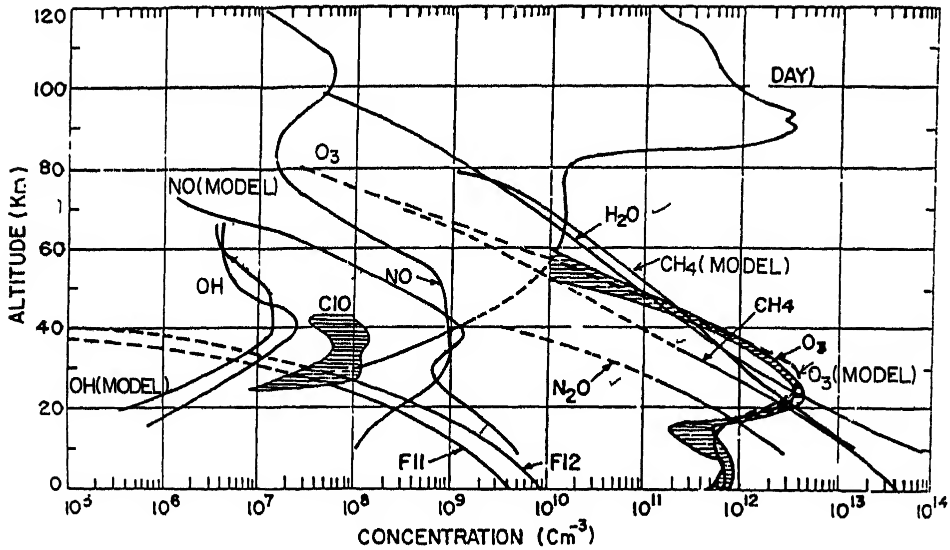

PROFILES OF IMPORTANT MINOR SPECIES

Fig.6 Reference profiles of important minor species as synthesised from Indian MAP programme along with model profiles derived by Beig and Mitra

and Mitra (*see* also Section 8) are also shown in the diagram These profiles are representative of equatorial conditions. NO values shown in the diagram are of interest in this connection.

5. ANTARCTIC OZONE DEPLETION

Since 1987 India has been participating in measuring ozone profile changes in its own Antarctic Stations as a part of the Antarctic Network over the entire year and particularly during the September, October, November season when the depletion begins and ends. In consonance with other observations, major ozone depletion was observed in the height ranges 12 to 24 km, and depletions were observed in all the years excepting 1988. A gradual deepening of the hole is seen as we go from 1987 to 1992. This is shown in Fig. 7.

The requirement that the temperature at the appropriate levels should be lower than about - 80°C is fulfilled in all the years excepting 1988 which, as mentioned earlier, is also the year for which ozone depletion is the least.

6. GLOBAL ENVIRONMENTAL CHEMISTRY

The basic elements of the middle atmospheric chemistry vis-a-vis those in the troposphere and the mesosphere (both in terms of neutral species and ionization) are shown in Fig. 8. Coupling from below and above through transport of fluxes from below (H_2O, N_2O, CH_4, CFC) and from above (NO) as well as direct injections at stratospheric levels (Cl and NO_x) are shown in Fig. 9.

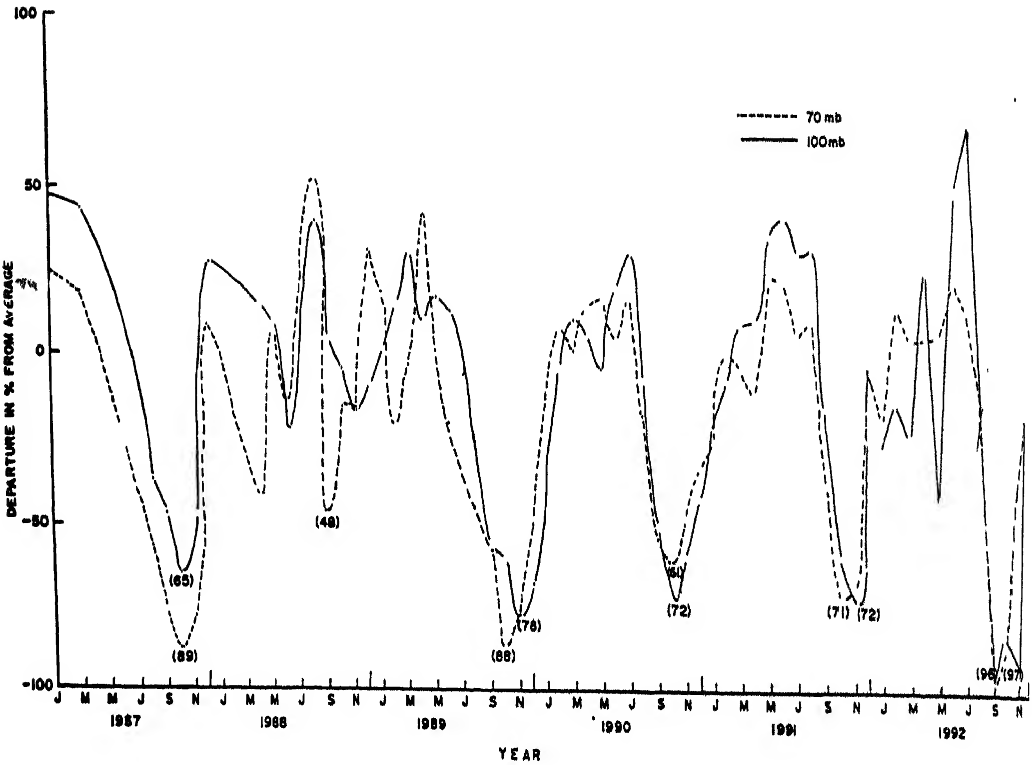

Fig 7 Trend of ozone concentration at 70 mb and 100 mb levels over Dakshin Gangotri/Maitri (after S.K. Srivastava)

The hierarchy of interest is:

Troposphere $\underline{H_2O}$, $\underline{O_3}$, $\underline{CH_4}$, <u>CFCs</u>, $\underline{N_2O}$, OH
Stratosphere $\underline{H_2O}$, $\underline{O_3}$, OH, NO, ClO, CH_4, <u>CFCs</u>
Mesosphere <u>NO</u>, H_2O, O_3, O.

Those underlined are the ones for which measurements were undertaken in India during IMAP. There are limited amounts of observations for nitric oxide for the mesosphere but none for the stratosphere or the troposphere. Water vapour measurements through radiosonde techniques give H_2O concentrations only up to 6 to 8 km. The earlier rocket-borne stratospheric H_2O measurements made by Soviet scientists with rockets launched from Thumba in late 70s resulted in concentrations

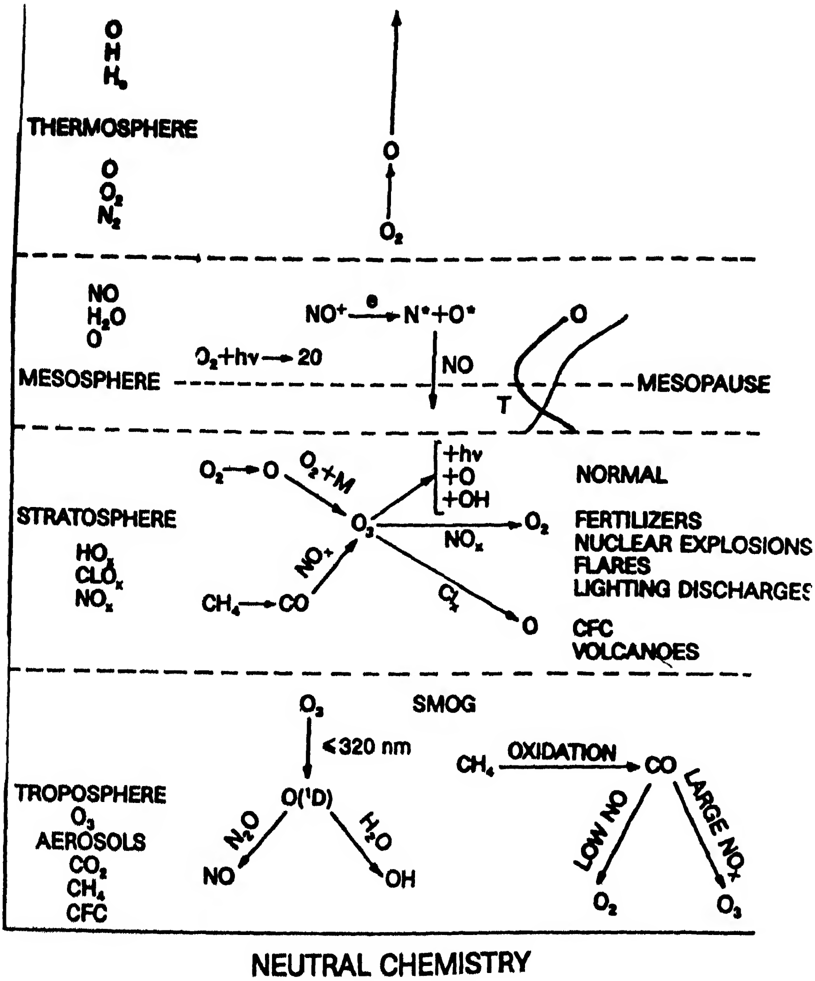

Fig.8 Changes in chemical reaction sequences as one moves up from the troposphere to the middle and upper atmosphere (after Mitra[20])

that are believed to be too large. This was later corrected through the use of balloon-borne payloads by Jayaraman and Subbaraya *et al.* in 1988. Another constituent of considerable impact is OH, the so-called atmospheric detergent. OH reactions with CH_4 and other greenhouse gases (GHG) determine their lifetimes. Determination of the spatial and temporal distributions of OH and their changes in future as GHG concentrations change, will form a critical activity in future.

Since forcing from below is very critically determined by the flux of CFCs, CH_4, CO_2, N_2O and H_2O (both of natural and anthropogenic origin), much of post-IMAP efforts has been concentrated on the determination of these fluxes. In fact, an

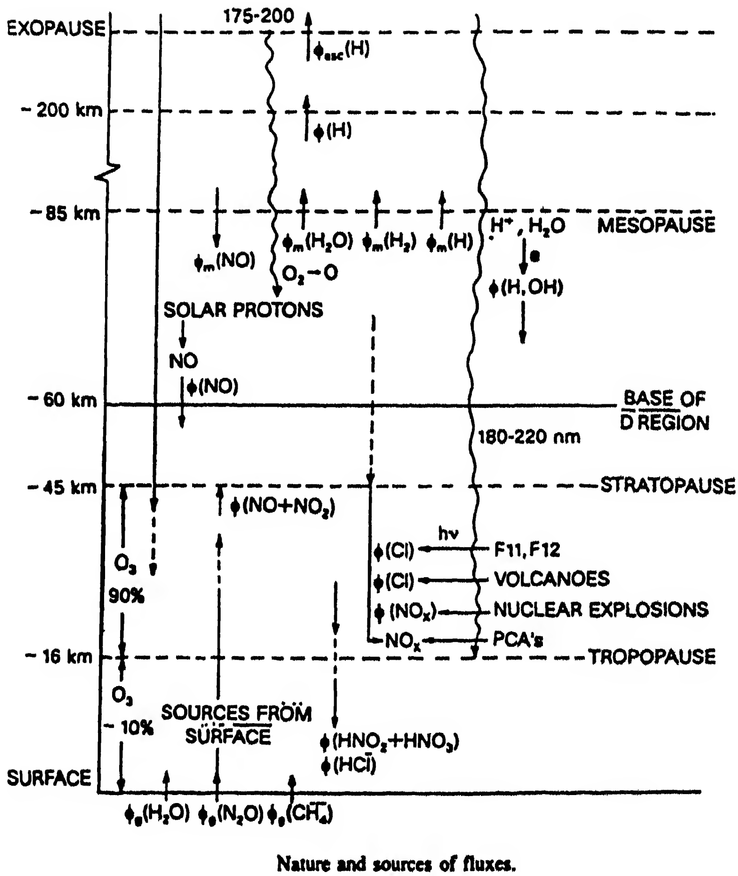

Fig.9 Transport of fluxes of atmospheric chemistry interest (after Mitra[20])

inventory of Greenhouse Gas Emission is now a major element of activity in most countries. Indian efforts have also been fairly significant in the last few years. An important effort in this direction was the 1991 Campaign on methane emission from paddy fields organised under the auspices of the National Physical Laboratory and the Indian Agricultural Research Institute, New Delhi. The main inventories of CO_2, CH_4, and N_2O are shown in Fig.10 and 11. (after Mitra[5]).

In all of these, the need for the use of standardized methodologies and of intercomparisons between the measurements has been repeatedly emphasized. While fluxes and concentrations at the surface have been emphasized, profile shapes have not had sufficient attention in the last few years.

7. OZONE AND UV-B RADIATION

A point to note is that while ozone reductions are significant in middle and high latitudes, there have been no measurable reduction in tropical regions. This is shown in Fig. 12. It is also clear from this figure that there is a low ozone belt in the tropical region which has hardly changed over the last decade or two.

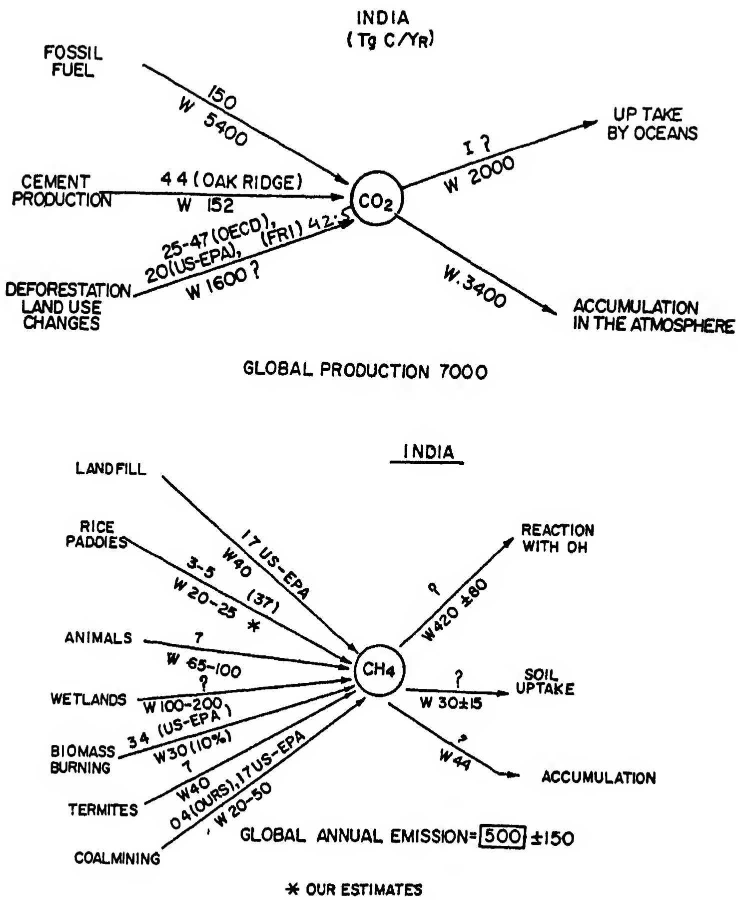

Fig 10 Sources and sinks of CO_2 and CH_4. The upper values refer to India, the lower values to world as a whole (after Mitra[20])

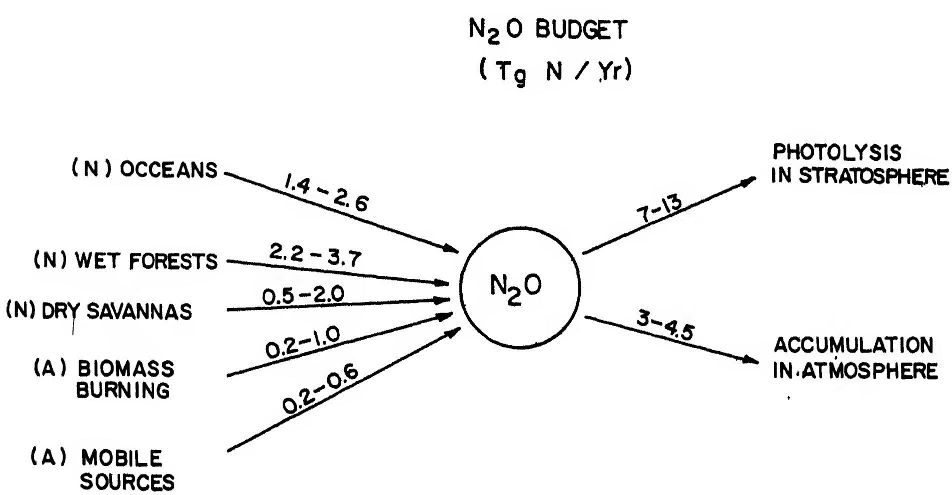

Fig 11 Sources and sinks for N_2O

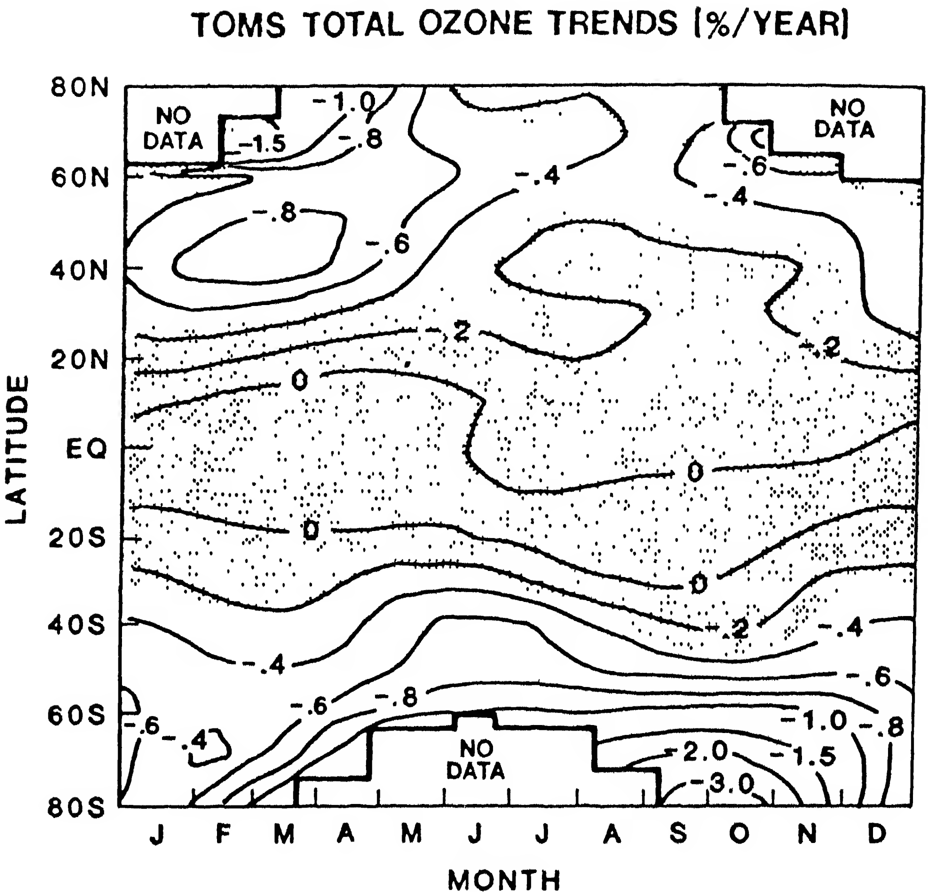

Fig 12 Ozone changes during the last decade (after Stolarsky *et al.*)

There are three specific major impacts of ozone changes. The first is the penetration of solar UV-B radiation through the stratosphere to the troposphere down to the ground and the upper layers of the ocean. This is one of the major programmes of SPARC. Modelling becomes difficult because of the presence of aerosols and the tropospheric clouds and also the uncertainties in the changes in tropospheric ozone. Nevertheless a number of models have been generated including one in India by the National Physical Laboratory. The modelled UV-B contours for the Indian subcontinent for a particular month is shown in Fig. 13. The second impact is in climate. It arises from the following: the CFCs have a positive greenhouse forcing effect – the estimated GWPs are 3400 and 7100 for CFC11 and CFC12 respectively for 100 years time horizon, but the reduction in ozone in the lower stratosphere caused by the increased atmospheric loading has a negative greenhouse forcing. Quantitative estimates depend on a number of factors: the magnitude of decrease, ozone profile changes, temperature effects. Not all these are adequately quantified yet, but the negative forcing appears to be almost completely compensating the warming effects of CFCs. As the atmospheric chlorine loading continues to decrease as a result of the implementation of the Montreal Protocol, this offset will decrease. Because of little or no change in the tropical regions in the ozone

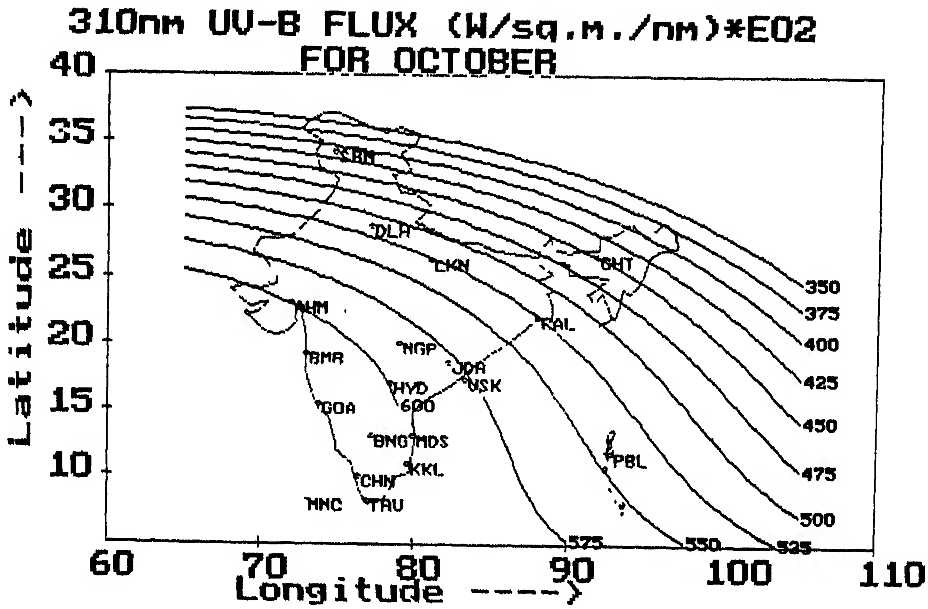

Fig 13 UV-B flux contours over the Indian subcontinent as calculated by NPL (Srivastava *et al*[6].)

profile, there is a latitudinal component in the offset for which no GCM studies are currently available. For Indian conditions the implications of no or little reduction and the consequence of varying ozone profile shapes need to be examined. So far global work in this aspect has only begun to be made and there is no work in India. A third impact concerns the increase on tropospheric ozone as a result of biomass burning which injects into the atmosphere a large quantity of NO_x. In fact, for tropical regions this is the most important aspect of ozone change and not the stratospheric ozone depletion. An example of tropospheric ozone increase from biomass burning in Congo region is shown in Fig. 14. Similar changes have been seen in Indian stations. Urgent work in this direction is necessary. An international programme called ITOY (International Tropospheric Ozone Year) is planned to look into this phenomenon quantitatively, in which Indian ozone network is expected to play a major role.

Of considerable interest are the various kinds of ozone changes from different types of anthropogenic and natural events. This is shown in Fig.15.

8. GLOBAL CHANGES AND THE MIDDLE ATMOSPHERE

Emphasis has been primarily on surface and near surface levels of climatic and other changes occurring from increasing concentrations of greenhouse gases. The mesosphere and thermosphere have been overlooked excepting recently for some efforts by Roble and Dickinson[7] and by Rishbeth[8]. While direct effects of radioactive forcing by increased concentrations of greenhouse gases are restricted to tropospheric levels, there can be consequent changes at higher levels. Using earlier developed models on the structures of the mesosphere, thermosphere and the ionosphere, Roble and Dickinson, Rishbeth and more recently Rishbeth and Roble[9]

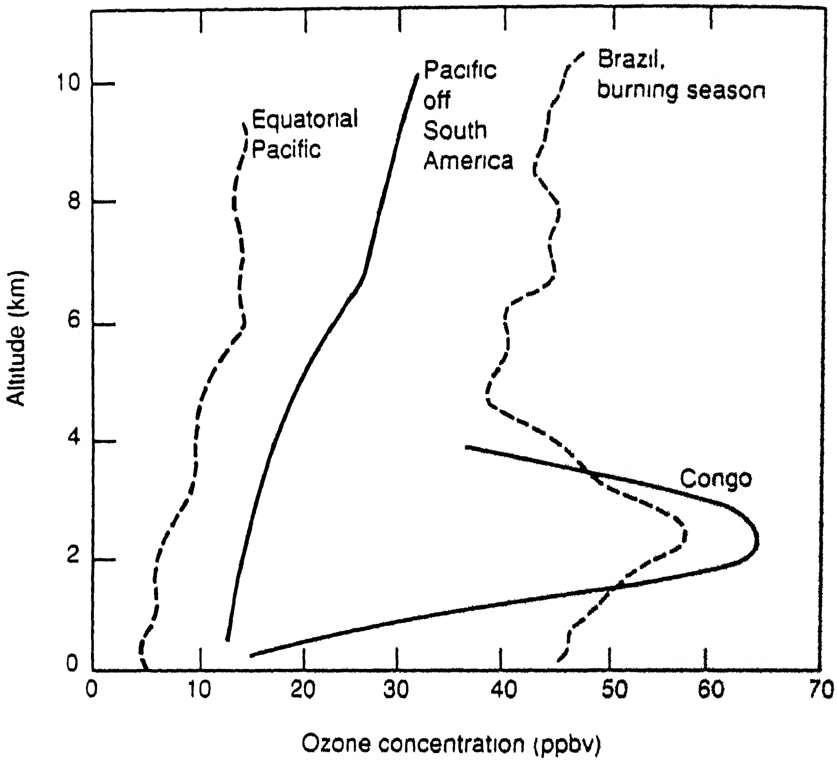

Fig. 14 Effect of biomass burning on tropospheric ozone (after Crutzen and Andreae, 1990)

have estimated changes in the middle and the upper atmosphere as well as in the ionosphere for a doubling of carbon dioxide. When these are combined with a number of calculations made by Brasseur *et al.*[10] on changes in the stratospheric and tropospheric regions, we find a pattern of the type given in Fig. 16. For the scenario of CO_2 doubling, a warming of about 4K at the surface changes into a cooling of ~10K in the stratosphere.

For the scenario of CO_2 doubling, the mesosphere is cooled by 10K and the thermosphere is cooled by 50K. The changes in the thermal structure necessarily change also the composition of the upper atmosphere. The consequent changes in the composition are[7] :

Per Cent Change in Density

	100 km	300 km
O_2	-40%	-60%
N_2	-40%	-60%
O	+20%	-40%

There are consequent changes in the ionization of the lower and middle atmosphere. These have been derived by Beig and Mitra[11] on the basis of a 2-d model. It appears that there are substantial changes in ion composition with major implica-

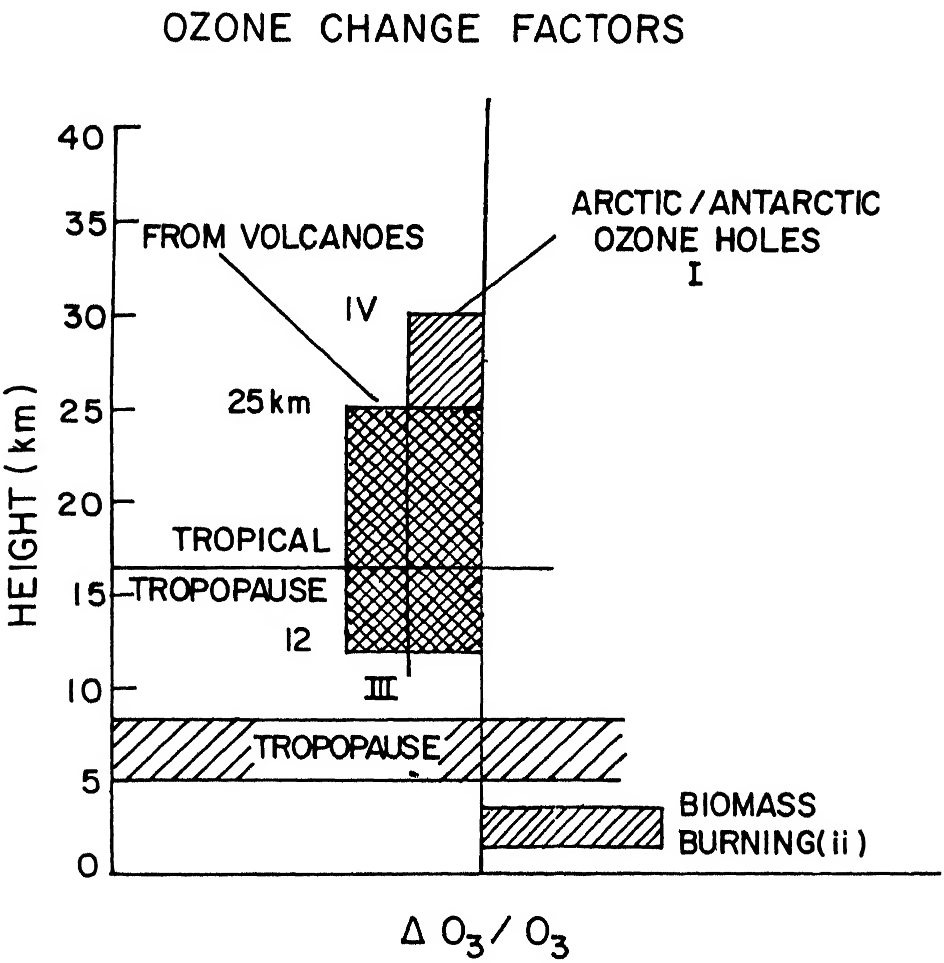

Fig.15 Types of changes in ozone profile from (a) Antarctic PSC's, (b) volcanic eruptions and (c) biomass burning

tions in global electrical circuit. One example of these calculations is shown in Fig. 17 and 18.

Observational evidence in support of this type of variation has also been looked for recently in a variety of ways: rocket, balloon and Lidar measurements of the atmospheric temperature, occurrence of noctilucent clouds, radio propagation measurements of various kinds These are shown in Table 2: the data cover segments of the last two decades. A synthesis of these results in terms of the temperature change from 1970 to 1990 is shown in Fig. 19 along with some theoretical calculations for this period.

9. MAJOR NEW FACILITIES

While many new facilities were introduced during MAP in India (a number of facilities came up such as laser heterodyning system, multiwavelength radiometers,

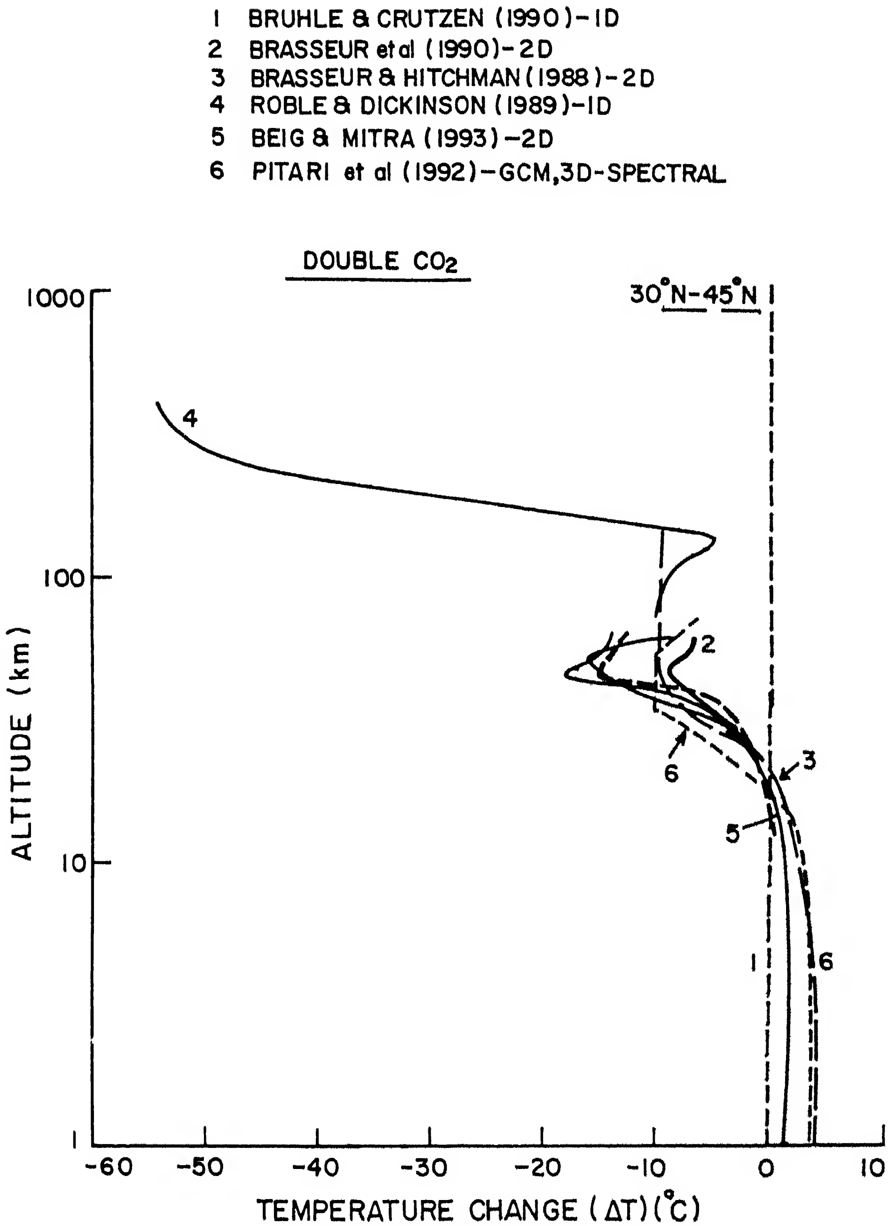

Fig 16 T vs height for 2 x CO_2 case

a Lidar at Trivandrum) and some of the most valuable observations came from the Lidar at the Observartory of Haute-Provence (France, 44°N, 6°E) operating since 1979, and the set of ST/MST radars at various places, several new facilities have come up more recently. These are new ST/MST Radars and UARS Satellites.

Amongst the new radars important additions from the tropical region were the Radar at Chung Li in Taiwan and the recently installed MST Radar at Gadanki near Tirupati in India.

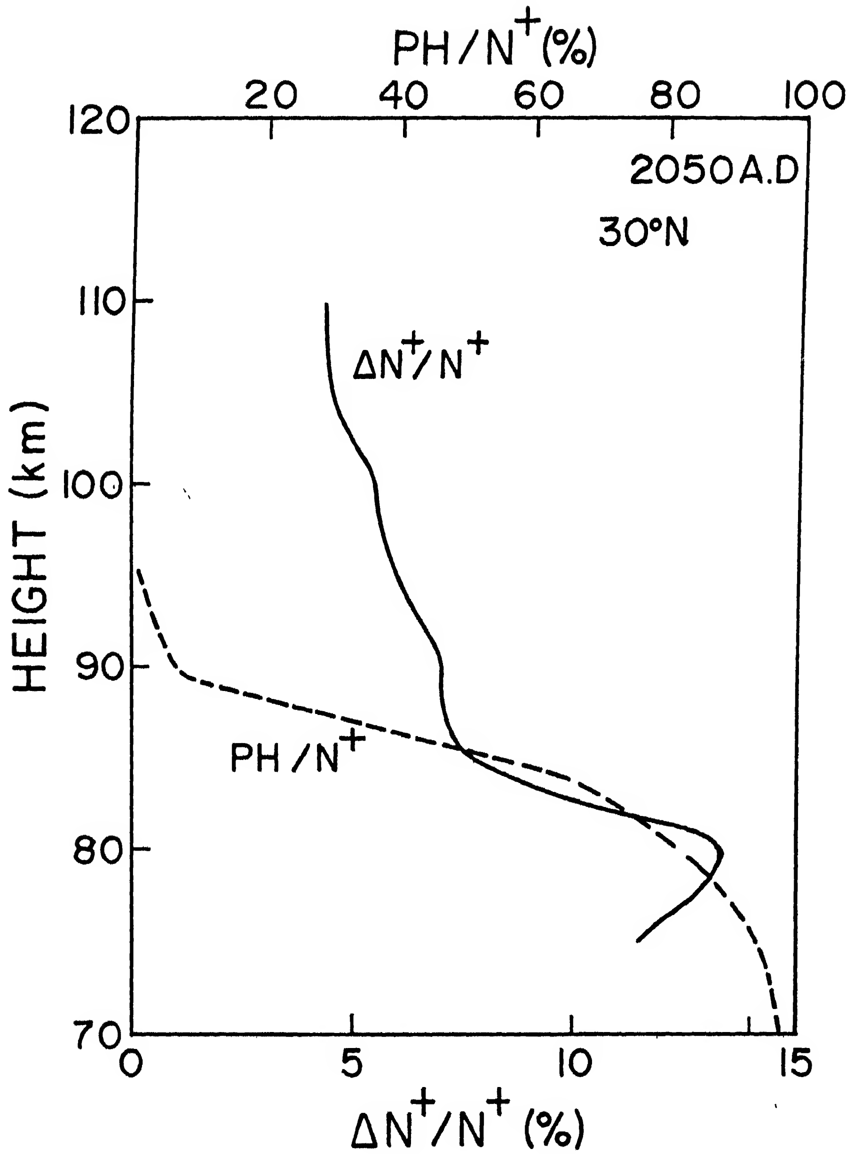

Fig 17 Global change and middle atmospheric ionization (after Beig and Mitra)

The Indian MST radar was commissioned on ST mode on 29 October 1990 and is now operating on MST mode. It operates on a frequency of 53 MHz with a peak power of 2.5 MW and an average power 60 kW. The antenna system is an array of 1024 yagi elements spread over an area of 136 m × 136 m with an effective area of 1.288×10^4 m^2 and a peak power aperture product of 3×10^{10} W.m^2. Five positions of beam have been selected: Zenith, 20 E-W and 20 N-S. A major point to note is that the scientific design has been completed entirely by Indian scientists and the fabrication has been undertaken by an Indian group, SAMEER. It is a national facility providing major opportunities for atmospheric research to Indian aeronomers.

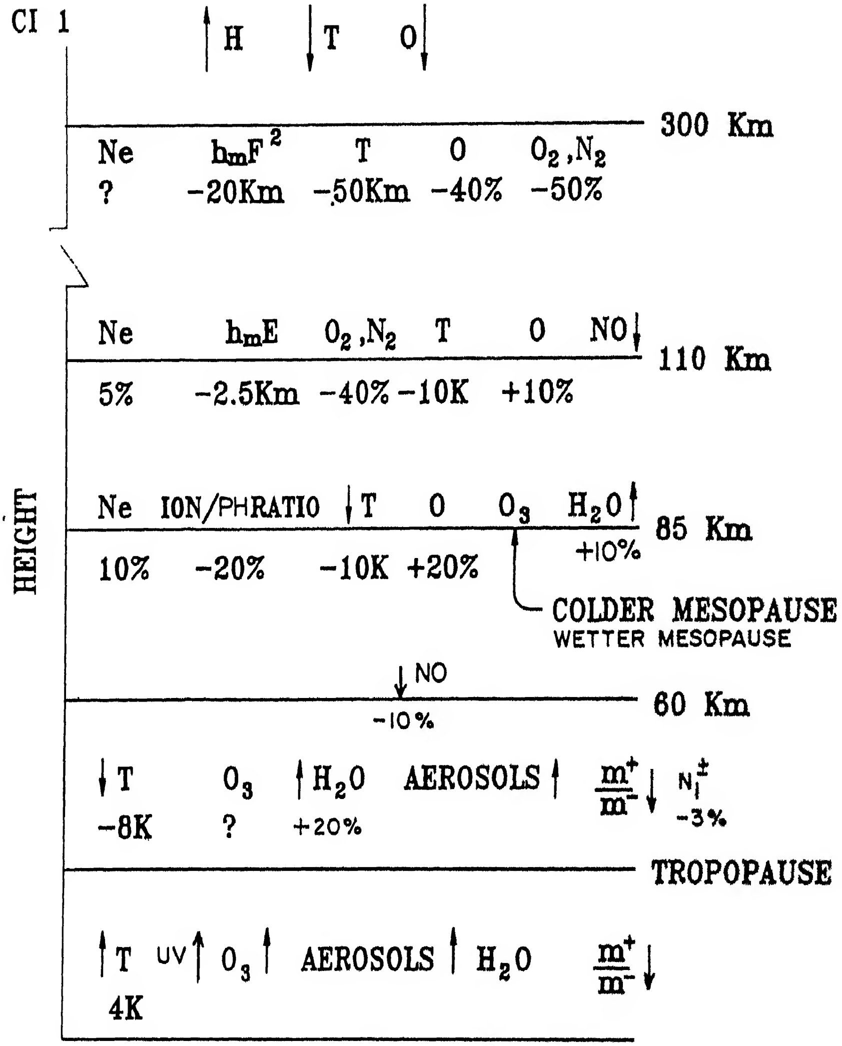

Fig 18 Nature of changes in minor species and ionization at different atmospheric levels for 2 x CO_2 scenario

The Indian radar is one of the few of its kind currently in existence or planned. Global distribution of ST/MST radars is shown below:

Global Distribution of ST/MST Radars

Facility Location	Location	Operating Frequency (MHz)	Peak Power Aperture Product (Wm^2)
Jicamarca, Peru	12°S,72°W	49.9	3.2×10^{11}
Poker Flat, USA	65°N,147°W	49.9	2.56×10^{11}
Mu, Japan	35°N,136°E	46.5	8.33×10^{9}
Arecibo, Puerto Rico	19°N,67°W	46.8	2.5×10^{9}

Facility Location	Location	Operating Frequency (MHz)	Peak Power Aperture Product (Wm^2)
Sousy, Germany	52°M,10°E	53.5	1.92×10^9
Tirupati, India	13°N,79°E	53.0	3.12×10^{10}
Aberystwyth, UK	52°N,40°W	47.0	1.25×10^9
Chung-li, Taiwan	25°N,121°E	52.0	5×10^8

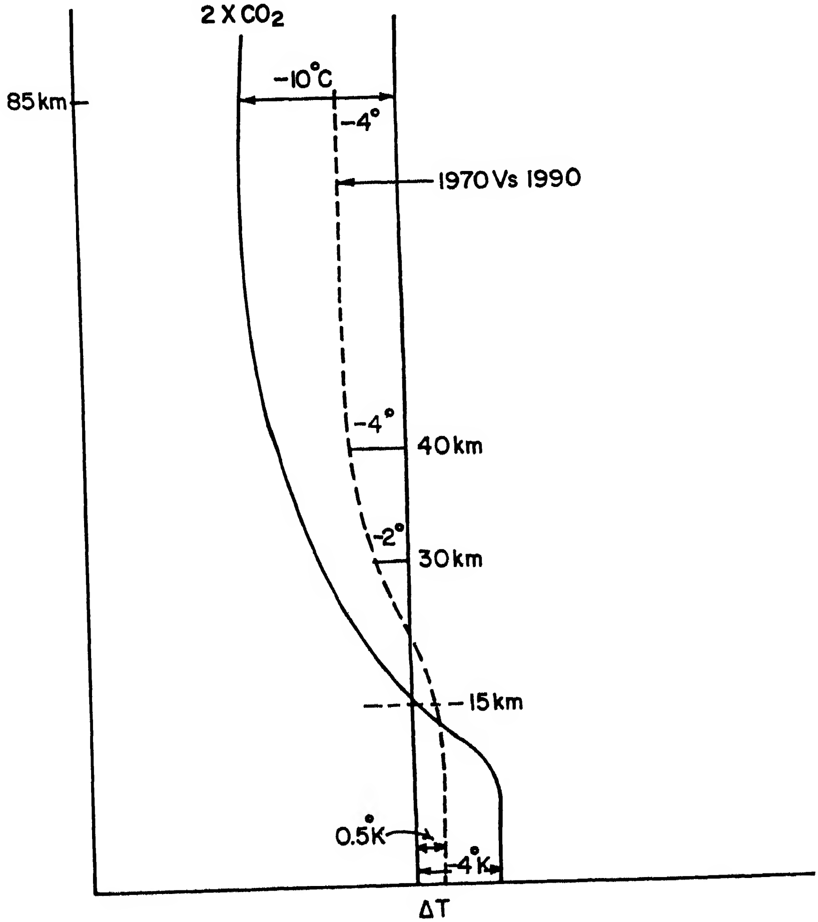

Fig.19 Observed changes in temperature as a function of height for the period 1970 to 1990

To many, MST radar heralds a new age to atmospheric physicists much the same way the radiosondes were decades ago. In the USA the technique is beginning to be used operationally for tropospheric weather prediction. One major reason is that it is the only instrument that can observe under all-weather conditions.

There are other exciting possibilities: capability to locate atmospheric fronts, ability to detect echoes from precipitation particles as much as from refractive index irregularities (shown by the Japanese radar at Shigaraki), real-time use of wind

profiles in nowcasting in regular use for the program for Regional Observing and Forecasting Services in the USA, determination of wind structures during cyclones (of the type done by Fukao with MU radar), freezing rain study capability, ability to monitor gravity waves and turbulence induced by the monentum flux, observations of thunderstorm reflectivities, the capability to monitor the behaviour of the tropopause breaks and to locate the breaks relative to fronts. In the Indian context, what advantages will accrue in the study and understanding of monsoon dynamics is not immediately clear, but one should be able to monitor changes in circulation patterns of interest. For the mesosphere, there is the distinct advantage of monitoring turbulence fields of spatial and time scales otherwise unavailable. On occasions of increasing reflectivity as during solar flares it should be possible to follow changes in increased scattered fluxes as the flare progresses. The Polar Summer Mesospheric Echoes (PMSE), coincident with NLC's as well as the newly detected 150 km echoes from equatorial regions, have created much interest. Returns have been observed from lightning discharges. For the Indian region the 150 km echo, returns from lightning discharges, and wind patterns during cyclones offer exciting possibilities

In addition, as a part of a project entitled "Study of Environmental Changes in Western Pacific Region", jointly organised by Japan and Indonesia, a Radar Observatory (60°s, 170°E) has been established within Pustiptek (National Center for Research, Science & Technology, about 27 km away from Jakarta). In this, two Doppler Radars, a Meteor wind radar and a Boundary Layer Radar (BLR) were set up in 1992 and have since been operating from November 1992.

A special advantage exists in Aberystwyth in Wales where a Lidar and the MST Radar are in simultaneous operation providing information of special value particularly at the mesospheric heights: new information is emerging from this simultaneous operation on anomalous radar returns from the mesopause region.

Perhaps the most important new addition was the launching of the Upper Atmosphere Research Satellite (UARS)[18] on 12 September 1991, containing four instruments to measure the height profiles of 15 important chemical species; two to determine atmospheric winds; and three to measure energy inputs from the Sun. This is the first systematic comprehensive study of the Earth's stratosphere and the mesosphere from a satellite. A series of papers in the June 1993 issue of *Geophysical Research Letters* give a first glimpse of the observations of ClO, O_3, $ClONO_2$, HNO_3, NO_2, H_2O, CH_4, N_2O, CFC12 as well as on stratospheric aerosols. Fig. 20 gives a summary of the measurement capability of this particular satellite.

10. NEW PROGRAMMES AND EVENTS

Of several new programmes and events in the post-MAP period, we will outline the following:

i) CEPEX
ii) DYANA
iii) Effects of Mt Pinatubo Volcanic Eruption

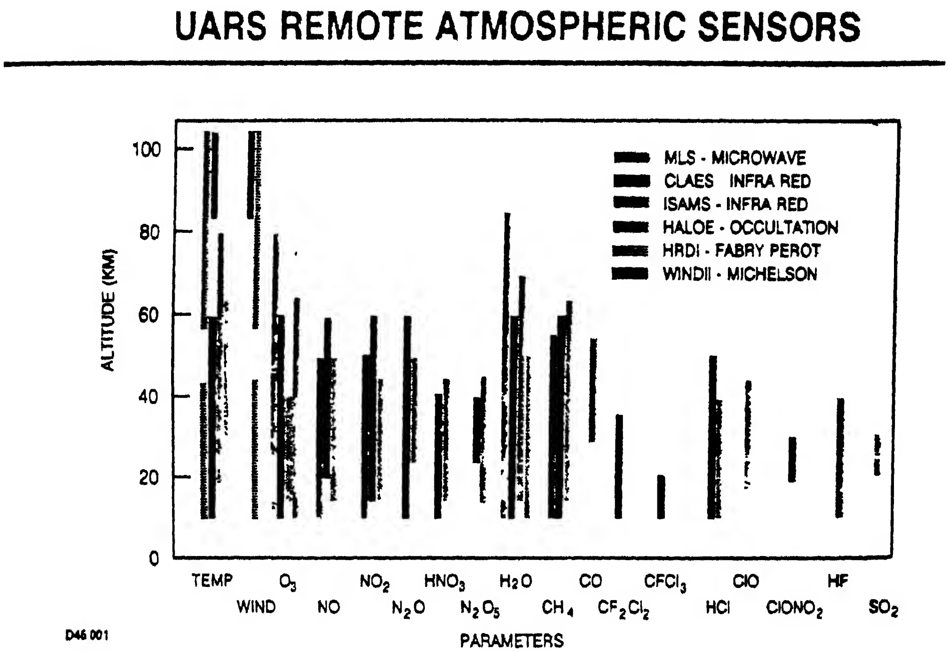

Fig 20 Measurement capability of UARS Satellite (after Reber, 1993)

CEPEX

This was a multiple-platform (surface, airborne and spaceborne platform) experiment to measure the so-called "supergreenhouse effect" and test the thermostat hypothesis for sea-surface temperature regulation. The mechanisms involved and the design of the experiment are shown in Fig.21. Measurements included:

(a) Radiation
Broadband longwave flux (4-50 μm)
Narrowband longwave flux (8-12 μm)
Longwave radiance (up, down and net)
Broadband solar flux (0-5 μm)
Narrowband radiance (visible and near IR)

(b) Atmospheric Dynamics
Analyzed winds, divergence and others (ECMWF analysis)
Vertical velocity from profilers (radar and wind profilers)
Horizontal winds (sondes and dropsondes)

(c) Evaporation, Precipitation, Clouds, Water Vapour and Ozone,
Evaporative and Sensitive Heat Flux (moorings)
Precipitation
Cirrus Cloud Bulk Properties (ER-2 and Learjet aircrafts, GMS, NOAA-9, 10, 11, 12)

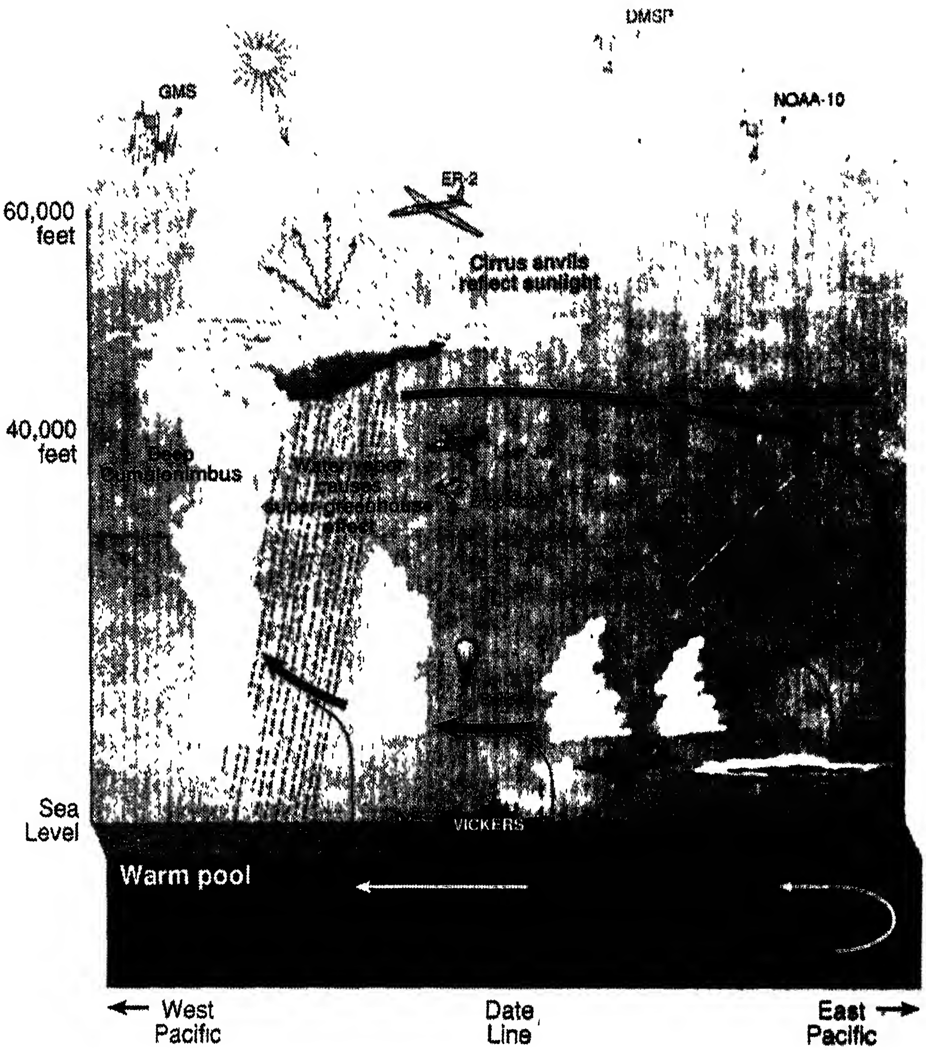

Fig 21 The design of CEPEX Experiment (after V Ramanathan)

Water vapour distribution (ER-2, Learjet, sondes)
(surface to 20 km)
Ozone (ER-2, ozonesondes)

The experiment was performed in March 1993. There is a proposal of mounting a similar campaign over the Indian Ocean at a future date.

DYANA

DYANA (DYnamics Adapted Network for the Atmosphere) was a multicountry experiment performed during the period January-March 1990 as a part of the STEP programme using a variety of rocket, balloon and groundbased equipment. One of

the objectives was to obtain the characteristics of the planetary scale waves in the low latitude middle atmosphere. Indian experiments were targeted for this particular objective. This was achieved through rocket launchings from Thumba and Balasore and balloon launchings from Thumba, Minicoy and Port Blair. In the campaign, Lidar observations of temperature (30-80 km) and ozone (20-45 km) were made by Japan and electron density profiles through rocketborne sensors over Volgogrod by a Russian group.

A proper evaluation of the campaign is yet to be made.

Mt PINATUBO VOLCANIC ERUPTION

The eruption of Mt Pinatubo (15.14°N, 120.35°E) in the Philippines on 15 June 1991 provided one of the most powerful tools for the study of the stratosphere in several major aspects The stratospheric clouds created by the very large amounts of SO_2 and other volcanic effluents were monitored by satellites, by NASA Wallops Flight Facility Electra aircraft, by a number of Lidars and by a host of groundbased systems. SO_2 emission was estimated to be 20 million tonnes (about 3 times that produced by El Chichon eruption), H_2SO_4/H_2O aerosol mass was around 20-30 megatonnes, stratospheric temperatures increased (by 3.5°C in September 1991 at 30 mb between equator and 30°N), a global mean climate forcing of - 4wm^{-2} (in early 1992) was predicted, exceeding the combined greenhouse gas warming; and in the Antarctic the ozone hole was observed to occur earlier and at lower levels than in other years. In India, there were unfortunately very few targeted observations.

Table 1 Proposed Reference Model for the Middle Atmosphere over India

Height km	Air number density (cm^{-3})	T K	O_3 cm^{-3}	N(noon) cm^{-3}	N^+ cm^{-3}	NO cm^{-3}	H_2O ppmv	CH_4 ppmv	N_2O ppbv	F11 pptv	F12 pptv
0	2.4(19)	300 15	8.6(11)				1(5)*	1 65	330	195	360
5	1.5(19)	270 15	5.0(11)				9(1)	1.65	330	195	360
10	87(18)	238 15	3.2(11)		2 5(3)		7	1 65	330	195	360
15	4 6(18)	205.65	4.1(11)		3 5(3)	1 0(8)	3	1.60	320	195	360
20	2.1(18)	208.35	1.78(12)		3.0(3)	2 5(8)	3	1.50	300	130	250
25	8 6(17)	219.85	3.14(12)		2 0(3)	6 0(8)	4	1.25	210	124	190
30	4.0(17)	231 35	2.81(12)		1 7(3)	9 0(8)	3	1 20	210		
35	1.9(17)	242 85	1.33(12)		1.3(3)	1.0(9)	35	0 60	40		
40	9.5(16)	254.35	5.42(11)		1.0(3)	- 1 0(9)	37				
45	4.5(16)	265.85	2.04(11)		8.0(2)	9 5(8)	5				
50	2.3(16)	268.15	6.84(10)		6.5(2)	9.0(8)	6.5				
55	1.2(16)	266.15	2.86(10)			6.0(8)					
60	6.6(15)	241.15	1.25(10)	10		2.5(8)					
65	3.3(15)	226.15	2.6(9)	61		1.5(8)					
70	1.6(15)	211.15	6.0(8)	250		8.0(7)					
75	7.5(14)	198.55	1.0(8)	510		2.5(7)					
80	3.3(14)	195.55	2.0(7)	740		1.4(7)					
85	1.6(14)	192.94		1.7(3)		1.2(7)					
90	7.2(13)	190.33		1.3(4)		2 0(7)					
95	3.0(13)	187.33		3.9(4)		2.5(7)					
100	1.2(13)	187.58		8.8(4)							

* variable

Table2: Global Change and Middle Atmosphere

(i)	Aikin *et al.*[12]	a) SSU Instrument Channel 47X Satellites, 44°N	1980-90	55 km	−(3.5±0.5) K/decade	
		b) Lidar HauteProvence	1980-90	55 km	−(0.25±0.10)K/decade	
(ii)	Datta, Chakravarty and Mitra[13]	Thumba rockets	1970-88	30 km	−2.3 K	
				40 km	−4 K	
(iii)	Angell[14]	Rocketsonde data	1973-85	26-35 km	−0.5 K/decade	
				36-45 km	−1.5 K/decade	
				46-55 km	−2.5 K/decade	
(iv)	Gadsen *et al.*	Noctilucent clouds	1964-88	85 km	−6.4 K (if no correction is made for change in water vapour concentration)	
(v)	Thomas *et al.*[15]	Noctilucent clouds	Over past century and a half	85 km	Attributes increase in frequency of occurrence of NLCs to increasing H_2O concentration from methane oxidation	
(vi)	Rind *et al.*[16]	Theory		55 km	−(1.5-2) K/decade	
(vii)	Taubenheium *et al.*[17]	LF Phase heights		80 km	−4°C (deduced from $\Delta p/p$ changes)	
(viii)	Labitzke *et al.*	Rockets averaged 10°N-90°N	1965-85	24 km	−0.24 K/decade	
(ix)	Beig and Mitra	Theory		20 km	$\frac{NPH}{PH}$	−3%
				40 km	"	−18%
				Mesosphere	$[NO^+ + O_2^+]/PH$	−40%

However, the Maitri ozone profiles[19] in 1992 showed a sharp fall in tropopause height and cooling in the season from May 1992 to November 1992, apparently associated with the volcanic cloud excursion to southern polar region. (Private Communication from S.K. Srivastava).

The eruption provides an outstanding test for chemical-climate modelling for troposphere-stratosphere regions. Ionic changes resulting from these effects are yet to be examined; such calculations can be rewarding.

11. CONCLUSIONS

The post-MAP period has seen an intensification in the work on the middle atmosphere in a broader frame connected, on the one hand, with the lower atmosphere through programmes such as IGBP and SPARC and on the other, with the upper atmosphere through programmes such as STEP. New insights are coming from emergence of ST/MST radars and the Lidars such as those in France and Aberystwyth. In India, the establishment of the MST Radar has provided new opportunities for low and middle atmospheric research to the Indian atmospheric science communities. A campaign was organized from 8 February 1992 to 7 April 1992 to operate the Radar on ST mode to determine the dynamics of the tropospheric-stratospheric region and the structure of the characteristics of the tropopause with particular emphasis on detection and characterisation of the conditions for tropopause "break". This information was necessary to understand the conditions under which transfer of gases like ozone and water vapour occur between the stratosphere and the troposphere. This in fact is one of the major target areas of SPARC.

ACKNOWLEDGEMENTS

I wish to acknowledge with grateful thanks the assistance received from Mr. R.K. Bhasin, Dr. G. Beig, Mr. T.K. Mandal and Mrs. Sudesh.

REFERENCES

1. Special Issue on Indian Middle Atmosphere Programme, *Indian J Radio & Space Phys.*, **13** (1989) (5&6), 165-314.
2. IMAP Final Report - 1, Balloon-borne Experiments for Middle Atmospheric Conductivity Campaigns, ISRO-IMAP-SR-39-92, ISRO, December 1992.
3. Krishnamoorthy K, Nair Prabha R, Prasad B.S.N., Muralikrishna N., Gayathri H.B., Narasimha Murthy B., Niranjan K., Ramesh Babu V., Satyanarayana G.V., Agashe V.V., Aher G.R., Singh Rishal & Srivastava B.N. Results from the MWR Network of IMAP, *Indian J. Radio & Space Phys.*, **22** (1991) 243-258.
4. IMAP Final Report II, Rocketborne experiments for D and E-Region Ionization Campaigns, ISRO-IMAP-SR-41-93, ISRO, July 1993.
5. Mitra A.P., *Greenhouse Gas Emissions in India*, Sci.Rep. 4 (Council of Scientific & Industrial Research, New Delhi), 1992.

6. Srivastava, B.N., Sharma M.C., Jain Meena & Iqbal Ahmad. *Atlas of Solar UV-3 Radiation, Erythemal Dose* and *Ozone over the Indian Subcontinent*, RSD, National Physical Laboratory, New Delhi), 1992.

7. Roble R.G. & Dickinson R.E. *Geophys. Res. Lett.*, **16** (12) (1989) 1441-1444.

8. Rishbeth H. *Planet. & Space Sci.*, **38**(7) (1990), 945.

9. Rishbeth H. & Roble R.G. *Planet. & Space Sci.*, **40**(7) (1992), 1011-1026.

10. Brasseur G., Hitchman M.H., Walters S., Dymek M., Falise E & Pirre M. *J. Geophys. Res.*, **95** (D5), (1990) 5639-5655.

11. Beig G & Mitra A.P., In course of publication.

12. Aikin A.C., Chanin M.L., Nash J & Kendig D.J. *Geophys. Res. Lett.*, **13** (3), (1991) 416-419.

13. Datta J, Chakravarty S.C. & Mitra A.P., In course of publication.

14. Angell J.K., *Mon. Weather Rev.*, **115** (1987) 2569-2577.

15. Thomas G.E., Olivero J.J., Jensen E.J., Schroeder W & Toon O.B., *Nature*, **338** (1989) 490-492.

16. Rind D., Suozzo R., Balachandran N.K., Prather M.J., *J. Atmos. Sci.*, (1990) 475-484.

17. Taubenheim J., Van Cossart, G. & Entzian G., *Adv. Space Res.*, **10** (10) (1990) 171-174.

18. Reber Carl A., *Geophys. Res. Lett.*, **20**(12), (1993) 1215-1218.

19. Srivastava S.K., In course of publication.

20. Mitra A.P., *Interactive processes in the Atmospheric Environment, Chemistry and the Environment*, edited by B.N. Noller and M.S. Chadha (Commonwealth Science Council, London) 1990.

MIDDLE ATMOSPHERIC CHEMISTRY

B.H. Subbaraya*

INTRODUCTION

In the earlier years, the programmes in middle atmospheric studies were largely restricted to the study of the D region ionization, its relation to solar activity and role in radio communication In the sixties and the seventies, ion chemistry of the D region became an important topic of study. Amongst the neutral species, the important role of the minor constituent ozone in solar UV absorption and the consequent effects on energetics and dynamics was well known. But as a research topic, its significance was restricted to its role as a tracer for atmospheric motions. The scene changed drastically in the seventies when the limitations of Chapman's[1,2] photochemical scheme for ozone was exposed by Johnston[3] and the role of catalytic reactions involving the HO_x[4], NO_x[5], and ClO_x[6,7] species was discovered. The consequent threat of a possible long-term global ozone depletion due to anthropogenic activities[8,9] made the study of Middle Atmospheric Chemistry a front-line research area during the decades of the seventies and the eighties.

Atmospheric Chemistry mainly concerns itself with trace gases, which exist in minute quantities - parts per million by volume at best, but more often in the range of parts per billion and even parts per trillion by volume. Ozone continues to hold centre stage and most other trace constituents acquire their importance because of the role they play in its chemistry, e.g. the nitrogen oxides, NO_x, the water derived radicals, HO_x, the chlorine and the bromine compounds. Ozone studies – modelling and observations–remain highly topical in the nineties due to the discovery of the Polar (Antarctic) Ozone Hole in the late eighties[10,11]. However , in recent years the recognition of the Global Warming problem due to increasing atmospheric abundances of the so-called greenhouse gases,[12,13] much of it due to anthropogenic influences, has added a new dimension to middle atmospheric chemistry, especially at tropospheric altitudes. During the past decade, several programmes in middle atmospheric chemistry have been developed in the country, significant results have been obtained and the programmes hold promise for the future.

**Physical Research Laboratory, Ahmedabad 380 009*

The Indian Middle Atmospheric Programme (1982-85-88) was formulated in the early eighties as a coordinated national programme for study of several aspects of middle atmospheric science that are special to the low latitude regions. This has largely set the tone for the programmes of the nineties. Many of the currently ongoing programmes and the developments envisaged during the next few years are relevant for the new international programme–STEP. Further, several initiatives have also been taken up as a result of the new International Programme on Global Change, the IGBP, which has a core programme on Atmospheric Chemistry, IGAC.

Ozone

The Dobson spectrophotometer network (Kodaikanal, Pune, New Delhi and Srinagar stations being maintained by the India Meteorological Department (IMD), Ahmedabad and Varanasi stations being maintained by the Physical Research Laboratory, Ahmedabad and the Institute of Geophysics of the Banaras Hindu University respectively) continues to be operational, making measurement of Total Ozone and Umkehr observations regularly and the data are being sent to the World Ozone Data Centre in Toronto, Canada. The data from the Mt Abu/Ahmedabad station, which has been in operation since 1951, was re-evaluated taking into consideration the station records of past calibrations, instrument settings, observational procedures, use of revised absorption cross-section etc., and a homogeneous time series has been constructed for the period 1951 to 1985[14]. This data set has been validated by comparison with TOMS data as well as data from other Dobson stations in the same latitude belt. The revised data set has been included in the Global Ozone Data used for long-term ozone trend estimates (Ozone Trends Panel, 1991). Figure 1 shows the revalidated time series for ozone for the period 1951-85. A similar exercise needs to be carried out for the data from the other Indian stations even though there are reports that the current data set for these stations is largely satisfactory[15]. The Indian Dobson network is unique and can provide valuable data from the tropical regions. The possible long-term ozone depletion is of the order of 1-2% per decade in middle latitudes and could be even smaller in low latitudes. Detection of these from the measurement records imposes stringent restrictions on the data quality[16] which was not recognized prior to the seventies. Hence the need to look into the past data and ensure its suitability for long-term trend studies. Re-evaluation is not special for the Indian stations. It is an exercise which has been going on all over the world during the past five to ten years[17].

A UV-B photometer network was set up during the IMAP period (New Delhi, Jodhpur, Waltair, Mysore and Trivandrum). The Indian subcontinent offers an ideal region for UV-B monitoring due to the wide range of variations from Trivandrum, a typical equatorial site, to Srinagar, a typical mid-latitude site and the large seasonal changes at some of the locations. Some of the stations like New Delhi and Trivandrum have collected more than ten years of data and attempts have been made to draw an erythmal map for the Indian region[18,19]. The Trivandrum data set shows a significant increasing trend of more than 1% per year over the ten-year period[20].

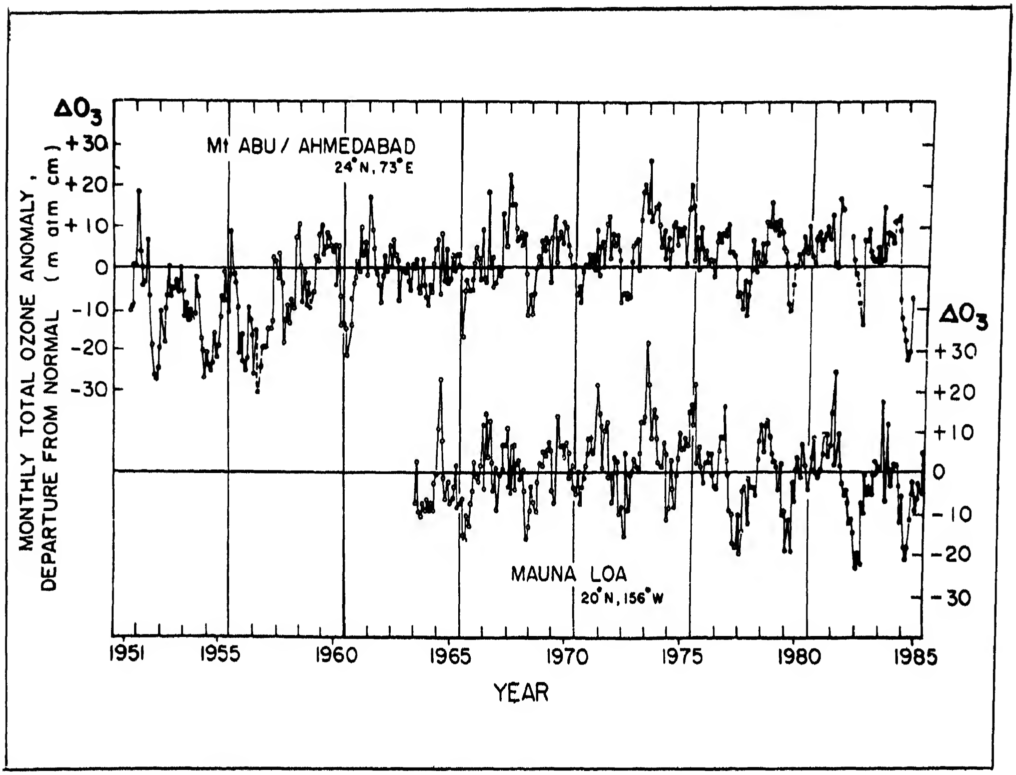

Fig. 1 Homogeneous time series for total ozone over Mt Abu/Ahmedabad (24°N, 73°E) for the period 1951-1985. Past data have been re-evaluated using station records of calibrations, instrument settings, revised absorption coefficients, etc. Also shown in figure are the data for the station Mauna Loa (20°N, 156°W) in the same latitudinal belt for comparison (after Angreji, 1989).

This increase, if interpreted in terms of ozone decrease, gives rise to a much larger decreasing trend in ozone over Trivandrum than is observed in other data sets for the equatorial regions. These observations need to be studied carefully for their cause. Attempts have also been made to use the ground reaching UV-B fluxes with suitable models to estimate total overhead ozone[21] and the estimated ozone values are compared with other available data. The results are quite satisfactory.

The Dobson spectrophotometer and UV-B network will continue to operate in the coming years. Simultaneous ozone and UV-B observations are very useful for model studies. The India Meteorological Department has plans to set up at least two Brewer spectrophotometers in India in the first half of the decade. The Brewer

instrument is an automatic computerized fast response instrument (in principle measurements can be made once in every two minutes) and can measure simultaneously total ozone, SO_2 abundances and ground reaching UV-B. In view of the overlapping of UV absorption features of O_3 and SO_2, in recent years there has been some concern about the accuracy of the Dobson Ozone Data obtained from urban polluted sites. Some of the Indian Dobson sites are not free from these concerns and hence the proposed operation of the Brewer spectrophotometer is important. The first instrument is likely to be set up at New Delhi during 1993-94. The location for the second instrument (likely to come up in 1994-95) is not yet decided. An advantageous location would be Trivandrum since New Delhi (urban polluted) and Trivandrum (marine relatively clean) offer two contrasting environments from the point of view of tropospheric chemistry and air pollution studies.

Ozone Vertical Distribution

Measurements of ozone vertical distribution are being made both by means of balloons and by rockets. The IMD balloon ozonesonde network consists of three stations – Trivandrum, Pune and New Delhi (a few sporadic measurements have been made from Hyderabad during IMAP) and rocket measurements generally made from Thumba during the eighties have been used to construct a mean ozone vertical distribution for the equatorial regions (Fig. 2), which shows several features

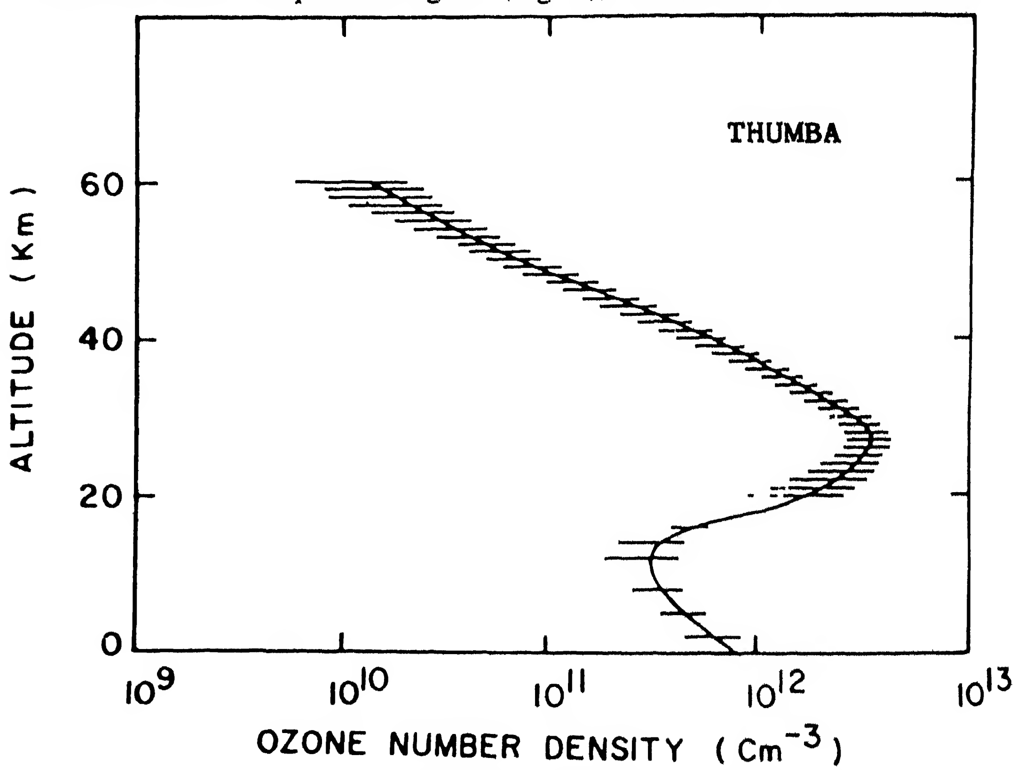

Fig 2 Mean ozone vertical distribution for the low latitude site, Thumba (8.5°N) based on rocket data for altitude region above 20 km and balloon ozonesonde data for altitudes below 20 km (after Subbaraya and Jayaraman, 1987).

different from the middle and higher latitudes[22]. The ozone maximum is reached at a higher level and the maximum concentrations are lower than those over middle and high latitudes. An attempt has also been made to study the day-to-night variations in the ozone vertical distribution[23] (Fig. 3) as well as perturbations in the ozone

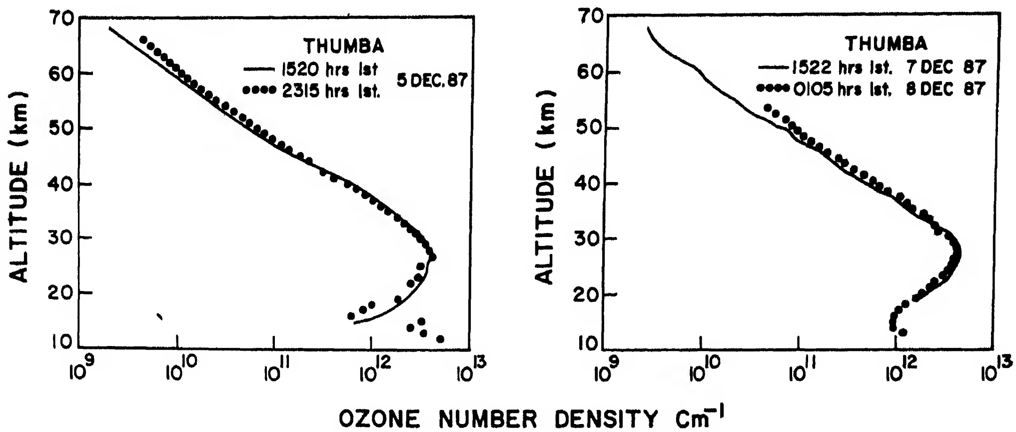

Fig. 3 Day-night variations in the ozone vertical distribution over Thumba (after Jayaraman *et al.*, 1989)

profile due to meteorological effects[24]. Major activities during the recent years have been the participation of the IMD balloon ozonesonde in the intercomparison experiment conducted at Vanscoy in Canada in 1991, the balloon campaigns conducted from the Indian station, Maitri, in the Antarctic and the DYANA campaign. The balloon ozonesonde measurements from the Antarctic during the ozone hole period show an interesting correlation of the ozone depletion with the tropospheric temperatures[25,26]. During March-June 1990 a number of rocket ozonesondes were flown from Thumba as part of the international campaign - DYANA (which was the first STEP coordinated programme). The data show that the mean ozone concentrations for March-April period are larger than those for the May-June period in the altitude region of 30-45 km (Fig. 4). The deviations from the mean reference profile are of the order of +15% for March-April and – 25% for May-June[27]. Ozone concentrations are larger in the night time than in day time at altitudes above about 45 km, confirming earlier results on day-night variations over Thumba, but the observed increases are larger than model estimates. Fig. 5 shows a comparison of the 1990 data with the data from the earlier campaigns at Thumba.

During the DYANA campaign, a Brewer spectrophotometer was operated at Thumba for about three months (March-June 1990). The instrument was loaned from Atmospheric Environmental Services, Canada, under a special arrangement with the Leningrad Institute for Atmospheric Sciences and the entire programme was coordinated under the ISRO-SCHM, the then Indo-Soviet scheme of collaboration. It was for the first time that such high time resolution (~ 2 min.) ozone measurements were made in India. On most clear days, the ozone values show a clear diurnal variation with a minimum around noon and maxima on either side (Fig. 6). The range of variations differs from day-to-day and lies between 4 and 12 DU representing a

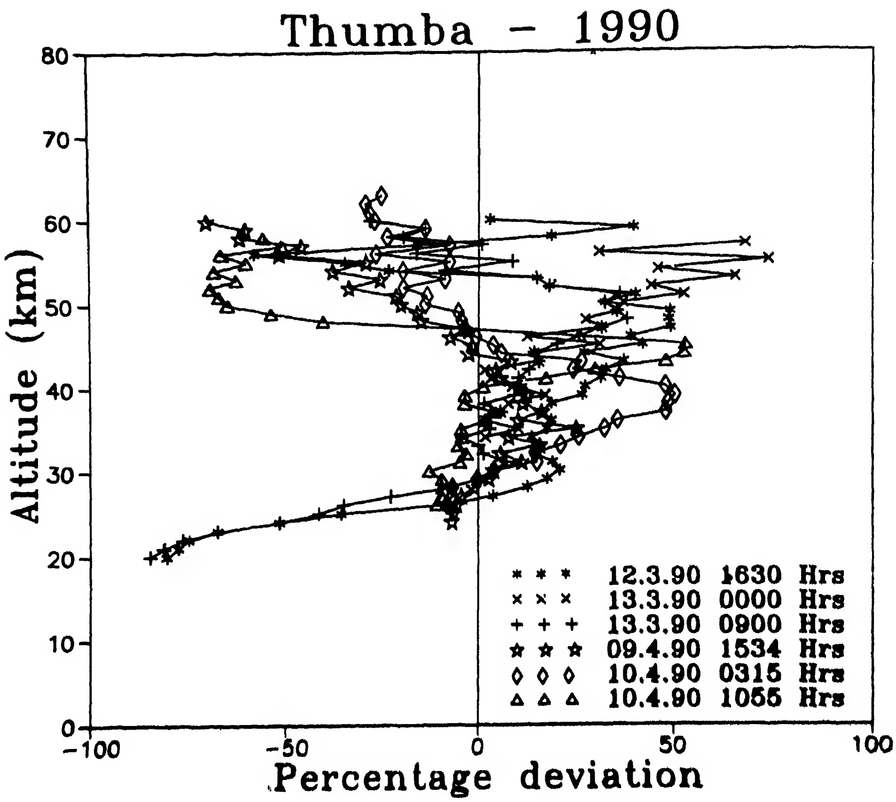

Fig 4 Deviation of the March-April 1990 rocket measurements of the ozone vertical distribution from the mean reference profile for Thumba (after Subbaraya *et al*, 1994).

change of 1.6 to 4% in total ozone. The data also show, apart from day-to-day variability, a clear 27-30 day periodicity (Fig. 7) and the familiar spring time increase in total ozone over Thumba[28].

A laser heterodyne system has been developed at National Physical Laboratory (NPL), New Delhi [29,30] for the measurement of ozone, water vapour and NO_2 vertical distributions. It is a versatile instrument and can in principle be used to make measurement of several other trace gases that are important in ozone chemistry[31], e.g. CFCs, but the present NPL setup needs some augmentation to make these measurements. NPL has also plans to install a similar system at the Indian station in Antarctic. This will be very useful for Antarctic Ozone Hole studies. Development of a microwave radiometer for ozone vertical distribution measurements has also been initiated at NPL This will be unique since this technique can be used both during night time and day time, but it will need proper validation/calibration using established techniques.

Other Trace Gases

A number of trace gases belonging to the NO_x and HO_x families and more recently chlorine-bearing and bromine-bearing compounds (CFCs, HCFCs, etc.)

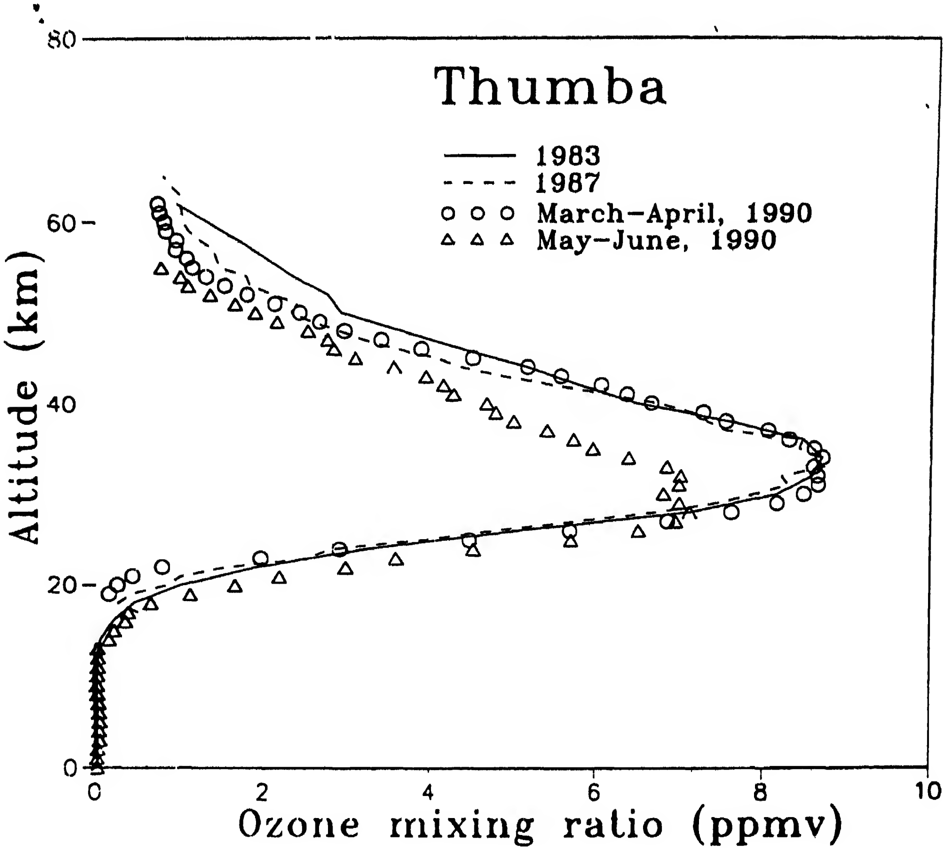

Fig 5 Comparison of the DYANA ozone profile measurements from the results of the previous ozone campaign at Thumba (after Subbaraya *et al*, 1994)

have been found to play an important role in ozone chemistry contributing to the Global Ozone Depletion and the Polar (Antarctic) Ozone Hole phenomena. In addition, a number of compounds, e.g. CO_2, CO, CH_4, N_2O and the CFCs play important roles in the Global Warming phenomenon Many of these gases are having significant anthropogenic sources and are long-lived (photochemical lifetimes of the order of tens to hundreds of years) and their atmospheric abundances are found to be increasing (IPCC, 1991). While the sources of these gases are variable over the globe (both natural and anthropogenic), in the lower troposphere they are globally well mixed. But in the upper troposphere and the stratosphere, their distributions exhibit significant spatial variations due to transport effects The vertical distribution in the tropics is important because the vertical uplift over the tropics and subsequent meridional transport makes the tropical troposphere the source region for the middle and high latitude stratosphere.

In recent years, a collaborative balloon programme between PRL, Ahmedabad and the Max Planck Institute for Aeronomie (MPAE) at Lindau, Germany, to measure the vertical distribution of trace gases in the tropical middle atmosphere was initiated under the ISRO-DLR scheme of collaboration. A composite payload of a cryogenic air sampler provided by MPAE and a multichannel sun-tracking radiom-

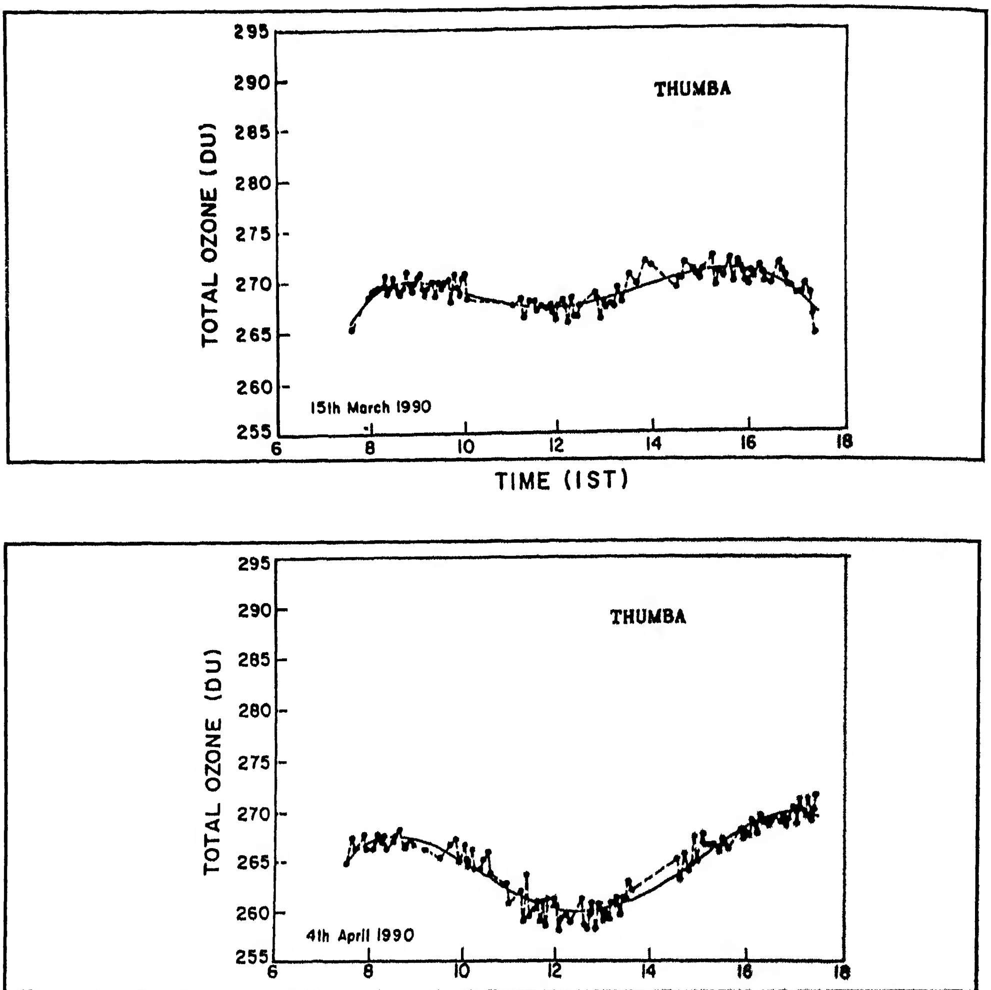

Fig.6 Typical diurnal variation of total ozone over Thumba for cloud-free days from the Brewer spectrophotometer measurements made during the DYANA campaign (after Subbaraya *et al.*, 1994).

eter provided by PRL have been flown from Hyderabad to collect air samples at different predetermined altitudes up to about 35 km. The collected air samples are analysed in the laboratory using GC and GC-MS techniques. The balloon experiments conducted from Hyderabad in March 1987 and April 1990 have yielded a complete data set of the vertical distribution of all trace gases of interest in stratospheric chemistry up to an altitude of 35 km[32]. Fig. 8-10 show some typical examples. For the first time the vertical distribution of the bromine-containing gas CH_3Br has been obtained up to stratosphere from the Hyderabad measurements. Contrary to earlier beliefs, significant abundance of this gas has been found in the stratosphere[33], making it an important source of bromine in the stratosphere. It has also been possible to estimate the atmospheric growth rates of some of the source gases. For example, the chlorofluoromethane F-12 has been found to be increasing at the rate of 4% per year. The halons 1211 and 1301 are increasing at the rate of 16% and 8% per year respectively.

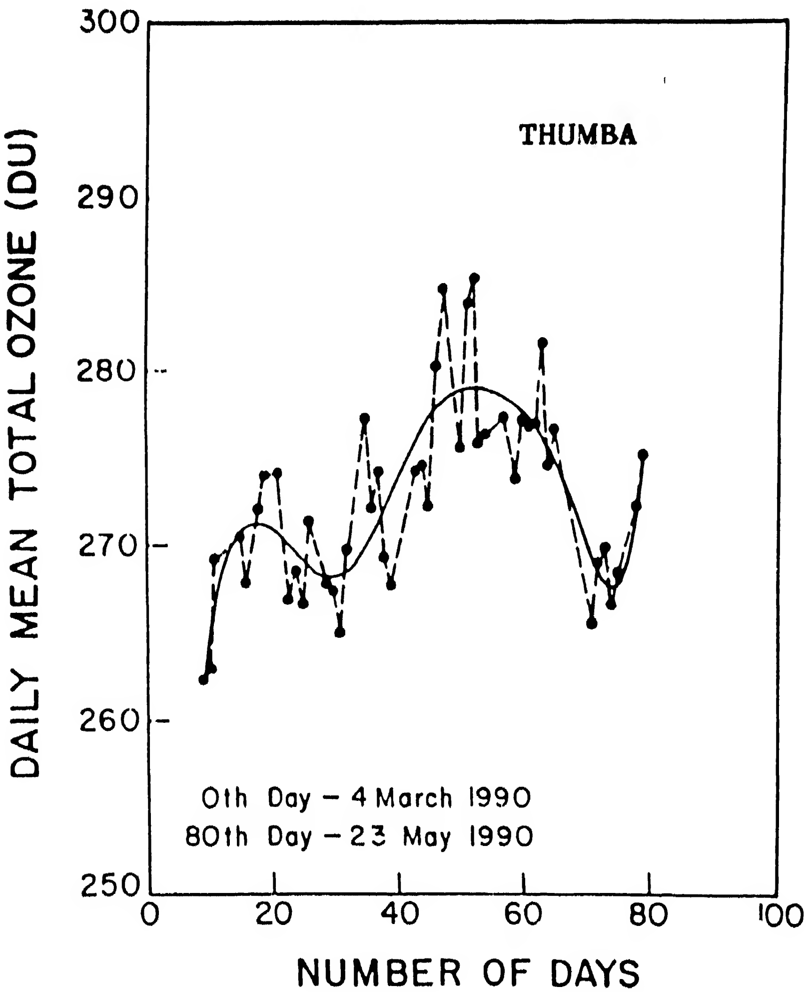

Fig 7 Day-to-day and longer-term variations in the Brewer spectrophotometer measurements made at Thumba during the March-June 1990 period (after Subbaraya *et al*, 1994)

Development of an indigenous cryosampler instrument has been undertaken by PRL/ISRO and the instrument is expected to be available soon. A few balloon launches from Hyderabad are planned for the coming years to determine the abundances and more importantly monitor the growth rates of these trace gases. Current and future growth rates of gases like F-11 and F-12, whose production and use is being curtailed (to be almost stopped by 1995) as a result of the Montreal protocol, can be used to validate current stratospheric photochemical models. For laboratory analysis, a facility with sophisticated gas chromatograph and a gas chromatograph mass spectrometer system have been set up at PRL. With these instruments, it will be possible to measure the abundances of trace gases over a wide range from parts per million down to parts per trillion (10^{-12}) by volume.

In the past few years, groundbased spectrophotometry in the visible and near ultraviolet has been successfully employed at IITM, Pune[34] and at PRL[35] to study

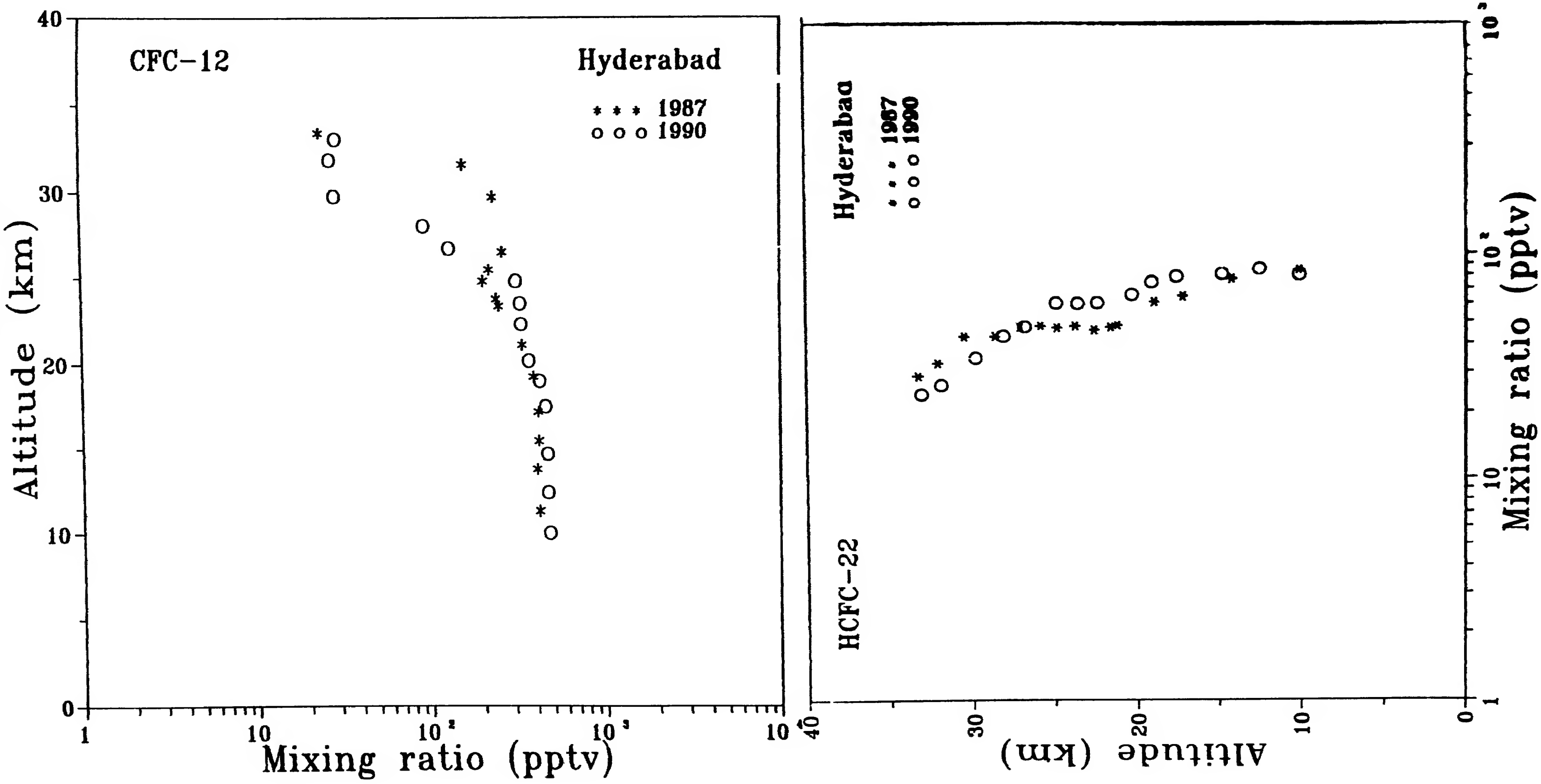

Fig 8 Vertical distribution of the trace gases, CFC-12 and HCFC-22 obtained from the balloon experiments conducted at Hyderabad

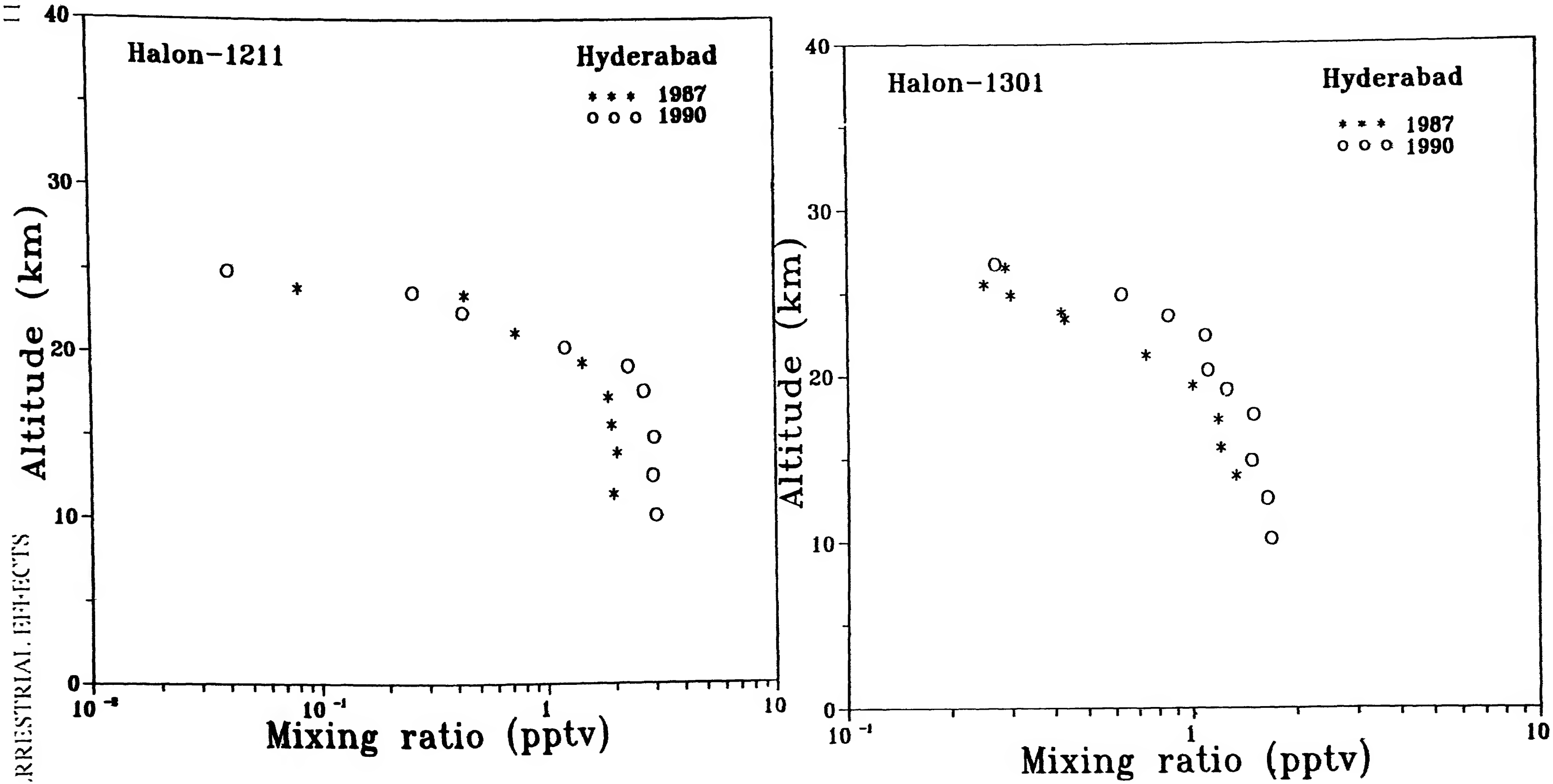

Fig 9 : Vertical distribution of the Halons 1211 and 1301 obtained from the balloon experiments conducted at Hyderabad. The data clearly show the increasing abundances of these gases in the atmosphere.

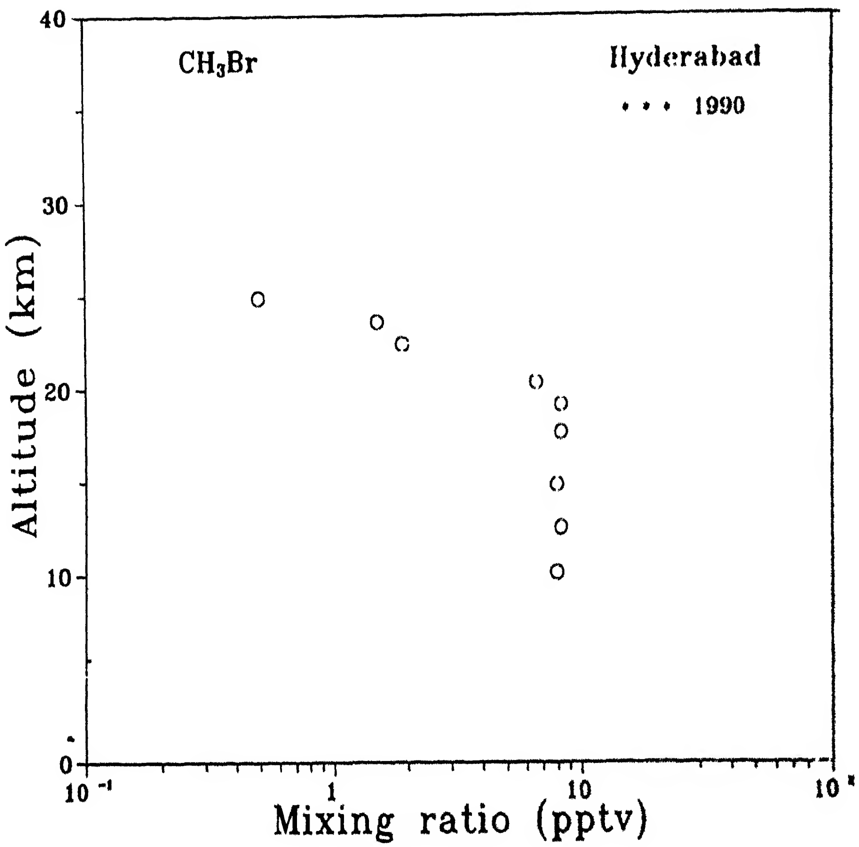

Fig 10 Vertical distribution of the bromine-containing gas CH_3Br obtained from the Hyderabad balloon experiments.

total columnar abundances of the gases NO_2 and NO_3. The data have been used to study the nocturnal and seasonal variations of NO_3 over Ahmedabad (Fig. 11). The total columnar abundances have been found to be an order of magnitude larger than at some of the other locations. The measured NO_2 concentrations show a good correlation with ozone concentrations[36] (Fig.12). At NPL, New Delhi, spectrophotometry in the near IR has been used for water vapour measurements[17]. In the coming years, these programmes will continue and there are plans to extend, especially in the IR for study of trace gases like CH_4, N_2O (and probably CFCs).

In recent years, under the International Geosphere-Biosphere Programme for study of various facets of Global Change, several new projects have been initiated all over the globe. An important project under this is Tropical Atmospheric Chemistry. The tropical regions are specially important since the troposphere here is thicker, there is abundant solar radiation throughout the year giving more scope to photochemistry and it provides almost half of the global fluxes of most of the trace gases whether they are of natural or photochemical origin. Further, as mentioned earlier, the tropical troposphere controls the mid-latitude stratospheric abundances of the long-lived trace gases due to the tropopause fold in the 20-30° latitude belt.

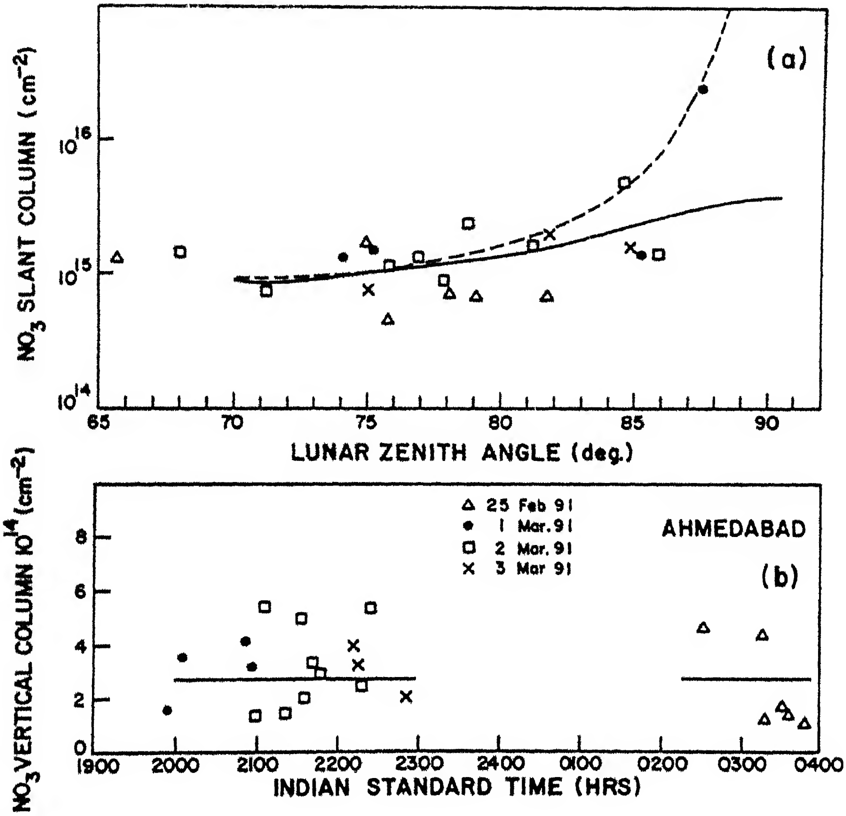

Fig.11 NO_3 column abundances over Ahmedabad obtained from visible absorption spectrometry (after Lal *et al.* 1993)

Hence the fluxes and abundances in the tropics are important from the global point as well.

Several IGBP initiatives have been introduced during the past 2-3 years in India by different groups. The major programme of interest from the Solar Terrestrial Physics point of view is the monitoring of the oxidants O_3 and OH. OH is difficult to measure directly, but can be inferred from O_3 and CH_4 measurements. A programme has been initiated under the ISRO-DOS Geosphere-Biosphere Programme to monitor ozone in ambient air at a few selected locations. The locations are chosen to be representative of different types of environments in the Indian sub-continent – urban polluted, rural, forest and remote pristine environments. The first station has been in operation at Ahmedabad since November 1991. The second station has recently been made operational at the MST radar site in Gadanki. The Ahmedabad measurements have been used to study the diurnal day-to-day and seasonal variations in surface ozone[18]. Fig. 13 shows typical diurnal variations of surface ozone at Ahmedabad and Mt Abu. While a clear noon-time maximum is seen at Ahmedabad, at Mt Abu there is a minimum in the forenoon hours. The observations are consistent with solar radiation-induced photochemistry of a polluted and NO-rich air over Ahmedabad, while over Mt Abu the ambient air is poor

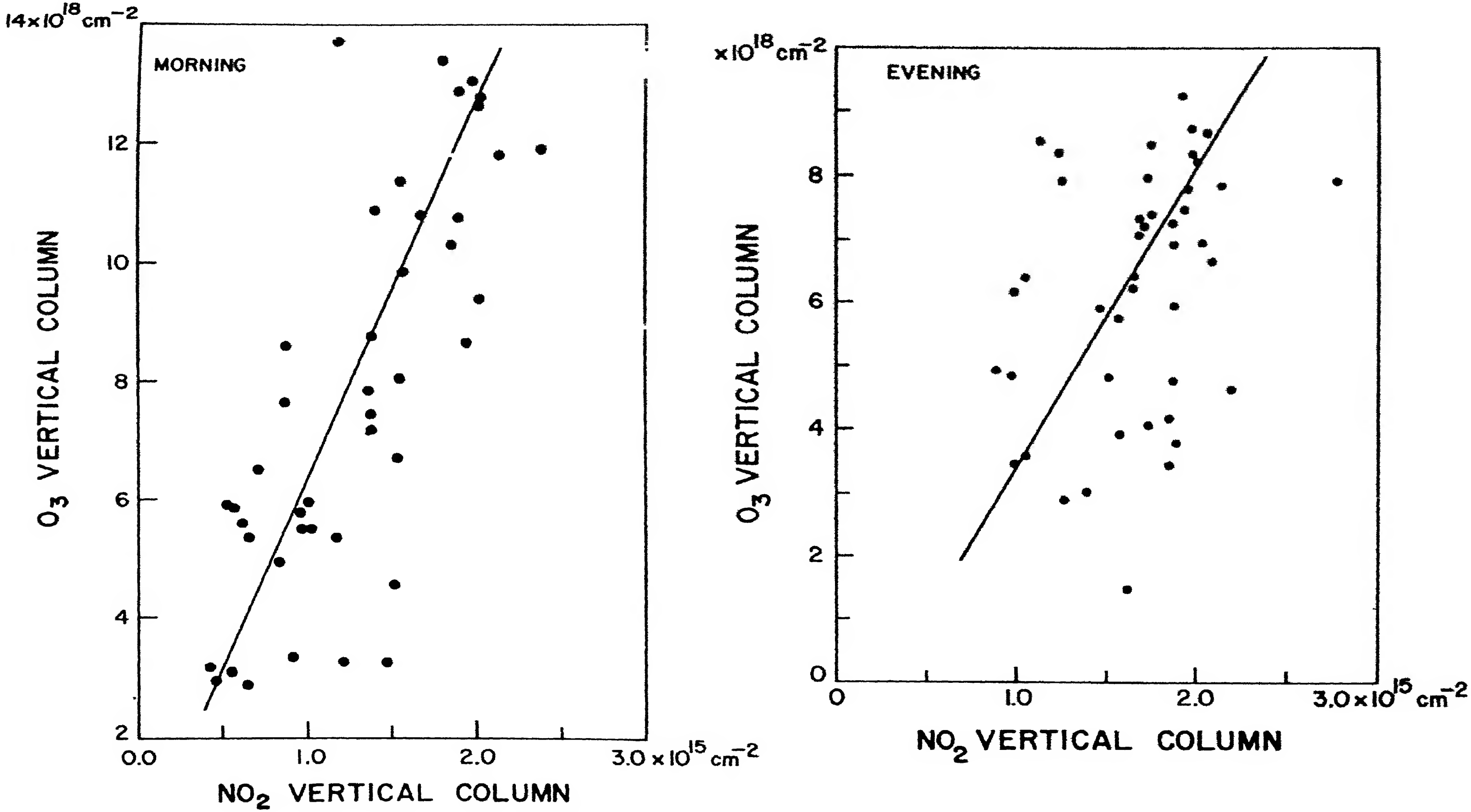

Fig. – Total column abundances of NO_2 obtained at Ahmedabad show good correlation between NO_2 and O_3 (after Lal *et al.* 1993). Morning and evening observations are separately shown.

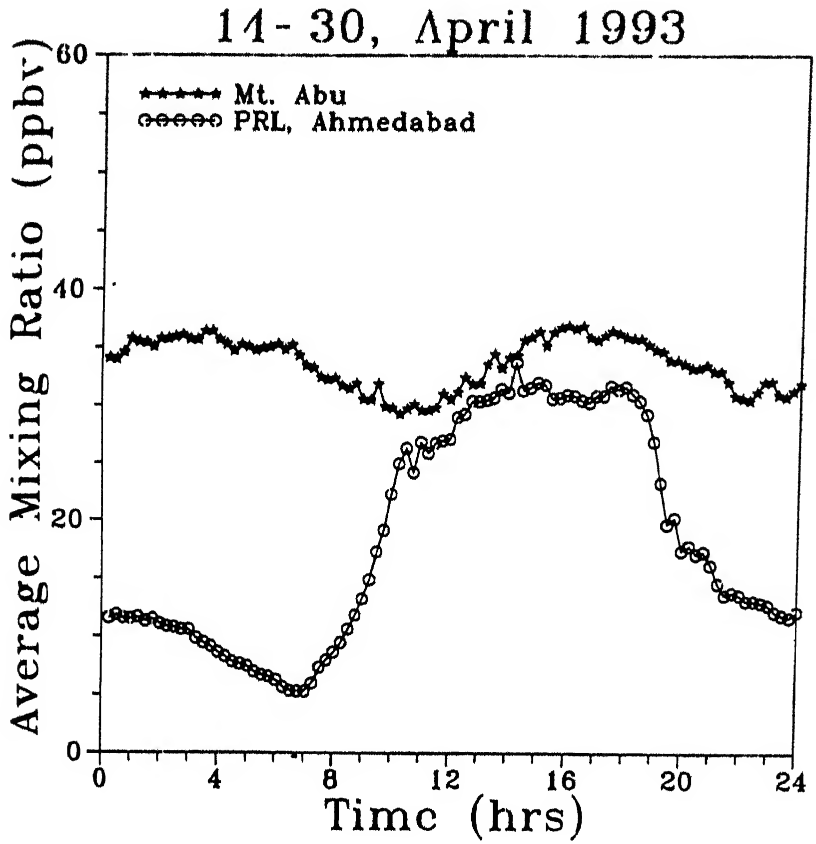

Fig.13 Diurnal variation of ambient air ozone mixing ratios at the PRL campus in Ahmedabad, which is a typical urban polluted site compared with simultaneous measurement at a remote site in Mt Abu (after Subbaraya *et al*, 1994).

in NO concentrations. The programme is being expanded to include a regular continuous monitoring of O_3 and NO_x and periodic gas sampling from these regions for measuring the ozone precursors – CH_4, CO, NMHCs, etc. The total programme will provide a comprehensive data set for modelling most aspects of tropical tropospheric chemistry.

The Indian subcontinent is geographically highly suited for tropospheric stratospheric exchange studies. It encompasses the ITCZ in the south and the tropopause fold between the mid-latitude and tropics in the north. Further, several meteorologically important features, such as the monsoon trough and the north westers, provide an opportunity to study the impact of meteorology on mid-latitude chemistry. Measurements across the exchange region are needed and high altitude aircrafts provide the best platforms. In recent years, some of the most significant results are obtained elsewhere in the globe using aircraft platforms. Instrumentation (sensors) capability exists in the country, but no suitable aircraft platform is available. Development of a DIAL laser system for ozone measurements in the troposphere as well as stratosphere (up to a height of about 25 km) is under consideration by several groups in the country. The Atmospheric Sciences Panel of

the Department of Science and Technology has identified this as a thrust programme for this decade and a position paper has been prepared[39]. If this programme materializes, it will provide a valuable tool for Tropospheric-Stratospheric Exchange studies, which is an important element in the International STEP programme.

Another lacuna on the national front has been in the area of satellite-based measurements. During the last two decades, major advances in Middle Atmospheric Chemistry and Dynamics have become possible because of data collected from satellites. In India, no such platform has so far been available. However, with the advent of the indigenous PSLV rocket, which will be flight-tested in 1994, and the Geostationary launch facility GSLV, which is likely to be a reality in the second half of the decade, there are possibilities of satellite remote-sensing of the middle atmosphere for chemistry and radiation studies.

In the area of mesospheric chemistry, progress in recent years has been far from satisfactory. Based on interest and initiatives from ionospheric (D region) studies, the sixties and the seventies saw several model studies of mesospheric chemistry. Several pioneering studies of mesospheric airglow -OH, $O_2{}^1\Delta g$ and sodium emissions were made in the earlier years. But most of these activities have decayed during the eighties in spite of the revival of interest in this area elsewhere in the globe. Ground-based airglow measurements have in the past proved valuable tools for studying atmospheric chemistry and dynamics. There have been significant advances in measurement techniques during the past decade. There is a need to take advantage of these developments in India. The IMAP ionisation campaign in the eighties also provided some scope for studies of nitric oxide variability in the mesosphere[40]. Rocket-borne payloads for measuring nitric oxide concentrations in the mesosphere and lower thermosphere have been developed by NPL and PRL. A well-planned coordinated study of nitric oxide variations in the equatorial mesosphere and lower thermosphere – with season and solar activity–will be a significant contribution to STEP.

REFERENCES

1. Chapman, S., *Mem. Roy Meteorol. Soc.*, **3** (1930) 103.
2. Chapman, S., *Phil. Mag.***10** (1930) 369.
3. Johnston, H.S., *Science*, **173** (1971) 517
4. Bates, D.R. & Nicolet, M., *J. Geophys. Res.*, **55** (1950) 301.
5. Crutzen,P.J., *Quart. J. Roy. Meteor Soc.*, **96** (1970) 320
6. Wofsy, S.C. & McElory, M.B., *Can. J. Chem.*, **52** (1974) 1582
7. Stolarski, R.S. & Cicerone, R.J., *Can. J. Chem.* **52** (1974) 1610
8. Molina, M.J. & Rowland, F.S., *Nature*, **249** (1974) 810
9. Nicolet, M., *Rev. Geophys. Space Phys.*,**13** (1975) 573.
10. Chubachi, S., *Mem. Natl. Inst. Polar Res.*, Special Issue No.34 (1984) 13.
11. Farman, J.C., Gardiner, B.G. & Shanklin, J.D., *Nature* **315** (1985) 207

12. Ramanathan, V., Cicerone, R.J., Singh, H.B. & Kiehl, J.T., *J.Geophys. Res.*, **90** (1985) 5547.
13. Mitchell, J.H.B., *Rev. Geophys.*, **27**(1990)115.
14. Angreji, P.D., ISRO-Scientific Report-ISRO -PRL-SR-34-89 (1989).
15. Rao, K., *Curr. Sci.*, **64** (1993) 344
16. Bojkov, R., Bishop, L., Hill, W.J., Reinsel, G.C. & Tias, G.C., *J.Geophys. Res.*, **95** (1990) 9785.
17. WMO Scientific Assessment of Ozone Depletion (World Meteorological Organization), 1991.
18. Srivastava,B.N., Sharma, M.C. & Tanwar, R.S., *Indian J. Radio and Space Phys.*, **18** (1989) 296.
19. Gayathri, H.B., Prasad, B.S.N.& Thukaram, M., *Indian J. Radio and Space Phys.*, **22** (1993) 306.
20. Mohan Kumar, G., Ph.D. Thesis, Cochin University, 1993.
21 Prasad, B S.N., Gayathri, H.B., Muralikrishna, N. & Murthy, B.N., Indian *J.Radio and Space Phys.*, **20** (1991) 18.
22. Subbaraya, B.H. & Jayaraman, A., *Adv. Space Res.*, **7** (1987) 119.
23. Jayaraman, A., Lal. S., Subbaraya, B.H., Zalpuri. K.S., Seshadri, N., Sreedharan, C.R., Vijay Kimar, R., Ignatov, V.M., Kokin, G.L., Perov, S.P., Shtrikov, O.V., Tishin, S.V. & Chizhov, A.F. in *Ozone in the Atmosphere,* (Edited by) R.D. Bojkov and P. Fabian (A. Deepak Pub. Co., USA) 1993 113.
24. Subbaraya, B.H., *Curr. Sci.*, **64** (1993) 339.
25. Srivastava, S.K., Paper presented at the National Space Science Symposium, Ahmedabad, 1992.
26. Sreedharan, C.R., Gulhane, P.M. & Kataria, S.S., *Curr. Sci.*, **64** (1993) 634.
27. Subbaraya, B.H., Jayaraman, A., Lal, S., Ramani, S.V., Thomas John, Zalpuri, K.S., Sreedharan, C.R., Srivastava, S.K., Perov, S.P., Kokin, G.A., Tishin, S.V., Byazankin, S.A., Shtirkov, O.V., Chizhov, O.V., Ignatov, V.M. & Uvarov, V.N., To appear in *J. Atmos. Terr. Phys.*, (1994).
28. Subbaraya, B.H., Lal, S., Venkataramani, S., Ishov, A.G., Perov, S.P. & McElroy, T.M., To appear in *J. Atmos. Terr. Phys.*, (1994).
29. Jain, S.L. & Arya, B.C , Res Rept NPL 87 C 50053, (NPL., New Delhi), 1987.
30. Jain, S.L., *Indian J. Radio and Space Phys.*, **18** (1989) 175.
31. Saha, A.K., *Indian J. Radio and Space Phys.*, **20** (1991) 381.
32. Borchers, R., Fabian, P., Singh, O.N., Lal, S. & Subbarya, B.H, in *Ozone in the Atmosphere,* edited by R.D. Bojkov and P. Fabian, (Deepak Pub. Co., USA) 1988, 290.
33 Lal, S., Borchers, R., Fabian, P., Patra, R.H. & Subbaraya, B.H., To appear in *Tellus* (1994).
34. Jadhav, D.B., *Indian J. Radio & Space Res.*, **21** (1992) 108
35. Lal, M., Siddhu, J.S., Das, S.R. & Chakrabarty, D.K., *J. Geophys. Res.*, **98** (1993) 23029.
36. Lal, M., Chakrabarty, D.K, Sddhu, J.S. & Das, S.R., *Indian J. Radio and Space Phys.* **22** (1993) 108.
37. Gosh, A.B., Sharma, R.C. & Reddy, B.M., *Indian J. Radio and Space Phys.*, **22** (1993) 38.
38. Subbaraya, B.H., Lal, S., Modh, K.S. & Manish Naja, in *Global Change Studies*, Scientific Report-ISRO-GBP-SR-42-94 (1994) pp. 5-15.
39 *Lidar Studies of the Atmosphere* (Department of Science & Technology, New Delhi) 1993
40. Chakrabarty, D K , Pakhmov, S.V. & Beig, G., in *Hand Book for MAP*, **29** (1989) 10.

EQUATORIAL MIDDLE ATMOSPHERIC DYNAMICS

B.V. Krishna Murthy*

INTRODUCTION

The atmospheric region between 10 and 100 km is generally considered to be the Middle Atmosphere. This region experiences wave forcing from atmospheric region below and heating due to ozone in the stratosphere. The wave forcing from below and the heat sources in the region itself give rise to a very wide range of oscillations and waves (in wind, temperature and pressure). The dynamics of the middle atmosphere at low latitudes is significantly different from that at middle and high latitudes. This is mainly because the decreasing effect of coriolis force at low latitudes. Whereas the synoptic scale flow at mid-latitudes is quasi-geostrophic, the flow at low latitudes becomes increasingly ageostrophic with decreasing latitude. Atmospheric waves in the low latitudes reflect the transition from quasi-geostrophic to ageostrophic motions in their horizontal structure showing nearly isobaric wind perturbations at the northernmost and southernmost extent and cross-isobaric flow near the equator. In the equatorial region, interaction between waves and the mean flow gives rise to strong long-period oscillations, namely Quasi-Biennial (QBO) and Semi-Annual (SAO) oscillations. Table I summarizes the different types of oscillations/waves of importance in the equatorial middle atmosphere.

Many scientific studies have been carried out in India on various aspects of equatorial middle atmospheric dynamics. Significant contributions have been made on the characteristics of long-period oscillations such as the QBO, equatorial waves and tides. The studies carried out are based mainly on wind and temperature data obtained from rocket and balloon soundings. Theoretical studies on equatorial wave propagation in the middle atmosphere have also been carried out.

In this report, a summary of the research work on middle atmospheric dynamics carried out in India in the last decade or so is presented.

*Space Physics Laboratory, Vikram Sarabhai Space Centre, Trivandrum 695 022.

Table 1 Different Types of Oscillations / Waves in Equational Middle Atmosphere

Type of oscillation/wave	Time scale	Main mechanisms/sources for generation
1. QBO	~26 months	Wave-mean flow interaction involving Kelvin and Rossby gravity waves
2. Annual oscillation	12 months	Latitudinal unequal solar heating.
3. SAO	6 months	Wave-mean flow interaction involving Kelvin waves and solsticial heating.
4. Plannetary waves (including equatorial waves)	2-40 days	Orographic, thermal forcing
5. Tidal oscillations	24 h, 12 h	Thermal (due to ozone and water vapour)
6. Gravity waves	~5 min to a few hours	Mountain waves, unsteady shear zones

Quasi-biennial Oscillation

Using M-100 data of winds and temperature over the period 1970-1986 at Trivandrum (8°33N, 77°E) and RH-200 rocket data of winds over the period 1979-1987 at Balasore (21.5°N, 7°E), Nagpal *et al.* (1989) and Sasi and Krishna Murthy (1991) studied the characteristics of QBO. Sasi and Krishna Murthy quantified the characteristics of QBO and their cycle-to-cycle variability. Their main results on QBO at Trivandrum are summarised below:

1. The easterly and westerly amplitudes of QBO show a broad maximum at ~30 km. Their amplitudes decrease rapidly above and below 32 and 25 km respectively.

2. The maximum amplitude (mean) of both easterly and westerly regimes of QBO is about 18 ms^{-1}. The QBO shows significant amplitudes in the altitude region 18 to 40 km.

3. The maximum easterly amplitudes show greater cycle-to-cycle variation than the maximum westerly amplitude. This implies greater cycle-to-cycle variation in the wave momentum flux deposited by the causative Rossby gravity waves and also planetary waves. The role of gravity waves also needs to be mentioned here.

4. The mean periods of easterly and westerly regimes are nearly constant with altitude except at lower altitudes. The period is generally longer for the westerly

regime than the easterly regime. The westerly regime following the El Chichon volcanic eruption is found to be particularly of longer duration.

5. The QBO in temperature shows a maximum mean amplitude (for both warm and cold regimes) of 3.4 K and the maximum occurs at 20 km for the warm regime and 19 km for the cold regime.

6. The cycle-to-cycle variation of temperature QBO is found to be quite large. The standard deviation of the mean amplitude is in the range 1-2 K.

Unlike at Trivandrum, the QBO amplitudes at Balasore do not show a prominent maximum with altitude and the amplitudes are quite small at Balasore compared to those at Trivandrum. The QBO periods at Balasore are nearly the same as those at Trivandrum in the altitude range 25-34 km, above and below which they are considerably shorter. The occurrence of the maxima of the easterly and westerly regimes at Balasore is found to lag that at Trivandrum by 1-2 months.

Sasi and Krishna Murthy (1991) found from their analysis of QBO at Trivandrum over the period 1970-1986 that geostrophic balance holds good approximately at altitudes below 25 km, whereas at altitudes above 25 km, significant deviations occur from geostrophic balance for some of the QBO cycles studied.

Reddy and Raghava Reddi (1986) from an analysis of QBO at Trivandrum, Ascension Island (8°S, 14.5°W) and Kwajalein (8.7°N 167.7°E) found that the characteristics of QBO are nearly the same at the three stations. This result indicates that there are no significant longitudinal differences in the QBO characteristics.

Annual and Semiannual Oscillations

The characteristics of the Annual (AO) and Semi-annual (SAO) oscillations have been studied by Reddy and Raghava Reddi (1986), Reddy *et al.*, (1986), Nagpal *et al.* (1989), and Jain and Rangarajan (1991).

Reddy *et al.* (1986), studying the AO in the zonal wind at Trivandrum (Thumba), SHAR (13.7°N, 80.2°E) and Balasore found that its amplitude shows a well-defined primary peak in the altitude range 12-15 km with altitude of the peak decreasing with latitude. A prominent secondary peak is shown near stratopause at Balasore. The AO amplitude is found to increase with increasing latitude except in the region 33-43 km. The height variation of AO phase (time of maximum of westerly wind) is smallest at Balasore and largest at Trivandrum.

Analysing the zonal wind data of Trivandrum, Ascension and Kwajalein for the study of longitudinal variations of AO, Reddy and Raghava Reddi (1986) reported that the AO amplitudes in the troposphere are much smaller at Ascension and Kwajalein compared to those at Trivandrum. They found that AO at Ascension and

Kwajalein has approximately the same amplitudes in the 35-45 km region in the year 1979 whereas in the following year 1980, AO at Trivandrum and Kwajalein has similar amplitudes in the altitude region 22-60 km. This indicates that in the stratosphere (and lower mesosphere) the longitudinal differences in AO amplitudes exhibit variations from year to year. Comparing the maximum stratospheric AO amplitudes at Balasore and Barking Sands (21.9°N, 159.6°W), Reddy and Raghava Reddi reported that it is greater at Barking Sands by a factor of 1.6-1.8 compared to that at Balasore. Further, the tropospheric AO amplitudes at Balasore are found to be greater than those at Barking Sands.

Investigating the SAO (in zonal wind) at Trivandrum, SHAR and Balasore, Reddy *et al.*(1986) found that its amplitude is small below 30 km and increases steadily from 30 to 60 km, exhibiting a broad maximum centred on 48 km. A secondary maximum is found to appear at 16 km. They also reported the absence of a substantial gradient of SAO amplitude in the 40-55 km range. The SAO phase (time of maximum westerly wind) is reported to decrease slowly with height in the region 30-60 km. Above 30 km, the SAO phase leads at Balasore compared to that at Trivandrum.

Studying the longitudinal differences using the data for the years 1979 and 1980, Reddy and Raghava Reddi reported that the maximum SAO amplitude (occurring near stratopause) at Trivandrum is 1.6 times that at Kwajalein and that at Ascension is 1.6 times that at Trivandrum. Moreover, the height extent with large SAO amplitude increases progressively from Kwajalein to Trivandrum to Ascension. At a latitude of ~21°N, the SAO amplitudes in the stratosphere did not exhibit any longitudinal differences as shown by the data at Balasore and Barking Sands.

Using the zonal wind data at Trivandrum, Kwajalein and Ascension covering a period of about 10 years, Reddy and Vijayan (1993) reported large cycle-to-cycle variation in the amplitudes of AO and SAO. They observed that in general, large SAO amplitudes (near stratopause) occur during the westerly phase of QBO (at 28 km) and smaller amplitudes during its easterly phase. A similar trend is observed for AO in the lower mesosphere (at 62 km), with large amplitudes prevailing during the westerly phase.

Analysing the tropopause characteristics in the Indian zone, Krishna Murthy *et al.* (1986) found that the amplitude of AO of tropopause pressure (P) and height (H) showed a minimum at ~ 17°N with a marked increase north and south of 17°N. There is a steady march of the phase (of AO) of P and H with latitude, with the maximum (in P and H) delayed progressively from 8° to 29°N. On the other hand, the phase of AO of tropopause temperature (T) decreased with latitude, i.e. the maximum occurred earlier at lower latitudes. The semi-annual components are found to be weaker than the annual components and they also showed a broad minimum (in amplitude) around 17°N. Krishna Murthy *et al.* reported that the phases of AO and SAO of P, H, and T showed very little variations from year to year. The behaviour

of the AO and SAO components was interpreted in terms of the surface equivalent potential temperature and cloud cover.

Raghava Redddi *et al* (1993) studied AO and SAO of temperature at mesospause levels from Meteor wind radar data at Trivandrum. From the amplitude decay of underdense radiometeor trails obtained from the Meteor wind radar, they derived the ambipolar diffusion coefficient (D). The amplitudes of AO and SAO of D have been interpreted in terms of the AO and SAO of mesopause temperature. They found that AO of mesopause temperature is much stronger than its SAO and that the CIRA atmospheric models do not reproduce the observed AO of mesopause temperature. They reported that taking into account AO and SAO, the mesopause temperature T_m can be represented as a function of day number d by :

$$T_m = 186.7 + 9.2 \cos (0.986\text{-}d - 309) + 5.8 (\cos 1.972 - 120)$$

Equatorial Waves

Using the altitude profiles of zonal and meridional winds in the height range 20-60 km from weekly RH 200 rocket launchings at Balasore and SHAR, Devarajan *et al.* (1985) deduced some of the characteristics of the equatorial atmospheric waves. According to their analysis the dominant vertical wavelengths (of the waves) in the zonal wind are in the range of 6-12 km in about 67% of the cases examined and the amplitudes are significantly greater during easterly background wind. The amplitudes are greater by about a factor of 2 at SHAR compared to those at Balasore. Corresponding wave perturbations are found to be absent, in general, in the meridional wind. These characteristics lead to the conclusion that the observed wavelike disturbances (in the altitude profiles of zonal wind) are the manifestation of Kelvin waves. In some cases, Devarajan *et al.* found the wave periods to be in the range 4-8 days. The short vertical wavelengths together with the short periods indicated the possible dominance of zonal wave number 2 during many wave disturbances. Devarajan *et al.* also reported that the more active periods of wave disturbances correspond to the easterly phase of SAO and the wave activity persisted for a longer duration when the AO and SAO are in easterly phase.

As part of the Indian Middle Atmospheric Programme (IMAP), scientific campaigns were conducted to obtain wind profiles using RH-200 rockets and balloons for the study of equatorial waves. The first campaign consisted of near simultaneous rocket and balloon launchings at Trivandrum, SHAR and Balasore on alternate days from 23 May to 12 June 1984 (Krishna Murthy *et al.*, 1986). The second campaign consisted of wind measurements using RH-200 rockets and balloons launched daily from SHAR for 45 days from 15 January to 28 February 1986 (Raghava Rao *et al.* 1990).

Krishna Murthy *et al.*(1986) found that the wind variance (of both zonal and meridional components) is maximum around 13 km and that at Trivandrum it is

greater than that at SHAR and Balasore The tropospheric data showed no significant vertical phase propagation for longer-period oscillations with period ~ 15.5 days, whereas shorter-period (~7.7 days) waves showed vertical phase propagation with a wavelength of ~ 7 km. As the peak in variance represents mainly a non-propagating disturbance, the observed peak (in variance) is attributed to the 15.5-day component.

In the region 23-35 km, Krishna Murthy *et al.* (1986) observed a strong maximum in the zonal wind variance while no phase change is seen in this altitude range. Above this altitude region, the long-period waves (~15.5 days) indicated a vertical wavelength of ~ 7 km with upward phase propagation, followed by a downward phase propagation. On the other hand, the short-period (7.7 days) waves showed no systematic phase variation with altitude. Krishna Murthy *et al.* inferred from these observations of no phase propagation in the region 23-35 km that this is a source (of wave disturbances) region. They suggested that ozone heating could provide the necessary energy for these disturbances.

Raghava Rao *et al.* (1990), from an analysis of the second campaign data, reported that waves with periods > 23 days reveal two height regions of enhanced amplitudes, one in the troposphere and another in the upper stratosphere/lower mesosphere. The vertical wavelengths have been estimated to be 34 km and 19 km in the troposphere and lower stratosphere respectively and 8 km in the upper stratosphere and lower mesosphere. Raghava Rao *et al.* suggested that the tropospheric waves to be Rossby waves of extra tropical origin penetrating to tropical latitudes. The stratospheric and mesospheric waves appear to be emanating from a source around the stratopause. Similar evidence has been found for the location of source region of wave disturbances with mean periods ~15.5 days from the first campaign results reported by Krishna Murthy *et al.* (1986).

Using wind data from high altitude balloon and rocket launchings at equatorial stations, Nagpal and Raghava Rao (1991) found observational evidence for the presence of long-period waves (period of 23-60 days) in the troposphere/stratosphere, particularly during winter months. They suggested that these waves are from mid-latitudes (Rossby waves). Using a 2-d dynamic wind model to simulate the easterly and westerly phases of SAO, Nagpal and Raghava Rao (1991) studied the implication of these waves in producing the easterly phase of SAO. They showed that momentum deposition by the Rossby waves propagating from mid-latitudes is a significant contribution to the easterly phase of SAO.

Reddy and Vijayan (1989) made quantitative theoretical estimates of the reflection and radiative damping of the Kelvin and Rossby gravity (RG) waves propagating upward in the 20-90 km region. They showed that for Kelvin waves, the reflected wave energy is generally less than 15% of the incident wave energy but the reflected wave amplitude can be 20-30% of the incident wave amplitude for many modes at 20 km altitude. In contrast, many RG wave modes suffer strong or total

reflection at various heights if they are not severely damped at lower heights. Reddy and Vijayan (1989) found radiative damping to be severe for Kelvin waves with periods greater than 6-8 days depending on background wind conditions. The radiative damping is found to be severe even in the lower stratosphere for Rossby-gravity waves with periods greater than 4 days. The damping rates and wave amplitudes showed strong dependence on background wind conditions. They found that Kelvin waves in the 2-8 day period range and RG waves in the 1.5-3 day range can propagate into the upper mesosphere/lower thermosphere without much attenuation depending upon wind conditions. Reddy and Vijayan had shown that some of the observed characteristics of the equatorial waves (Kelvin and Rossby gravity waves) can be explained on the basis of their theoretical results.

Using stratospheric and mesospheric wind data from M-100 rocket launchings at Trivandrum, Raghava Reddi *et al.* (1988) detected a quasi 2-day oscillation in the zonal and meridional wind components and found its amplitude to be > 15 m/s at altitudes > 40 km. The vertical wavelength is obtained to be ~30 km in the 40-60 km region and ~20 km in the 60-80 km region. From the range of vertical wavelengths and the sense of rotation of the wind vector, they concluded that the quasi 2-day wave could be a lower mode of RG wave.

Tidal Oscillations

Diurnal and semidiurnal tides in the altitude region 20-65 km have been studied by Sasi and Krishna Murthy (1990, 1993) and Krishna Murthy *et al.* (1992) as part of DYANA (Dynamics Adopted Network for the Atmosphere) programme.

Sasi and Krishna Murthy (1990) observed that the tidal components at Balasore showed significant seasonal variations. The observed diurnal tides in the zonal and meridional components showed, in general, good agreement with the theoretical predictions for the three seasons (summer equinoxes, winter) except the zonal component in winter. This disagreement in winter is attributed to planetary wave disturbances. Sasi and Krishna Murthy (1990) found that the observed semi-diurnal amplitudes to be much greater than the theoretically predicted values. The observed phases showed good agreement with the theoretical values for equinox seasons whereas for summer and winter seasons they differ considerably from theoretical values. They also found evidence for the presence of non-migrating tides (Krishna Murthy *et al.* 1992; Sasi and Krishna Murthy, 1993).

Analysing the data of meteor wind radar at Trivandrum, Raghava Reddi *et al.*(1993) observed that in the altitude region ~ 85-100 km, in addition to the diurnal (1,1) mode, the evanescent mode, characteristics of mid-latitudes, and the symmetric (1,3) mode could also be present. They found that for the semi-diurnal tide, the strongest mode is not always the (2,2) mode and the higher order (2,4) and (2, 5) could be present with significant amplitudes.

REFERENCES

Devarajan, M., Reddy, C.A. & Raghava Reddi, C., (1985). *J. Atmos, Sci.* **18**, 1973.

Jain, A.R. & Rangarajan, G.K., (1991). *Indian J. Radio Space Phys.*, **20**, 409.

Krishna Murthy, B.V. Indukumar, S. Raghava Reddi, C. Raghava Rao, R. & Rama, G.V., (1986) *Indian J.Radio Space Phys.*, **15**, 125.

Krishna Murthy, B.V., Parameswaran, K. & Rose, K.O., (1986) *J. Atmos, Sci.*, **43**, 914.

Krishna Murthy, B.V., Perov, S.P. & Sasi, M.N., (1992) *J. Atmos. Terr. Phys.*, **54**, 881.

Nagpal, O.P., Jain, A.R. & Dhaka, S.K., (1989). *Indian J. Radio Space Phys.*, **18**, 233.

Nagpal, O.P. & Raghava Rao, R., (1991). *J. Atmos. Terr. Phys.*, **53**, 1181.

Raghava Rao, R., Suhasini, R., Sridharan, R., Krishna Murthy, B.V. & Nagpal, O.P., (1990) *Proc. Indian Acad. Sci.*, **99**, 413.

Raghava Reddi, C., Getha, A. & Lekshmi, K.R., (1988). *Ann Geophysicae*, **6**, 231.

Raghava Reddi, C., Rajeev, K. & Ramkumar, G., (1993). *J. Geophys. Res* (in press)

Raghava Reddi, C., Rajeev K. & Ramkumar G., (1993). *J. Atmos. Terr. Phys.* (in press)

Reddy, C.A. & Raghava Reddi, C. (1986). *J. Atmos. Terr. Phys.*, **48**, 1085.

Reddy, C.A., Raghava Reddi & Mohankumar K.G., (1986). *Quart. J.R. Met. Soc.*, **112**, 811.

Reddy, C.A. & Lekshmi Vijayan, (1989). *Quart. J.R. Met. Soc.*, **115**, 1273.

Reddy, C.A. & Lekshmi Vijayan, (1993). *Adv. Space Res.*, **13**, 373.

Sasi, M.N. & Krishna Murthy B.V., (1990). *J. Atmos. Sci.*, **47**, 2101.

Sasi, M.N. & Krishna Murthy, B.V., (1991). *J. Atmos. Terr. Phys.*, **53**, 1173.

Sasi, M.N. & Krishna Murthy, B.V., (1993). *J. Geomag. Geoelect*, (in press)

PLANETARY ATMOSPHERES AND IONOSPHERES

K.K. Mahajan, J.Kar and H.O. Upadhyay*

This article is a brief 'Status Report' in the area of 'Planetary Atmospheres and Ionospheres'. A short account of the planetary explorations is given and the major characteristics of the planetary atmospheres and ionospheres which have resulted from these explorations are described. Results on solar wind interaction with the nonmagnetic planets in the light of Viking and Pioneer Venus missions are also given. Major Indian contributions are summarised and various outstanding problems and future Indian experimental and theoretical plans are briefly stated.

1. INTRODUCTION

All planets, with the exception of Mercury, have extended atmospheres. The chemical composition can, however, be different. The Earth's atmosphere, for example, consists of 78% nitrogen, 21% oxygen and 1% argon, while atmospheres of Venus and Mars are CO_2-dominated. Jupiter, Saturn and Uranus have mainly hydrogen, helium and small amounts of methane. It is now recognised that although all the terrestrial planets started with a similar composition, these went through important evolutionary changes during their long history of about 4.5 billion years. Various parameters like the mass of the planet, its distance from the Sun and its internal structure have played a crucial role in the planetary evolution, since these parameters controlled the escape of lighter gases, the outgassing from the interior, and the chemical reaction between atmospheric gases and crustal rocks. In spite of such varied composition, all planets have ionised regions in their upper atmospheres, called the ionospheres, produced mainly by solar radiations. In this article, we shall give a short account of the planetary explorations, cover major characteristics of the planetary atmospheres and ionospheres, give a summary of major contributions from India in this area, state the various outstanding problems, and finally enunciate plans for future work, mainly in the country.

*National Physical Laboratory, New Delhi 110 012.

2. PLANETARY EXPLORATIONS

Planets are being explored by space techniques since early sixties Three types of missions have been employed in these explorations and these are:

1. Fly-bys
2. Orbiters
3. Orbiters cum landers.

The first successful planetary mission was the American spacecraft Mariner 2 which flew by Venus at a distance of about 35,000 km. This was followed by a large number of missions which are summarised in Fig.1. The missions have been superposed on the sunspot cycle. It can be noted that for most of the planets observations exist for low as well as high levels of solar activity.

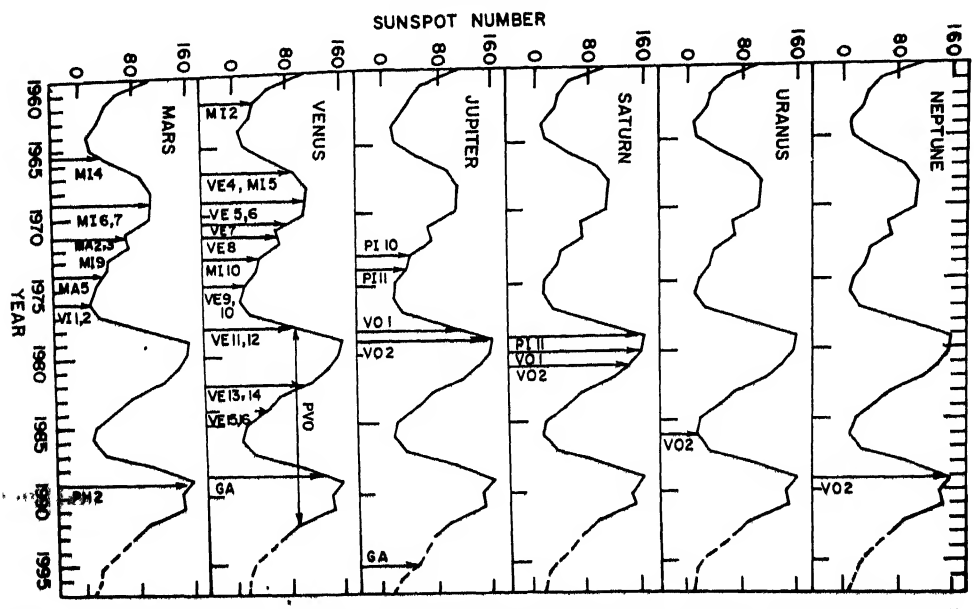

Fig 1 Successful planetary missions to various planets (Venus is the most explored planet, especially in the light of the recent Pioneer Venus mission).
Symbols: GA-Galileo, MA-MARS, MI-Mariner, PH-PHOBOS, PI-Pioneer, VE-Venera, VI-Viking, VO-Voyager.]

Although the earliest missions were fly-bys, Mariner-9 was the first spacecraft to orbit a planet, other than the Earth. It provided an extended period of observations for the ionosphere and upper atmosphere of Mars. Viking mission had both landers and orbiter. The Viking landers made *in-situ* measurements in the atmosphere and ionosphere of Mars. Pioneer Venus has been the most successful mission. It had both landers and orbiter. The orbiter explored Venus directly for about 14 years and had a large number of ionospheric and atmospheric experiments. The giant planets viz. Jupiter, Saturn, Uranus and Neptune, have been explored by Pioneer 10, 11 and/ or Voyager 1 and 2 Only Voyager 2 has visited all these four planets. All missions to giant planets have been fly-bys.

3. MAJOR RESULTS

Planetary explorations have given real surprises about the structure and constitution of ionospheres and upper atmospheres of almost all the planets. For example, a quantitative knowledge of the upper atmosphere of Mars began with the Mariner 4 radio occultation data in 1965 (Kliore *et al.* 1965)[1]. Earlier to these measurements the Mars ionosphere had been predicted by Kliore *et al.* (1965)[2] to have the ionization peak at 3 times the observed altitude, with seven times the observed density. A model of the upper atmosphere of Mars with no CO_2 and several times the observed exospheric temperature was postulated by McElroy *et al.* (1965)[3]. At Venus, for example, only from the PV mission the ionosphere was found to be composed of molecular oxygen ions and not carbon dioxide ions, as had been thought earlier. Further, the temperature of the daytime Venus atmosphere was found to be about 300 K, much smaller than 700 K – the temperature at the surface. Similarly, new discoveries have been made about the solar wind interaction at Venus. These have then been extrapolated to Mars too. Major results on the atmospheres of most of the planets were reviewed by Mahajan & Kar (1988)[4]. In what follows, we shall summarize the main results emphasizing the advances made since then, under three headings, namely the neutral atmosphere, the ionosphere and the solar wind interaction. References to original papers will be kept to a minimum. However, while discussing Indian contributions, references to major Indian works will be given.

Neutral Atmospheres of Terrestrial Planets

The neutral composition of Venus and Mars is shown in Fig. 2. For comparison the composition of the Earth's thermosphere is also shown. The Venus thermosphere shown in the figure is based upon the direct measurements by the neutral mass spectrometer on the Pioneer Venus Orbiter (Niemann *et al.* 1980)[5]. The dashed lines show the daytime measurements, while the solid lines show the nighttime measurements. Up to about 200 km, CO_2 dominates and above it, atomic oxygen takes over – up to about 300 km 'cold' O dominates and above 300 km 'hot' O dominates. This dominance continues up to altitudes as high as 3500 km. This is a very important result, and is very relevant to the escape of O due to solar wind interaction. At Mars CO_2 is the major neutral constituent up to about 200 km, above which the models by Fox and Dalgarno (1979)[6] indicate O to be the dominant constituent. These models are reproduced in Fig. 2c. Atomic oxygen has not been measured. Direct measurements of CO_2, O_2, NO, CO and N_2, as made by the neutral mass spectrometer on Viking 1 (Nier and McElroy 1977)[7] are also shown. At Mars cold H is the dominant constituent above 500 km and is due to low gravity there. (This is in contrast to Venus where hot O is the major neutral constituent up to about 3500 km). The composition of the Earth's thermosphere is shown in Fig. 2b. As can be noted, N_2 is the major constituent up to about 200 km, above which O dominates. At higher altitude, in the exosphere, H becomes the dominant constituent. Earth's thermosphere is the hottest, with Tex increasing with solar activity and with a day-

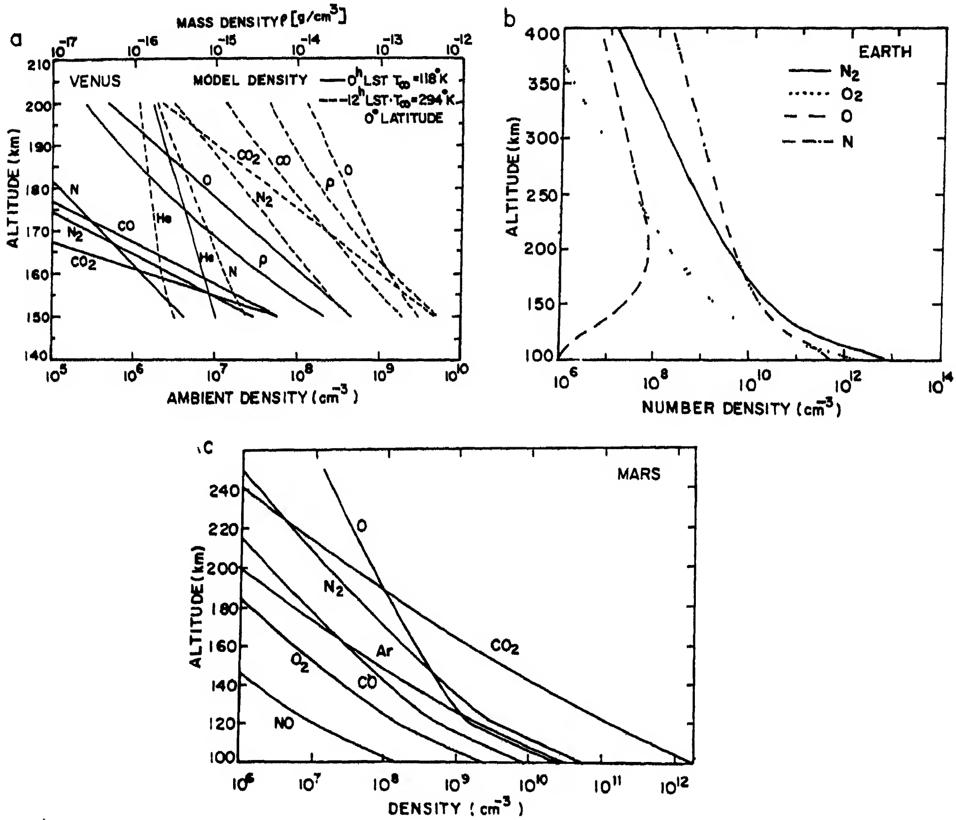

Fig.2 The neutral composition of Venus, Earth and Mars thermosphere [The Venus thermosphere is shown in Fig 2a (after Niemann *et al* 1980) [5] Fig 2b shows the Earth's thermosphere based on the MSIS 86 model for $F_{10.7}$=150 (Hedin 1987)[61]; and Fig. 2c the Mars atmosphere (after Fox and Dalgarno 1979)[6] In Fig 2c, the modelled profiles are compared to some of the densities measured by Viking 1. The CO_2, O_2 and NO measurements are represented by solid circles, the CO and N_2 densities by crosses, and Ar densities by open squares

to-night ratio of 1.3. The daytime temperature during medium solar activity is around 1000 K. Fig. 3 shows a comparative study of atmospheric temperatures of the three planets.

Due to the Pioneer Venus mission, Venus is now the most explored planet. This mission, as mentioned earlier, lasted for nearly 14 years. The Pioneer Venus Orbiter, which started sampling Venus in December 1978, continued sampling until October 1992, when it ran out of fuel and burnt off in the Venus atmosphere. Important results on the Venus atmosphere include the strong winds that carry constituents of the atmosphere across the terminator from the dayside to the nightside, where they descend into the lower atmosphere, the very low nightside temperature, the great bulges in hydrogen and helium densities found in the predawn section and enormous deuterium, larger by a factor of 100 relative to Earth (Hunten, 1989)[8]. The predawn bulges require a super-rotation with a period of about 6 days, imposed on the predicted flow. There is very little thermal escape, even of lighter gases like hydrogen and helium. The non-thermal escape is also at a low rate. The high

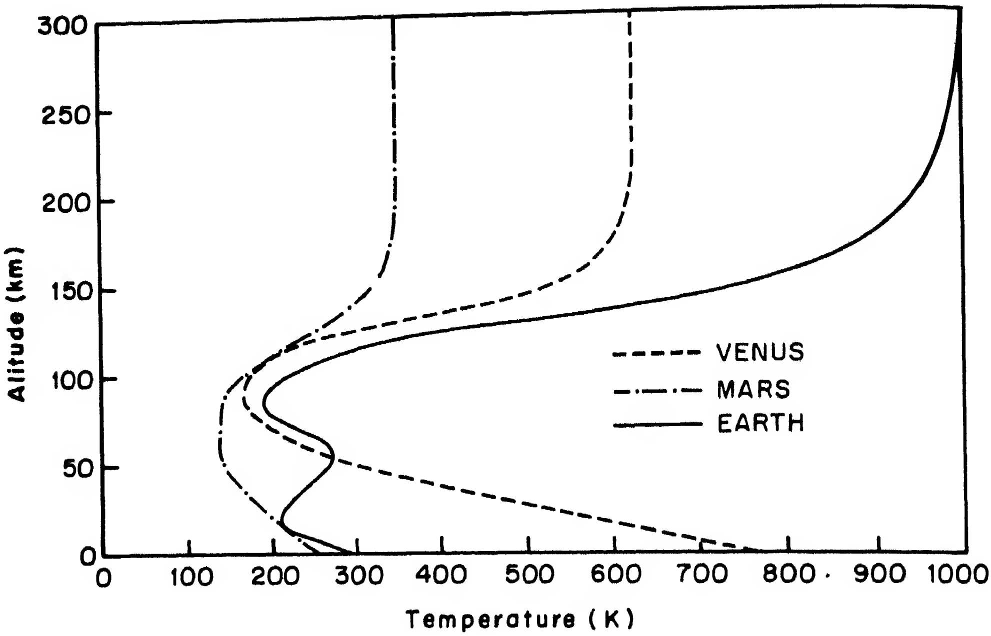

Fig 3 Examples of temperature distributions for Venus, Mars and the Earth [(after Bauer, 1973)[10]

deuterium to hydrogen ratio, on the other hand, is a strong evidence of massive loss of hydrogen (and thus of water), at least in the past, if not the present.

Neutral Atmosphere of Giant Planets

Atmospheres of all the giant planets are composed mainly of hydrogen and helium; all exhibit minor components dominated by CNO compounds, as expected from cosmic abundances. However exploration by Pioneer and Voyager spacecrafts and the improvements in ground-based and airborne telescope measurements have brought to light some differences in composition. In contrast to the common view two decades ago about similar composition and elemental abundances close to solar values (*see* e.g. Gautier and Owen, 1989)[9], strong differences exist in the He/H ratio in the atmospheres of Jupiter, Saturn, Uranus and Neptune. Further, the deuterium to hydrogen ratio at Jupiter and Saturn seems to be equal to protosolar value, but significantly higher at Uranus. Atmospheres of all giant planets have been enriched in carbon, the enrichment increases as one moves away from Sun. In addition, differences in thermal structure also exist. Jupiter, Saturn and Neptune exhibit substantial internal sources of energy while Uranus exhibits only a very weak source of energy, consequently the convection is expected to be rather small within Uranus.

There is a lot of similarity in the thermal structures of the four giant planets, as can be noted from Fig. 4 (Bauer, 1973)[10]. All have tropospheres, stratospheres and mesospheres at about the same altitudes. This similarity results from equilibrium between similar sources and sinks of radiative energy. The thermospheres of these planets are quite hot, as observed with radio and UV steller occultation techniques.

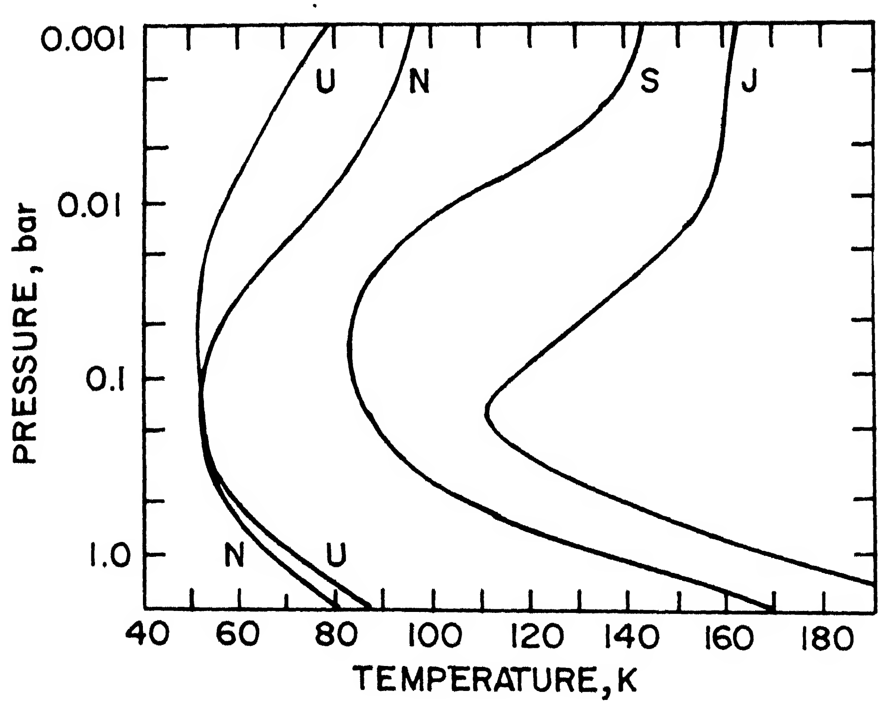

Fig 4 Temperature profiles of Jupiter, Saturn, Uranus and Neptune [(after Gautier and Owen, 1989)[9]

Exospheric temperature at Jupiter and Saturn has been computed to be 1100 K and 800 K respectively, while it is around 750 K at both Uranus and Neptune.

Ionosphere and Ion Compositions of Terrestrial Planets

Pioneer Venus was the first spacecraft to enter the Venus ionosphere to make direct measurements, although altitude profiles of electron density at the planet had earlier been obtained by the radio occultation technique by several Mariners and Venera spacecrafts. The Pioneer Venus mission very satisfactorily answered questions like: what is the ion composition of the Venus ionosphere? what is the plasma temperature? how does the composition of the neutral atmosphere affect the ionosphere? what is the source of variability of the ionosphere? how do ionosphere and upper atmosphere respond to changes in the solar EUV? and the solar wind? and why is there a nightside ionosphere in spite of a large night at Venus? (Brace *et al.* 1989)[11]. These questions had been raised before the start of the mission. However a large number of discoveries were also made during the first two years of the mission, when the periapsis was maintained deep in the ionosphere. For example, a large bulge of hydrogen and helium ions was found in the predawn ionosphere.

This suggests, as mentioned earlier, that the thermosphere of Venus must be rotating faster than the planet, a result consistent with the recent theory on atmospheric super-rotation (all atmospheres rotate faster than their planets). Another surprising result was, that although ionospheric electron densities showed a strong control of solar EUV, the ionospheric temperatures exhibited no detectable effect. The Venus

ionosphere also showed a much higher concentration of deuterium ions than that of Earth's ionosphere. These observations suggest again that Venus originally may have had a lot of water that is no longer present. Transport of dayside ions to the nightside was detected, which explains the maintenance of the night ionosphere, although evidence has also been presented for local production. Relative importance of the two sources varies with solar activity. Larger flows occur at solar maximum when the dayside density is high, while local production is more important at solar minimum when the nightward flow is low. The nightside ionosphere has been found to be very hot – the electron temperature does not show any change between day and night. In addition, there are holes in the otherwise dense nightside ionosphere. Superthermal ions and electrons have been detected, mainly above the ionopause. Fig. 5 shows an overview of the Venus environment.

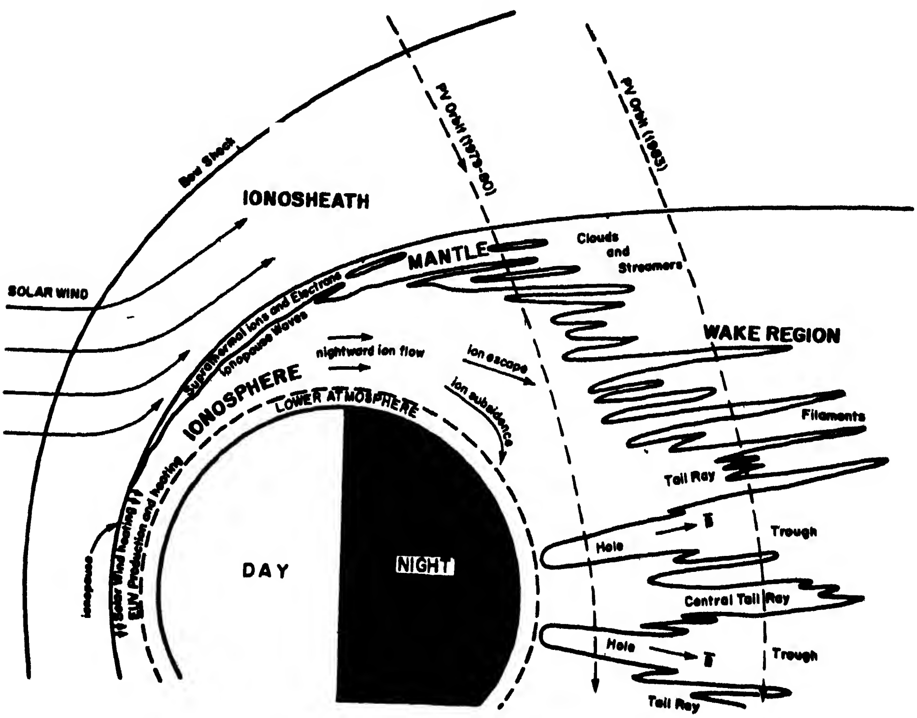

Fig.5 Sketch showing the Venus Iono-tail structure, based on PVO crossing of high altitude nightside ionosphere (after Brace *et al* 1987)[62].

The last *in-situ* data sent by the Pioneer Venus Orbiter (PVO) during its 'entry' phase in 1992 pertains to a period of low solar activity. Measurements from the ion mass spectrometer indicate that O^+ ion density in the midnight sector decreased from solar maximum (SCmax) concentration by at least an order of magnitude at all altitudes. In contrast, O_2^+, the major ion at the main ionospheric peak at 140 km, exhibited a much smaller decrease. This clearly establishes that, unlike SCmax times, O^+ ions transported from the dayside are not the major source of the nightside ionosphere of Venus at low solar activity. Instead, the observed excess production of mass 28 ions (over chemical production) provides strong evidence of electron

impact ionization at these times. In general, the nightside ionospheric states were strikingly similar to the "disappearing" ionosphere conditions, observed only sporadically at SCmax. The preliminary magnetometer data show evidence of strong horizontal magnetic fields pervading the nightside ionosphere. Also there is evidence of rapidly drifting plasma and 30-100 eV superthermal O^+ ions. Qualitatively, similar results were observed by the electron temperature probe, the average electron density (Ne) at altitudes between 170 and 400 km being about a factor of 5 lower during the entry phase. An important new result was the observation of small-scale waves in Ne having horizontal wavelengths of the order of a km between 140 and 150 km. This may be associated with a plasma instability triggered by the dominant particle impact ionization.

There have been no direct measurements of the Mars ionosphere after the Viking landers, but the analogies with the PVO results at Venus have resulted in a great deal of new knowledge. It has been concluded that Mars has either no or very weak magnetic field. The plasma scale heights in the topside ionosphere indicate a large solar activity change, which has been interpreted as a solar activity effect in the thermospheric temperatures. The weakness of the Mars magnetic field has been confirmed by the PHOBOS mission which has also provided evidence for large outflows of the Martian ions.

Fig. 6 shows the ion composition at Venus and Mars. For comparison, ion composition of Earth's ionosphere is also given. The Venus measurements are from the ion mass spectrometer on PVO (Taylor *et al.* 1980)[12]. The Mars measurements are by the Viking retarding potential analyser (Hanson *et al.* 1977)[13] and are compared with the calculations of Fox and Dalgarno (1979)[6] (solid curves).

Ionospheres of Giant Plants

Observations of radio emissions at 20 MHz provided the first impetus for studying the ionosphere of Jupiter. These were explained as possible plasma oscillations of Jupiter's ionosphere, thus requiring peak electron densities of the order of 5×10^6 cm^{-3}. Rishbeth (1959)[14] immediately explained these high densities by proposing that H^+ ions were formed by photoionization of H, produced from total dissociation of H_2. By making a comparative study with the F_1 region of the Earth's ionosphere, Rishbeth obtained a value of 50 cm^{-3} s^{-1} for H^+ production rate and by using radiative recombination as the loss mechanism for H^+, he obtained the desired electron density. McElroy (1973)[15] pointed out that direct photoionization of H is not an important source of H^+, but it is the dissociative photoionization of H_2 which is the major source of H^+. This is so because atomic hydrogen is about 3 orders of magnitude smaller than molecular hydrogen in the main ionospheric region.

Since the above observations of radio emissions, ionospheres have been detected and measured at all the giant planets by the Voyager mission. Ion production is mainly thought to be due to solar EUV, although galactic cosmic rays, and

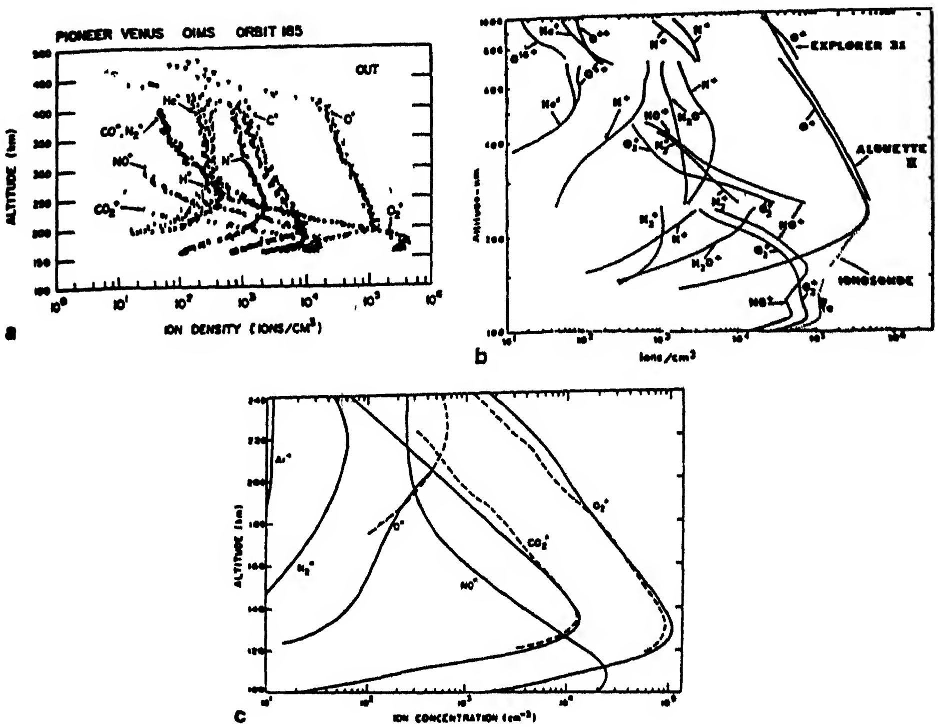

Fig.6 The ion composition of Venus, Earth and Mars ionospheres. [Fig. 6a, shows the distribution of the major ions in the Venus thermosphere near solar maximum conditions at small solar zenith angles as measured by the PVOIMS (after Taylor *et al.* 1980)[12]. Fig. 6b shows the ion composition of the Earth's ionosphere based on ion mass spectrometer data. Fig. 6c shows the Viking retarding potential analyzer observations (Hanson *et al.* 1977)[11] (dashed curve) compared to the calculations of Fox and Dalgarno (1979)[6] (solid curve)

precipitating particles at all latitudes are also considered to be important. H_2^+ ions have the highest production rate, between 90 - 95% of all ions produced. Under certain circumstances, when H_2 is vibrationally excited, the reaction of H^+_2 with H_2 produces H_3^+, which could be the major ion at or below the main ionospheric peak at Jupiter and Saturn (Majeed and McConnel 1991)[16]. H^+ will remain the major ion on the topside ionosphere. H_3^+ was first spectroscopically detected on Jupiter's auroral region by Baron *et al.* (1991)[17]

A lot of excitement was initially generated by the so-called 'electroglow' phenomenon, wherein a non-solar excitation mechanism was needed to explain the intense dayside Lyman and Werner band UV airglow emissions from H_2 observed by the Voyager in Jupiter, Saturn, Uranus and Neptune. However, the source seemed to have a solar control, in view of the observed near absence of the phenomenon on the nightside. The most likely cause of this phenomenon is solar fluorescence scattering of H_2 rather than photoelectron acceleration (Yelle, 1988, Wait *et al.* 1988:)[18,19]

The ionospheres of the giant planets get weaker as one moves away from the Sun. At Jupiter peak electron density is more than $10^5 cm^{-3}$, while it is smaller by an order

of magnitude at Saturn. At Uranus and Neptune the peak density is close to 10^3 cm^{-3}. Fig. 7 compares sample Ne-h profiles at the four planets. Fluctuations in the observed profiles have been smoothed and thus the profiles are only symbolic to show the major characteristic – the large decrease in the peak density from Jupiter to Neptune. This large decrease from Jupiter to Uranus and Neptune is not consistent with the photochemistry and therefore a few additional loss processes like water from the rings at Saturn and influx of methane from the rings at Uranus have been invoked (*see* review by Mahajan and Kar, 1988)[4]. Outflow of plasma along field lines has also been considered as a possible loss mechanism. All the four planets have magnetic fields, some highly tilted and offset from the planet's centre (namely Uranus and Neptune).

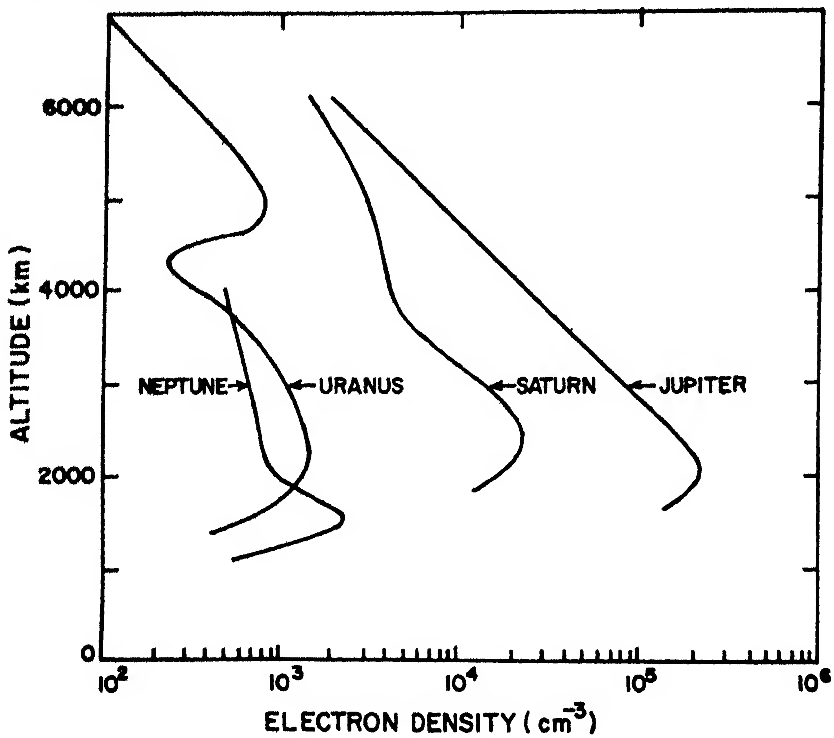

Fig.7 Electron density profiles of Jupiter[63], Saturn[64], Uranus[65] and Neptune[66]. Profiles have been smoothed to show the gross features.

Solar Wind Interaction

The magnetic field of all the giant planets is sufficiently strong and, therefore, their ionospheres are protected from the solar wind by their magnetospheres. The terrestrial planets have weak or no magnetic field and so solar wind interacts directly with these planets. In the following, we discuss the interaction at Venus and Mars.

Solar Wind Interaction at Venus

Although it was known before the PVO mission that intrinsic magnetic field of

Venus was much smaller than that of the Earth, yet it was not clear if it had any role in the interaction of solar wind. The PVO measurements have established that the magnetic field of Venus is too weak to play any role in the solar wind interaction. Consequently the solar wind interacts directly with the ionosphere and atmosphere of Venus. A very important result noted right in the beginning of the mission was the large variability in the upper boundary of the ionosphere, called the ionopause, which was found to be controlled by the solar wind dynamic pressure, P_{SW}. Fig. 8 taken from Taylor *et al* (1979)[20] shows an example of large changes in the ionosphere, following changes in P_{SW}. The solar wind interaction results in a magnetic cushion or a magnetic barrier acting both as a lid on the ionosphere and as an obstacle to the solar wind flow The solar wind pushes the magnetic field down towards the planet which in turn pushes on the ionosphere. The plasma pressure is generally large enough to stand off the solar wind. The strength of the magnetic field increases to the necessary value to balance the solar wind, thereby putting a lid on the ionosphere. It is to be noted that there is little or no direct coupling between the solar wind and the atmosphere of the planet. The coupling, however, occurs above the ionopause where neutral atoms of oxygen get ionized and are then picked up by the solar wind flow. The neutral atmosphere can be removed by this mass-loading, but this process is very slow. It has been calculated that 10^{26} ions are removed each second, which means that only about three feet of water, globally, could be removed from the surface of Venus since its formation (Russell, 1989)[21].

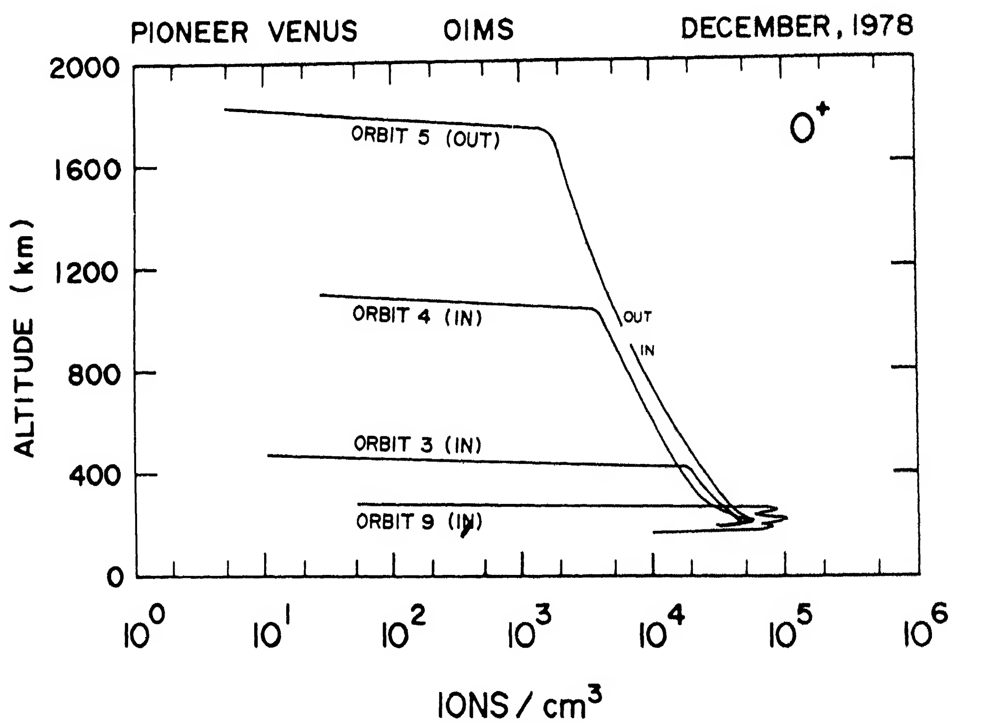

Fig.8 Altitude profiles of O^+ densities from a series of PVO orbits, showing the variability of ionopause (after Taylor *et al* 1979)[20]

A very surprising and unexpected result of the solar wind interaction at Venus was the discovery of flux ropes – coils of twisted magnetic field which seem to be connected to the solar wind's magnetic field (Russell *et al.* 1979)[22]. These flux ropes form at the ionopause and sink into the ionosphere. When P_{SW} is low, the ionosphere is virtually free of magnetic field, except for these flux ropes. However, when P_{SW} increases, the ionosphere gets fully magnetised (Luhmann *et al.* 1980)[23]. The intensity of magnetization depends upon the intensity of P_{SW}.

The extensive data on bow-shock during the solar cycle have revealed that the bow-shock moves outward and inward with the rise and fall of sunspot number. This motion is a result of the greater mass loading due to higher hot O density during solar maximum (Russell *et al.* 1988)[24].

The solar wind interaction has profound effects on the structure of Venus ionosphere. During high solar activity, the Venus ionosphere is rather robust (high plasma pressure), and therefore, it stands off the solar wind at greater heights in the topside ionosphere. However, during conditions of very high P_{SW}, the balance height between P_{SW} and plasma pressure moves down to lower altitudes and we get a depressed ionosphere having the scale height of the parent neutral gas (Mahajan *et al.* 1989)[25]. This condition is expected to be rather quite frequent during low solar activity when plasma pressure falls below P_{SW}. Fig. 9 illustrates the scenario during low and high solar activity conditions.

VLF waves have been detected by the Electric Field Detector on the Pioneer Venus Orbiter, thus providing evidence of lightning at Venus. These waves appear to occur more frequently over some geographic regions, a result consistent with the property of terrestrial waves generated by lightning.

Solar Wind Interaction at Mars

The Mars-2, Mars-3 and Mars-5 provided the first simultaneous measurements of plasma and magnetic field in martian environment, in the early seventies. Existence of a detached bow-shock, a very thick tail with the downstream flow of planetary plasma, a high altitude dayside obstacle to the solar wind flow with underlying planetary plasma embedded in a moderately strong magnetic field and a boundary layer with traces of pick-up ions in the ionosheath, were some of the major results from these measurements. The PHOBOS-2 plasma package has provided much more extensive data on the solar wind interaction at Mars (*Nature*, 19 October 1989)[26]. Observations of the bow-shock location and the structure of the magnetotail of Mars by the PHOBOS spacecraft and of Venus by the Pioneer Venus Orbiter show the solar wind interactions with these two planets to be quite similar. Both Venus and Mars have mainly induced magnetospheres and magnetotails which stand off the solar wind flow.

The PHOBOS-1 and PHOBOS-2 spacecrafts were launched on 7 and 12 July

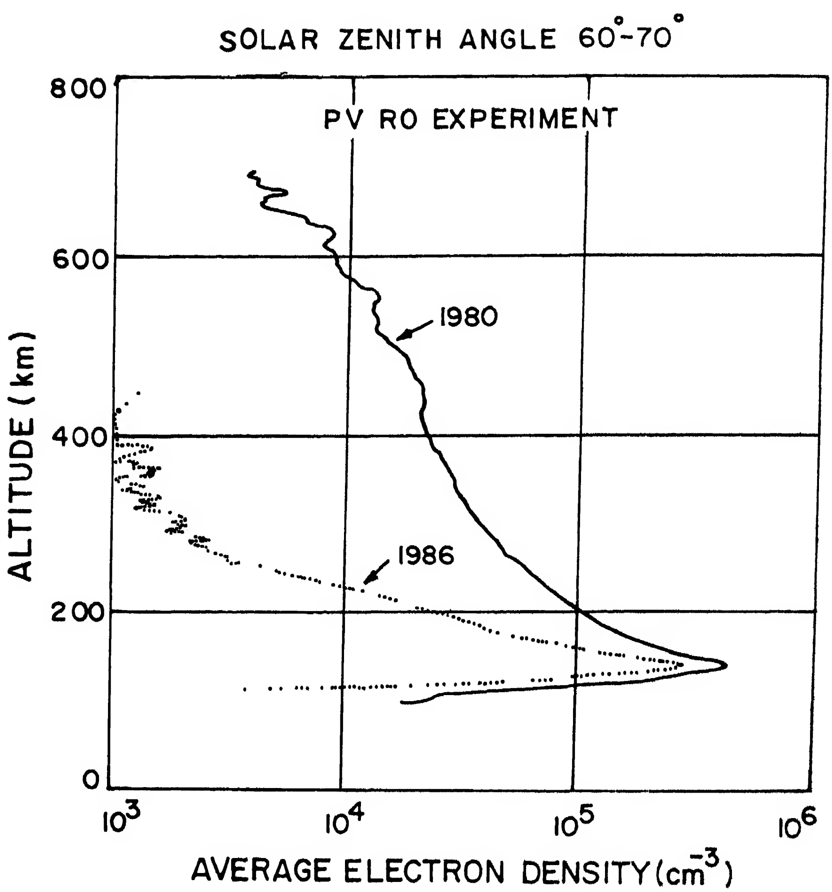

Fig.9 Average electron density profiles from PV radio occultation experiment showing the solar cycle effect on the dayside ionopause. The 1980 and 1986 profiles are the average of 6 and 10 individual profiles respectively (after Knudsen *et al.* 1987)[67].

1988 respectively. Radio communication with PHOBOS-1 was lost during the Earth to Mars cruise phase. PHOBOS-2 was inserted into an elliptical orbit around Mars on 29 January 1989. On 27 March 1989, radio contact with PHOBOS-2 too was lost. Although the PHOBOS-2 mission could not carry out the planned scientific programme, yet during its short lifetime of 2 months, this spacecraft returned unique scientific data. In the upstream sub-solar region (bow-shock and magnetosheath), magnetic field, plasma waves and particles were measured. The plasma programme of the PHOBOS mission allowed features of the magnetic field and characteristics of plasma in the equatorial region of the martian tail to be measured.

A major question about the martian magnetosphere is the nature of the martian wake – whether the tail is induced or intrinsic. Statistical analysis of the PHOBOS magnetograms by some workers show that the martian magnetic tail is induced. If there is an influence of the martian intrinsic magnetic field on the magnetotail of Mars, that influence is weak. The most persistent feature of the martian magnetospheric cavity is the dominance of ionospheric ions. Fig. 10 shows the number density and flow velocity for H^+ ions and the number density of O^+ and molecular ions during the

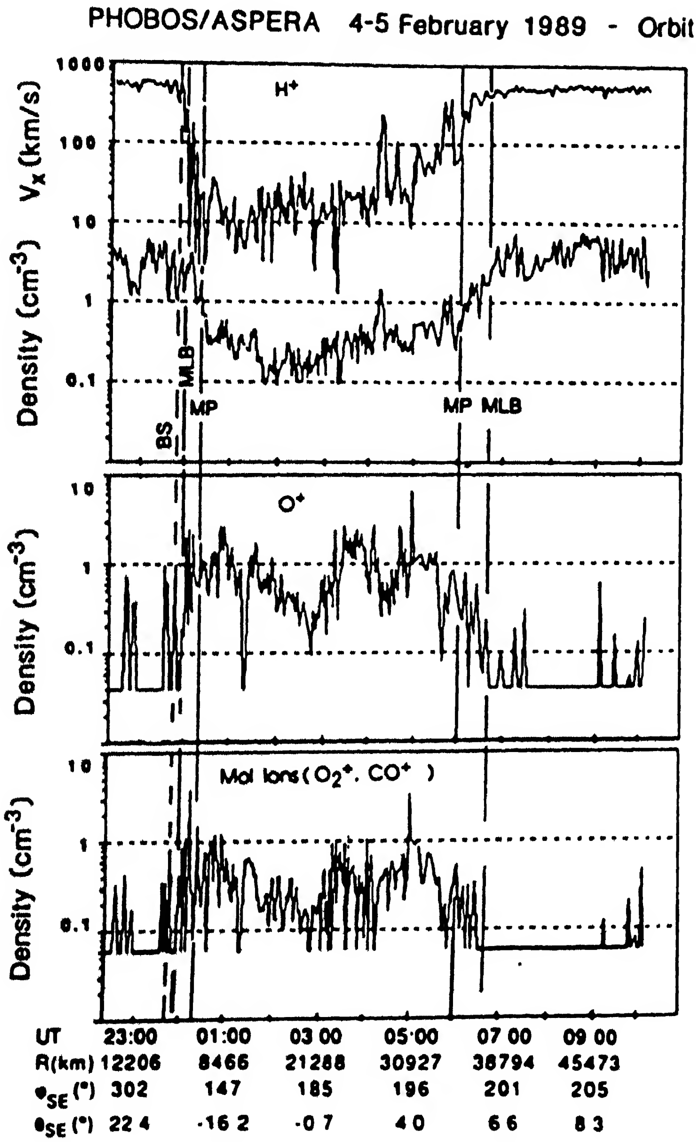

Fig. 10 Number density of O^+ and molecular ions in the Mars magnetosphere measured by the ion composition experiment ASPERA on PHOBOS-2 Notice that at times the molecular ion density exceeds the O^+ density (after Lundin et al 1989)[68]

crossing of the martian tail. Large increases of energized ionospheric ion densities accompanied by strongly reduced H^+ ion densities can be noted. The O^+ density is twice the molecular ion density but locally molecular ions may even dominate the ionospheric outflow. Oxygen ions are up to ten times more abundant than protons inside the martian magnetosphere, which implies not only a fast loss of atmosphere from Mars but probably efficient transfer of solar wind energy to the martian ionosphere without a significant mass transfer of solar wind plasma into the inner martian magnetosphere (Lundin *et al.* 1990)[27]. An escape flux of $7 \times 10^{27} s^{-1}$ for H^+ ions has been estimated by Lundin and Dubinin (1992)[28]. If the escaping particles are O^+

ions, the maximum rate would be $4 \times 10^{26} s^{-1}$ (or $2 \times 10^{26} s^{-1}$ for O_2^+) which is equivalent to escape of 11 kg atmosphere/s.

Major Indian Contributions

Research in planetary atmospheres started at various centres in India in the early eighties. This was mainly due to the success of Pioneer Venus mission and due to the availability of UADS data from the World Data Center. Pioneer and Voyager missions to the giant planets had also provided enough information for some theoretical and analytical work on these planets. In what follows, we bring out a summarised account of the various significant contributions from India. For simplicity we shall do this planetwise.

Venus

Much of the Indian contribution on the venusian upper atmosphere relied on the *in-situ* data from the Pioneer Venus Orbiter(PVO). The group at NPL used these data to study the variability of the ionosphere of Venus and its interaction with the solar wind. It was shown that some of the variability in the dayside ionosphere could be attributed to solar flares (Kar *et al.*,1986)[29]. The large-scale horizontal magnetic fields that are sometimes observed in the dayside ionosphere could also strongly affect the altitude profile of the plasma density (Kar *et al.*,1987)[30] even near the terminator. These magnetic fields were shown to have a strong correlation with the solar wind dynamic pressure (P_{sw}) implying that the fields are generated in a continuous mode rather than episodically (Kar and Mahajan, 1987)[31]. These large-scale magnetic fields ultimately dissipate in the collisionally dominated lower ionosphere. This, along with particle precipitation from solar wind, should lead to some neutral heating. However, a study of the exospheric temperatures (Tex) inferred from neutral density scale heights shows no linear correlation between P_{sw} and Tex (Kar *et al.* 1991)[32]. The effect of P_{sw} on the ionopause and plasma energetics were also studied. It was shown that the density ionopause (the critical factor which determines the amount of plasma supplied to the nightside) near the terminator remains quite high (400-500 km) even for very high P_{sw} (Kar *et al.* 1992)[33]. This implies that a significant flow of plasma to the nightside is still possible, contrary to earlier understanding In another work relevant to the maintenance of nightside ionosphere, it was shown that the main ionosphere above 200 km shows a positive response to variations in solar EUV flux contrary to earlier results (Ghosh *et al.* 1993)[34]. Early results indicated that electron temperatures (Te) on the dayside ionosphere had a statistically linear relationship with P_{sw} (Mahajan *et al.*, 1988)[35] implying that Te variability in the dayside is essentially controlled by solar wind heating. But a more careful analysis later showed that Te in the ionosphere does not show any orbit-to-orbit variability and that most of the variability in Te is in the ionopause and is inversely related to Ne (Mahajan *et al.* 1994)[36] as shown in Fig. 11. The observed sharp rise in Te in the ionopause region is attributed to the steep fall in Ne. This is so because local equilibrium exists there due to large horizontal

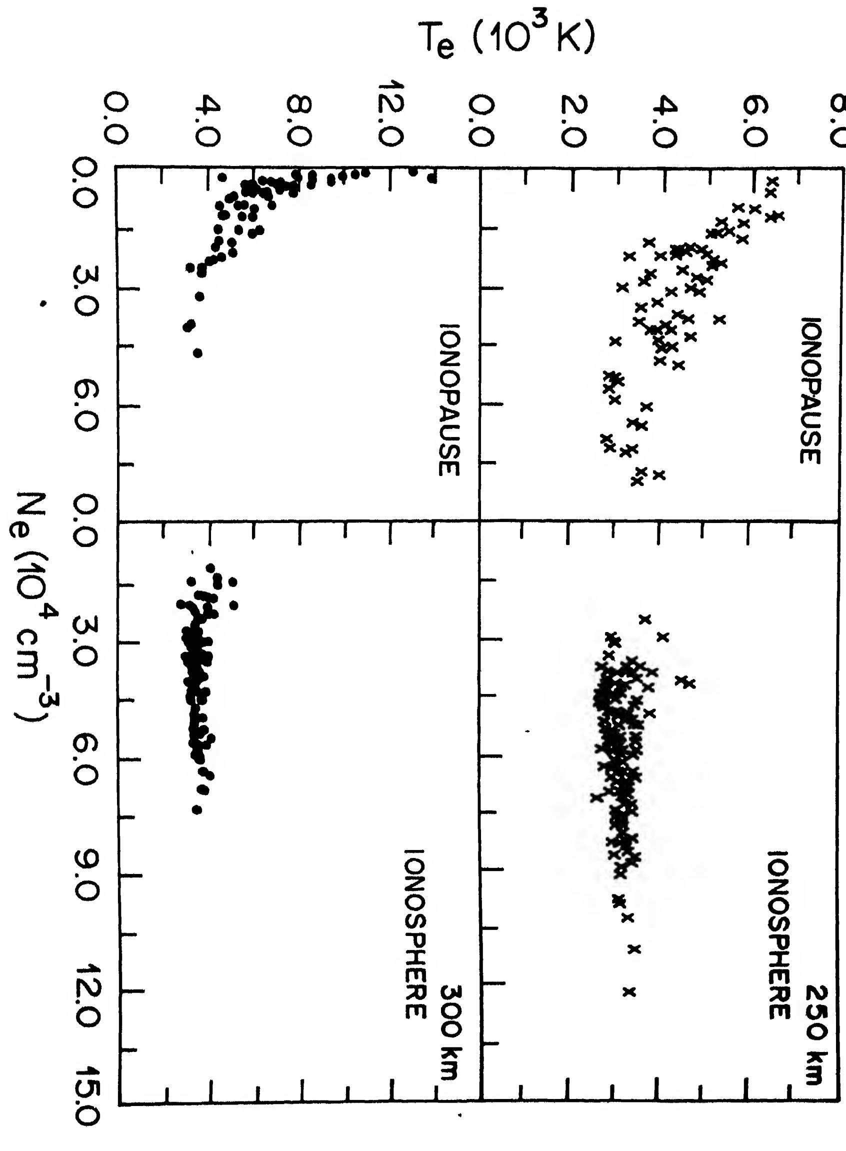

Fig.11 A plot of Te against Ne for dayside orbits with SZA < 60° at 250 and 300 km Left hand panels have data from the ionopause region. The right hand panels contain data from the main ionosphere. A negative correlation between Te and Ne can be noted in the ionopause region [(after Mahajan *et al* 1994)[36].

magnetic fields. Solar wind does not seem to play any major role in the thermal structure of the Venus ionosphere.

The group at Banaras Hindu University has been involved primarily in theoretical modelling of the ionosphere of Venus. Upadhayay and Singh (1990)[37] modelled the neutral densities as well as steady state plasma densities in the range 100-800 km. While their results agree with those of other models below 250 km, these deviate considerably above this altitude. They attributed this to dynamical processes. Orbits with extremely high ionopause have been interpreted as evidence of hot oxygen at altitudes as high as 3000 km by Mahajan *et al.* (1992)[38]. However, the extremely high ionopause encountered on orbit 422 (2800 km) was sought to be explained in

terms of plasma transport processes and effects of solar coronal transients by Singh and Upadhyay, (1990)[39]. Assuming photochemical equilibrium, Balachandraswamy (1991)[40] calculated the electron and ion density profiles in Mars and Venus in the altitude range 100-300 km. He obtained good agreement with observations below 200 km for both the ionospheres. The energetics and the maintenance of the nightside ionosphere were also modelled using a spectral technique by Singhal and Whitten (1991)[41]. The nightside ion densities showed a sharp decrease as the ionopause altitude was lowered to 300 km, while the effect of viscosity on the nightward flow velocity becomes appreciable above an altitude of 400 km. Another source for the nightside ionosphere is particle precipitation. Singhal and Haider (1982)[42] used a generalised yield spectrum approach to calculate the volume excitation rates for various atmospheric species as well as volume ionization rates resulting from precipitating electrons in the 30-500 eV range. Several bands of CO_2,N_2 and $O(^1D)$ were found to be strongly excited by low energy electron precipitation.

The magnetometer aboard the PVO observed low frequency waves in the magnetic field in the ionopause region in subsolar locations. These waves were explained in terms of flute instability by Singh and Upadhyay (1989)[43]. The Electric Field Detector aboard PVO also observed waves in four different channels. Singh and Upadhyay (1993)[44] studied the wave attenuation along the Venus-ionosphere waveguide. They showed that the signals (assumed to be generated by lightning) can travel considerable distance and can ultimately leak out through the ionospheric 'holes' in the nightside of Venus.

Mars

In contrast to Venus, not much observational data exist on the upper atmosphere of Mars, the last and the only direct measurements being made by Viking 1 and 2 in 1976. However, there is an increased focus on Mars at the present time. The PHOBOS mission, albeit only partially successful, stimulated research on the ionosphere of Mars and its interaction with solar wind. It is still not clear whether the solar wind interaction of Mars is primarily magnetospheric or Venus-like (atmospheric). Mahajan *et al.* (1992)[45] showed that the solar wind interaction region extended down to about 160 km during the Viking measurements thus grossly eroding the molecular O_2^+ layers as shown in Fig. 12. This should result in an outflow of ionospheric O_2^+ ions which were indeed observed by the ASPERA instrument on PHOBOS 2 in the magnetotail region of Mars. This process constitutes a significant loss of atmospheric constituents. However, Kar (1993)[46] pointed out that in the past, Mars probably had an intrinsic magnetic field which would have been strong enough to have a magnetospheric interaction with the solar wind thereby shielding the atmosphere from direct erosion. Another instrument aboard PHOBOS-2, the hyperbolic electrostatic analyser, had measured electron fluxes within the energy range 3-480 eV. Haider *et al.* (1992)[47] showed that the impact ionization from possible precipitation of these electrons could be sufficient to maintain the nightside ionosphere of Mars.

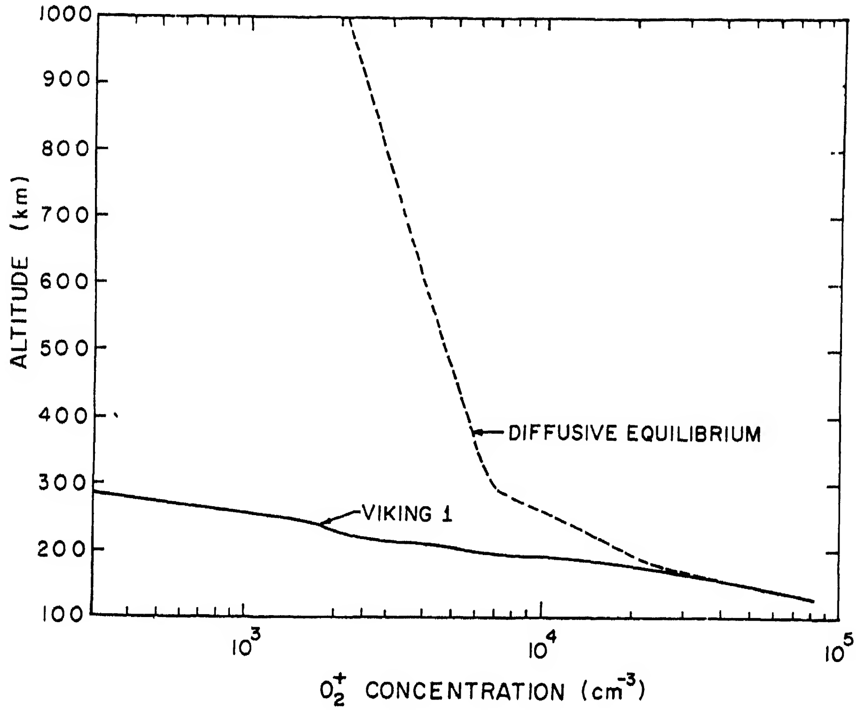

Fig 12 The expected O_2^+ profile under diffusive equilibrium above 160 km for Viking 1 and the observed O_2^+ profile (marked as Viking 1) The observed O_2^+ profile has been grossly eroded by the solar wind interaction (after Mahajan *et al* 1992)[15].

Outer planets

On outer planets the only experimental data are those supplied by the Pioneer and the Voyager spacecrafts. Hence the Indian efforts, as elsewhere, have been primarily theoretical. Using Voyager data, Mahajan (1981)[48] discovered an equatorial anomaly in the ionosphere of Jupiter much like the one existing in the Earth's ionosphere as shown in Fig. 13. Raghavarao and Dagar (1983)[49] calculated the dynamo region to extend from 130 to 330 km on Jupiter (referred to 43.8 mbar pressure level) and also gave an estimate of the intensity of the current density and latitudinal extent of the equatorial electrojet. Subsequently a similar equatorial anomaly was also observed at Saturn (Mahajan *et al.* 1985, 1986)[50,51]. A surprising result from the Voyager observations is the high thermospheric temperatures ($\geq$1000 K) on the outer planets Apart from the suggested heat sources, possible localised heating at Jupiter could also take place by frictional dissipation of Io-related Alfven waves (Kar and Mahajan, 1986)[52].

The group at BHU has been actively involved in modelling the various aeronomical processes at the outer planets. Haider (1986)[53] used the Analytical Yield Spectrum (AYS) approach to estimate the photoelectron fluxes in the atmosphere of Titan for a purely N_2 atmosphere. Singhal and Haider (1986)[54] further calculated the intensities of some N_2 band emissions in Titan. They concluded that the intensity of Lyman-Birge-Hopfield (LBH) bands observed by Voyager 1 can be explained in terms of

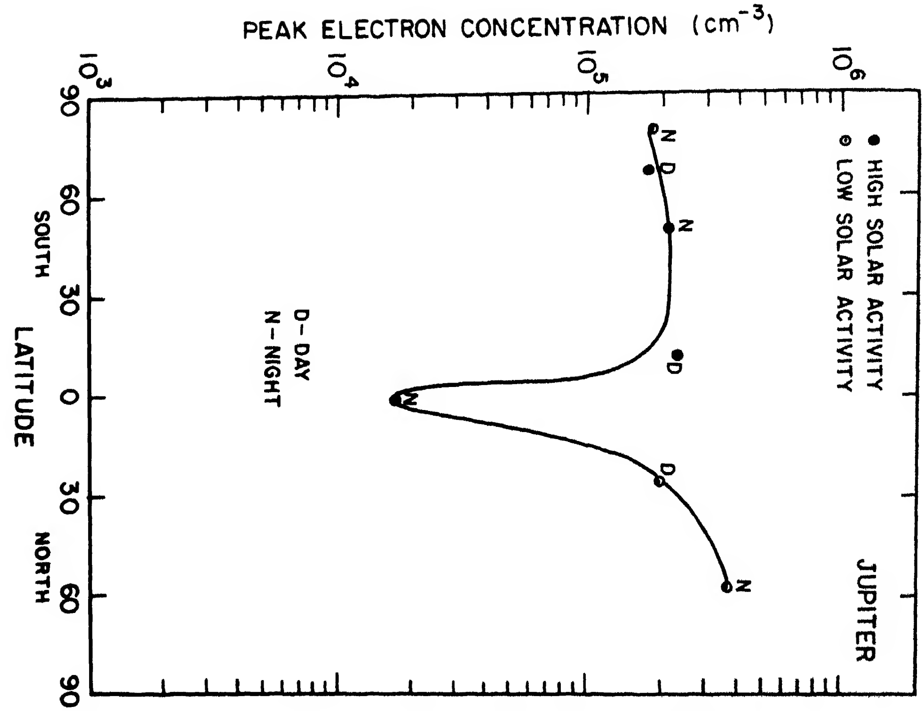

Fig.13 Plot of peak electron density with latitude showing the equatorial anomaly in the ionosphere of Jupiter (after Mahajan, 1981)[18]

solar EUV radiation alone, while the calculated Birge-Hopfield (BH) band emissions are too small compared to the observed intensity. The emissions resulting from atmospheric interaction with magnetospheric electrons or solar wind electrons fall short of observed intensities by an order of magnitude or more. The same AYS technique was used to calculate the photoelectron and auroral electron fluxes in cometary ionospheres by Bharadwaj *et al.*(1990)[55]. It was further extended to Neptune by Bharadwaj and Singhal (1990)[56] to calculate the H_2 band emission rates at subsolar locations from photoelectrons as well as at auroral latitudes from precipitating electrons. They predicted the total auroral H_2 band intensity to be about 900R assuming the electron energy flux to be the same as that at Uranus. They had also estimated a dayglow intensity of 20R of this band from the photoelectron source. The Voyager 2 reported Lyman alpha airglow emission intensity to be 10R on Neptune, which is quite close to the estimated value. A puzzling result from the Voyagers was the observation of intense dayside Lyman and Werner band UV airglow emissions from H_2 at Jupiter, Saturn and Uranus. Singhal and Bharadwaj (1991)[57]studied the energetics of photoelectrons in the presence of parallel electric fields at Uranus using a Monte Carlo technique. They found the parallel electric fields (produced by ionospheric dynamo action) are capable of producing about 20% of observed electroglow emission. Parallel electric fields are not however capable of energizing low energy protons to produce appreciable H Lyman alpha emission through direct collisions with H_2 (Bharadwaj and Singhal, 1993)[58]. Hot H atoms (resulting from charge exchange of accelerated protons) may instead be a potential source of enhanced Lyman alpha emissions by scattering solar Lyman alpha.

Recently Singhal *et al.* (1992)[59] made a detailed study of electron precipitation (10-100 keV) processes in the auroral regions of Jupiter using the continuous slowing down approximation. On the other hand, Singh (1991)[60] used the same approach to study the possibility of the auroral emissions on both Jupiter and Saturn resulting from energetic proton precipitation. He found the range of proton energy compatible with observed emission intensities to be about 1-1000 keV.

FUTURE DIRECTIONS

It is now well recognized that investigations of other planetary atmospheres is vital for the understanding of the evolution of our own atmosphere. In the last two decades space probes have extended the scope of aeronomical studies to the fringe of the solar system, thus opening up a very exciting and fertile area of research. India has a long tradition of research in upper atmospheric phenomena. This experience will be invaluable in studies of atmospheres of other planets. A number of important Indian contributions have come in the last decade. But much more can be done and needs to be done.

India already has a vigorous space science programme, which might involve launching of planetary probes sometimes in the future. However, a great deal can be learnt by using the existing data. There now exists a vast database on the atmosphere of Venus. The Voyagers 1 and 2 also provided a lot of data on the outer planets. All these data are well archived and can be easily accessed by Indian scientists using elecronic mail or otherwise. All the spacecraft missions to various planets threw up a number of puzzles some of which are yet to be solved. These as well as other interesting aeronomical investigations can be done using these data. An interesting possibility is comparative study of various recorded solar phenomena as their effects propagate out and affect different planetary environments. These data can also act as benchmarks for theoretical models that may be developed by Indian scientists.

Ground-based observations have led to many interesting results in planetary atmospheres. A case in point is the recent discovery of tenuous atmospheres on Mercury and Moon. Such ground-based observations can be undertaken by Indian scientists.

Io is the second innermost moon of Jupiter. Its orbit lies within the Jovian magnetosphere. Four neutral clouds (viz. sodium, potassium, oxygen, and sulphur) and plasma in the form of torus have been detected on Io by remote observations of cloud emission lines. The scientists at Physical Research Laboratory (PRL) plan to measure sodium and sulphur emission lines on Io from the Earth. Ground-based observations in the planetary tail are also possible by Doppler imaging spectrometer, which can measure the Doppler shift of the emission of ionized species as a function of distance from planets. Measurements of plasma outflow at comet Halley have been made by PRL scientists using this technique. These programmes are very

promising and need to be continued in future.

Another area where Indian scientists can possibly play a role is laboratory studies of aeronomically important chemical reactions. In particular, a variety of chemical reactions including hydrocarbons occur on the outer planets for which the reaction rates are very poorly known Any Indian contributions in this area will be greatly valued by the theoretical modellers. Most of solar energy is emitted between 0.2 and 2.0 μm. The solar radiation in this range interacts with material. So laboratory measurements can help calculate real (n) and imaginary (k) part of the complex refractive index for modelling the structure of planetary atmospheres.

As discussed already theoretical models of the aeronomical processes on outer planets have already been undertaken by Indian scientists. However, this is presently limited to only a group or two. It is necessary to involve more scientists in this area.

OUTSTANDING PROBLEMS

The field of planetary atmospheres and ionospheres is indeed a frontier area of research. With the exceptions of Venus, the planetary missions have just given us only very sketchy information about the planets. The only direct measurements at Mars, as stated earlier, are due to Viking landers of 1976. For the giant planets, no direct measurements have yet been made, although Galileo is expected to provide *in-situ* data at Jupiter, and Cassini is planned to make similar attempts at Saturn. No mission like PVO is in sight for Mars. Consequently the field of planetary atmospheres has unlimited opportunities for excellent research. We list below some of the outstanding problems for each of the planets.

VENUS

1. Why do the atmospheres of Venus and other planets superrotate ?
2. Why is there so much variability of the neutral atmosphere during the night ?
3. Is there a solar activity change in Tex and, if so, is it consistent with the 50% increase from solar max to solar min seen in the scale height of Ne-h profile for radio occultation measurements ?
4. How did hydrogen escape at an enhanced rate in the past and what are the current nonthermal processes for escape of hydrogen ?
5. Why does the electron temperature remain the same during day and night ?
6. Does solar wind contribute anything to electron and ion heating ? How much of the solar wind is absorbed by the ionospheres ?
7. How are mass, momentum and energy transferred from the solar wind to the upper atmosphere and ionosphere ?

8. Are there important latitudinal variations in the ionosphere (and atmosphere)?
9. How are holes caused in the nightside ionosphere ?
10. What causes the wavelike structure in the plasma and magnetic field in the nightside of dawn and dusk terminators ?
11. What are the relative contributions of particle ionization and dayside transport for maintenance of the nightside ionosphere ?
12. How are ionopause waves, plasma clouds and streamers formed in the far downstream ?
13. How are superthermal ions generated and what is their role in the Venus environment ?
14. What is the mechanism for high ionopauses ?
15. Is the ionopause of Venus predictive ?

MARS

1. Why was there so much variability in the thermal structure between the Viking 1 and Viking 2 landers ?
2. Does *T*ex show as large a solar activity change as exhibited by plasma scale heights deduced from radio occultation measurements ?
3. Has Mars any intrinsic magnetic field ?
4. How do the upper atmosphere and ionosphere respond to duststorm ?
5. Where does the ionopause occur ?
6. How does ionosphere respond to changes in the solar wind ?
7. How far does the solar wind penetrate ?

OUTER PLANETS

1. Why are the exospheric temperatures so high ?
2. Why does D/H change from one planet to the other ?
3. What causes superrotation of the atmospheres ?
4. What is the cause of equatorial anomaly ?
5. Why is there so much of stratification in the ionosphere ?
6. What are the reasons for departure from photochemical equilibrium ?
7. What is the role of water, methane, and dynamics ?

Acknowledgements

For the Pioneer Venus results we have heavily depended upon the report "Pioneer Venus Orbiter-Ten Years of Discovery", published from NASA Ames Research Center, Moffett Field, California, USA, August 1989.

REFERENCES

1. Kliore, A.J., Cain, D.L., Levy, G S., Eshleman, V.R., Fjeldbo, G. & Drake, F.D., *Astronaut.*, **7**, (1965). 72.
2. Kliore, A.J., Cain, D.L., Levy, G.S, Eshleman, V.R, Fjeldbo, G. & Drake, F.D., *Science*, **149**, (1965). 1243.
3. McElroy, M B, Ecuyer, J.L. & Chamberlain, J W., *Astrophys. J.*, **141**, (1965). 1523.
4. Mahajan, K.K. & Kar, J, *Space Sci. Rev.*, **47**, (1988). 303.
5. Niemann, H.B., Kasprzak, W T. Hedin, A.E., Hunten, D.M & Spencer, N.W., *J. Geophys. Res.*, **85**, (1980). 7817.
6. Fox, J.L. & Dalgarno, A., *J. Geophys Res.*, **84**, (1979). 7315.
7. Nier, A.O & McElroy, M B, *J. Geophys. Res.*, **82**, (1977). 4341.
8. Hunten, D.M., "*A Report of the Pioneer Venus Science Steering Group*" edited by L. Colin (NASA Ames Research Center, Moffett Field, California), (1989). p. 12.
9. Gautier, D. & Owen, T.C., *Origin and Evolution of Planetary and Satellite Atmospheres*, edited by S.K, Atreya, J.B., Pollack, and M.S., Matthews, The University of Arizona Press, Tucson), (1989) p. 487.
10. Bauer, S.J., *Physics of Planetary Ionosphere* (*Springer-Verlag, Berlin*). (1973).
11. Brace, L.H, "*A Report of the Pioneer Venus Science Steering Group*", edited by L. Colin (NASA Ames Research Center, Moffett field, California), (1989). p. 16.
12. Taylor, H.A Jr., Brinton, H.C., Bauer, S.J., Hartle, R.E., Cloutier, P.A. & Daniell, R.E., *J. Geophys. Res.*, **85**, (1973). 7765.
13. Hanson, W.B., Sanatani, S.& Zuccaro, D.R., *J. Geophys. Res.*, **82**, (1977). 4351.
14. Rishbeth, H., *Aust. J. Phys*, **12**, (1959). 466.
15. McElroy, M.B, *Space Sci. Rev.*, **14**, (1973). 460.
16. Majeed, T. & McConnel, J C., *Planet. Space Sci.*, **39**, (1991). 1715.
17. Baron, R., Joseph, R.D., Owen, T., Tennyson, J. Miller, S. & Ballester, G.E., *Nature*, **353**, (1991). 539
18. Yelle, R.V, *Geophys. Res. Lett.*, **15**, (1988). 1145.
19 Wait, J.H, Chandler, M.O., Yelle, R.V., Sandel, B.R. & Cravens, T.E., *J. Geophys. Res.*, **93**, (1991). 14295.
20. Taylor, H.A. Jr., Brinton, H C., Bauer, S.J., Hartle, R.E., Donahue, T.M., Cloutier, P.A., Michel, F C., Daniell, R.E. & Blackwell, B.H., *Science*, **203**, (1979). 752.
21 Russell, C T., *A Report of the Pioneer Venus Science Steering Group*, edited by L., Colin, (NASA Ames Research Center, Moffett field, California), (1989). _ p. 26.
22. Russell, C.T., Elphic, R.C. & Slavin, J.A., *Science*, **203**, (1979). 745.
23. Luhmann, J.G., Elphic, R.C., Russell, C.T., Mihalov, J.D. & Wolf, J.H., *Geophys. Res. Lett.*, **7**, (1980). 917

24. Russell, C.T., Chou, E , Luhmann, J G., Gazıs, D , Brace, L H. & Hoegy, W.R., *J. Geophys. Res.*, **92**, (1988). 5461.

25. Mahajan, K.K , Mayer, H.G., Brace, L.H. & Cloutier, P.A., *Geophys Res. Lett.*, **16**, (1987) 757

26. *Nature*, October 19, (1989) **341**

27 Lundın, R *et al* *Geophys. Res. Lett.*, **17**, (1990). 873.

28. Lundın, R , & Dubının, E.M , *Adv Space Res* **12** (9) (1992). 255

29. Kar, J , Mahajan, K K , Srilakshmı, M V. & Kohlı, R , *J Geophys Res.*, **91**, (1986). 8986.

30 Kar, J., Mahajan, K K. & Srılakshmı, M.V , *Adv. Space Res.*, **7**, (1987). 111

31. Kar, J & Mahajan, K.K , *Geophys Res Lett* , **14**, (1987). 507

32 Kar, J., Paul, R , Kohlı, R., Mahajan, K.K , Kasprzak, W.T , & Nıemann, H B , *J Geophys. Res.*, **96** (1991) 7901.

33 Kar, J., Mahajan, K K , Ghosh, S., & Brace, L.H , *J Geophys. Res* , **97**, (1991) 13902

34. Ghosh, S., Mahajan, K.K. & Brace, L.H , *J. Geophys. Res* , **98**, (1993). 19293.

35. Mahajan, K K , Paul, R. & Kar, J , *Indıan J. Radio Space Phys.* **17**, (1988). 50

36 Mahajan, K K., Ghosh, S , Paul, R. & Hoegy, W R., *Geophys. Res. Lett.*, **21**, (1994) 77

37 Upadhyay, H.O & Sıngh, R.N., *Adv Space Res* , **10**, (5), (1990). 41

38. Mahajan, K K , Ghosh, S ,Sethı, N K & Kohlı, R , *Geophys. Res Lett.*, **19**, (1992). 1627.

39 Sıngh, R N. & Upadhyay, H.O., *Curr. Scı* , **59**, (1990). 565

40 Balachandraswamı, A C , *Indian J Radıo Space Phys* , **20**, (1991). 68.

41. Sınghal, R P & Whıtten, R C , *Indian J. Radıo Space Phys* **20**, (1991) 150

42 Singhal, R.P. & Haider, S A., *Indıan J Radıo Space Phys* , **11**, (1989) 15.

43. Sıngh, R.N. & Upadhyay, H O., *Proc IndianAcad. Scı (Earth and Planet. Sci)*, **93**, (1989). 297.

44. Sıngh, R.N & Upadhyay, H.O , *J Geomag. Geoelectr.*, **45**, (1993).383.

45. Mahajan, K.K., Kar, J. & Kohli, R (1992). COSPAR Meetıng, Washıngton DC, USA, to appear ın *Adv Space Res.* (1994).

46. Kar, J., *Geophys. Res. Lett.*, **17**, (1990). 113.

47. Haıder, S A. *et al.* *J. Geophys. Res.*, **97**, (1992). 10637.

48. Mahajan, K.K., *Indıan J Radio Space Phys.*, **10**, (1981). 211.

49. Raghavarao, R. & Dagar Ratı. *Planet Space Sci* , **31**, (1983). 633.

50. Mahajan, K.K., Kar, J & Srılakshmi, M.V., *Indian J. Radıo Space Phys* , **14**, (1985). 143.

51 Mahajan, K K., Kar, J. & Srılakshmı, M V., *Indıan J Radıo Space Phys* , **15**, (1986).61.

52 Kar, J. & Mahajan, K.K., *J. Geophys. Res.*, **91**, (1986). 7101.

53. Haıder, S.A., *J Geophys. Res* , **91**, (1986). 8998.

54. Sınghal, R.P. & Haıder, S.A , *Indian J Radio Space Phys* , **15** (1986). 46.

55. Bhardwaj, A., Haıder, S.A & Sınghal, R.P., *ICARUS*, **85**, (1990). 216.

56 Bhardwaj, A & Sınghal, R.P , *Indıan J. Radıo Space Phys.*, **19**, (1990). 171.

57. Sınghal, R.P & Bhardwaj, A., *J. Geophys Res.*, **96**, (1991) 15963.

58. Bhardwaj, A. & Sınghal, R.P., *J. Geophys Res* , **98**, (1993). 9473.

59. Sınghal, R P., Chakravarty, S.C , Bhardwaj, A & Prasad, B., *J. Geophys Res.*, **97**, (1992). 18245.

60. Singh, V., *Indıan J. Radıo Space Phys.*, **20**, (1991). 140.

61 Hedın, A.E , *J. Geophys. Res.*, **92**, (1987). 4649.

62. Brace, L.H. *et al* *J Geophys. Res* , **92**, (1987) 15.

63. McConnell, J.C., Holberg, J.B., Smith, G.R., Sandel, B.R., Shemansky, D.E. & Broadfoot, A.L. *Plane. Space Sci.*, **30**, (1982). 151.
64. Lindal, G.F., Sweetnam, D.N. & Eshleman, V.R., *Astron. J.*, **90**, (1985). 1136.
65. Lindal, G.F., Lyons, J.R., Sweetnam, D.N., Eshleman, V.R., Hinson, D.P. & Tyler, G.L., *J. Geophys. Res.*, **92**, (1987). 14987.
66. Tyler, G.L. *et al. Science*, **246**, (1989). 1466.
67. Knudsen, W.C., Kliore, A.J., & Whitten, R.C. *J. Geophys. Res.*, **92**, (1987). 13391.
68. Lundin, R. *et al. Nature*, **341**, (1989). 609.

[redacted]

[redacted]